Process Optimization and Environmental Assessment of Municipal Solid Waste Conversion to Liquid Fuels and/or Chemicals

By:

Aviwe Hlaba

MEng: Chemical Engineering

In fulfilment of the Requirement for the Degree of Masters of Engineering: Chemical Engineering, Faculty of Engineering & the Built Environment

Cape Peninsula University of Technology.

Cape Town

April 2020

Process Optimization and Environmental Assessment of Municipal Solid Waste Conversion to Liquid Fuels and/or Chemicals

Aviwe Hlaba

Supervisors:

Otolorin Adelaja Osibote and Oluwaseun Oyekanmi Oyekola

Declaration

I, Aviwe Hlaba, declare that the contents of this dissertation/thesis represent my own unaided work and that the dissertation/thesis has not previously been submitted for academic examination towards any qualification. Furthermore, it represents my own opinions and not necessarily those of the Cape Peninsula University of Technology.

Signed : Date :

Executive Summary

South Africa currently faces an energy security issue with regards to the country's rather insignificant petroleum reserves. The Fischer-Tropsch Synthesis process has found great application in converting the reserves available to products of economic value in terms of fuels and chemicals finding the adequate application at Sasol and Petro SA alike. However, in the realisation of the fact that coal is a high pollutant and natural gas reserves at a critical low with Sasol and Petro SA respectively, new innovations have become of critical importance. Solid waste management has become an ever-growing problem world-wide due to rapid urbanization and population growth. South Africa was found to have generated 9 million tons of general waste in 2011 with the Western Cape generating 675 kg/capita/annum. The convention of management has been that of landfilling however, this method is fast becoming insignificant due to the lack of space and detrimental nature to the environment. Considering the energy security issue South Africa is facing, and the global drive of finding alternate sources of fuel with the depletion of fossil fuel, attention has turned to MSW as a sustainable source of energy while remediating its effect on the environment. Thermochemical conversions of Municipal Solid Waste (MSW), this presents an attractive means of harnessing the potential value in this waste stream thus thermochemical conversion poses an attractive means of converting this waste stream into valuable fuel products.

In the realisation of the 2 problems of energy security and solid waste disposal, Biomass to Liquid (BTL) technology was found to be the most suitable to tackle these issues. BTL is an established process that uses the thermal conversion of biomass into various liquid fuels products through a series of technologies. MSW is highly heterogeneous which poses a processing challenge, unlike virgin biomass which is normally used in BTL technologies. The study investigated the production of high-quality syngas through an Aspen simulation of thermal gasification which would be suitable for liquid fuels and chemicals via Fischer-Tropsch synthesis to bridge the energy security issue in South Africa. As the study also possesses an environmental facet, it was necessary to assess the pollution load caused by the process of landfilling in terms of Heavy Metals and Radionuclides which will be determined by means of radionuclide analysis and heavy metal analysis. The procedures were accomplished by use of the gamma-ray spectroscopy, High Purity Germanium detector, (HPGe) and Inductively Coupled Plasma Optical Emission Spectrometry, (ICP-OES) methods.

The study was conducted by making use of Refuse Derived Fuel (RDF) pellets produced from the MSW. 4 Different binders in form of corn starch, guar-gum starch, waste palm oil and waste engine oil were used in the production of the pellets, thus the effect of this on energy content

and thermal degradation behaviour was studied. The energy content of MSW in Cape Town was investigated using a bomb calorimeter and the thermal degradation behaviour was studied using Thermogravimetric Analysis (TGA). The South African Government, through the National Development Plan of South Africa, aims to provide access to the grid and off-grid electrical power to a minimum of 95 % of the population by 2030, of which 20 GW of the required 29 GW required for this needs to come from alternative and renewable energy sources. This study using the MSW from the City of Cape Town Municipality in South Africa shows that the MSW has a calorific value of approximately 19 MJ/kg which is significantly high, meaning that the waste can be directly used as fuel in many applications but more importantly that of electricity generation. The calorific value for the pelletised waste was found to be higher at an average of 23.9 MJ/kg which can be compared with South African coal being 25.1 MJ/kg. Using TGA, 3 distinguishable major mass loss regions were found between temperatures 55 – 265 ℃, 270 – 410 ℃ and 410 – 502 ℃. The total sample reduction was found to be more than 90 % on average which is a reduction of the waste.

Heavy metals and Radionuclides (HM and R) are abundant in various types of municipal solid waste, including industrial waste, construction waste, medical waste, and household waste. Products containing HM and R are commonly disposed of in MSW or hazardous waste landfills and dumpsites. Approximately an average of 0.8 to 3 kg per capita per day of MSW is generated by suburban areas in South Africa. This method of managing or processing the waste has fast become inadequate and hence the need for new innovations. This has led to the focus on thermochemical conversion as an alternative. The soil is amongst the most considerable sources of radiation exposure to human beings and the migration for the transfer of radionuclides to the immediate environment. Exposure is a direct result of gamma-ray emissions that are produced by the most common terrestrial radionuclides, which are the member of the ^{238}U and ^{232}Th series and ^{40}K of which concentrations differ with respect to the type of soil and the geology of the area. Environmental pollution by chemicals and heavy metals such as Cd, Ni, Zn, and Pb etc., showed a great increase in recent times due to various industrial operations including that of MSW disposal. All heavy metals at high concentrations have strong toxic effects and are regarded as environmental pollutants.

Naturally occurring radionuclides activity was investigated at landfill sites from the City of Cape Town using a Hyper-Pure Germanium (HPGe) detector with appropriate shielding coupled to a Palmtop Multichannel Analyzer. Activity concentrations of the radionuclides ^{238}U, ^{232}Th and ^{40}K were obtained from the activity concentrations of their respective daughter radionuclides. To obtain the overall combined effect in terms of activity concentration from the 3 parent radionuclides, the radium equivalent was calculated and 38.273, 41.019 and 83.007 Bq/Kg were

obtained from Bellville, Coastal Park, and Vissershok respectively. Other radiological hazards in terms of Internal and External hazard indices and Representative hazard index were determined and found to be within safe limits. The dose rate in the air at 1m above the ground was determined to obtain a characteristic of the external gamma-ray and was found to be 17.490, 18.609 and 38.667 nGy/y for Bellville, Coastal Park, and Vissershok respectively. The health effects of the radiation in terms of annual effective dose and excess lifetime cancer risk were determined to be 0.031 mSv/y and 0.0961×10^{-3} which are lower than limits set by the United Nations Scientific Committee on the Effects of Atomic Radiation (UNSCEAR) and the Nuclear Industry Association of South Africa (NIASA).

The gasification part of the study was through process simulation models on ASPEN Plus Process simulation software. This investigation proposes a model of syngas creation from Refuse Derived Fuel (RDF) Pellet gasification with air in a fixed bed reactor. The model (utilizing Aspen Plus process simulation software) is utilized to model the anticipated results of RDF gasification and to give some processes fundamentals concerning syngas generation from RDF gasification. The fixed bed reactors are an updraft fixed bed reactor which can be divided into 3 sections which are drying, pyrolysis and gasification. The model is based on a combination of models that the Aspen Plus simulator provides, representing the three stages of gasification. Thermodynamics package used in the simulation comprised the Non-Random Two-Liquid (NRTL) model. The model works on the principle of Gibbs free energy minimization and was validated with experimental data of MSW gasification found in the literature. The RYield module was combined with the RGibbs module to describe pyrolysis section, while the RGibbs module was used for the gasification section individually. Proximate and ultimate analysis of RDF pellets and operating conditions used in the model are discussed. The sensitivity analysis module of Aspen Plus was used to research the effect of air equivalence ratio, ER and temperature value on the syngas composition, and carbon conversion. The results indicate that higher temperature improves gasification as the composition of H_2 and CO increase, as well as carbon conversion until a temperature of 900 ℃ and higher air equivalence ratio increases the carbon conversion while decreasing syngas quality as there is an increase in CO_2 and H_2. The most suitable binder for the gasification of RDF derived from MSW is maize starch, with the optimal process parameters for the production of syngas being that of temperature at 780 ^{0}C and airflow rate of 6 kg/hr which translates into a fuel-to-air feed ratio of about 1:2. Results obtained are in good agreement with the experimentally measured data in the literature.

This thesis is dedicated to my late father Mandlenkosi Welcome Hlaba (1939 – 2010) and my great mother Nomvuyiso Irene Hlaba

For their love, hard work, sacrifice, encouragement and never-ending belief in me and my dreams. They are the reason I am where I am today.

Acknowledgements

First and foremost, I would like to give thanks to my Heavenly Father God, for even giving me the opportunity to pursue this qualification as well as the strength and guidance he has bestowed upon me allowing me to complete my studies.

Thanks to my parents for all they have done in bringing me up and making sure I always have the opportunities to pursue everything that I have ever dreamt of in life. Without fail, you have always supported me without ever questioning my ambitions, even when you might have not fully agreed with some of my endeavours. You have never failed to stand by me.

A big thank you to my mother for remaining a strong pillar of support after the passing of my father. You made sure that the only pain we felt as your children were the grief of losing him. You worked hard to ensure we remained financially stable enough to continue and finish my university studies in pursuit of my dream of being a Chemical Engineer. You are my hero and I will forever be grateful to you.

My sincere gratitude to my academic parents, Dr Otolorin Adelaja Osibote and Mr Ademola Rabiu. As much as we have had our fair share of disagreements, especially with Dr Osibote, you have always found a way to make me pull through and deliver the goods. No matter how much I disappointed you and angered you at times, you never stopped believing in me and my ability to produce quality research deliverables. Through a very difficult time, you pushed me all the way to ensure that our work was completed and with top quality. Without your guidance and expertise, this dream of mine would have never materialised.

I would like to acknowledge the financial support given by the Deutscher Akademischer Austauschdienst and the National Research Foundation (DAAD/NRF) Scholarship towards this research. Opinions expressed in this thesis and the conclusions arrived at, are those of the author, and are not necessarily to be attributed to the DAAD/NRF.

Table of Contents

List of Notations

HM and R	Heavy Metals and Radionuclides
FBR	Fixed-Bed Reactor
ER	Equivalence Ratio
TGA	Thermo Gravimetric Analysis
ICP-OES	Inductively Coupled Plasma - Optical Emission Spectrometry
GC-MS	Gas Chromatography-Mass Spectrometry
MSW	Municipal Solid Waste
BTL	Biomass to Liquid
RDF	Refuse-Derived Fuel
FT	Fischer-Tropsch
CV	Calorific Value
LHV	Lower Heating Value
MHV	Medium Heating Value
HHV	Higher Heating Value
NRP	Non-Recyclable Plastic
η_m	Gasification efficiency (%)
H_g	Heating value of the gas (kJ/m^3)
Q_g	Volume flow of gas (m^3/s)
H_s	Lower heating value of gasifier fuel (kJ/kg)
M_s	Gasifier solid fuel consumption (kg/s)
HPGe	High Purity Germanium

FWHM	Full Width at Half Maximum
keV	Electronvolt
Eff'	Absolute efficiency at specific photopeak energy after attenuation correction
Eff	Efficiency prior to specific photopeak energy attenuation correction
μ(E)	Mass attenuation at a specific gamma energy E
ρt	Average sample mass per unit area.
A	Net peak area
LT	Live time
b	Branching ratio (gamma-ray emission probability corresponding to the photopeak energy)
m	Sample mass
Eff'	Absolute efficiency at a specific photopeak energy
Bq	Becquerel
Ra_{eq}	Radium Equivalent
H_{in}	Internal Hazard Index
H_{ex}	External Hazard Index
Iγr	Representative Level Index
I_{geo}	Geo-accumulation Index
ELCR	Excess Lifetime Cancer Risk

List of Tables

List of Figures

CHAPTER 1. INTRODUCTION

As predicted by the South African National Development Program, the nation's economic growth and energy sector will be promoted by means of adequate investment into the energy infrastructure by the year 2030 (National Planning Commision, 2012). Grid and off-grid availability of 95 % of the population according to the program shall be reached at least. Undisrupted economic activity will also be ensured by substantial electrical energy and liquid fuel supply for South Africa (National Planning Commision, 2012).

An additional 29 000 MW of electrical energy was deemed a necessity for the year 2013 in South Africa, of which 20 000 MW of that extra power was proposed to need to come from renewable energy sources in the place of coal as reported in the plan (Department of Energy, 2015). "Load Shedding", is term or name given to a relief strategy implemented by the Electricity Supply Commission (ESKOM) to try and mitigate the imbalance of demand to supply of electrical power in South Africa. The strategy induces planned power cuts in order for ESKOM to be able to cope with the load requirements, necessitating the need of energy security for current and upcoming advancements in technology (Department of Energy, 2015).

The Department of Energy (DoE) aims in South Africa, respectively, at making a complete change in the energy sector through uniform approach, through a secure and balanced energy mix of stable and well-regulated electricity supplies and demand. In view of reducing the carbon emissions of energy and other industrial activities, the implementation of policies to mitigate climate change, particularly under the Paris Agreement on Climate Change, has become of paramount significance to the DoE (Department of Energy, 2015, Rogelj et al., 2016).

Municipal Solid Waste (MSW) is a solid waste created through the disposal of publicly used products of general daily use. Cape Town Municipality's annual waste generation figures are 1.9 megatons as recorded on the website of the City (City of Cape Town, 2009b, Department of Environmental Affairs and Tourism, 2012, Engledow, 2007). In 2011, 59 million tons of general waste was produced in South Africa, of which 5,8 million had been recycled, while 53,2 million remainings were disposed of as shown by the modelled results (Department of Environmental Affairs and Tourism, 2012).

The composition of general waste in South Africa as contributed by industrial, commercial and household waste streams can be represented in terms of 6 % plastic, 7 % paper, 4 % glass, 1 % tyres, 13 % organic waste, 21 % construction and demolition waste, and 34 % non-recyclable municipal waste.

Landfilling is the most highly used mechanism of waste disposal in the majority of developing countries due to the low cost and convenience it presents regardless of the environmental shortcomings that stem from it (Adefeso et al., 2012, Adesuyi et al., 2015, Aucott, 2006, Odukoya and Abimbola, 2011). The average waste disposal in the world is 85 per cent, while more than 95 per cent is disposed of using the landfill system in South Africa alone (Department of Environmental Affairs and Tourism, 2012, Department of Water Affairs & Forestry, 1998). Landfills pose adverse short and long-term effects on the environment, especially when they are not adequately operated and managed. Short term effects include air pollution, noise, the wind scattered litter, unpleasant odour and flies, while the long-term effects pose a much more adverse threat to human, plant and animal life in the fact that landfills may pollute groundwater sources through leachate and landfill gas generation (Adefeso et al., 2012, Ademola et al., 2015, Adesuyi et al., 2015, Aucott, 2006).

In light of these and many other negative environmental factors posed by landfilling operations, it is then clear, the importance of the production of renewable energy sources such as RDF as they effectively solve the problem of obtaining renewable and sustainable energy sources and also lessen the negative effects posed by landfilling operations to the environment.

Heavy metals and radionuclides (HM and R) are commonly found in a range of urban solid waste, including industrial waste, building material, medical waste and home waste. The heavy metals include mercury, lead and cadmium. The metals are purposely added to certain consumer and industrial products, namely batteries, switches and in certain pigments. Products containing heavy metals and radionuclides are commonly disposed in MSW or hazardous waste landfills and dumpsites (Aucott, 2006). Weak landfill siting, design and operation were one of the historic problems with municipal waste disposal which have adverse consequences on the quality of life of surrounding residents and the immediate environment (Department of Environmental Affairs and Tourism, 2006). If ill-managed, leachates from landfills percolate into the underlying soils of the landfill site. This can cause contamination of the food chain due to the fact that soil acts as a sink for heavy metals which have the ability to migrate towards a column of water or accumulate in plants (Odukoya and Abimbola, 2011). In particular, the method of landfilling as a disposal mechanism for MSW is increasingly recognized globally as an unsustainable waste management method. With many cities in the world, waste-to-energy (WTE) engineering is increasingly getting positive recognition. These can be categorized as biotechnology/chemical, physical and thermal.

The main characteristic of Biological/Chemical technologies is low-temperature operations of under 200 °C which have a low reaction rate since the response rate is directly proportional to

the reaction temperature (Fogler, 2006). These innovations include the manufacture of products in multiple phases by physical chemistry and chemical processes. Compost, chemicals and electrical energy are amongst a wide variety of obtainable by-products.

The changes in the organic fraction of the MSW feedstock are addressed by Physical Technologies. These organically-based materials can be separated, shredded and dried to formally produce materials called waste-based fuel (RDF). This fuel can be used as densified or pelletized homogeneous pellets for thermal technology.

In contrast to organic/chemical technologies, thermal technologies work at much higher temperatures between 400 and 5000 °C (Fogler, 2006). The key by-product of currently most applicable thermal technologies is usually electricity. Thermal technologies include advanced combustion, incineration, pyrolysis and gasification thermal conversion processes. The goal is to identify and optimise an existing gasification process for MSW to obtain the maximum achievable yield of syngas. This will be done while taking into consideration the environmental impact of the gasification process in terms of the heavy metal content in the ash residual and possible heavy metal contamination in the product syngas. The syngas product will be analysed to determine suitability for Fischer-Tropsch synthesis in terms of the H_2/CO and heavy metal contamination. A suitable syngas product would then ascertain an alternative measure of treating MSW rather than the landfilling practice while obtaining worth from the process in terms of fuels and/chemicals.

1.1 Background and Motivation

South Africa currently faces an energy security issue with regards to the country's rather insignificant petroleum reserves. The Fischer-Tropsch Synthesis process has found great application in converting the reserves available to products of economic value in terms of fuels and chemicals. In the production of petroleum syngas, Sasol uses coal gasification. However, because of its polluting nature, coal is a rather "dirty" source of fuel. Nevertheless, the stocks are small in Petro SA's process of converting natural gas into liquid fuel. On the other hand, MSW offers a sustainable source of raw material, non-exhaustible and non-seasonal for this process. The Treasury estimates averaging 0.8-3 kg per person per day of solid waste in a South African suburban area. This is quite a significant amount if all the MSW participants in a certain state, city or metropolitan area are included. About 1.9 megatons of waste are made annually in the city, as reported on the website of the City of Cape Town Municipality. MSW management approaches in most developing countries are most commonly applied by means of incineration, combustion and other forms of disposal in the form of glass and plastic recycling. The primary focus of this study will be to optimize the operation of an effective

reactor in MSW gasification to obtain total syngas yield suitable for further processing in order, by means of the Fischer-Tropsch synthesis, to obtain fuels and/or chemicals. This system will then analyse the environmental impact relative to that of the convention on waste disposal, with respect to the heavy metal content of the material gas and the ash content of the thermochemical process. As part of the environmental assessment, radionuclide analysis will also be conducted on the landfill soil samples as to give an indication of the effect that landfilling practices have on natural background radiation Radionuclide analysis of the soil samples will be carried out by means of the gamma-ray spectroscopy method. Inductively Coupled Plasma Optical Emission Spectrometry (ICP-OES) will study the heavy metal content of the ash residual from the gasification.

1.2 Problem Statement

Biomass to Liquid (BTL) is an established process that uses the thermal conversion of biomass into various liquid fuel products through a series of technologies. However, unlike virgin biomass, MSW is highly heterogeneous which poses a processing challenge. There are also many compounds in MSW that will adversely affect the catalyst performance and processing equipment. This study will investigate different process conditions and feed characteristics to maximize the yield of syngas using a simulation generated from Aspen Plus. Heavy metals and Radionuclide analyses will be conducted on landfill soil samples to assess the effect the current landfilling practice of solid waste disposal on the environment.

1.3 Aims and Objectives of the Study

The study will investigate the production of syngas by means an Aspen Simulation of thermal gasification which would be of adequate quality for liquid fuels via FT synthesis and/or chemicals production i.e. methanol, to bridge the energy security issue in South Africa. An environmental assessment will be conducted to assess the pollution load of the current waste disposal practice of landfilling to emphasise the importance of finding alternative means of waste processing. This will be achieved via the following objectives:

1) Investigate the pollution load of the landfilling process in terms of HM and R levels.

2) Aspen Simulation of syngas production through MSW gasification using a known process.

3) Optimisations of the gasification system in order to maximize the yield of syngas. These include feedstock characteristics, gasification temperature and air flowrate.

1.4 Research Questions

1) What is the environmental impact of the current waste disposal method of landfilling in terms of the HM and R level?
2) What are the optimal conditions (feedstock characteristics, gasification temperature and airflow rate) to maximise syngas yield?
3) What is the composition of the product gas from the gasification process?
4) Is the H_2/CO ratio adequate in accordance with FT Synthesis for fuel production or chemical product (methanol)?

1.5 Scope of the study

The type of thermochemical conversion process that will be considered is that of an Aspen Simulation for thermal gasification of MSW-RDF pellets to produce the syngas. This thesis will focus on the optimisation of the gasification process parameters (feedstock characteristics, gasification temperature and airflow rate) for the maximum yield of a syngas product that would be suitable for liquid fuels via FT synthesis and/or chemicals production i.e. methanol, in terms of H_2/CO ratio.

1.6 Significance of research

The outcomes of this research will provide a much-needed understanding of the thermochemical conversion process MSW as an alternative means of processing the already environmentally detrimental waste stream other than the current method of landfilling. It will contribute towards the current global drive of obtaining alternate sources of energy other than fossil fuels. The research will provide insight in terms of the optimum process parameter requirements for the maximum yield of a syngas product that would meet the requirements of the Fischer-Tropsch Synthesis process to produce fuels and/or chemical i.e. methanol. This, in turn, will contribute towards reducing or even eliminating the negative environmental aspect of solid waste management in terms of the pollution load caused by the heavy metals and radionuclides (HM and R) present in the MSW which is currently disposed of by landfilling.

1.7 Thesis delineation

This thesis will focus on the optimisation of process parameters required for the maximum yield of syngas by means of thermal gasification of MSW-RDF pellets. The environmental analysis will also include heavy metal and radionuclide analysis of the landfill soil. Fischer-Tropsch Synthesis will not be done however, the product syngas from the gasification process

will be analysed to see if it will meet the requirements for FT-Synthesis for fuels and/ or chemicals i.e. methanol, production in terms of H_2/CO ratio obtained from the simulation process.

1.8 Thesis outline

Chapter 1 is an introductory chapter which describes what municipal solid waste is and current management and disposal methods thereof. In this chapter, the concept of Waste-to-Energy research is introduced and a general overview of current methods and technologies available. The chapter includes a problem statement the describes the current state of affairs in South Africa in terms of energy supply deficiencies and solid waste disposal as well as how the project will be able to combat both problems at once. The aim, objectives and research questions are detailed in this chapter explain how the project will address the issues described in the problem statement.

Chapter 2 is a literature review chapter which discusses what MSW is as well as the current method of disposal in South Africa and the Environmental impacts them stem from this method. The chapter also discusses how MSW can be used as an alternative source of fuel in incineration processes or as a direct fuel for furnace operations. The BTL process is also discussed in terms of current industry trends as well as how the process can be applied for MSW in processes like pyrolysis and gasification.

Chapter 3 focuses on the environmental issues associated with MSW and its disposal in landfills. The chapter discusses heavy metal and radionuclide analysis. The procedures used as well as results and conclusions obtained from these analyses are discussed in this chapter gives an overview of how current MSW disposal in South Africa affects the environment.

Chapter 4 discusses the Biomass to Liquid or BTL process and how it can be applied as an alternative treatment for MSW alleviating the negative environmental impact stemming from its disposal while addressing the energy crisis in South Africa. The stages of RDF pellet production are discussed as well as the necessary characterisations with the methods used and their results obtained thereof. Calorific value determination, TGA and proximate analysis are the analyses discussed in terms of RDF production. This chapter also discusses the gasification simulations conducted on Aspen Plus and the results obtained thereof including conclusion and recommendations.

Chapter 5 is the general conclusion and recommendations from the overall project in terms of all the results obtained and how they impact the on the significance of the study. This

chapter concludes on how the research questions were answered and to what degree were they successful in achieving the set objectives.

CHAPTER 2. LITERATURE REVIEW

2.1 Municipal Solid Waste

Municipal solid waste (MSW) is a general waste that includes everyday items that are publicly disposed of and also known as litter, garbage, and waste. The municipality of Cape Town estimates that townships generate about 1.9 megatons of waste every year (City of Cape Town, 2009a, Department of Environmental Affairs and Tourism, 2012, Engledow, 2007). System waste data show that South Africa as a whole created 59 million tons of general waste in 2011 (Department of Environmental Affairs and Tourism, 2012). Recycling operations were projected at only 5.8 million tons, with a balance of 53 million tonnes.

2.1.1 Composition of MSW

The composition of South African general waste, as contributed by manufacturing, industrial and household waste sources, can be expressed in plastic, paper, glass, rubber, organic waste, building and demolition waste and non-recyclable municipal waste. Pulp, plastics, glass and pneumatic were the main recyclables.

Table 2-1: Modelled Waste Data (Department of Environmental Affairs and Tourism, 2012).

General Waste 2011	**Generated**	**Recycled**	**Disposed**	**Recycled**
	1×10^6 Tonnes			%
Municipal waste	7.88	-	7.88	0
Organic waste	2.95	1.03	1.92	35
Construction and demolition waste	4.73	0.756	3.97	16
Paper	1.69	0.966	0.728	57
Plastic	1.28	0.230	1.05	18
Glass	0.938	0.300	0.637	32
Metals	3.12	2.49	0.624	80
Tyres	0.247	0.00987	0.237	4
Other	36.2	-	36.2	0
Total general waste [T]	59.0	5.79	53.2	10

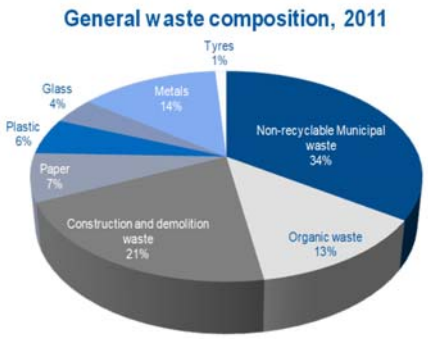

Figure 2-1: The waste composition for general waste, 2011 (percentage by mass) (Department of Environmental Affairs and Tourism, 2012)

Back in time, only a few characterization studies have been carried out regarding the composition in the MSW, especially in Cape Town and Gauteng Province of South Africa. In relation to the natural portion of the product, it can be divided into putrescible, green and garden waste. Nonetheless, the creation and classification of the streams as agricultural waste means that Cape Town alone is very similar to the Gauteng region.

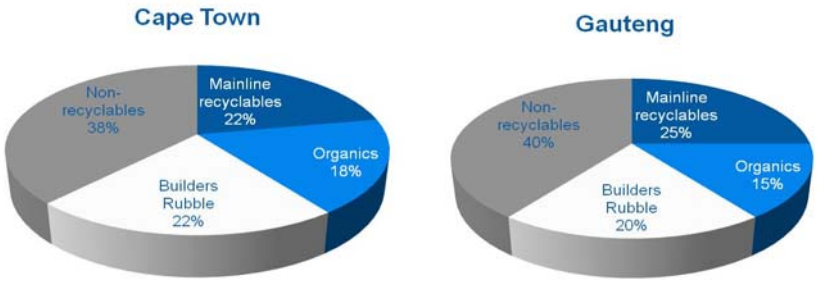

Figure 2-2: Municipal waste composition (Percentage by Mass) (Department of Environmental Affairs and Tourism, 2012)

2.2 MSW Management

Burning and depositing in landfill sites is widely used for handling MSWs in most developing countries, with reuse of glass and plastics. Nonetheless, these approaches are inherently ineffective and endanger the environment, public health, air quality, land, and groundwater. (Adefeso et al., 2012). In general, the landfill industry is increasingly regarded as an inefficient waste management system because of its negative environmental effects as regards pollutants. (Adesuyi et al., 2015, Aucott, 2006, Department of Environmental Affairs and Tourism, 2006, Odukoya and Abimbola, 2011).

2.2.1 Landfilling

A waste dump or landfill is an area or piece of land allocated for waste storage by methodology (Gdp, 2003). The word landfilling applies to the removal of waste on land, whether by means of excavation filling or over - the-ground construction, whereby the term filling is used only in the technical sense. Because the waste disposal process is the simplest and most convenient, waste has traditionally been disposed of on land (Department of Water Affairs & Forestry, 1998). It is estimated that more than 95% of the waste produced in South Africa is disposed of via landfill, whereas the total figure is estimated at more than 85% (Department of Environmental Affairs and Tourism, 2006, Department of Water Affairs & Forestry, 1998). Either recycling through resource recovery or through volume reductions, regardless of any strategies to reduce waste, some kind of residual waste remains, and waste is created on an ongoing basis. Figure 2.3 shows the role of a landfill site as the primary means of disposal in a waste management process. Deposits which are not controlled can, in the short and long term, have adverse effects. Short-term consequences can include noise, flies, odour, air pollution, unsightliness and wind scattered litter. Problems like water pollution and waste gas production have long-term effects (Adefeso et al., 2012, Ademola et al., 2015, Adesuyi et al., 2015, Aucott, 2006, Department of Water Affairs & Forestry, 1998). The long-term effects are normally caused by wrong site selection, development, planning and/or operation.

The municipal district of Cape Town consists of a solid waste management system that collects, cleanses areas and disposes of waste in the municipal area of Cape Town. The main objective of this city division is to incorporate waste management systems in a manner that not only provides basic services but minimizes the environmental impact of waste and increases the related economic activity (City of Cape Town, 2009a). A waste management system similar to the one shown in Figures 2-3 is run by the municipality of Cape Town. The individual or organization shall temporarily store all waste generated in large bags or reject bags in order to wait for municipal workers to collect it on specific days. Waste is collected from the various areas and transported to nearby waste sites nearest a particular area or the larger transportation stations. Individuals and residents may drop their waste and must not wait until the city collects it. Residents are able on any day of the week to drop bulky garages or garden waste, builders 'scrap or recyclable. One can freely drop a maximum load of 1.5 tons of non-hazardous waste. There are currently 25 drop-offs operating in the city. Selected waste disposal systems are able to accept special waste for recycling which fall within the recovery/treatment section such as used motor oil and metals and canned waste, cardboard, paper and polystyrene, as well as electronic waste (e-waste). In the case of widely moving distances between internal and external waste collection networks, the transfer station facilities

will then be used to unload waste. The waste is then compacted into containers of approximately 20 tons each and transported to the dumpsite by road or rail. Cape Town currently operates three transfer stations: Athlone, Swartklip and the Integrated Waste Management Facility of Kraaifontein (City of Cape Town, 2009a). Approximately 50 and 40 containers are transported by rail and road to the Vissershok site at Athlone and Swartshaklip transfer stations. Kraaifontein's Integrated Waste Management Facility functions more than just a transfer station, as it is also fitted with a recycling facility, material rehabilitations system and waste transfer station. The chipping system for garden waste can be used in this facility and at other drop-off sites and then transferred to the composting industry. Waste collected and deemed recyclable will be sorted, segregated, baled and then sold by a vendor. Eventually, waste considered non-recyclable and waste not processed at transfer stations such as hazardous waste, medical waste, sludge and heavy loads of debris from developers are sent to landfills. Cape Town currently has three Vissershok, Bellville and Coastal Park operational landfills. The City of Cape Town embarked on the construction of another Integrated Waste Management Facility at the Bellville landfill site in 2015, operating in the same manner as the Kraaifontein facility.

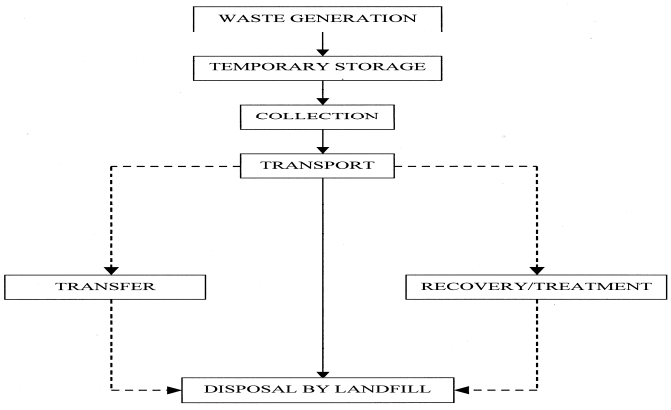

Figure 2-3: Schematic of how waste management works on a general basis (Department of Water Affairs & Forestry, 1998).

2.3 MSW as Alternative Source of Fuel/Energy

2.3.1 Calorific Value

The heat value or energy value for any material, food or gas is usually the amount of energy resulting from the total fuel combustion of the substance with units of energy by unit volume or by unit mass. Generally, the standard CV expression units are MJ / kg, of which the SI units or in English units are Btu / lb. The CV of fuel would depend on an assumption in the ultimate combustion products concerning water molecules. The highest heating value (HHV) is referred

to as if the water is condensed from combustion products. This condensation accounts for the entire fuel heating quality, including reactive heat and latent heat. When the air in the final combustion products is vaporised, the steam is not reduced into liquid water, so that latent heat is not absorbed by it, then it is called the lower heating value (LHV).

The CV of fuel is usually measured by experiments using a device known as a bomb calorimeter in HHV conditions. In an oxygen-rich environment, the machine burns in a sealed vessel a small amount of fuel. The calculation of the Calorific Value is then quantified by the product of the fluid mass multiplied by the specific heat of the fluid, which is then multiplied by the difference in temperature (net increase). The resulting calorific value for the fuel being analysed is known to be collected at a constant volume, following that the fuel has undergone the process of combustion in a vessel with a fixed or set volume vessel (Digital Data Systems, 2010, Parr Instrument Company, 2007).

As a general rule, the calorific value of ordinary MSW may be approximated to be 20 MJ/kg, with the exception of scenarios whereby the MSW bulk composition consists of 1 substance in majority such as polyethene, which has approximately double the energy content of MSW (Rand et al., 1999). According to Zafar (2015), the calorific value of raw MSW in the Saudi Arabia region is approximately 4.18MJ/kg and between 8 – 11 MJ/kg in the United Kingdom as reported by Department for Environment Food & Rural Affairs (2013). Studies conducted in Changzhou and Guangzhou in China show raw MSW of 3 to 4 MJ / kg, while Italy has reports of 10 to 4.8 MJ / kg and 10.5 to 16.17 MJ / kg respectively in Kuala Lumpur, Malaysia and Parona (Zhang et al., 2008). The difference in calorific value is attributed to the abundance of certain materials as mentioned earlier in the instances where the energy content is higher, and lack of it where it is lower. These substances are also referred to as non-recyclable plastics, NRP's. Table 2.2 shows in detail the energy content in their respective constituents.

Table 2-2: Calorific Value of non-recyclable plastics (NRP) broken down into the different constituents that make up the material (Themelis and Mussche, 2014)

Materials	**% in NRP**	**MJ/kg**	**MJ/kg NRP**
Polyethylene terephthalate (PET)	12.4%	24	2.93
High density polyethylene (HDPE)	17.8%	44	7.76
Polyvinyl chloride (PVC)	5.5%	19	1.05
Low density polyethylene/ Linear low-density polyethylene (LDPE/LLDPE)	19.6%	28	5.39
Polypropylene (PP)	13.9%	44	6.08
Polystyrene (PS)	8.70%	41	3.56
Other	22.0%		5.55
Total NRP	100%		31.96

2.3.2 Incineration

Incineration is a waste treatment process that involves the combustion of the organic portion of waste material (Knox, 2005). Combustion is a chemical reaction when oil, primarily fossil fuel, responds to heat by oxygen in the air (Himmelblau and Riggs, 2012). In fossil fuel, the heat released is used to power boiler, furnace, oven, the internal combustion engine and other operating equipment. Combustion is an exothermic reaction that is formed in combination with fire, carbon dioxide and air. As combustion is a chemical reaction, it can be described by 2.1 to 2.3 reactions (Bairnes, 2013)

$$\boldsymbol{CH_4 + 2O_2 \rightarrow CO_2 + 2H_2O + HEAT} \quad (2.1)$$

$$\boldsymbol{C + O_2 \rightarrow CO_2 + HEAT} \quad (2.2)$$

$$\boldsymbol{CH_4 + 2O_2 \rightarrow CO_2 + 2H_2O + HEAT} \quad (2.3)$$

The sole purpose of combustion is to burn fuel to retrieve energy in the most efficient mannerism possible. To achieve a high level of efficiency, it is essential to ensure that all the fuel burns with minimal to no losses. System efficiency is directly proportional to the amount of energy obtained and equal to system costs.

Complete combustion ensures that 100 % of the fuel energy is obtained if full burning takes place (Himmelblau and Riggs, 2012). Only by adding excess air into the combustion process will total combustion be assured. Excess air increases the quantity of oxygen and nitrogen in

the flame, increasing the chance of oxygen mixing with the gas. With the introduction of additional heat, turbulence increases, and the combustion cycle improves. Better mixing of fuel and air improves combustion efficiency by increasing reaction chances between the two materials. Excess air has its positive characteristics since it limits the amount of carbon monoxide produced, but the drawback is that it often causes more heat losses, and it is therefore important to regulate, and track, excess air carbon emissions so that the combustion process is as efficient as possible. Time, temperature and turbulence is a major factor of the combustion process. Over time, it is vital that the fuel is allowed to burn enough time in order to prevent large quantities of energy from being left in the oil. Long periods, however, lead to long flames which inevitably lead to improper mixing. With the correct time balance and mixing as a result of turbulence, complete combustion is achieved, flame retardation is minimized and combustion safety improves. For decades energy recovery from urban solid waste has been applied in its simplest form. The combustion or incineration of waste such as wood boards and various household goods was the first energy recovery method of waste solely for the purpose of heating (Lee, 1996). This waste incineration technology formed the basis for the recovery of energy from MSW in modern times. Burning transforms solid waste into heat, flue gas and ash. The combustion of 1.5 million tons of MSW generates 15% of the district heating needs in Sweden (Rand et al., 1999).

In the cement industry, MSW also finds use as a fuel. Cement is extremely fossil-fuel based and accounts for around 5% of the world's current anthropogenic carbon dioxide emissions (Hasanbeigi et al., 2012). MSW is a world-wide validated energy recovery process, but due to the existence of poly-vinyl chlorides (PVC), most environmental concerns arise at low temperatures. The average temperature of the raw material in a cement kiln increases to 1,450 °C and the raw material fuses into small clinker pellets. The high-temperature process of clinker production then resolves environmental concerns (Hasanbeigi et al., 2012, Patel and Chauhan, 2014). The worldwide production is projected to grow from about 2.540 million tons (Mt) in 2006 to between 3.680 Mt (low estimate) and 4.380 Mt (high estimate) in 2050. Cement demand and production are projected to increase in 2006. In China, India, and other Asian developing countries the largest share of this development will be achieved. The significant increase in cement production is related to the significant increase in total energy consumption and CO_2 emissions in the sector. The use of alternative sources can contribute towards reducing the rapid rate of depletion of fossil fuel supplies and also help reduce CO_2 emission from the industry if alternative fuel includes lower carbon emission factors or biomass (Hasanbeigi et al. 2012).

In combustion, fuel from waste can also be used for the generation of electricity or combined heat and power, also abbreviated as CHP (Department for Environment Food & Rural Affairs, 2013). The probability of using an incineration plant for power production depends on whether customers can use the available power. In most cases, electricity is easily shared across the national grid to end-users. The heat produced by an incinerator can be used to heat up a boiler as a furnace fuel to generate steam that can then be used to power a turbine to produce electricity. The average net energy supply per ton of municipal waste is approximately 2/3 MWh of electricity and 2 MWh of district water (Reno Sam & Ramboll 2006). Therefore, burning about 600 metric tons (660 short tons) of electricity per day produces approximately 400 MWh (17 MW of power constantly 24 hours) of electricity per day and 1200 MWh of heating energy every day.

2.3.3 Pyrolysis

Pyrolysis is defined as the thermal degradation of organic materials in the absence of oxygen. Pyrolysis is an old process of oil-producing, known as pyrolytic oil since it is a well-known thermo-chemical technique. The oil is a mixture of organic chemicals and water. The other components of the pyrolysis cycle include oil, gas and solid char (He et al. 2010). As a general overview, two features of the system of pyrolysis can be identified. For optimizing the yield of the fluid material, the first one called the flash pyrolysis is important. The second, known as modern or traditional pyrolysis, is used to optimize gas yield. The traditional form is the commonly preferred method for high-temperature conditions at low heat, long gas resistance and catalyst presence (He et al., 2010). Traditional pyrolysis is also favoured when solid char production is at the forefront.

He et al. (2010), using a fixed bed reactor downstream at a temperature ranges of 750 to 900 ° C, and calcined dolomite as a catalyst, have investigated bench output using pyrolysis. The existence of the dolomite catalyst had a major impact on the development of material and gas composition, and important catalytic performances on an increase in gas yield and lower oil yield and carbohydrate compared to non-catalytic processes were demonstrated. Higher temperatures lead to higher MSW conversion and substantially higher H_2 and CO levels into syngas output. Because Fischer–Tropsch synthesis for the production of transport fuel, syngas from MSW pyrolysis is highly desirable, it can also be used as a fuel, with a lower heating content of 13,87 MJ / N m^3, directly as a medium heating value (MHV) fuel. A Columbia University study showed that the oils obtained from a system of fast pyrolysis mainly contain 10 compounds, namely benzene, toluene, styrene, limonene, 2,3-dimethyl-1-heptene, benzoic acid, ethylbenzene, indole, xylene and d-allose. (Kwon et al., 2010). The study was performed

using a reactor with a marginal heating speed of 800 °C/min. The presence of CO_2 was shown to significantly decrease the oil products while the presence of hydrocarbons containing 1 carbon (C1) to 5 carbons (C5) was found to significantly increase in the gaseous and non-condensable phases. The pyrolysis effect of particle size has been studied using a fixed bed reactor at a temperature of 800 °C (Luo et al., 2010). Samples of 0–5 mm, 5–10 mm and 10–20 mm were analysed in sizes. The results show that the smaller the particle size, the greater the gas production with less charcoal and tar. It was also found that a smaller size of particles also can increase the CO, H_2 and ash and carbon content of the carbon dioxide.

2.3.4 Gasification

In synonymous nature to combustion, gasification is a thermal process that makes use of high temperatures to break down fuel, usually in the form of waste (Friends of the Earth, 2009). The main difference in both processes is the use of less oxygen than conventional combustion methods for the gasification process. In a more technical definition, the thermal conversion of organic products at high temperatures and reduced conditions can be defined as the main processing of permanent gases with smaller products such as char, water and condensing gas. The resulting gas compound is called syngas by a gasification system (Breault, 2010). Essentially, gasification is a cycle between the above-mentioned combustion (thermal oxygen degradation) and pyrolysis (thermal degradation when oxygen is missing) (Niu et al., 2014). Solid fuel is typically made up of carbon, oxygen and hydrogen. However, nitrogen and sulphur may be a contributory factor but in small amounts (FAO Forestry Department, 1986). The solid fuel is warmed by the combustion of a fraction of the fuel during conventional gasification processes. In order to achieve reduction, the combustion gasses are then transferred to a bed of fuel at high temperatures. The reactions in the combustion section are listed for this stage. The water vapour and carbon dioxide are converted to carbon monoxide, hydrogen and methane, the main component of which is the fuel source gas in all gasification processes (FAO Forestry Department, 1986). Like any chemical reaction, gasification can also be shown by reaction equations and the most significant reactions in the reduction zone are shown in the following way (Breault, 2010):

$$\boldsymbol{C + CO_2 \leftrightarrow 2CO \ \ (+164.9\frac{kj}{mol})} \tag{2.4}$$

$$\boldsymbol{C + H_2O \leftrightarrow CO + \ H_2(+122.6\frac{kj}{mol})} \tag{2.5}$$

$$\boldsymbol{CO + H_2 \leftrightarrow CO + H_2O \ \ (+42.3\frac{kj}{mol})} \tag{2.6}$$

$$\boldsymbol{C + 2H_2 \leftrightarrow CH_4 \ \ (0\frac{kj}{mol})} \tag{2.7}$$

$$\boldsymbol{CO + 3H_2 \leftrightarrow CH_4 + H_2O\ (-205.9\frac{kj}{mol})} \quad (2.8)$$

As mentioned earlier, the initial steps of the gasification process are described by combustion, thus, the above equations commence from that step. Equations (2.1) and (2.2) describe the core reactions in reduction and the energy of the reactions show that they require heat, thus, this will result in reduced gas temperature during the reaction (FAO Forestry Department, 1986). Reaction (2.6) defines the equilibrium between water and gas. The value of the equilibrium constant water gas (K_{WE}) is determined for each temperature by the ratio between, in principle, the product of carbon monoxide (CO) and water vapour (H_2O) concentrations to the product of carbon dioxide (CO_2) and hydrogen (H_2). Throughout fact, the composition of balance of the gas is only accomplished in the case of an appropriate reaction rate and time. The reaction rate decreases with the dropping temperature. The reaction rate is so low below 700 ° C for the water-gas balance that the mixture is said to be "frozen."

The gas composition then remains unchanged. In order to convert the carbonaceous materials into gaseous products, the gasification process uses an agent which can be air, oxygen, hydrogen or even steam(Sadaka, 2015).

Air Gasification

This is the simplest gasification process since air is the gasifying agent. In excess character formed by pyrolysis in the reactor, a low supply of air is combusted (usually at an equivalence ratio (ER) of 0,25) (Sadaka, 2015). Nonetheless, the gas is a low energy material and consists of primarily air-diluted hydrogen carbon monoxide. The heating value of the gas varies from 3.5–7.8 MJ / Nm^3, which in turn makes it ideal for applications in engines and boilers. The reactor temperature depends primarily on the feedstock level and the airflow rate since air is the gasification agent. Low bed temperatures are a direct consequence of extremely low inlet air into the system causing lower gas production and increased tar yields.

Oxygen Gasification

The amount of nitrogen introduced into the system must, therefore, be kept to a minimum, to ensure that a consumer gas that can be transported efficiently within a pipeline network and that in turn can easily find applications for process energy or even a synthesizer gas that can be used to produce chemicals and fuels. It means that the material gas has no nitrogen traces so that this principle is viable (Sadaka, 2015). An oxygen supply or plant nearby would make this possible, but the required installation costs could be raised. Niu et al. (2014) stated that the gas evolution characteristics showed that H_2 and CO formation are directly proportional to temperature, although inversely proportional to CO_2 and CH_4 outputs. This study was

conducted by MSW in four waste materials, namely paper, wood, textiles and kitchen waste that were individually oxygen-gasified in a fixed bed reactor (FBR). Temperature between 700 and 900 °C and ER range 0.14–0.32 have been investigated for LHV, the yields of products char, tar, gas and the composition of gas elements. The LHV of the syngas produced was found to be within a range of 6–10 MJ/m^3 with a specific temperature proportionality of up to 800 °C (Niu et al., 2014). The fuel gas components and LHV of syngas decreased as the ER increase increased, while the CO_2 production increased linearly. The correct ER was recorded for the range of 0.18 to 0.23 for high-quality syngas. Higher ER and temperature are more suitable in fabric and garbage gasification for higher gasses and lower tar and char levels.

Hydrogen Gasification

The feedstock is gasified under high-pressure conditions in the presence of H_2. In this process, it is crucial for most products in the gas phase to maintain strict reaction conditions. This process is less desired to the required level of control and hydrogen needs to be readily available (Niu et al., 2014). An increase in temperature from 426 to 760 °C increased CO and hydrocarbon gases from (8 % to 18 %) and (4 % to 63%), respectively as reported by Weil et al. (1987). The pre-heated hydrogen mixture with peat was tested at the entry point of a fluidized bed reactor. The gasifier was run in an isothermal heating mode as an induced flow reactor.

Steam Gasification

In comparison to air gasification, steam should be the sole gasification agent, an external energy source is needed for steam gasification (Niu et al., 2014). Air and steam mixture is also common practice for gasification agents, as the combination contributes to supplying the necessary energy because of the exothermic nature of the burning biomass. This will benefit from high temperatures through the devolatilization cycle of bio-mass to create specific gases. Steam reacts with CO in order to create H_2 and CO_2, which is referred to as the reaction of water-gas shift. Steam gasification produces a more energy-intensive supplier gas in comparison with air. A study by He et al. (2010) on the catalytic steam gasification of dolomite as the catalyst shows that the calcination of dolomite is better than natural dolomite. The presence of steam meant that tar was completely decomposed by an increase of the temperature from 850 °C to 950 °C. A bench-scale downstream FBR was used in this study for MSW gasification. The purpose of the study was the investigation of the effect of catalyst and reactor temperature on the yield of syngas where the composition of the material was investigated in a 750-950 °C, at a steam-to-MSW ratio of 0.77 and at a weight hourly rate of 1.29 h^{-1} (He et al., 2010). High temperatures have led to an increase in the output of H2 and

CO, increasing efficiency in carbon conversion and dry gas yield. MSW was shown to be within the range of 36.35-70.21 mol% for catalytic steam processing types where char had the highest ash content at 950 °C of 84.01%. The contents are determined to be negligible for hydrogen, nitrogen and sulphur.

Gasification Efficiency

When it comes to the determination of the technical operation and economic feasibility of a gasification process, it is paramount to determine the process efficiency (FAO Forestry Department, 1986).

$$\boldsymbol{\eta_m = \frac{H_g \times Q_g}{H_s \times M_s} \times 100} \qquad (2.9)$$

Where:

η_m : gasification efficiency (%)

H_g : heating value of the gas (kJ/m^3)

Q_g : volume flow of gas (m^3/s)

H_s : lower heating value of gasifier fuel (kJ/kg)

M_s : gasifier solid fuel consumption (kg/s)

Gasifier Types

Regarding the fact that in a gasifier, there is an interaction between the gasification agent and the fuel, the gasifier types are named according to the manner in which the gasification agent is introduced to the reactor vessel. There are 3 fundamental types of gasifiers namely, updraught, downdraught and cross-draught (E4tech, 2009, FAO Forestry Department, 1986, Rajvanshi, 2014).

The updraught gasifier depicted in Figure 2.4 below is supplied with fuel from the upper part, and gasification agent intake is at the bottom of the reactor (Rajvanshi, 2014). The gas product transports tars and volatility produced by the gasification process and leaves the material atop the reactor (E4tech, 2009, FAO Forestry Department, 1986). Ash is collected from the grate on the reactor bottom. Combustion reactions occur in the vicinity of the grid at the end of the reactor, resulting in the more important reduction reactions in the gasifier (FAO Forestry Department, 1986). The benefits of the modified gasifier are the low-pressure drops, good thermal performance and a slow tendency to form slag (Rajvanshi, 2014). Other advantages of

this type of gasifier include its simplicity, the high carbon burning out and internal heat exchange leading to low gas exit temperatures and high efficiency of equipment (FAO Forestry Department, 1986). The drawbacks of the gasifier type include high sensitivity to tar and fuel humidity, relatively long time to start an IC-engine, poor response capability for heavy gas loads (Rajvanshi, 2014).

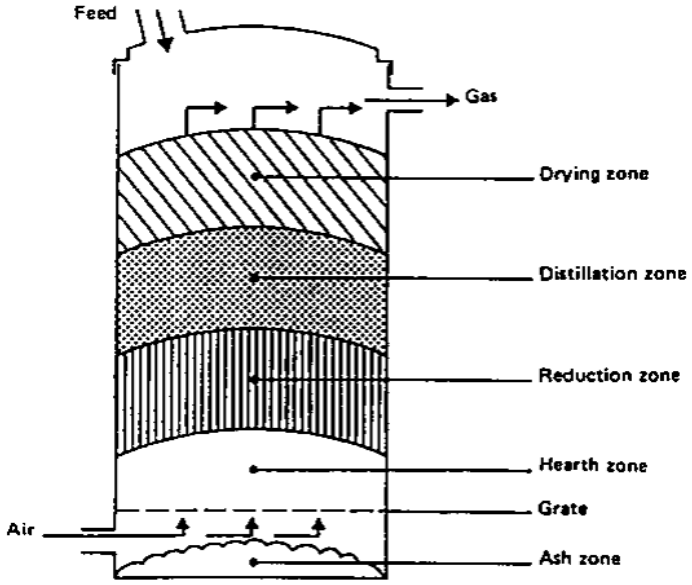

Figure 2-4: Updraught Gasifier (FAO Forestry Department, 1986).

The downdraught gasifier depicted in Figure 2.5 below is supplied with fuel from the top of the vessel and is also called the co-current gasifier type (E4tech, 2009). This form of gasifier was a solution to the problem of the gas flow's tar entrenchment (FAO Forestry Department, 1986). The material gas is removed from the gasifier so that the fuel and the gas travel in the same direction. A part of the fuel fed into the gasifier is burned to create a layer of warm coal, and the acid and tarry distillation products from the gas oil go through the vessel's throat and thus into permanent gasses as fairly high-quality gas syngas (FAO Forestry Department, 1986, E4tech, 2009, Rajvanshi, 2014). The primary advantage of downdraught gasifiers is the potential to create a producer gas free of tar that can be used in the engine (FAO Forestry Department, 1986). Flexible load adaption and low exposure to carbon, dust and tar content of feedstock offer additional advantages (Rajvanshi, 2014). The downside of a downdraught gasifier is that the particle size of feedstock is not too small and the vessel's designs are often very large (FAO Forestry Department, 1986, Rajvanshi, 2014). Regarding the number of fuel particles, fluffy materials with low density lead to flux problems and a huge pressure drop that requires the fuel to be pelleted or briquetted before being fed into the gasifier. Further downdraught gasifier drawbacks in comparison to updraught gas are due to their lower

efficiencies, which are directly caused by the lack of internal exchange of heat and the decreased heating cost of consumer gas.

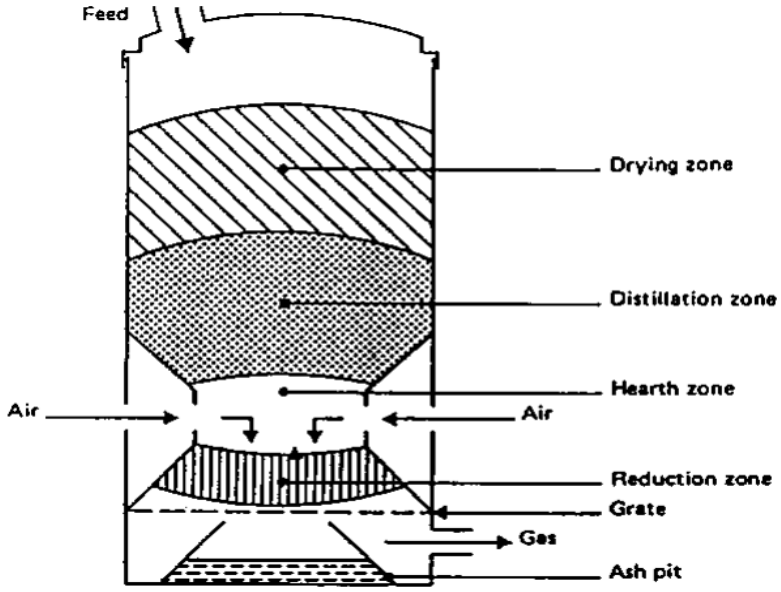

Figure 2-5: Downdraught Gasifier (FAO Forestry Department, 1986).

In theory, the cross-draught gasifier is a modification for the use of coal. Charcoal gasification results in the oxidation area with high temperatures of more than 1500 °C, which contributes to material difficulties. The gasifier fuel itself acts as an insulation against too high temperatures in the cross-draught gasifier (FAO Forestry Department, 1986). The benefits of this kind of gasifier include their short design height that allows economically viable small-scale operations (FAO Forestry Department, 1986, Rajvanshi, 2014). This is because the gas purification, which only includes a cyclone and heat filter, is relatively simple. Fast response times and versatility in gas production include other advantages (Rajvanshi, 2014). The inconveniences of cross-draught gasifier are the limited capacity for char conversion and very high sensitivity to high-pressure drop slag formation (FAO Forestry Department, 1986, Rajvanshi, 2014).

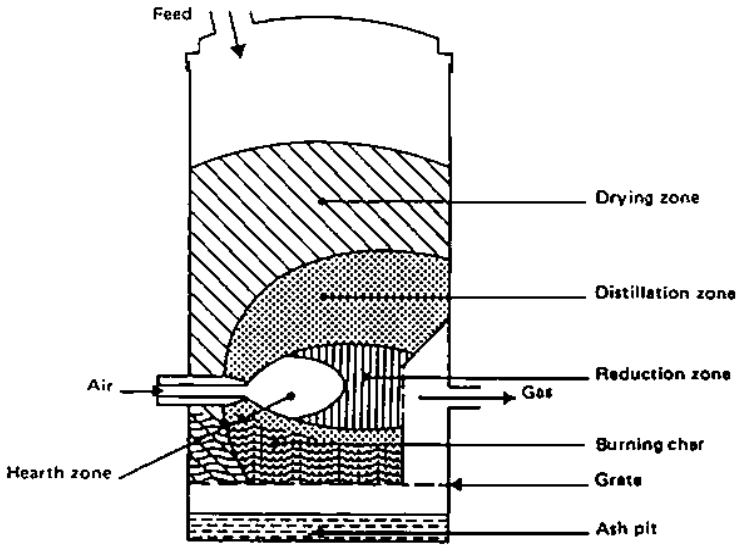

Figure 2-6: Cross-draught gasifier (FAO Forestry Department, 1986).

Characteristics of Gasifier Fuels

Under experimental or laboratory conditions, a wide range of carbonaceous and biomass fuel can be gasified. Nonetheless, the most accurate assessment of a gasifier is that it is capable of mixing biomass fuel with a necessary amount of air of less than stoichiometric (20% - 40%) and that it is able to produce a consistent gas product that can economically attract the customer (Rajvanshi, 2014). In order to accomplish this objective, the gasifier fuel properties have to be studied and fuel needs to be processed. It is therefore logical that there is no universal gasifier capable of handling all or most forms of fuel (FAO Forestry Department, 1986, Rajvanshi, 2014). A gasifier is extremely fuel-specific, with each type of gasifier working satisfactorily for stability, gas performance, efficiency and pressure losses (Rajvanshi, 2014). The following criteria can be used to identify the fuel as good or bad :

- Energy Content
- Bulk Density
- Moisture Content
- Volatile Matter (Tar)
- Ash Content and Ash Chemical Composition
- Slagging Characteristics

The size of the gasifier is directly proportional to the energy content and mass density of the gasifier fuel because power is available for longer periods at a load (Rajvanshi, 2014).

The humidity content of a fuel is dependent on the form, source and treatment of the fuel. The use of low-moisture fuel is more preferable as heat losses occur on the evaporation of humidity before the gasification is substantial and the gasification energy budget is affected (Rajvanshi, 2014). High humidity also stresses the cooling and filtering equipment by increasing the pressure fall through these units as fluid is condensed. The humidity of the carburant must be decreased in some way by pre-treatment to achieve the desired level of less than 20% of dryly defined moisture content (FAO Forestry Department, 1986, Rajvanshi, 2014).

In the design of the gasifier or the layout of the gas cleaning section to eliminate the tars from the consumer gas, detailed measures are necessary to determine the amount of Volatile Content present in the gasifier feedstock (FAO Forestry Department, 1986). Tar is one of the most dangerous components of the product gas from a gasification system because of its propensity to accumulate in the carburettor (Rajvanshi, 2014). The temperature and heat level are dependent on the physical properties of the tar and its appearance ranges from watery brown (60 %) to black and extremely viscous (7% of water). Filters and coolers also refer to gas cleaning techniques intended for tar extraction. A gasifier is well-designed if less than 1g / m^3 of tar is produced. The downdraught gasifier is generally considered to be an option in terms of reduced tar production but the downdraught process does not fully alienate the tar due to the localized inefficient processes taking place at the throat of the gasifier (Rajvanshi, 2014).

Ash is the oxidized mineral material following full fuel combustion (Rajvanshi, 2014). Ash may cause a number of problems, particularly with up and downdraught gasifiers, in gasification operations. In addition, ash appears to trigger scorching, which prevents the feed fuel's downward slowing in the gasifier. This slashing can also lead to too much tar forming, which can cause air channelling, which makes the risk of explosion worse, in addition to the impediment of fuel movement due to ash (FAO Forestry Department, 1986, Rajvanshi, 2014). The formation of slag is mainly dependent on three factors: fuel ash content, ash melting properties and the gasifier temperature profile (FAO Forestry Department, 1986). In particular, fuel containing ash content less than 6 % was observed without slagging. The slagging property of fuels between 6 and 12 % of the ash content depends largely on the melting point of the ash, which is then determined by the fact that trace elements are present that result in eutectic mixtures of a low melting point (FAO Forestry Department, 1986). Severe slagging can be highly expected for fuels with an ash content exceeding 12%.

Table 2-3: Slagging of agricultural residues in a small laboratory down draught gasifier (Jenkins, 1980)

Slagging Fuels	Ash Content %	Degree of Slagging
Barley straw mix	10.3	Severe
Bean straw	10.2	"
Corn stalks	6.4	Moderate
Cotton gin trash	17.6	Severe
Cubed cotton stalks	17.2	"
RDF pellets	**10.4**	**"**
Pelleted rice hulls	14.9	"
Safflower straw	6.0	Minor
Pelleted walnut shell mix	5.8	Moderate
Wheat straw and corn stalks	7.4	Severe

However, the slag can be overcome by using either the gasifier at low temperatures which keep the temperature far below ash-flow or by maintaining a temperature above the ash melting points (Kaupp and Goss, 1987). The first process is therefore done by injection of steam or water while the latter by means of provisions to clear the molten slag from the gasifier's oxidation region. It is, therefore, necessary to note that these methods have been only thoroughly tested and demonstrated in two gasifier fuels, namely charcoal and wood, as the primary fuels of World War 2 (Rajvanshi, 2014).

2.4 Current Developments in MSW Gasification and BTL Research

Taking into account the current state of usable fossil fuels in the world and their adverse consequences in relation to their negative impact on the environment (carbon footprint) a push to make energy sources more sustainable and renewable has emerged. With MSW also becoming a global problem in terms of disposal as the method currently being used of landfilling, especially in developing countries, is fast becoming obsolete due to problems of space and environmental issues in terms of pollution due to heavy metal contamination of the soil and groundwater streams as well as radionuclide activity concentrations, the two problems form solutions of each other. MSW gasification thus marries the two by making use of the MSW to be disposed of as feedstock to produce syngas, which can then be further processed to produce fuels and chemicals or used directly to power gas turbines for power generation.

Research on MSW gasification in Pakistan with the aim of syngas production has shown that this can be a successful process not only to help resolve the solid waste problem but also to reduce waste disposal through landfilling methods. The plant capacity of the studied facility has been determined based on feed supply and an automated carbon capture process called

the selexon method (Shehzad et al., 2016). Higher moisture content has also been found to be harmful to the performance of the syngas, and large amounts of MSW require high heat input, which in turn increases process costs. The highest effect in terms of operating conditions on the syngas composition was found to come from the temperatures of gasification. This analysis of the fluidized bed gasifier performance was conducted by simulation on ASPEN Plus (Shehzad et al., 2016).

At the Huazhong University of Science and Technology, research was also conducted to generate hydrogen-rich gas or syngas by catalytic gasification using steam as a gasifying agent and dolomite as a downstream catalyst. The study was conducted using a fixed bed reactor with a bench scale. With the presence of steam, the catalytic quality of the calcined dolomite was found to be higher, tar was completely decomposed as temperature increases from 850 to 950 °C with a sample temperature range of 750 to 950 °C (He et al., 2009). The development of H_2 and CO, combined with the improved carbon conversion efficiency with high temperatures and dry gas extraction, was found directly proportionate to the temperatures. The highest H_2 of 53.29 mol% and the highest H_2 yield of 38.60 mol H_2/kg MSW was observed at a maximum temperature of 950 °C (He et al., 2009). The total yield potential was found to be 70.14 in terms of mol H_2/kg dry MSW at 900 °C while syngas generated from catalytic steam gasification ranged from 36.35 to 70.21 mol% (He et al., 2009). The residual char was found to have negligible hydrogen, nitrogen and sulphur content while the ash content was found to be highest at a temperature of 950 ℃ being 84.01 % of the char.

A study conducted by Couto, Silva, and Rouboa in Portugal showed that increasing CO_2 content improves the conversion of carbon and CO_2 and improved cold gas efficiency while suppressing the production of tar (Couto et al., 2016). With regard to the ability to modify the H_2/CO ratio, air-CO_2 combinations can then be used for FT-synthesis based on catalysts and particularly for chemical products, such as urea, methanol and acetic acid.

A gasification analysis of 2 types of solid collected fuels, one as unsorted waste streams from local waste producers following an active hygiene process mainly composed of plastics, textiles, and a low biomass and paper content also referred to as trommel rejects in the study in question, further to be referred to as RT. The other fuel was derived from a mixture of mixed domestic waste streams with substantial biomass material, wastepaper and non-recyclable plastics also referred to as fluff further to be referred to as FL in the study in question. The study was carried out by the Catalonia Institute of Energy Research Thermochemical Conversion Unit. The study was done using a fluidized bed reactor in laboratory size, evaluating the gasification efficiency and the syngas value with temperature, dust, or dolomite, and air or steam parameters of 750 and 850 °C bed material and gasification agents

respectively. The efficiency of the gasification in syngas value was evaluated with concentrations of small contaminants such as tar, N, S and Cl. In the case of calcined dolomite as bed material with a higher gasification temperature of 850 °C, syngas performance was also improved with a rising H_2/CO ratio, carbon conversions and a decrease of tar (Recari et al., 2016). Either air or steam was found to increase the heat content of the fuel, but further work was recommended to understand fully the emission of minor pollutants under these operating conditions.

During the simulation of gasification, the Ministry of Défense, Health and Environmental Technology at Ming Chi University has studied the effects of operating temperature on syngas composition, total gas yield and gas heating quality. Together with two additives, CaO and activated carbon as stage 2 bed material, a 2-stage fluidized bed gasifier was used. The temperatures measured were 700, 800 and 900 ° C. When the operating temperature rose from 700 to 900 ° C, the molar percentage of H_2 in the material syngas increased from 19.4 to 29.7 mol% (Liu et al., 2016). It was also found to increase the overall gas yield and gas heating quality. The molar percentage of H_2 rose when CO_2 dropped when CaO was used as an additive in the commodity fuel. It was found that the use of activated carbon as an additive raises the molar percentage of CH_4 in the syngas as well as the overall yield of fuel and gas heating quality. Full gas yield and gas heating quality were found to be significantly increased by activated carbon while CaO had better effects on H_2 output (Liu et al., 2016).

A 160 MW thermal waste gasifier used solid recycled fuel for landfilling in Lahti, Finland. The gasification syngas generated is then cooled and cleaned before being moved to a gas-fired boiler for steam production, which is then used for district heating and grid power generation (European Biofuels Technonology Platform, 2016). The process uses a fluidized bed (CFB) atmospheric pressure gasifier with air being the gasifying component. The gasification process temperature ranges from 850–900 °C. The commodity gas is then cooled to a temperature of 400 °C from the gasification temperature in order to solidify the corrosive compounds in the gas so that they can be filtered out (Lahti Energia, 2016).

In June 2014, Enerkem opened a commercial-scale MSW-to-ethanol plant in Edmonton City, Canada. The plant produces and retails biofuels of the next generation by thermal gasification from non-recyclable and non-compostable MSW. Before a catalytic conversion process, the resulting syngas from the gasification process is then washed and refined to produce methanol and ethanol. The Enerkem Alberta Biofuels facility is the world's first major collaboration of this nature between metropole and a waste-to-biofuels producer with an annual production capacity of 38 million litres of biofuel (European Biofuels Technonology Platform, 2016, Vierhout, 2016).

CHAPTER 3. ENVIRONMENTAL ANALYSIS

3.1 Radionuclide Analysis of Landfill soil

Naturally Occurring Radioactive Materials (NORM) is any material of natural origins that contains elements that are radioactive and is found in the environment (Canadian Nuclear Safety Commission, 2004). Natural radioactivity originates from extra-terrestrial and radioactive elements present in the earth's crust. The earth's radioactivity can be grouped into three categories, Primordial, Secondary and Cosmogenic radionuclides. Approximately 90 % of the radiation exposure to human beings can be attributed to natural origins such as exposure to radon gas, cosmic radiation and surface-dwelling radionuclides (Ademola et al., 2015). The soil is amongst the most considerable sources of radiation exposure to human beings and the migration for the transfer of radionuclides to the immediate environment (Ahmad et al., 2015). Exposure is mainly through direct external exposure or through the incorporation of the radionuclides into the body by means of inhalation or ingestion (Jabbar et al., 2010). Exposure is a direct result of gamma-ray emissions that are produced by the most common terrestrial radionuclides, which are the member of the Uranium (^{238}U) and Thorium (^{232}Th) series and Potassium (^{40}K) of which concentrations differ with respect to the type of soil and the geology of the area. All uranium isotopes are radioactive in nature, and when they decay, produce an array of other radioactive secondary elements that will continue on this trend of decay until stable nuclei are reached. Synonymous with uranium, thorium also follows the same trend of decay in the formation of various secondary naturally occurring radioactive nuclei as uranium since they both share a similar attribute of significantly long half-lives. This phenomenon of systematic radioactive decay of these two primordial naturally occurring radioactive elements into various radionuclides is commonly referred to as the decay series of that specific element (Jabbar et al., 2010, Mehra and Singh, 2011, Navas et al., 2002). Potassium is regarded as one of the most abundant isotopic elements of natural origins on the earth's surface as it makes up more than 2 % of the earth's crustal mass (Jabbar et al., 2010). Due to its biological structure, Potassium is regarded as the most significant natural source of radioactivity which is ingested by humans.

Traditionally, the radionuclide analysis is conducted by the method of window analysis. This method is used to determine, amongst other nuclides, primordial Uranium (^{238}U), Thorium (^{232}Th) and Potassium (^{40}K) concentrations in the sand, soil and ore from gamma-ray measurements (Newman et al. 2008). Window analysis is conducted by the analysis of individual gamma-ray energy lines in the given spectrum by setting appropriate regions of interest, called windows, around the photopeaks of interest. It is then possible to extract

activity concentrations by making use of the appropriate gamma-ray branching ratios, measurement time, sample mass, and the applicable photopeak detection efficiency, by computing the peak area under the region of interest. This is done after correcting for the continuum and background radiation (Newman et al., 2008). The sample analysed needs to have been sealed for approximately 28 days in order to achieve secular equilibrium in the ^{228}Th sub-series of the ^{232}Th series and the ^{226}Ra sub-series of the ^{238}U series. When secular equilibrium is reached, the best way to then determine the activity concentrations is by making use of the weighted average of activity concentrations calculated for each of the gamma-ray energy lines selected for analysis.

3.1.1 Methodology

3.1.1.1 Source of sample

MSW in Cape Town, South Africa is composed of approximately 38 % non-recyclable waste, 22 % mainline recyclables, 22 % builders' rubble and 16 % organic waste of which only the recyclable waste is not going to the landfill site (City of Cape Town, 2009b, Department of Environmental Affairs and Tourism, 2012). Building materials alone are known to contain natural radioactivity which now poses the threat of the increase in the concentration of the naturally occurring radionuclides already present in the surface soil of the landfill sites' soil when during disposal of the builders' rubble (Faheem et al., 2008). It is thus important to monitor the hazard of radiation imposed by the practice of using landfills for the disposal of Municipal Solid Waste.

The aim of this study is to conduct radionuclide analysis on environmental soil samples collected from the 3 active landfill sites in Cape Town, South Africa, namely Vissershok, Bellville and Coastal Park of which are operated by the City of Cape Town Municipality. Vissershok, with GPS location (-33.773931, 18.545786), shown in Figure 3.1 below, is the largest landfill site in the Cape Town municipal area covering 150 hectares of land situated just approximately 500m away from the Cape Farmlands area.

Figure 3-1: Vissershok Landfill demarcated in red dashed lines with Cape Farms on the far right

The second largest being the Bellville site, shown in Figure 3.2 below, is 73 hectares in size situated in the Bellville south industrial area (33.9356509, 18.6552615). Nearby residential areas include Belhar 23 and the Cape Peninsula University of Technology (CPUT) Bellville campus less than 400 m from the site respectively.

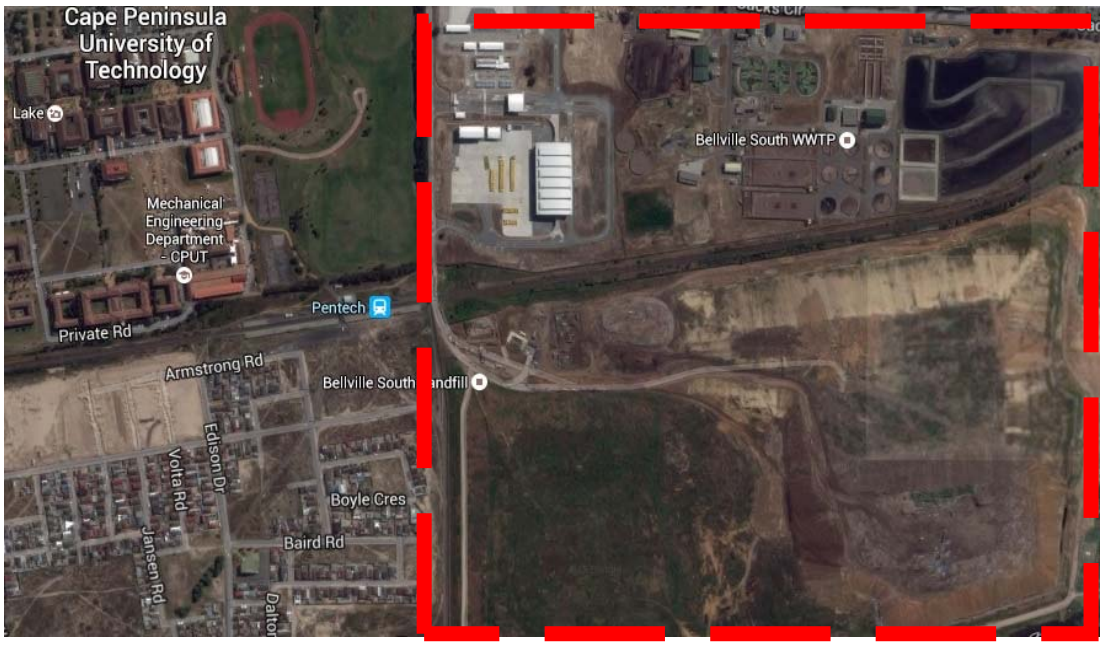

Figure 3-2: Bellville landfill site demarcated in red dashed lines (far right) with CPUT and Belhar 23 on the left

Lastly, the Coastal Park landfill (-34.0170711, 18.3298305), shown in Figure 3.3 below, is the smallest at 68 hectares is situated in the Muizenberg area along the coast just 1km away from the nearest residential area of Muizenburg.

Figure 3-3: Coastal Park Landfill site

In conducting this analysis, the objective is to quantify the activities of the naturally occurring radionuclides namely ^{238}U, ^{232}Th and ^{40}K in the landfill soil samples and thereof assess the gamma-radiation emitted from the soil which in turn will give an indication of the dose that humans are potentially exposed to from the landfill radioactivity.

A total number of 42 soil samples were collected at approximately 1 kg each. This number is made up of 14, 10 and 18 soil samples from the Bellville, Coastal Park, and Vissershok landfills respectively. Soil samples were collected at a depth of approximately 5 - 10 cm depth at the base of the landfill sites. In order to ensure each sample set is a fair representation of each landfill site, the samples were collected at approximately 40 – 50 m apart in order to cover a reasonable amount of ground in the landfill sites, hence the varying number of samples as per the varying size of each landfill site. The samples were collected using handheld garden shovels and heavy-duty refuse bags.

3.1.1.2 Sample Preparation

Samples were air-dried by spreading them over polyethene sheets at room temperature for a period of 5 to 7 days depending on the requirements with regards to each samples' moisture content. This was done in a controlled environment in order to prevent resident dust contamination. After drying is accomplished, the samples are then homogenized by means of a crushing and grinding process to attain a pre-set particle size according to specifications dictated by the analytical requirements. The ground samples were then passed through a sieve of 35 mm mesh. The samples were then stored in air-tight Marinelli beakers with geometry which is identical to that of the reference material. The beakers containing the samples were

hermetically sealed and stored for a period of approximately 4 weeks before gamma-ray spectrometry commenced. This is to ensure that secular radioactive equilibrium was reached after their progeny. Then the soil samples were analyzed for radionuclides.

3.1.1.3 Gamma-ray Measurements

Radionuclide analysis of the soil samples was carried out by means of the gamma-ray spectroscopy method. The analysis setup comprised of a Hyper-Pure Germanium (HPGe) detector coupled via a computerized interface to a Palmtop Multichannel Analyzer (MCA). The detector was a coaxial n-type detector with an energy resolution of 2.0 keV (full width at half maximum, FWHM) at 1332 keV, shielded with lead blocks in order to prevent scattered radiation from the shield. The efficiency of the detector, which is typical of HPGe detectors was 30 % (Khandaker, 2011). Each sample was analyzed for naturally occurring radionuclide activity for a period of 86400 seconds and the accumulated spectra data were analyzed by the palmtop MCA software (MCA8k-01). The absolute efficiency at specific photopeak energy was determined using equation 2.1 (Jabbar, 2010):

$$\boldsymbol{Eff' = Eff.e^{-\mu(E)\rho t}} \qquad (3.1)$$

where:

Eff′ = Absolute efficiency at specific photopeak energy after attenuation correction

Eff = Efficiency prior to specific photopeak energy attenuation correction

μ(E) = Mass attenuation at a specific gamma energy E

ρt = Average sample mass per unit area.

The activity concentrations of the various radionuclides were determined using equation 2.2 stipulated below (El-Sayed, 2014, Jabbar, 2010, Jabbar et al., 2010, Oladapo et al., 2012, Tzortzis et al., 2003):

$$\boldsymbol{A = \frac{C}{LT \times b \times m \times Eff'}} \qquad (3.2)$$

where:

A = Net peak area

LT = Live time

b = Branching ratio (gamma-ray emission probability corresponding to the photopeak energy)

m = Sample mass

Eff' = Absolute efficiency at a specific photopeak energy

The results of the radionuclide analysis show the activity concentrations of the progenies relating to the parent radionuclides of ^{238}U, ^{232}Th, and ^{40}K respectively. The progenies or daughter radionuclides identified were Radium (^{226}Ra), Lead (^{214}Pb), Bismuth (^{214}Bi), Actinium (^{228}Ac), Thallium (^{208}Tl) as well as the individual naturally occurring radionuclide Potassium (^{40}K).

The activity concentration, in Bq/Kg, of the landfill soil samples under investigation, in terms of the common terrestrial radionuclides which are members of the ^{238}U and ^{232}Th series and ^{40}K, were computed using the photopeaks of the gamma-ray spectra of the decay series as per methodology. Since the parent radionuclides do not inherently emit intense gamma rays but have progenies with more intense gamma rays and equal in activity to their parents at secular equilibrium, the radionuclide analysis was dependent on the detection of the emissions from these progenies.

The results of the activity concentrations were obtained using the gamma-ray energy lines of the various radioactive daughter elements that were identified. ^{226}Ra activity was determined using the 186 keV gamma-ray energy line while the daughters ^{214}Pb and ^{214}Bi were computed using the photopeaks in gamma-ray energy line ranges of 241.9 – 351.9 keV and 609 – 2203.7 keV gamma-ray energy lines respectively. The 338.2, 795, 911 and 968 keV gamma-ray energy lines were used to identify the ^{228}Ac radionuclide and the 583, 860 and 2614.6 gamma lines were used to identify ^{208}Tl. ^{40}K, being the single naturally occurring radionuclide, its energy line of 1460 keV was used to identify the parent radionuclide (Mehra and Singh, 2011, Navas et al., 2002, Sundareshan, 2013). Table 3-1 shows details of the lines used for identifying these radionuclides and thus computing the activity concentrations.

Table 3-1: Gamma-ray energy lines used for activity concentration determination with the associated branching ratios

Series/Radionuclide	Nuclide	Energy (keV)	Branching Ratio
^{238}U	^{226}Ra	186.1	0.0617
	^{214}Pb	241.9	0.0750
	^{214}Pb	295.2	0.1850
	^{214}Pb	351.99	0.3579
	^{214}Bi	609.3	0.4479
	^{214}Bi	768.4	0.0480
	^{214}Bi	934	0.0303
	^{214}Bi	1120.4	0.1480
	^{214}Bi	1238.8	0.0586
	^{214}Bi	1377.6	0.0392
	^{214}Bi	1729.6	0.0288
	^{214}Bi	1764.6	0.1536
	^{214}Bi	2204.9	0.0486
^{232}Th	^{228}Ac	338.3	0.1125
	^{228}Ac	794.9	0.0434
	^{228}Ac	911.2	0.2660
	^{228}Ac	969	0.1617
	^{208}Tl	583.2	0.3041
	^{208}Tl	860.6	0.0447
	^{208}Tl	2614.5	0.3570
^{40}K	^{40}K	1460.8	0.1067

3.1.2 Results and Discussion

Table 3-2 is a summary of the radionuclide analysis obtained from the 3 different landfill sites in the Cape Town Municipal area. Results are presented in terms of the range in which the activity concentrations were found at each sample site in terms of the radionuclides as well as the mean/ average values for each radionuclide.

Table A-1 in the appendix shows the detailed activity concentrations for each sample at each site for all identified radionuclides as well as the standard deviation or error (σ) for the radionuclide analysis results obtained. There might be uncertainty linked to results due to interference caused by x-ray lines of 92.6 keV of Bi, Po, U, and Th as well as the 63.7 keV lines from the corresponding Thorium series. Another factor that may lead to an increase in random error is the self-absorption of the low gamma-ray energies in the samples in question which is significantly dependent on the density and varying composition of the sample, for this reason, any photo-peak below the 100 keV mark was ignored (Papp et al., 1997).

Table 3-2: Summary of activity concentrations in terms of range and the average obtained for each radionuclide identified

	Radionuclide	Bellville	Coastal Park	Vissershok
Activity Range	Ra	3.044 - 15.198	7.0593 - 8.9646	8.5736 - 21.4017
	Pb	7.935 - 12.169	8.2780 - 8.4119	12.4880 - 24.0184
	Bi	3.599 - 14.757	6.6662 - 14.8040	13.3038 - 31.5813
	Ac	5.244 - 14.081	11.7142 - 12.0620	15.5573 - 33.1001
	Tl	5.960 - 19.480	17.5867 - 20.6316	18.6132 - 41.6325
	K	53.971 - 137.923	80.4208 - 97.4471	175.3260 - 477.5319
	Radionuclide	**Bellville**	**Coastal Park**	**Vissershok**
Activity Averages	Ra	8.452	8.012	14.730
	Pb	7.895	8.345	18.233
	Bi	8.232	10.735	22.141
	Ac	10.351	11.888	23.908
	Tl	12.663	19.109	27.724
	K	90.241	88.934	315.886

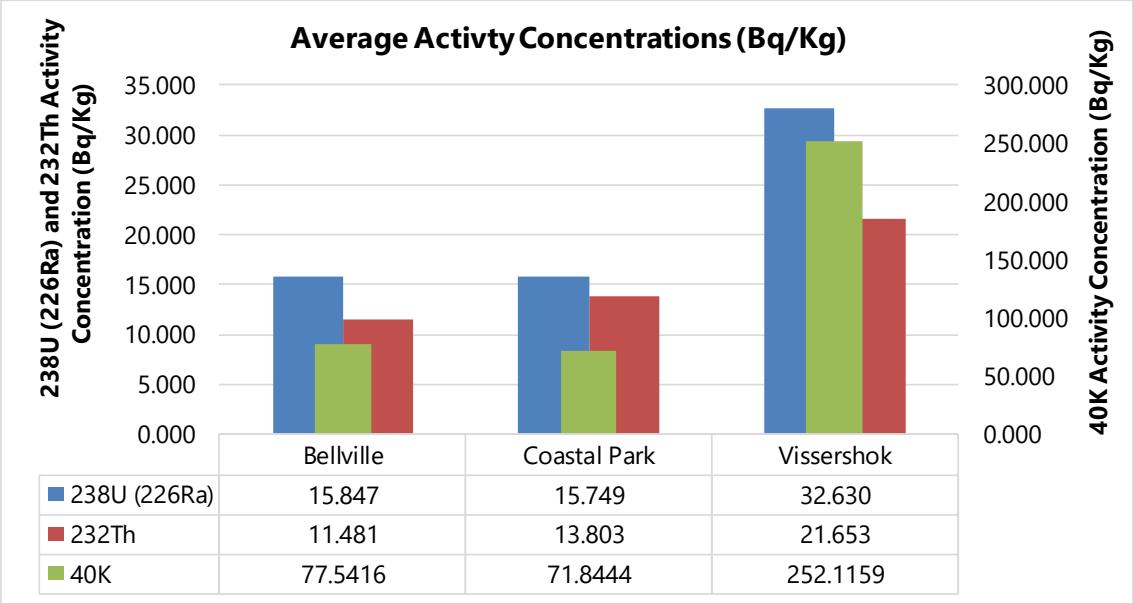

Figure 3-4: Summary of results showing the activity concentrations of ^{238}U, ^{232}Th and singly occurring ^{40}K in (Bq/Kg) as an average of each radionuclide from all samples in each site

In order to obtain the activity concentrations of the parent radionuclide ^{238}U and ^{235}U, gamma-ray energies of 186 keV from ^{226}Ra were used, under the assumption that $^{235}U/^{238}U$ isotopic ratio is constant for varying sample type and composition at 7.2×10^{-3} (Mehra and Singh, 2011). Regarding the fact that secular equilibrium can be assumed as reached between ^{238}U and ^{232}Th and their respective decay products as per methodology waiting period, ^{238}U and

^{232}Th activity concentrations were determined by computing the mean activity concentrations of their decay products, namely ^{226}Ra, ^{214}Pb and ^{214}Bi for ^{238}U and ^{228}Ac and ^{208}Tl for ^{232}Th (Harb et al., 2008). The results obtained are summarized in Figure 3.4.

In consideration of the results obtained, it can be distinguished that the ^{238}U activity concentration in the Bellville site (prefix bv) ranges between 8.750 and 24.189 Bq/Kg with a mean concentration of 15.847 Bq/Kg. Activity for ^{232}Th at the same site ranges between 7.774 – 18.331 Bq/Kg with an average of 11.791 Bq/Kg and ^{40}K averaging at 77.542 Bq/Kg range 45.031 – 122.041 Bq/Kg.

The Coastal Park landfill site shows a ^{238}U activity range of 14.618 – 16.880 Bq/Kg with an average activity of 15.749 Bq/Kg while ^{232}Th and ^{40}K averaged at 13.803 and 71.844 Bq/Kg with ranges 13.069 – 14.536 Bq/Kg and 63.910 – 79.779 Bq/Kg respectively while at the Vissershok site, ^{238}U activity concentration was found in the range 23.917 – 41.273 Bq/Kg with an average of 32.630 Bq/Kg, 15.783 – 26.154 Bq/Kg with a mean activity of 21.653 Bq/Kg for ^{232}Th and 155.766 – 352.432 Bq/Kg at an average activity of 252.116 Bq/Kg for ^{40}K.

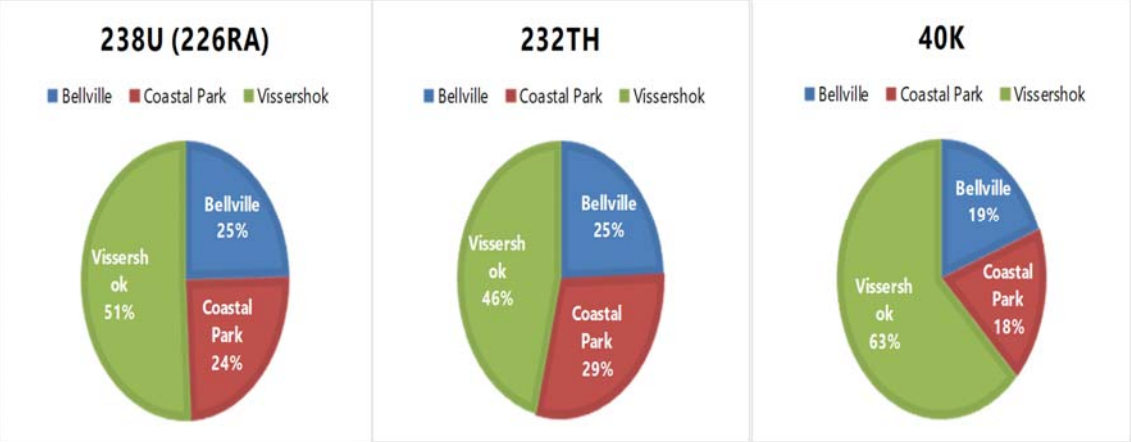

Figure 3-5: Percentage contributions of radionuclide activity concentrations from each landfill site.

Figure 3-5 shows the percentage contribution of each parent radionuclide from each landfill site. It can be deduced from the figure that the Visserhok landfill site has the highest activity concentrations of all 3 parent radionuclides as compared to the other 2 landfill sites which agree with Figure 3-4. This can be attributed to that Vissershok is the largest of the 3 landfill sites and hence has a vaster range of waste being disposed of at the site including high volumes of builders' rubble which constitutes to the high levels of ^{40}K as Vissershok contributes 64 % of the singly occurring radionuclide, which is common in most building materials.

A comparison of the mean activity concentrations for each radionuclide from other countries around Africa and the rest of the world are presented in Table 3.3. The results presented from other countries were from radionuclide analysis conducted on soil samples from those areas. The results obtained from the current study show that the average activity concentrations for each radionuclide were lower than most of the activities obtained in the other regions, even though these samples were obtained from landfill sites in Cape Town.

Table 3-3: Mean activity concentrations for soil samples around the world

Location	**Mean Activity Concentrations (Bq/Kg)**			**Source**
	$^{238}U(^{226}Ra)$	^{232}Th	^{40}K	
Botswana	34.8	41.8	432,7	(Murty & Karunakara 2008)
Windhoek Namibia	24.8	35.2	517.9	(Oyedele 2006)
South Western Nigeria	54.5	91.1	286.5	(Ajayi 2009)
South Sinai Egypt	46.4	65.8	1186.5	(Darwish et al. 2015)
Algeria	50.0	25.0	370.0	(Sroor et al. 2001)
Al Qasseem Saudi Arabia	9.3	12.3	535.0	(El-Taher & Al-Zahrani 2014)
Central Kutahya Turkey	33.0	32.0	255.0	(Sahin & Cavas 2008)
Himachal Pradesh India	44.2	93.1	174.5	(Singh et al. 2003)
United States	40.0	35.0	370.0	(Sroor et al. 2001)
World Mean	32.0	45.0	420.0	(Sroor et al. 2001)
Landfills Cape Town South Africa	21.4	15.6	133.8	Current Study

It is of great importance to also asses the correlations between the 3 radionuclides ^{238}U (^{226}Ra), ^{232}Th and ^{40}K. The correlation is done by plotting one radionuclide to another in a histogram and plotting a regression line to obtain the correlation factor which is the R^2 value on the graphs. The correlations obtained between ^{238}U (^{226}Ra) and ^{40}K, ^{238}U (^{226}Ra) and ^{232}Th, and ^{232}Th and ^{40}K were found to be 0.886, 0.884 and 0.841 respectively. The correlation factor of all 3 comparisons is high averaging at 0.871 which is very close to 1. Linear regression was done on the plots, meaning that the correlation between the radionuclides is almost perfectly linear. This means that the radionuclides' occurrences in the samples are evenly distributed. The correlation of the radionuclides is shown in Figure 3-6. The linear nature of the regression also gives testament to the composite nature of the samples as there are no distant outliers in the data.

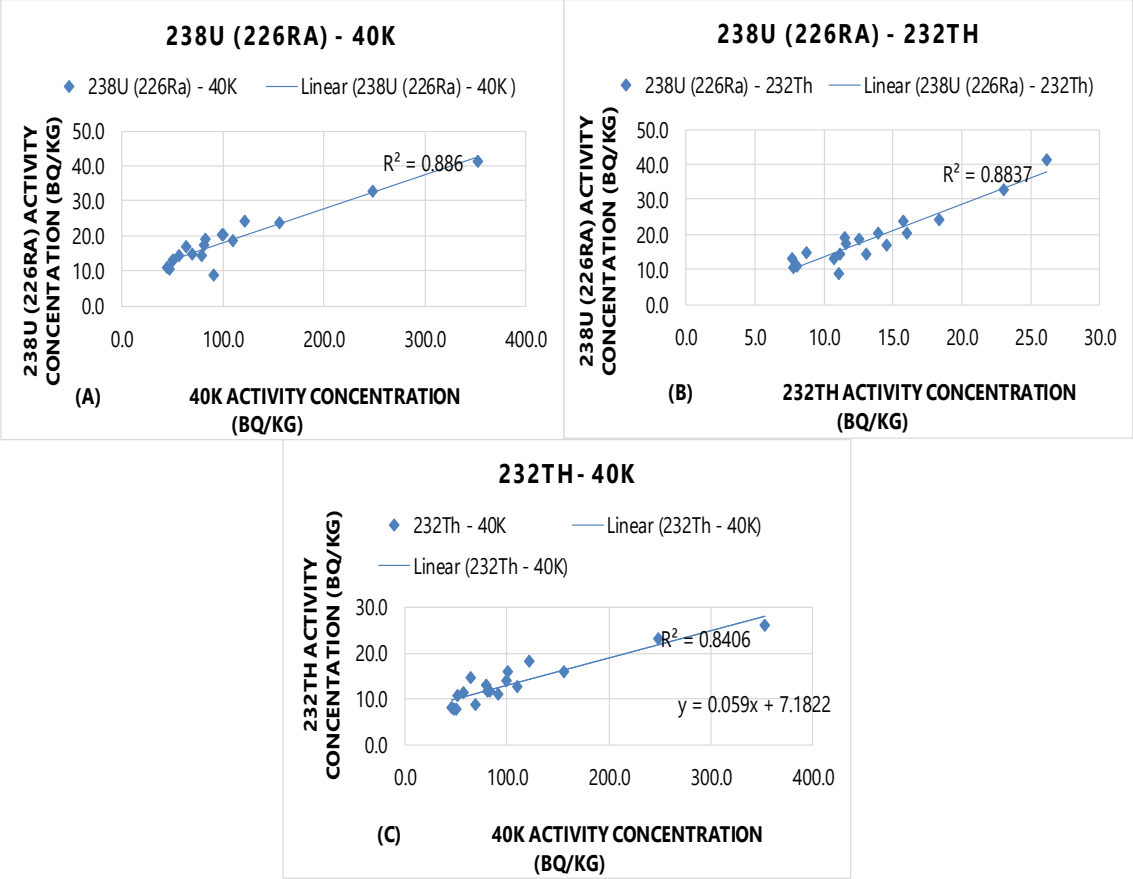

Figure 3-6: (a) ^{238}U (^{226}Ra) – ^{40}K, (b) ^{238}U (^{226}Ra) – ^{232}Th and (c) ^{232}Th – ^{40}K correlations in landfill soil samples of the City of Cape Town municipality.

Several radiological parameters were determined from the activity concentrations obtained from the soil samples. The parameters include the radium equivalent, external and internal hazard indices, representative gamma index, absorbed dose rate, annual effective dose rate (indoor and outdoor), lifetime dose rate, and the excess lifetime cancer risk.

Radium Equivalent: The distribution of the naturally occurring radionuclides ^{238}U (^{226}Ra), ^{232}Th and ^{40}K are not by any means uniform in the soil. Therefore, in order to compare the combined radiological effect of the soil containing these radionuclides by a single quantity, a collective index called the Radium Equivalent was used to describe the gamma radiation from the varying mixtures of the radionuclides in the soil (El-Sayed, 2014, Mehra and Singh, 2011, Oladapo et al., 2012). The radium index is calculated by the equation 3.3 (Yang et al., 2005).

$$\mathbf{Ra_{eq} = C_{Ra} + 1.43C_{Th} + 0.077C_K} \quad (3.3)$$

Where C_{Ra}, C_{Th} and C_K are the activity concentrations of ^{226}Ra, ^{232}Th and ^{40}K respectively. The index represents a weighted total of the above-mentioned radionuclides' activity concentrations on the basis of an assumption that states that 1 Bq/Kg of ^{226}Ra, 0.7 Bq/Kg of

^{232}Th and 13 Bq/Kg of ^{40}K produce an equal amount of gamma radiation dose rates (Alzahrani et al., 2011, Harb et al., 2008, Papp et al., 1997). The results obtained for the 3 sites in this study are summarized in Table 3.4.

The results obtained show that the Vissershok landfill has the highest amount of radiation at 79.608 Bq/Kg. This site also showed the highest amounts of the activity concentrations of the 3 radionuclides ^{238}U (^{226}Ra), ^{232}Th and ^{40}K. This can be attributed to that fact that Vissershok is the largest of the 3 landfill sites and most amounts of all types of waste, ranging from motor oil, household, medical and industrial waste are disposed of at this site. This then explains the overall high radiation activity at this landfill site. Coastal Park landfill displayed the second-highest amount of radiation with regards to the radium equivalent. Breaking down this reading of 38.042 Bq/Kg, it was noticed that potassium was particularly high as compared to the other radionuclides. This can be attributed to the fact that the Coastal Park landfill was mostly used for the disposal of builders' rubble. According to research conducted around the world, it was observed that building materials show a particularly high radioactivity concentration of potassium (Eisa and Mohamed, 2010, El-Taher, 2012, Zalewski et al., 2001). Similarly, with the Coastal Park site, the Bellville site exhibited a synonymous distribution of the 3 radionuclides and having a radium equivalent of 31.610 Bq/Kg. The Bellville reading is a bit lower compared to Coastal Park since the Bellville site had an evener distribution of household, builders' rubble and garden waste compared to coastal park and had a lower thorium concentration compared to coastal park.

External Hazard Index: This is a commonly used hazard index to denote the external exposure and is obtained using the equation 3.4 (Ajayi, 2009, Anekwe and Avwiri, 2016, El-Taher and Al-Zahrani, 2014, Sroor et al., 2001) :

$$\mathbf{H_{ex}} = \frac{\mathbf{C_{Ra}}}{\mathbf{370\ Bq/kg}} + \frac{\mathbf{C_{Th}}}{\mathbf{259\ Bq/kg}} + \frac{\mathbf{C_{K}}}{\mathbf{4810\ Bq/kg}} \qquad (3.4)$$

Where C_{Ra}, C_{Th} and C_K are the activity concentrations in Bq/kg for ^{226}Ra, ^{232}Th and ^{40}K respectively, as with the other indices to be discussed. This is a model proposed by several authors which creates a scenario for a room in the house where the inhabitants live with infinitely thick walls without windows and doors (United Nations Scientific Committee on the Effects of Atomic Radiation, 2010). The value of the external hazard index must be less than unity, which essentially means that the objective of the index is to maintain the radiation dose to the accepted dose limit of 1 mSv/y which corresponds to the upper limit of Ra_{eq} 370 Bq/kg (Ajayi, 2009, Darwish et al., 2015, El-Taher and Al-Zahrani, 2014).

The calculated values for the external hazard index illustrated in Table 3.4 range from 0.103 – 0.224 with a mean value of 0.146 and a standard deviation of 0.068. All the values obtained are below the critical value of unity being 1 which corresponds to the accepted dose limit of 1 mSv/y.

Internal Hazard Index: In addition to the external irradiation, radon along with its short-lived products are regarded as hazardous to respiratory organs through inhalation of alpha particles emitted from these products. The internal exposure to radon and its daughter products are quantified by the internal hazard index which, which needs to be less than 1, is given by the following equation (Ajayi, 2009, Darwish et al., 2015, El-Taher and Al-Zahrani, 2014):

$$\mathbf{H_{in}} = \frac{\mathbf{C_{Ra}}}{\mathbf{158\ Bq/kg}} + \frac{\mathbf{C_{Th}}}{\mathbf{259\ Bq/kg}} + \frac{\mathbf{C_K}}{\mathbf{4810\ Bq/kg}} \quad (3.5)$$

The calculated values of the external hazard index presented in Table 3.4 were found to range from 0.146 to 0.312 with a mean value of 0.204 and standard deviation of 0.094. All the values obtained do not exceed the recommended limit of 1 with Bellville landfill site showing the lowest at 0.146 and Visserhok the highest at 0.312.

Representative level index: This index is used for the approximation of gamma radiation associated with natural radionuclide activity in the soil and is defined by the following equation (Ajayi, 2009, Darwish et al., 2015, El-Taher and Al-Zahrani, 2014, Sroor et al., 2001):

$$\mathbf{I_{\gamma r}} = \frac{\mathbf{C_{Ra}}}{\mathbf{150\ Bq/kg}} + \frac{\mathbf{C_{Th}}}{\mathbf{100\ Bq/kg}} + \frac{\mathbf{C_K}}{\mathbf{1500\ Bq/kg}} \quad (3.6)$$

The values obtained for the representative level index as presented also in Table 3.4 were found to range from 0.272 to 0.602 with a mean value of 0.388 and a standard deviation of 0.185. The limit for the representative level index is set to be ≤ 1 (Ajayi, 2009), of which all the values obtained fall below the limit. Figure 3.7 illustrates a plot of the representative level index as well as the external and internal hazard indices respectively.

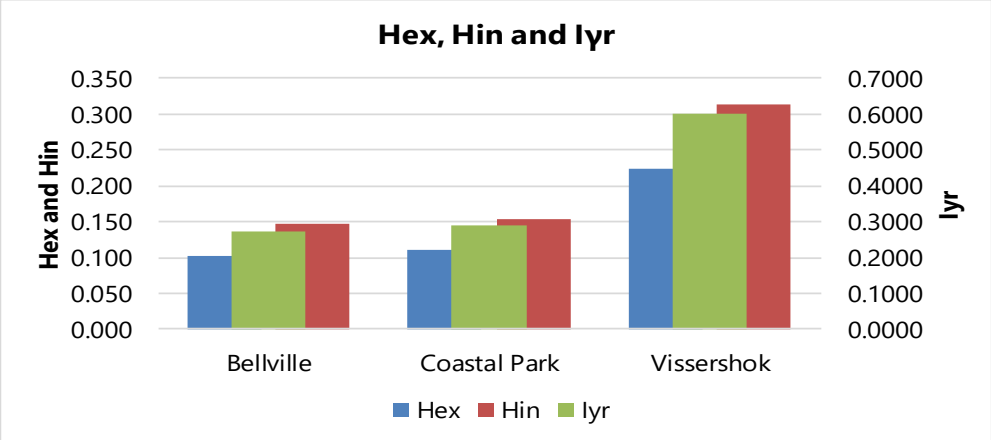

Figure 3-7: Average activity internal and external hazard indices with representative level index in landfill soil

Therefore, it can be concluded that based on these results, with respect to the radium equivalent, internal and external hazard indices, as well as the representative level index, there is no evidence of any threat of a health hazard from the landfill soil of Bellville, Coastal Park and Vissershok respectively regarding gamma radiation.

Table 3-4: Radium equivalent for soil samples from respective sites

	Radium Equivalent (Bq/Kg)	**Hex**	**Hin**	**Iyr**
	38,2	0,103	0,146	0,272
	41,0	0,111	0,153	0,291
	83,0	0,224	0,312	0,602
Mean	54,1	0,146	0,204	0,388
Standard Deviation	25,1	0,068	0,094	0,185

Absorbed dose rate: To provide a characteristic of the external gamma-ray, it is necessary to calculate the absorbed rate at 1m above the ground. The absorbed dose rate D (nGy/h) was calculated using equation 3.7 (United Nations Scientific Committee on the Effects of Atomic Radiation, 2010):

$$\mathbf{D = 0.462C_{Ra} + 0.604C_{Th} + 0.0417C_{K}} \quad (3.7)$$

The values obtained for absorbed dose rate in the air at 1m above ground averaged at 17.490, 18.609 and 38.667 nGy/h for the Bellville, Coastal Park, and Visserhok landfills respectively. The United Nations Scientific Committee on the Effects of Atomic Radiation (UNSCEAR) reports a global average of approximately 55 to 60 nGy/h absorbed rate 1m above the ground of which all 3 sites are lower (Mehra and Singh, 2011, Oladapo et al., 2012, United Nations Scientific Committee on the Effects of Atomic Radiation, 2010). Results in summary in table 3.5.

Annual effective dose rate: It is also necessary to assess the overall effects of this radiation on health due to the absorbed dose rate. This is done by determining the annual effective dose rate E (mSv/y) using equation 3.8 (United Nations Scientific Committee on the Effects of Atomic Radiation, 2010):

$$\boldsymbol{E = D(nGy/h)\ \times 8760(h/y) \times 0.2 \times 0.7(Sv/Gy) \times 10^{-6}} \quad (3.8)$$

Equation 3.8, as used by the UNSCEAR takes into account a conversion coefficient of 0.7 Sv/Gy from the absorbed dose in air 1m above the ground and outdoor occupancy factor of 0.2 (Mehra and Singh, 2011, Oladapo et al., 2012). The annual effective dose rate for indoors was also determined which then considers an indoor occupancy factor of 0.8, being the fraction of time spent indoors, instead of 0.2 which the corresponds to the fraction of time spent outdoors in equation 3.8 above (El-Taher and Al-Zahrani, 2014, United Nations Scientific Committee on the Effects of Atomic Radiation, 2010). To approximate the annual effective dose, the conversion coefficient from the absorbed dose in the air to effective dose needs to be taken into consideration, as well as the outdoor occupancy factor (El-Taher and Al-Zahrani, 2014). The annual effective dose rates determined using the outdoor occupancy factor for outdoor terrestrial gamma radiation in landfill soil were 0.0214, 0.0228 and 0.0474 mSv/y for Bellville, Coastal Park, and Vissershok respectively, which are all lower than the reported global average of 0.07 mSv/y (United Nations Scientific Committee on the Effects of Atomic Radiation, 2010). The corresponding values for annual effective dose rate for indoor exposure were found to be 0.086, 0.091 and 0.190 mSv/y for Bellville, Coastal Park and Vissershok landfill sites respectively. The results obtained for all 3 sites fall under the world-wide average of 0.34 mSv/y. It can be deduced from the result of absorbed dose rate and annual effective dose rate that the soil in the 3 City of Cape Town landfill sites still fall under the category of normal levels of radiation, meaning the soil radioactivity of the sites remains less hazardous to the environment and human health. Summary of these result given in Table 3.5.

Table 3-5: Summary of results for absorbed dose rates and annual effective dose rate (indoor and outdoor) per year for each site.

Site	D(nGy/h)	E(mSv/y)Outdoor	E(mSv/y)Indoor
Bellville	17.5	0.021	0.086
Coastal Park	18.6	0.023	0.091
Vissershok	38.7	0.047	0.190

These results are also lower in comparison to the combined limit of indoor and outdoor annual effective dose rate specified by UNSCEAR of 0.460 mSv/y for terrestrial radionuclides of an area regarded to have normal background radiation (Oladapo et al., 2012). These results also

meet the standards set out by the Nuclear Industry Association of South Africa (NIASA) that state that no member of the general public may receive more than 1 mSv/y in addition to natural background exposure of approximately 2.4 mSv/y (Lindell, 1987). Figure 3.8 is a graphical representation of the average values for the radium equivalent, absorbed dose rate (D) and annual (outdoor) effective dose rate (E).

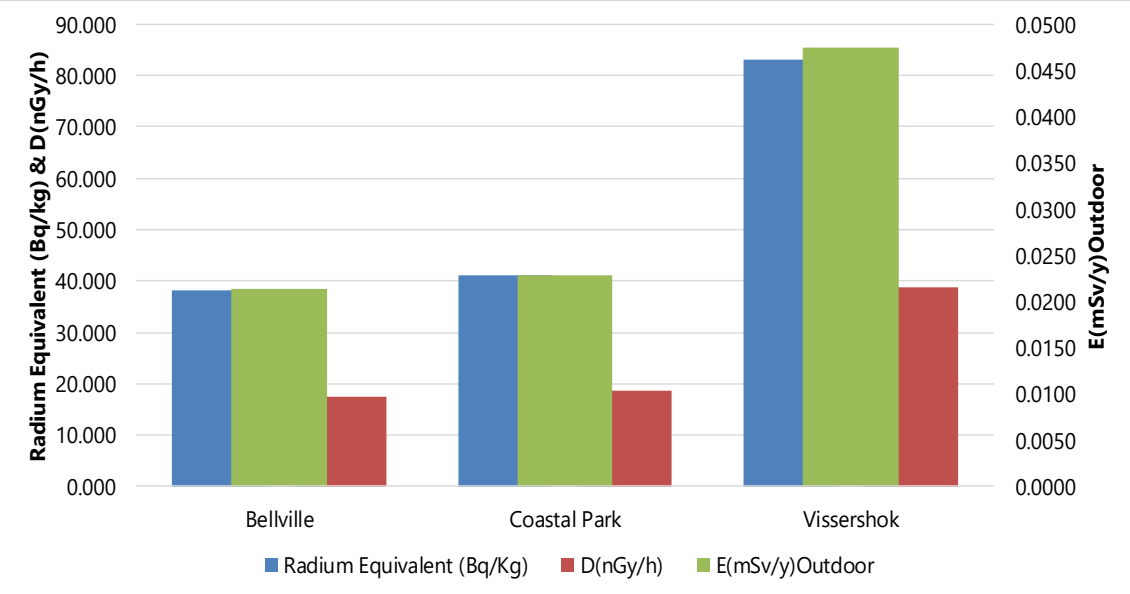

Figure 3-8: Radium equivalent, absorbed dose rate (D) and annual (outdoor) effective dose rate (E).

Excess lifetime cancer risk (ELCR): This describes the probability of developing cancer in a population of individuals over a lifetime at a specific level of exposure. This was calculated using equation 3.9 (Anekwe and Avwiri, 2016, Darwish et al., 2015, El-Taher and Al-Zahrani, 2014):

$$\mathbf{ELCR} = \mathbf{E} \times \mathbf{DL} \times \mathbf{RF} \qquad (3.9)$$

Where E is the annual effective dose rate (mSv/y), DL is the duration of life or life expectancy of which is 62.9 years in South Africa (Staff Writer, 2016), and RF is the risk factor (Sv^{-1}) which indicates fatal cancer per Sievert. The International Commission on Radiological Protection (ICRP 106), for stochastic effects, used a value of 0.5 for RF for the public (Anekwe and Avwiri, 2016, Darwish et al., 2015, El-Taher and Al-Zahrani, 2014). The results for the ELCR are presented in Table 3.6:

Table 3-6: Annual effective dose rate with lifetime dose and ELCR

Site	D(nGy/h)	$E(mSv/y)_{Outdoor}$	Lifetime Dose (mSv)	ELCR
Bellville	17.490	0.0214	1.3492	0.0675
Coastal Park	18.609	0.0228	1.4355	0.0718
Vissershok	38.667	0.0474	2.9828	0.1491

The results obtained for ELCR are 0.0675, 0.0718 and 0.1491 ($\times \mathbf{10^{-3}}$) lifetime cancer risk. The presented values are lower than the global average of 0.29 ($\times \mathbf{10^{-3}}$) lifetime cancer risk presented by the UNSCEAR (United Nations Scientific Committee on the Effects of Atomic Radiation, 2010).

3.1.3 Conclusion

Radionuclide analysis of soil samples from 3 active landfill sites around the City of Cape Town Municipal area was conducted. The analysis was carried out by means of gamma-ray spectroscopy with a Hyper-Pure Germanium detector with appropriate shielding connected to a Palmtop Multichannel Analyzer.

The radioactivity concentrations of ^{238}U (^{226}Ra), ^{232}Th and ^{40}K were obtained from averaging out the radioactivity concentrations of their respective daughter radionuclides in soil samples from the Bellville, Coastal Park, and Vissershok landfill sites.

With the assumption of secular equilibrium being attained, the dose rate in air 1m above ground and the effective annual dose rates were determined The results obtained show that the landfill sites meet global standards set out by UNSCEAR and South Africa's NIASA in terms of the maximum allowable emissions in terms of the dose rate in air and effective annual dose rates respectively.

3.2 Heavy Metal Analysis of Soil Samples

One of the most prevalent environmental impacts associated with the disposal of municipal solid waste in landfill sites is the influence of heavy metals. The extent of the effect of heavy metals is found to contrast with respect to the prevailing conditions at the landfill site and its binding forms (Karim et al., 2014). Regarding the fact that the landfills are open to the atmosphere, the exposure to atmospheric conditions causes different effects due to oxygen diffusion. The binding of metals to Manganese (Mn), and Iron (Fe) oxide increase in conditions of high redox, whereas binding to carbonate, organic compounds and sulphides show inverse proportionality (Prechthai et al., 2008). The degradation rate and buffer capacity of the landfill

site are greatly influenced with the increased possibility of oxygen diffusion through the upper layer of the landfill and with sufficient moisture content (Bozkurt et al., 2000, Prechthai et al., 2008).

Environmental pollution by chemicals and heavy metals such as cadmium (Cd), nickel (Ni), zinc (Zn), lead (Pb) etc., showed a great increase in recent times due to various industrial operations including that of municipal solid waste disposal (Waoo et al., 2014). All heavy metals at high concentrations have strong toxic effects and are regarded as environmental pollutants. The effects of toxic metals that may induce symptoms and disease can be allocated into two categories that are often overlapping yet distinct. The categories are direct toxic effects that damage tissues and interfere with the body's regular metabolic processes and displacement or depletion of essential nutrients leading to nutritional deficiencies and associated health concerns (The Environmental Illness Resource, 2016). Reports by nutrition researcher Robert Goyer state that cadmium, lead, mercury, and aluminium are toxic metals that may interact metabolically with nutritionally essential metals. Impairment of cognitive development such as development disorders, degenerative diseases of the nervous system inclusive of Alzheimer's, Parkinson's and multiple sclerosis (MS), problems with skeletal development and maintenance (e.g osteoporosis), kidney disorders, and blood disorders are diseases associated with toxic metals (The Environmental Illness Resource, 2016).

The Comprehensive Environmental Response, Compensation, and Liability Act (CERCLA) area 104 (I), as corrected by the Superfund Amendments and Reauthorization Act (SARA), requires the Agency for Toxic Substances and Disease Registry (ATSDR) and the Environmental Protection Agency (EPA) to set up a list, arranged by priority, of substances that are most normally found at facilities on the National Priorities List (NPL) and which are resolved to represent the most huge potential risk to human well-being due to their known or suspected lethality and potential for human exposure at these NPL locals. CERCLA likewise requires this list to be overhauled occasionally to mirror extra data on unsafe substances. In CERCLA, it is known as the priority list of unsafe substances that will be a contender for toxicological profiles (Registry, 2018). This substance priority list is updated and distributed on a 2-year premise, with a yearly casual survey and correction. Each substance on the list is a possibility to wind up the subject of a toxicological profile arranged by ATSDR. The listing algorithm organizes substances in view of recurrence of occurrence at NPL destinations, danger, and potential for human exposure to the substances found at NPL locales.

The ecological effect of metals and the contamination level in the soil samples can be resolved with the assistance of two parameters; the enrichment ratio (ER) and geoaccumulation index (I_{geo}) (Nowrouzi and Pourkhabbaz, 2014). The enrichment factor (EF), because of its all-inclusive

equation, is a generally straightforward and simple device for surveying the degree of enrichment and looking at the contamination of distinctive environmental media (Benhaddya and Hadjel, 2013). The ER is a normalization technique proposed by Simex and Helz (1981) to evaluate the concentration of the metals. It normalizes metal concentration as a proportion to another constituent of the soil. Rubio et al. (2000) expressed that there is no agreement about the most suitable soil constituent to be utilized for normalization. Among those utilized have been Al, Fe, total organic carbon, and grain size. The constituent decided, for this reason, ought to likewise be related to finer particles (identified with grain size) and its focus ought not to be anthropogenically adjusted (Ackermann, 1980). The EF is characterized as follows (Ergin et al., 1991) :

$$\boldsymbol{EF} = \frac{\left(\frac{\boldsymbol{M}}{\boldsymbol{Fe}}\right)_{\boldsymbol{Sample}}}{\left(\frac{\boldsymbol{M}}{\boldsymbol{Fe}}\right)_{\boldsymbol{Background}}} \quad (3.10)$$

where $(M/Fe)_{Sample}$, is the proportion of metal and Fe concentrations in the sample, and $(M/Fe)_{Background}$, is the proportion of metal and Fe concentrations of the background. The world mean shale, as well as the world, mean soil, are among the materials regularly utilized to give background metal levels. As per Zhang and Liu (2002), EF values in the vicinity of 0.5 and 1.5 demonstrate the metal is totally from crustal materials or natural processes, though EF values more prominent than 1.5 suggest that the sources will probably be anthropogenic.

Geochemical index (I_{geo}) was initially expressed by Muller (1969) to decide and characterize metal contamination in soil by contrasting current concentrations and preindustrial levels, I_{geo} is figured as follows:

$$\boldsymbol{I_{geo}} = \boldsymbol{log_2[C_n/1.5B_n]} \quad (3.11)$$

where C_n is the measured concentration in the soil for the metal n, B_n is the background value for the metal n (Turekian and Wedepohl, 1961), and factor 1.5 is utilized considering conceivable varieties of the background data due to lithological variations.

The hazard evaluation technique (risk assessment) on the soil is broadly applied to the health risk assessment of heavy metals exposure to surface dust (Zheng et al., 2010, Chang et al., 2009, Ferreira-Baptista and De Miguel, 2005). The pathways of contaminations connected to the surface dust entering the human body are hand-to-mouth ingestion, dermal retention and mouth and nose inhalation. The measurement gotten by means of every one of the three ways was figured utilizing equations (3.12) - (3.14) (USEPA, 1996, United States Environmental Protection, 1989).

$$D_{ing} = C \times \frac{IngR \times EF \times ED}{BW \times AT} \times 10^{-6} \quad (3.12)$$

$$D_{inh} = C \times \frac{InhR \times EF \times ED}{PEF \times BW \times AT} \quad (3.13)$$

$$D_{dermal} = C \times \frac{SL \times SA \times ABS \times EF \times ED}{BW \times AT} \times 10^{-6} \quad (3.14)$$

Where D_{ing} is the everyday measurement by means of hand-to-mouth ingestion of substrate particles; D_{inh} is the day by day dosage by means of inhalation of resuspended particles through mouth and nose; D_{dermal} is the day by day dosage by means of dermal retention of trace components in particles clung to uncovered skin. The other parameters significance and values are presented in Table 3-7 below:

Table 3-7: Parameter meaning and value of daily dose model of heavy metals in urban surface dust (Ma and Singhirunnusorn, 2012)

Parameter	Meaning and Unit	Values		Reference
		Child	Adult	
C	Exposure-point concentration, mg/µg	95%UCL		This Study
IngR	Ingestion rate, mg/d	200	100	(EPA, 2001)
InhR	Inhalation rate m^3/d	7.6	20	(Van den Berg, 1995)
PEF	Particle emission factor, m^3/kg	1.36 X 10^9		(EPA, 2001)
SA	Exposure skin area, cm^2	2800	5700	(EPA, 2001)
SL	Skin adherence factor mg/(cm^2h)	0.2	0.7	(EPA, 2001)
ABS	Dermal absorption factor, unitless	0.001		(Ferreira-Baptista and De Miguel, 2005)
ED	Exposure duration, y	6	24	(EPA, 2001)
EF	Exposure frequency, d/y	180		(Ferreira-Baptista and De Miguel, 2005)
BW	Average body weight, kg	15	70	(United States Environmental Protection, 1989)
AT	Average time, d	ED X 365 (non-carcinogens) 70 X 365 (carcinogens)		(United States Environmental Protection, 1989)

For non-carcinogens the dosages computed for every component and exposure pathway are in this way divided by the corresponding reference dose (RfD) to give a hazard (HQ), Hazard index (HI) is equivalent to the entirety of HQ. On the off chance that the estimation of HQ or HI is less than one, it is trusted that there is no huge danger of non-cancer-causing impacts. On the off chance that HQ or HI surpasses one, at that point quite possibly non-cancer-causing

impacts may happen, with a likelihood which tends to increase as the estimation of HQ or HI expands (EPA, 2001). For carcinogens, the dose is multiplied by the corresponding slope factor (SF) to create a gauge of cancer risk (CR). The level of cancer risk related with exposure to this component in road dust in the scope of limit values (10^{-6} to 10^{-4}), above which ecological and administrative organizations consider the hazard unsuitable (United States Environmental Protection, 1989). Hazard Index technique and cancer risk strategy were utilized to survey human wellbeing danger of heavy metals exposure to surface dust in Cape Town landfill sites. In this study, Zn, Cr, Cd, Se, Sb, Cu, Pb, Ni and As were identified as possible hazards for the community.

3.3 Identified Heavy metals and their potential Health Risk

Zinc (Zn) is a basic component required by the human body. It is generally found in nutritious supplements. Be that as it may, the high concentration of zinc in the body may influence the wellbeing. Zinc is among the most widely recognized components in the Earth's crust. Zinc is found noticeable all around, soil, water and is available in all sustenance. In nature, zinc is as sulphide. Zinc mixes are generally utilized as a part of the industry. Ingesting large amounts of zinc for a while may cause frailty, harm the pancreas, and decline levels of high-thickness lipoprotein cholesterol (Zheng et al., 2010).

Chromium (Cr) can exist in a few oxidation states, which are Cr (II), Cr (III), Cr (VI) and Cr (VI) of which the last is the most solvent and unsafe to human. Exposure to an abnormal state of chromium causes skin disturbance, and harm to the liver, respiratory organs, and kidney. Illnesses related to high exposure to Cr are lung malignancy, puncturing of the nasal septum. EPA and the Research on malignancy and the National toxicology program order Cr as classification one cancer-causing agent (Zhong et al., 2016).

Cadmium (Cd) is for the most part found in earth's crust. It occurs in a blend with zinc. It is an inescapable by-product in enterprises of copper and lead extraction. It might likewise be found in pesticides. It is discharged into nature through weathering of rocks, timberland fires, and volcanoes, while whatever is left of Cd is brought into the earth through anthropogenic exercises (Johri et al., 2010). People interact with Cd for the most part through food that is exceptionally rich in Cd and that increases the convergence of Cd in the human body. A portion of the food containing Cd are mushrooms, liver, and dried kelp. Smokers get exposed to a high concentration of Cd. Tobacco smoke transports Cd into the lungs. Cadmium enters the human body by inward breath and ingestion of nourishment and water containing Cd. It doesn't generally infiltrate the human body through the skin so dermal transport is of low risk. Cadmium is perceived by the EPA as the most lethal component. A few illnesses related to the

exposure to high concentrations are a bone break, harm to the focal sensory system, mental clutters, and conceivable DNA harm or tumour development (Huang, 2004).

Selenium (Se) occurs normally as a metalloid component, which is fundamental to human well-being in low sums, however, is destructive in high concentrations (Greer, 1986). The occupational-related inward breath exposure may happen in the metal, selenium-recuperation, and paint production environments. In these conditions, exposure of people to hydrogen selenide - the most poisonous selenium compound which exists as a gas at room temperature brings about bothering of the mucous films, aspiratory enema, serious bronchitis, and bronchial smelling salts, though inward breath of selenium dust can cause aggravation of the layers in the nose and throat, bronchial fits, and synthetic pneumonia (World Health Organization, 1996).

Antimony (Sb) is known as a worldwide contaminant. The dangers of the exchange of Sb from the earth to people are very desperate and genuine (Wu et al., 2011). The contamination of Sb is a worldwide issue in view of its danger to people and the imperative part of Sb in causing illnesses of liver, skin, respiratory and cardiovascular systems (Schnorr et al., 1995, Kuroda et al., 1991, Girgis et al., 1970). It has been recorded as a priority heavy metal toxin of enthusiasm for the United States and the European Union (Council Directive, 1976, United States Environmental Protection Agency, 1979). Sb is presented in the earth through modern exercises and the utilization of Sb items, for example, fire retardants. It enters the human body for the most part by the inward breath, skin contact and by eating nourishment containing antimony (De Boeck et al., 2003). The world health organisation (WHO) and the expert committee on food additives (ECFA) have not assessed the security of Sb. Be that as it may, the EPA in the US has given an oral measurement of 0.4 ug/kg of body weight every day for Sb (World Health Organization, 2011).

Copper (Cu) is an exceptionally rudimentary substance that occurs naturally in the earth and spreads through the earth through characteristic marvels. People generally utilize copper. For example, it is applied in the industries and in agricultural practices (Lenntech, 2018b). With global copper production continually on the rise (Kilian, 2017, Agency Staff, 2018), this fundamentally implies increasingly copper winds up in the earth. Streams are depositing muck on their banks that are tainted with copper, because of the transfer of copper-containing wastewater. Copper enters the air; air will stay there for an eminent timeframe before it settles when it begins to rain. It will then wind up predominantly in soils (Lenntech, 2018b). Therefore, soils may likewise contain huge amounts of copper after copper from the air has settled. Copper can be discharged into the earth by both normal sources and human exercises. Cases of regular sources are wind-blown dust, rotting vegetation, forest fires and ocean spray. A few

other cases of human exercises that add to copper discharge are mining, metal generation, wood creation and phosphate manure creation. Since copper is discharged both normally and through human movement it is extremely across the board in the earth. Copper is frequently found close to mines, industrial settings, landfills and waste transfers (Lenntech, 2018b). Copper can be found in numerous sorts of sustenance, in drinking water and in the air. Thus, we ingest large amounts of copper every day by eating, drinking and breathing. The assimilation of copper is fundamental since copper is a trace element that is basic for human wellbeing. Although people can deal with relatively vast concentrations of copper, a lot of copper can, in any case, cause prominent medical issues. Copper fixations in the air are normally very low so introduction to copper through breathing is unimportant. In any case, individuals that live close to smelters that process copper metal into metal, do encounter this sort of introduction. Individuals that live in houses that still have copper plumbing are presented to, therefore, amounts of copper than a great many people since copper is discharged into their drinking water through erosion of channels. In the workplace, a copper infection can prompt an influenza-like condition known as metal fever. This condition will go following two days and is caused by over sensitivity (Lenntech, 2018b). Long haul exposure to copper can cause disturbance of the nose, mouth, and eyes and it causes cerebral pains, stomach aches, unsteadiness, regurgitating and looseness of the bowels. Deliberately high takes-up of copper may cause liver and kidney harm and even fatality. Regardless of whether copper is cancer-causing has not been resolved yet (Gallagher and Perlman, 2013). There are logical articles that show a connection between long-haul exposure to high concentrations of copper and a decrease in intelligence with youthful teenagers (Rossi et al., 2006, Prohaska, 2000).

Industrial exposition to copper exhaust, dust, or fogs may bring about metal smoke fever with atrophic changes in nasal mucus layers. Chronic copper poisoning brings about Wilson's Disease, portrayed by hepatic cirrhosis, cerebrum harm, demyelination, renal illness, and copper deposition in the cornea (Gallagher and Perlman, 2013, Lenntech, 2018b). At the point when copper winds up in the soil, it firmly appends to natural matter and minerals. Accordingly, it doesn't travel extremely far after discharge and it barely ever enters the groundwater. In surface water, copper can travel great distances, either suspended on ooze particles or as free particles. Copper does not separate in the earth and hence, it can gather in plants and creatures when it is found in soils (Lenntech, 2018b).

Lead (Pb) is a standout amongst the most studied heavy metals because of its wide industrial application. There are a few different ways that people can be exposed to lead (Pb). The significant sources are toxic paint, lead-defiled water, assembling of lead batteries, elastic

items, glass and other lead-containing items (Lenntech, 2018b). It has cancer-causing properties and influences respiratory and process frameworks. Pb metal is especially unsafe to kids as it harms their insight and sensory systems (Zhong et al., 2016). Despite the fact that debate still exists in regards to the levels at which Pb poisonous quality shows itself clinically, there is a boundless acknowledgement that Pb is neurotoxic (Gallagher and Perlman, 2013). Lead occurs organically in nature. Be that as it may, most lead concentrations that are found in the earth are a consequence of human exercises. Because of the utilization of lead in fuel, an unnatural lead-cycle has comprised. In automobile engines, lead is singed, with the goal that lead salts (chlorines, bromines, oxides) will begin. These lead salts enter nature through the exhausts of cars. The bigger particles will drop to the ground promptly and contaminate soils or surface waters, the smaller particles will travel long separations through the air and stay in the environment. Some portion of this lead will fall back to earth when it is drizzling. This lead-cycle caused by human creation is substantially more reached out than the normal lead-cycle (Lenntech, 2018b).

Nickel (Ni) is normally found in a blend with sulphur, oxygen, and sulphides in the world's crust joined with different components. Most nickel on Earth is difficult to reach since it is secured away in the planet's iron-nickel molten core, which is 10 % nickel (Lenntech, 2018c). Ni is brought into the earth amid nickel mining and by industries that utilize nickel or nickel mixes (Von Burg, 1997). It is likewise discharged in the climate by oil-burning power plants and junk incinerators. Ni occurs in the earth at low levels. The real wellspring of exposure to nickel is by the inward breath of air, smoking tobacco-containing Ni, skin contact with soils. Patients at hospitals might be exposed to Ni in prosthetic body parts produced using nickel-containing compounds. Exposure of an unborn child to nickel is through the exchange of nickel from the mother's blood to embryo blood. The wellbeing impacts from exposure to high concentrations of nickel are: incessant bronchitis, diminished lung capacity, and growth of the lung and nasal sinus, have happened in individuals who have inhaled dust containing certain nickel mixes (Li et al., 2008). EPA has grouped nickel refinery dust and nickel subsulfate as a human cancer-causing agent.

Arsenic (As) is a naturally occurring component that is broadly appropriated in the Earth's crust. It is found in water, air, sustenance, and soil (National Institute of Environmental Health Sciences, 2017). It occurs in soil and minerals and it might enter the air, water, and land through the breeze blown dust and water run-off (Lenntech, 2018a). Researchers, paediatricians, and general well-being advocates are progressively worried about the more unpretentious and long-extend wellbeing impacts of low-level exposures to people, particularly for new-born children and kids presented to arsenic in water and a few nourishments, for example, rice-

based items, amid delicate windows of advancement (National Institute of Environmental Health Sciences, 2017). Arsenic cannot be mobilized effectively when it is stationary. Because of human exercises, principally through mining and smelting, normally stationary arsenic have likewise mobilized and would now be able to be found on numerous a larger number of spots than where they existed normally (Lenntech, 2018a). Exposure to inorganic arsenic can cause different wellbeing impacts, for example, bothering of the stomach and digestion tracts, diminished generation of red and white blood cells, skin changes and lung aggravation. It is recommended that the take-up of huge measures of inorganic arsenic can escalate the odds of tumour advancement, particularly the odds of improvement of skin cancer, lung disease, liver malignancy and lymphatic disease (Lenntech, 2018a).

3.3.1 Methodology

3.3.1.1 Reagents and Chemicals

All reagents were analytical grade and were obtained from Sigma Aldrich, South Africa. The reference material, Estuarine sediment (trace elements) (BCR-277R) was purchased from the European Community Bureau of Reference, IRMM, Belgium of which BCR is a registered trademark of European Commission. The list of reagents and instruments used is presented below:

- 0.11 M acetic acid
- 0.1M hydroxyl ammonium chloride
- 8.8 M H2O2
- 1 M ammonium acetate
- Aqua Regia
- 5% nitric acid, HF was replaced by nitric acid

3.3.1.2 Equipment

- End-to-end shaker
- Centrifuge sigma 2-16
- 30 mL centrifuge tube
- Mettler AE 163 weighing balance.
- Sieves
- ICP-OES

3.3.1.3 Microwave Digestion

Scientists have been given the ability to study both decomposition and develop standardized methods for preparing for subsequent molecular analysis through the ability to control temperature and heating rate given by microwave technology. The EPA developed three general standard sample preparation methods that employ the use of microwave energy namely Method 3052, Method 3051A, and Method 3051 while other methods include the ASTM D5258-92 (Kingston and Haswell, 1997). Samples that are to be digested need to be dried. Drying samples with organic compounds that are to be analyzed pose a potential problem, especially if the sample contains volatile analytes. Hot plate drying techniques pose the threat of overheating and losses, however, microwave aided heating allows for lower temperatures as the sample dries with decreasing temperature allowing the retention of volatile analytes (Kingston and Haswell, 1997). Organic analytes generally need extraction and separation from a matrix in an appropriate solvent. This is done through digestion. Microwave digestion comprises of combining the sample matrix and acids in a pressurized vessel and increasing the temperature of the solution past the boiling point of the acid which increases the digestion rate. Microwave digestions allows for shorter digestion times counted in minutes instead of hours, zero losses in terms of volatile elements and complete recovery of Mercury, Arsenic, Cadmium etc., improved laboratory conditions due to eliminated acid fumes, no sample contamination from the environment as well as cross-contamination and easily reproducible (Martin and Coughtrey, 1982). Microwave digestion is recognized extensively as the most robust technique for sample preparation intended for Atomic Absorption (AA), Inductively Coupled Plasma Optical Emission Spectrometry ICP-OES or Inductively Coupled Plasma Mass Spectrometry (ICP-MS) analyses (Hamid, 2015).

3.3.1.3.1 Microwave Digestion Procedure

The technique that was utilized as a part of this venture for the extraction of heavy metals was the altered BCR Sequential Extraction. This 4-stage consecutive extraction technique has likewise been utilized as a part of past examinations and shows more data on the distinctive types of metals in the soil (Wali et al., 2014, Rao et al., 2008). All Glassware used were stored in diluted nitric acid and left-over night for the elimination of impurities or to avoid contamination; they were washed and rinsed with distilled water before using them. All soil samples were sieved to < 63 micrometres and 63 to <150 micrometres because the majority of particles that adhere to hands are < 63 micrometres in diameter yet risk assessments for sediment remediation are typically based on sediment samples sieved to < 250 micrometres. A mass of 250 mg of sample and 8 ml of Aqua regia (a mixture of one-part nitric acid and three parts hydrochloric acid) was transferred into microwave vessels and was left in contact overnight. Each time 3 samples were placed in the microwave carousel, together with a blank

which was prepared with supra-pure acids. After cooling, the sample was digested and was filtered with Whatman no.42 filter paper, since microwave digestion left solid residues in the digests; then they were transferred to a 50-ml flask and were brought to volume. The digests and the blanks were analysed with ICP-OES. A schematic representation of the extraction method is shown in Figure 3.9 below:

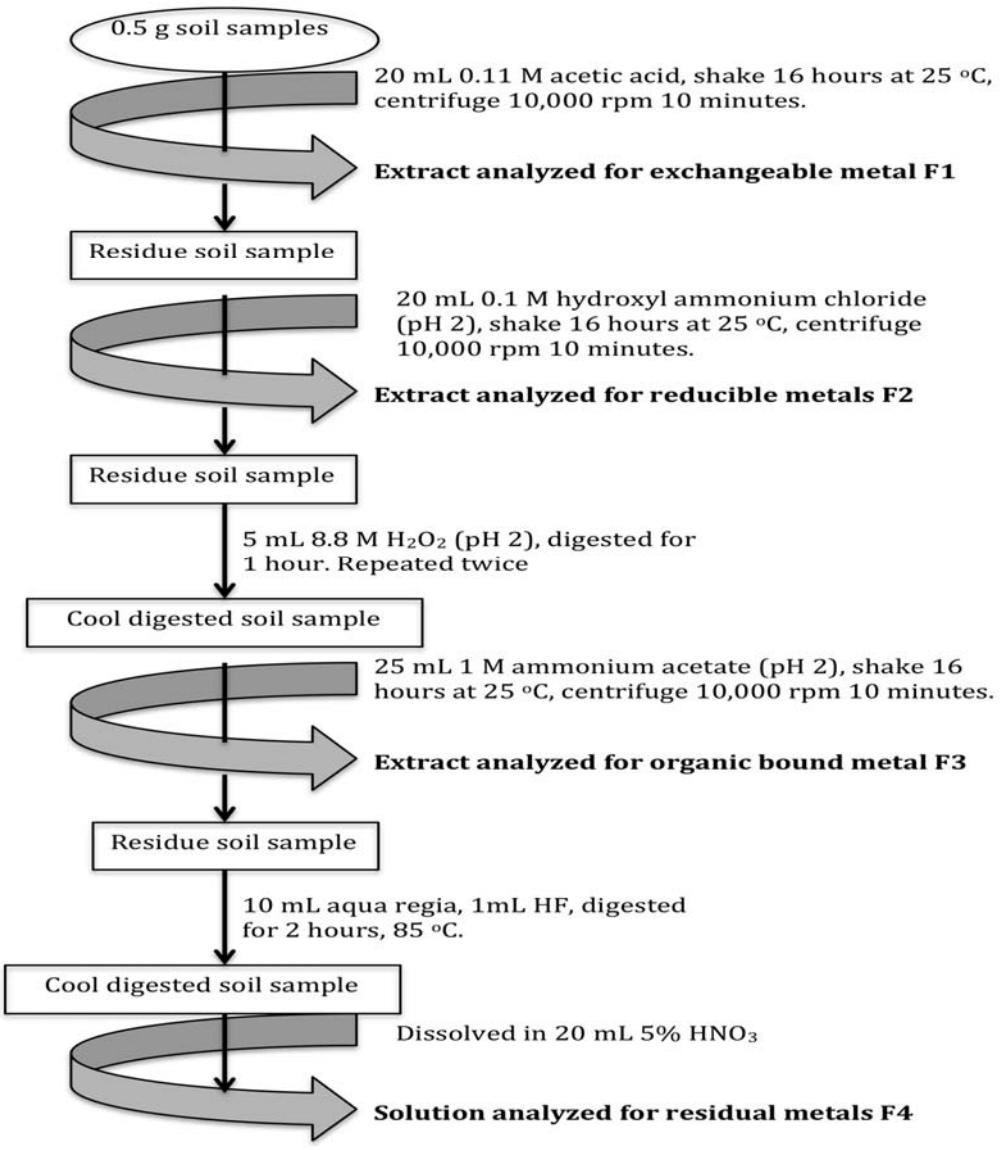

Figure 3-9: Schematic diagram of the extraction method

Table 3.8 below shows the parameters at which the microwave digestion is operated under. Furthermore, Figure 3.10 shows the apparatus used to conduct the microwave digestion in question.

Table 3-8: Operational parameters for microwave digestion

No	Steps	Power (W)	Time (Min)	Fan level
1	Power ramp	900	5:00	1
2	Power hold	900	20:00	1
3	Cooling		15:00	3

Upper limits for control parameters:

- Pressure increase Rate: 0.5 bar/s
- Pressure: 80.0 bar
- Microwave Power: 900 W
- Internal temperature: 280 °C
- IR temperature: 280 °C
- Vessel: 50 mL Glass
- Sample: 250 mg
- Control mode: Pressure

Table 3-9: Anton-Paar Microwave Reaction System – Multiwave Pro Specifications

Subsystem	Firmware Version	Hardware Version	Serial Number
Instrument Type	Multiwave	.	91136346
Instrument	1.10.4711.4		
Data Model	207		
Operating System	3.911		
Multiwave CPU Board	1.000.036	1.000.001	18347593
Multiwave Power Board	15.0		

Figure 3-10: Anton-Paar Microwave Reaction System – Multiwave Pro

3.3.1.4 Inductively Coupled Plasma Optical Emission Spectrometry

Inductively Coupled Plasma Optical Emission Spectrometry, ICP-OES is one of the most powerful and popular analytical tools for the determination of trace elements in a myriad of sample types. The technique is based upon the spontaneous emission of photons from atoms and ions that have been excited in an RF discharge. Liquid and gas samples may be injected directly into the instrument, while solid samples require extraction or acid digestion so that the analytes will be present in a solution. The sample solution is converted to an aerosol and directed into the central channel of the plasma. At its core the inductively coupled plasma (ICP) sustains a temperature of approximately 10 000 K, so the aerosol is quickly vaporized. Analyte elements are liberated as free atoms in the gaseous state. Further collisional excitation within the plasma imparts additional energy to the atoms, promoting them to excited states. Sufficient energy is often available to convert the atoms to ions and subsequently promote the ions to excited states. Both the atomic and ionic excited state species may then relax to the ground state via the emission of a photon. These photons have characteristic energies that are determined by the quantized energy level structure for the atoms or ions. Thus, the wavelength of the photons can be used to identify the elements from which they originated. The total number of photons is directly proportional to the concentration of the originating element in the sample. The instrumentation associated with an ICP-OES system is relatively simple. A portion of the photons emitted by the ICP is collected with a lens or a concave mirror. This focusing optic forms an image of the ICP on the entrance aperture of a wavelength selection device such as a monochromator. The wavelength exiting the monochromator is converted to an electrical signal by a photodetector. The signal is amplified and processed by the detector electronics, then displayed and stored by a personal computer (Xiandeng and Bradley, 2000).

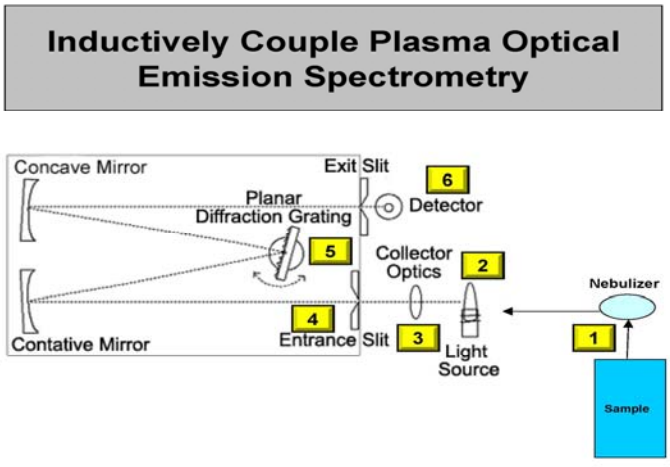

Figure 3-11: Inductively Coupled Plasma Optical Emission Spectroscopy (ICP-OES) (Jack, 2005)

3.3.2 Results and Discussion

Metal chemical speciation completed by sequential extraction of the metals is fundamental to the metal mobility (Tessier et al., 1979). The outcomes acquired demonstrate that the measures of heavy metals extracted from each fraction have significant variations with some metals and less with others per site as presented. The order of mobility of the metals considering their plenitude in the fractions is exchangeable metal > reducible or bound to oxide metal > organic bound metal > residual metals (Tessier et al., 1979). Oxides exist as nodules and bond between particles. These oxides hold trace metals and can be mobilized under reducing and acidic conditions (Ashraf et al., 2012). In the Bellville, all the identified metals were found be most abundant in the residual fraction with abundances ranging from 50.8 % to 85.5 % as presented in Figure 3-12. These heavy metals are contained in the crystal grids of minerals with solid ties and subsequently, they will not be discharged into the earth (Ashraf et al., 2012, Ogundiran and Osibanjo, 2009, Ideriah et al., 2013, Borgese et al., 2013). Metals present in the residual fraction are a measure of the level of natural contamination. The higher the metals exhibit in this portion, the lower the level of contamination (Howari and Banat, 2001).

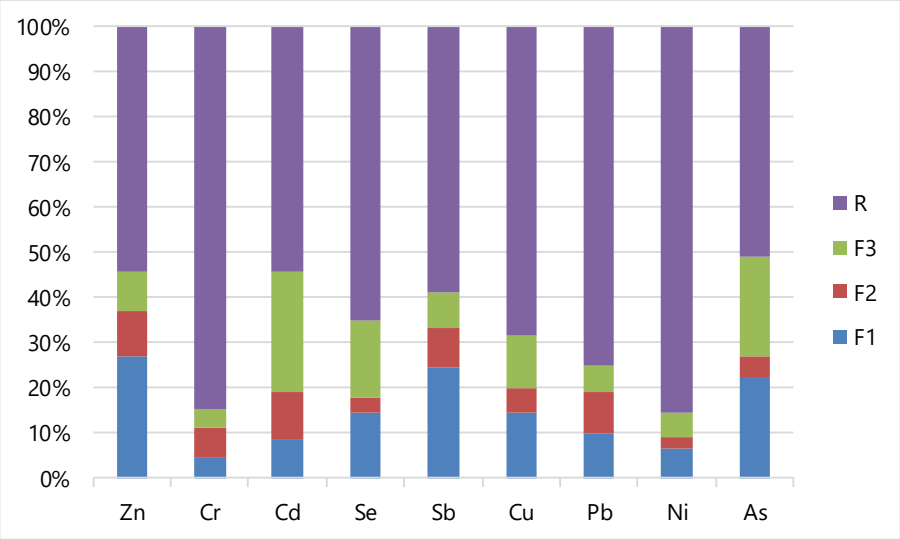

Figure 3-12: Bellville landfill metal chemical speciation is given by % abundance of each metal in each fraction of sequential extraction.

In Coastal Park, 4 of the 9 identified metals were most abundant in the residual fraction namely Cr (78.4±7.7 %), Cu (50.0±17.1 %), Pb (65.9±16.9 %) and Ni (66.8±11.8 %). Zn and Cd were found to be most abundant in the exchangeable fraction for Coastal Park with 38.8±21.6 % and 39.4±20.5 % abundance respectively for each. Se and Sb were found to be almost evenly

distributed between the residual fraction and the exchangeable fraction with Se being 30.9±17.0 % in the exchangeable fraction and 34.9 %±15.3 % in the residual fraction. While Sb was 34.3±14.2 % in the exchangeable fraction and 34.8±12.8 % in the residual fraction. As in Vissershok site was most abundant in the exchangeable fraction at 32.5±18.7%. A significant amount of As was also evenly spread between the organically bound fraction and residual fraction being 25.6±8.4 % and 28.7±12.6 %. The organic fraction is generally steady in nature, however, can be activated under solid oxidizing conditions because of degradation of organic matter (Huang et al., 2007, Tessier et al., 1979). The exchangeable stage represents the mobile and bioavailable heavy metal fraction. In this stage, the heavy metals have more labile limits and can be effectively discharged into the earth. The presence of heavy metals in this stage where they can be taken up by plants from the soils is the most unsafe to the environment (Ashraf et al., 2012). The Coastal Park site metal chemical speciation is presented in Figure 3-13.

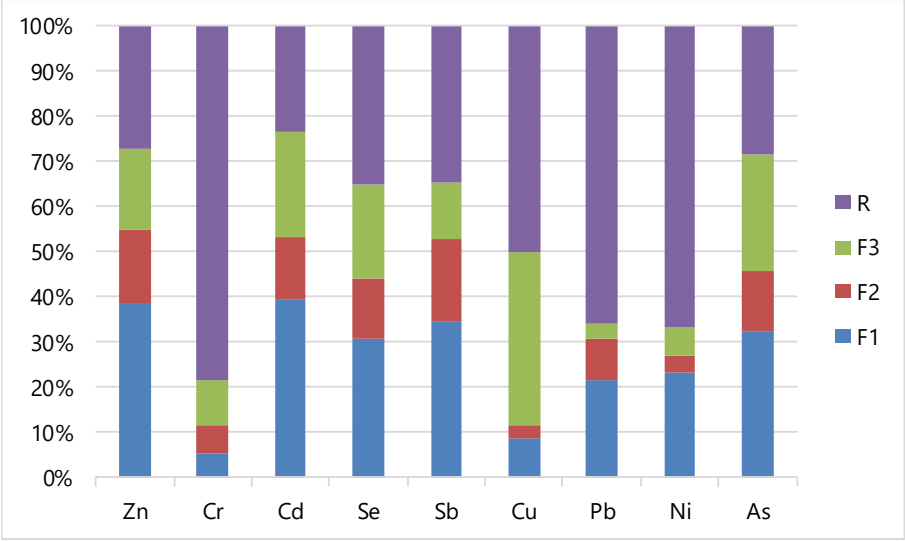

Figure 3-13: Coastal Park site metal chemical speciation given by % abundance of each metal in each fraction of sequential extraction.

Vissershok site metal speciation results showed that all the metals analysed were abundant in a combination of the fractions done in the sequential extraction method adopted for this study. Cr, Cu, Pb and Ni were most abundant in the residual fraction with abundances of 82.6±5.0 %, 61.5±16.2 %, 68.4±13.1 % and 68.3±18.9 % respectively. Zn in Vissershok site was almost evenly distributed in the exchangeable and reducible or bound to oxide metal fraction being 28.0±11.2 % and 23.3±10.4 % respectively. This then effectively makes Zn more abundant in the 2 phases when combined as they both form part of the mobile phases. In terms of the amount in the reducible or bound to oxide fraction, oxides hold trace metals and can be activated under reducing and acidic conditions (Ashraf et al., 2012). On account of Zn,

its higher extent (51.39%) is related to oxides and exchangeable fraction and just on account of an adjustment in the redox conditions towards reductive ones, Zn would be discharged from oxides. Accordingly, such changes must be normal from an anthropogenic effect (Ashraf et al., 2012). All the other remaining metals being Cd, Se, Sb, and As were more abundant in a combination of the 3 phases forming the mobile phases than in the residual fraction. The low abundance of metal in the residual fraction contrasted with its plenitude in other geochemical stages shows higher mobility of the metal in the earth. This demonstrates that these metals would effortlessly be discharged to the earth and possibly be exceedingly toxic. Figure 3-14 shows the graphical representation of the Vissershok site metal chemical speciation.

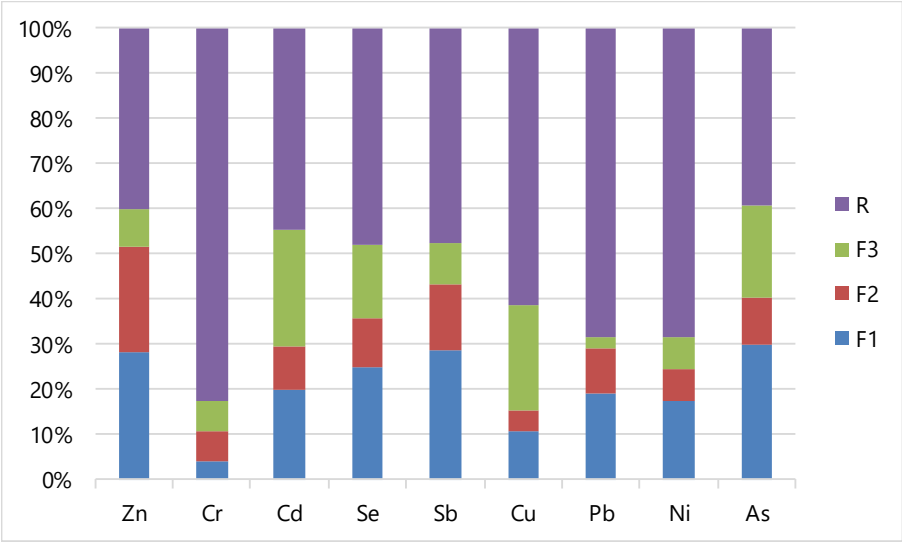

Figure 3-14: Vissershok site metal chemical speciation given by % abundance of each metal in each fraction of sequential extraction.

The sum of concentrations of metals in various geochemical stages can be utilized to express the potential mobility of metals. The potential mobility of metal can be surveyed by adding up the results of the exchangeable fraction, reducible or bound to oxide fraction and the organic bound fraction (Huang et al., 2007). Bellville site showed that all the metals have potential mobility of less than 50%, meaning that the metals are less likely to be discharged into the environment because the abundance of the metals is largely in the residual fraction. In analysing the results for Coastal Park site, Pb and Ni were found to 34.1% and 32.2% likely to be discharged into the environment with Cu being on the 50% mark of potential mobility. The potential mobility of the rest of the analysed metals was above 50% ranging between 65.1% and 76.3%, meaning that these metals are easily discharged into the environment with the potential of being highly toxic. In Vissershok site, Cu, Pb and Ni had a potential mobility of 38.5%, 31.6% and 31.7% respectively, meaning these metals are less likely to mobilize into the

environment while the rest of the metals were found to be more like to mobilize with potential mobility ranging from 52.5% to 60.6% These results are presented in Figure 3-15.

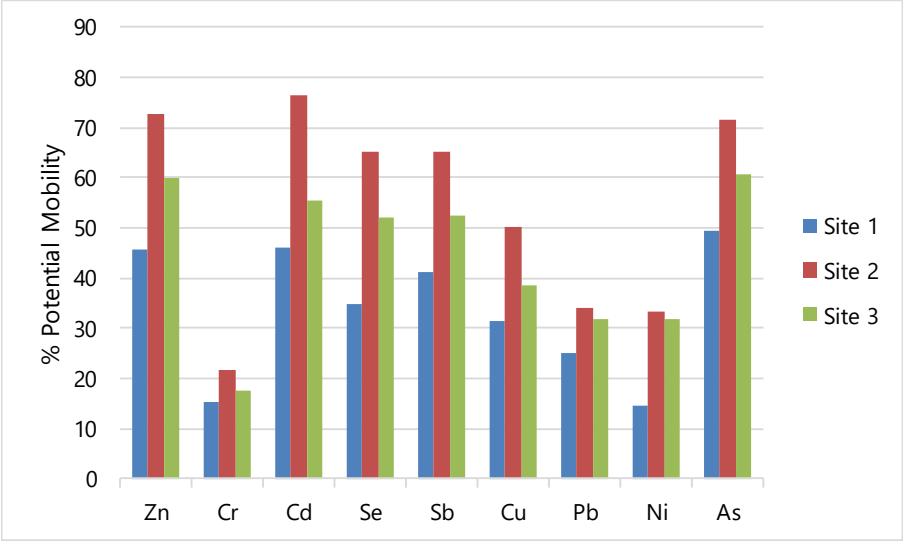

Figure 3-15: % Potential mobility of metals in the 3 different landfill sites.

It is of high importance calculate the geo-accumulation index (I_{geo}) in order to assess the level of contamination, if any, for the 9 metals considered for this study. Considering that the index considers pre-industrial or in this case, pre-landfill activity concentrations and concentrations during the period of landfill operations, the control sample was taken in areas where there is no landfill activity to use as background concentrations for each metal. Table 3-10 shows the scale of the pollution intensity for geo-accumulation. The geo-accumulation index of each metal for all 3 landfill sites is presented in Figure 3-16.

Table 3-10: Scale of the pollution intensity for the geo-accumulation index values (I_{geo}) classes with respect to the soil quality (Zamani-Ahmadmahmoodi et al., 2013).

Class	Value	Soil Quality
0	$I_{geo} \leq 0$	Practically uncontaminated
1	$0 < I_{geo} \leq 1$	Uncontaminated to moderately contaminated
2	$1 < I_{geo} \leq 2$	Moderately contaminated
3	$2 < I_{geo} \leq 3$	Moderately to heavily contaminated
4	$3 < I_{geo} \leq 4$	Heavily contaminated
5	$4 < I_{geo} \leq 5$	Heavily to extremely contaminated
6	$5 > I_{geo}$	Extremely contaminated

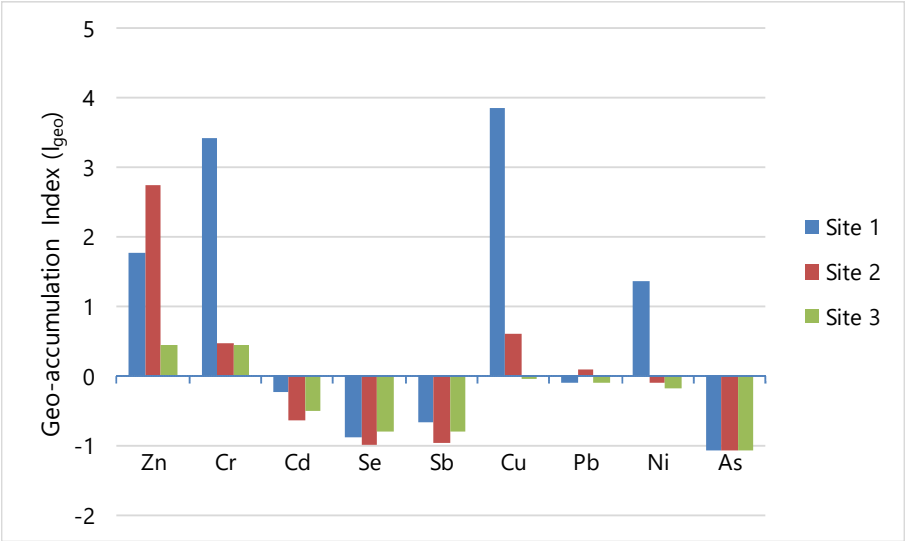

Figure 3-16: Geo-accumulation index of each metal for each landfill site

Bellville site shows that Cu and Cr were at a class 4 contamination level meaning that the site is heavily contaminated with Cu and Cr while Zn and Ni were in class 2 contamination level meaning the site is moderately contaminated with these metals. The metals Cd, Se, Sb Pb and As were all found to be at class zero contamination, meaning that the site is practically uncontaminated with regards to these metals. Coastal Park site Zn contamination was found to be a class 2 classifying the site as moderate to heavily contaminated with Zn. Coastal Park site had Cr, Cu and Pb at class 1 meaning the soil is uncontaminated to moderately contaminated with regards to these metals. The rest of the metals were found to be at class zero contamination. Regarding the geo-accumulation index for Vissershok site, only Zn and Cr were found to be at class 1 contamination while the rest of the metals were all found to be class zero for this site.

After examining the chemical speciation and risk to the environment because of the heavy metals, their potential antagonistic health effects caused by exposure to the landfill soil were evaluated. The reference measurement values and the slant factors were taken from the US Department of Energy's RAIS (Risk Assessment Information System) aggregation (U.S. Deparment of Enegry, 2000). On account of Cu, Sb and Zn, the inhalation reference concentration values (RfCi) were substituted with reference dose values (RfD) after considering the correction factor (U.S. Deparment of Enegry, 2000). The statistical manipulation depends on the assumption that after inhalation, the retention of the molecule bound toxicants will bring about comparative health effects as though the particles had been ingested (Ferreira-Baptista and De Miguel, 2005). The contents of metals bound to the mobile fractions of the

considered metals were utilized to figure the chemical daily intake (D_{dermal}, $D_{ingestion}$, $D_{inahaltion}$) for assessment of exposure.

Table 3-11 shows the results obtained in calculating the Hazard Index (HI) for possible non-carcinogenic health effects and Cancer Risk (CR) for all the metals considered, for each landfill site and for both adults and children. HI was assumed to be the sum of all the Hazard Quotients (HQ's) made up of Dermal, Ingested and Inhalation pathways. All the HQ values for all metals in all the sites were found to be below the limit HQ=1, meaning all sites were currently at no risk of detrimental non-carcinogenic health effects from neither of the 3 pathways for both adults and children. HI was also found to be below the threshold of HI=1 for all the metals in all the sites meaning there is currently no risk of non-carcinogenic health effects for both adults and children. For the Bellville site, the HI values for adults ranged between 1.40×10^{-4} and 7.45×10^{-2} and ranged between 6.03×10^{-6} and 3.87×10^{-1} for children. The HI ranges for Coastal Park site were 9.99×10^{-5} - 2.20×10^{-1} and 4.82×10^{-6} - 7.63×10^{-1} for adults and children respectively. For Vissershok site, the HI ranges for adults and children were 1.04×10^{-4} - 1.38×10^{-1} and 6.41×10^{-6} - 4.27×10^{-1} respectively.

Table 3-11: Hazard Index (HI) and Cancer Risk (CR) values for all 3 landfill sites with regards to all metals analyzed

				Bellville					
Parameters	**Zn**	**Cr**	**Cd**	**Se**	**Sb**	**Cu**	**Pb**	**Ni**	**As**
HI Adults	7.45E-02	1.43E-03	2.56E-04	2.89E-03	1.28E-02	1.16E-02	2.93E-04	1.40E-04	1.64E-02
HI Children	2.66E-05	4.21E-03	2.93E-02	3.59E-03	2.52E-02	6.87E-06	6.03E-06	7.51E-04	3.87E-01
CR Adults	2.96E-08	2.14E-06	1.56E-06	0.00E+00	0.00E+00	1.63E-07	2.93E-06	2.34E-06	7.36E-06
CR Children	2.01E-12	6.32E-06	1.79E-04	0.00E+00	0.00E+00	1.84E-11	6.03E-08	1.26E-05	1.74E-04
				Coastal Park					
Parameters	**Zn**	**Cr**	**Cd**	**Se**	**Sb**	**Cu**	**Pb**	**Ni**	**As**
HI Adults	2.20E-01	6.04E-04	4.22E-04	5.61E-03	1.30E-02	6.02E-04	3.62E-04	9.99E-05	2.60E-02
HI children	2.21E-05	1.64E-03	2.90E-02	1.19E-02	2.79E-02	7.59E-06	4.82E-06	6.83E-04	7.63E-01
CR Adults	8.73E-08	9.07E-07	2.58E-06	0.00E+00	0.00E+00	8.50E-09	3.62E-06	1.68E-06	1.17E-05
CR Children	1.66E-12	2.46E-06	1.77E-04	0.00E+00	0.00E+00	2.04E-11	4.82E-08	1.15E-05	3.44E-04
				Vissershok					
Parameters	**Zn**	**Cr**	**Cd**	**Se**	**Sb**	**Cu**	**Pb**	**Ni**	**As**
HI Adults	1.38E-01	4.56E-04	3.48E-04	4.95E-03	1.14E-02	3.80E-04	3.05E-04	1.04E-04	2.24E-02
HI children	1.58E-05	1.47E-03	2.63E-02	1.46E-02	3.97E-02	8.95E-06	6.41E-06	5.65E-04	4.27E-01
CR Adults	5.48E-08	6.84E-07	2.12E-06	0.00E+00	0.00E+00	5.37E-09	3.05E-06	1.74E-06	1.01E-05
CR Children	1.19E-12	2.20E-06	1.60E-04	0.00E+00	0.00E+00	2.40E-11	6.41E-08	9.48E-06	1.92E-04

When considering the carcinogenic risk CR, the safe range is from CR = $1x10^{-6}$ to $1x10^{-4}$. In analysing the results for Bellville site, it can be observed that for adults, the results of Cr fall below or within the safe range for all the metals ranging from 0 to 7.36×10^{-6}. With regards to children, CR for the metals Cd and As was above the threshold range being 1.79×10^{-4} and 1.74×10^{-4} for each metal respectively. This means children are at risk of developing cancerous health effects from exposure to these metals near or at this landfill site. The range of CR in the case of children in Bellville site was found to be 0 to 1.79×10^{-4}. The same trend was observed for Coastal Park site and 3 whereby there was no carcinogenic risk found for adults because all CR values for all the metals were lower or within the threshold range. The CR range for adults in Coastal Park site and Vissershok site was $0 – 1.17 \times 10^{-5}$ and $0 – 1.01 \times 10^{-5}$ respectively. The same was also true regarding the cancer risk for children as both Coastal Park site and Vissershok site had CR values above the threshold range for the metals Cd and As for both sites. CR for children in Coastal Park site with regards to these metals was found to be 1.77×10^{-4} and 3.44×10^{-4} for Cd and As respectively. In the Vissershok site, the CR values for Cd and As were found to be 1.6×10^{-4} and 1.92×10^{-4} respectively. This means that from Coastal Park site and Vissershok site, children are at the risk of developing cancerous health effects from exposure to Cd and As from these landfill sites. The ranges for CR regarding children in Coastal Park site and Vissershok site were $0 – 3.44 \times 10^{-4}$ and $0 – 1.92 \times 10^{-4}$ as presented in Table 3.11.

3.3.3 Conclusion

In this study, the results for heavy metal analysis for landfill soil samples in the City of Cape Town Municipality show that, in terms of metal chemical speciation, all the distinguished metals were found to be most copious in the residual part with plenitudes going from 50.8% to 85.5% with regards to Bellville site meaning there are limited chances of them being discharged into the earth. In Coastal Park site, 4 of the 9 distinguished metals where most copious in the residual portion to be specific Cr (78.4±7.7 %), Cu (50.0±17.1 %), Pb (65.9±16.9 %) and Ni (66.8±11.8 %). Zn and Cd were observed to be most copious in the exchangeable part for Coastal Park site with 38.8±21.6 % and 39.4±20.5 % abundance separately for each. Se and Sb were observed to be equitably conveyed between the residual and exchangeable portion with Se being 30.9±17.0 % in the exchangeable division and 34.9 %±15.3 % in the residual part. While Sb was 34.3±14.2 % in the exchangeable part and 34.8±12.8 % in the residual fraction. In Vissershok site, Cr, Cu, Pb, and Ni were for the most part found in the residual fraction with plenitudes of 82.6±5.0 %, 61.5±16.2 %, 68.4±13.1 % and 68.3±18.9 % separately. Zn in Vissershok site was equitably conveyed in the exchangeable and reducible or bound to oxide metal part being 28.0±11.2 % and 23.3±10.4 % individually. All the other remaining metals being Cd, Se, Sb, and As were more abundant in a combination of the 3

phases forming the mobile phases than in the residual fraction. Bellville site demonstrated that every one of the metals has potential portability of under 50 %, implying that the metals are more averse to be released into the earth because the abundance of the metals is in the residual fraction. In Coastal Park site, all metals but Pb and Ni had potential mobility of more than 50 % meaning that these metals are easily discharged into the environment with the potential of being highly toxic. The same potential mobility was witnessed in Vissershok site with an addition of Cu to the metals less like to be discharged into the environment. Results for geo-accumulatio index indicated that Bellville site was heavily contaminated with Cu and Cr while moderately contaminated with Zn and Ni. Coastal Park site demonstrated moderate contamination for Zn and was uncontaminated to moderately contaminated with Cr, Cu, and Pb. Vissershok site was uncontaminated to moderately contaminated with Zn and Cr. With regards to the health risk assessment, it was concluded that all the sites had no threat of any health risk being associated with exposure to the landfills for any of the studied metals for both adults and children of non-carcinogenic nature. In terms of the cancer risk, it was found that there is no threat to adults from the landfill sites through exposure to the metals observed in the study for adults, however, it was found that children are at risk of contracting cancerous health effects from exposure to Cd and As from the landfill sites.

CHAPTER 4. BIOMASS TO LIQUID

4.1 Refuse Derived Fuel (RDF)

South Africa's most abundant energy source is coal and most of the coal is of low quality, low heating value and high ash content. Per the Electricity Supply Commission, also known as "ESKOM" in South Africa, the organization relies on this coal to generate 90% of South Africa's electrical energy supply. Even with the coal, South Africa is still facing a crisis in terms of balancing power supply with demand which has resulted in ESKOM resorting to a relief procedure known to South African citizens as "Load shedding". Sasol uses the gasification of coal to produce syngas as raw material for petroleum production. However, coal is somewhat, "dirty" source of fuel due to its polluting nature. Petro SA converts natural gas into liquid fuels, however, reserves are low. MSW, on the other hand, offers a sustainable, non-exhaustible and non-season dependent source of raw material to produce any form of energy. RDF is a form of fuel that is derived from numerous types of wastes including MSW. RDF is largely composed of combustible types of waste such as non-recyclable plastics, cardboard, paper, labels and other corrugated materials (Williams, 1998). MSW is a fuel of inferior quality as a raw form. Thus, in order to improve the fuels consistency, storage and handling characteristics, combustion behaviour and calorific value, it is important to produce RDF from it (Zafar, 2015).

4.1.1 RDF Production and Characterisation

MSW poses a processing challenge due to its heterogeneous nature. The production of RDF pellets is put in place as a remedial strategy to this. However, due to different locations and sometimes seasonal waste, the pellets themselves may still have differing characteristics in terms of composition. To limit the variations of the RDF properties in terms of the composition and thermal properties. There are 2 generic types of tried and tested RDF systems with adequate commercial applications in the United States and parts of Europe like the United Kingdom in the form of coarse RDF which are the pellets and fluff RDF (Williams, 1998). This study focuses mainly on the production of coarse RDF Pellets. A Johannesburg Stock Exchange-listed company by the name of Interwaste announced the launch of South Africa's first RDF plant in February of 2016 (Van Der Merwe, 2016). The existing plant is said to have an annual capacity of 12 000 tons of waste converted into alternative fuel for use in South Africa's manufacturing sector as reported by the CEO of Interwaste. The South African white paper on renewable energy 2003 set out a target of 10 000 GWh of energy from alternative and renewable sources of energy by the year 2013 (Department of Minerals and Energy, 2003). While South Africa has an abundance of sunlight and wind in term of electricity generation, the potential for RDF should not be underestimated. According to the Director of Technical

Services at Interwaste, the main problem for RDF in South Africa is that the country simply could not afford it. The European model uses highly sophisticated technology and costs approximately € 45 per ton of waste which converts to R 648.53 South Africa Rands (Van Der Merwe, 2016).

As with any other process, pelletisation of MSW has some advantages and disadvantages. The advantages of waste pelletisation are as follows:

1. MSW in pelletized form provides a homogenous feed, this then alleviates the hassles of controlling the flow rate of a reactor, prediction of conditions, and controlling of the system.
2. Pelletized waste has reduced storage requirements. Waste materials are compressed when in the form of pellets, therefore, requiring less space compared to untreated waste (Belgiorno et al., 2003).
3. Untreated MSW has a limit in terms of storage in waste bags when collected at the waste collection centre since it runs a risk of firing and bacterial pollutants when stored for more than 3 days.
4. Transportation and handling costs are significantly lower as pelletized waste provides an efficient way for loading, unloading and handling of the waste from the waste collection centre to the process plant.
5. Distribution of the waste and odour problems in the environment would be controlled better by waste pelletisation (Uslu et al., 2008).

The disadvantages of pelletisation lie in the fact that when the density by compaction is increased, the active surface area will be decreased then the reaction rate will be decreased and the reaction time will be increased.

The unit operations applied to produce the RDF pellets are as follows:

4.1.1.1 Pre-treatment

4.1.1.1.1 Separation

The separation process starts with the collection of un-segregated municipal waste, including organic waste (primarily food waste) and materials like paper, cloth, plastic and wood that provide the calorific value required to burn. Before these can be formed into pellets, however, the combustible wastes must be separated from non-combustibles such as glass and metal, and the larger items must be broken into smaller pieces. Ideally, during the separation stages, hazardous materials would be removed completely. All sorts of ferric and non-ferric metals must be detected and are removed from the waste stream via magnetic separation. Separated

metals can be recycled. The reason is that even a very small amount of metal could destroy the pellet mill equipment.

4.1.1.1.2 Drying

This important step in the process differs in each facility depending on the investment or land availability. Solar drying is not possible during rainy seasons, and most facilities run at a fraction of their capacity during the rains, sending most of the waste to landfills. Mechanical drying, on the other hand, requires significant amounts of energy that could easily render RDF plants unprofitable without huge government subsidies.

To produce a pellet of good quality, an important factor of the feedstock, namely the moisture content needs to be taken into consideration. The moisture content of the untreated MSW tends to be high and it has a direct influence on the gas composition as well as the energy balance of the process. Taking the viewpoint from a gasification perspective, high moisture is undesirable because more energy will be required for evaporation. Depending on the required product gas and the process design, controlling moisture content is of paramount importance. The desirable feedstock moisture content for applications in gasification is in the range of 10-15 %. This is because when the wet produced pellet is dried, it develops cracks due to lack of moisture leaving the pellet fragile (Kahl, 2003). When the moisture content is below the range, it is also observed that there is increased friction between the feedstock and the dies in the pellet which can ultimately lead to blockages in the pellet mill (Cummer and Brown, 2002, Lestander et al., 2009, Uslu et al., 2008, Zafar, 2009). There is a vast range of driers that can be employed to achieve the desired moisture content and they can be classified into categories of conduction, convection, radiation, depending on the methods of heat transfer used (Baker, 1997, Grossel, 1998), with the majority of the drying equipment being convective with a statistic of 85 % to be exact (Grossel, 1998). The difference between convective and conductive driers is that with the former, the materials and drying medium are in direct contact whereas, with the latter, the materials dry by means of indirect heating. They can also be continuous or batch based on the mode of operation. Another way in which drying equipment can be categorised would be with regards to the type of vessel employed for the operation such as pneumatic spray, tray rotary drum and fluidized (Baker, 1997, Grossel, 1998). When it comes to the drying of MSW, there lies the possibility of emissions during the drying process caused by the evolution of volatile organic compounds and this phenomenon occurs when the drying operation is conducted at temperatures exceeding 100 °C (Cummer and Brown, 2002). Another hazardous matter to be taken into consideration in the drying process lies in the risk of firing the drying vessel due to combustible gases exploding which might have been evolved during drying. The process becomes dangerous when conducted at high temperatures and the

concentration of oxygen in the vessel is in excess of 10 % because an explosion is highly likely to occur (Cummer and Brown, 2002). The selection of a dryer is dependant on a variety of factors such as the required quality of the product, the particle size, energy requirements, environmental impact as well as the residence time (Baker, 1997, Cummer and Brown, 2002, Grossel, 1998). Driers that run in continuous process configuration have residence times varying from minutes up to 2 hours operating with atmospheric pressure and hot air as the drying medium as most dryers are convective (Baker, 1997, Grossel, 1998). One of the most common dryers used in commercial and industrial scale for the application of biomass drying is the Rotary cascade dryer. The dryer consists of a cylindrical shell with a diameter in the range 1m to 6 m inside the shell. The dryer has vanes that elevate materials and flood them through the cylinder with an angled slope in order to allow the materials to move through the drier during rotation (Cummer and Brown, 2002).

4.1.1.1.3 Size Reduction

The dimensions of raw waste are usually too large for processing equipment such as pellet mills, thus warranting a size reduction step in pre-treatment process for RDF production because most pellet mills range from 30 mm to 50 mm particle size (Agricon, 2017). This step may involve a single or a number of processes such as crushing or milling, grinding and shredding (Sahraei-nezhad and Akhlaghi-boozani, 2010).

A hammer mill was used in this study for the size reduction step and its operations are depicted in Figure 4.1 below. Hammer mills are the most commonly used machine in this process. They are regarded as most appropriate for waste material because of their low cost of energy in comparison with other size reduction machinery (Sahraei-nezhad and Akhlaghi-boozani, 2010). Hammer mills consist of rotating sets of swinging steel hammers through which the waste is passed whereby the machine can reduce the size of the waste to an 80 mm fluff like material (Sahraei-nezhad and Akhlaghi-boozani, 2010). The components of a hammer mill include a rotor disc with hammer rods for the hammer as well as a motor for rotating the rotor disc (Brown, 2014). The energy-efficient grinding process is given by the turning rotor at elevated speeds inside the mill chamber which allows the hammers to swing as the waste material is fed into the mill and the material is crushed or shattered by repeated hammer impacts, particle to particle impacts, and collisions with the grinder walls of the chamber in combination (Brown, 2014, Sahraei-nezhad and Akhlaghi-boozani, 2010).

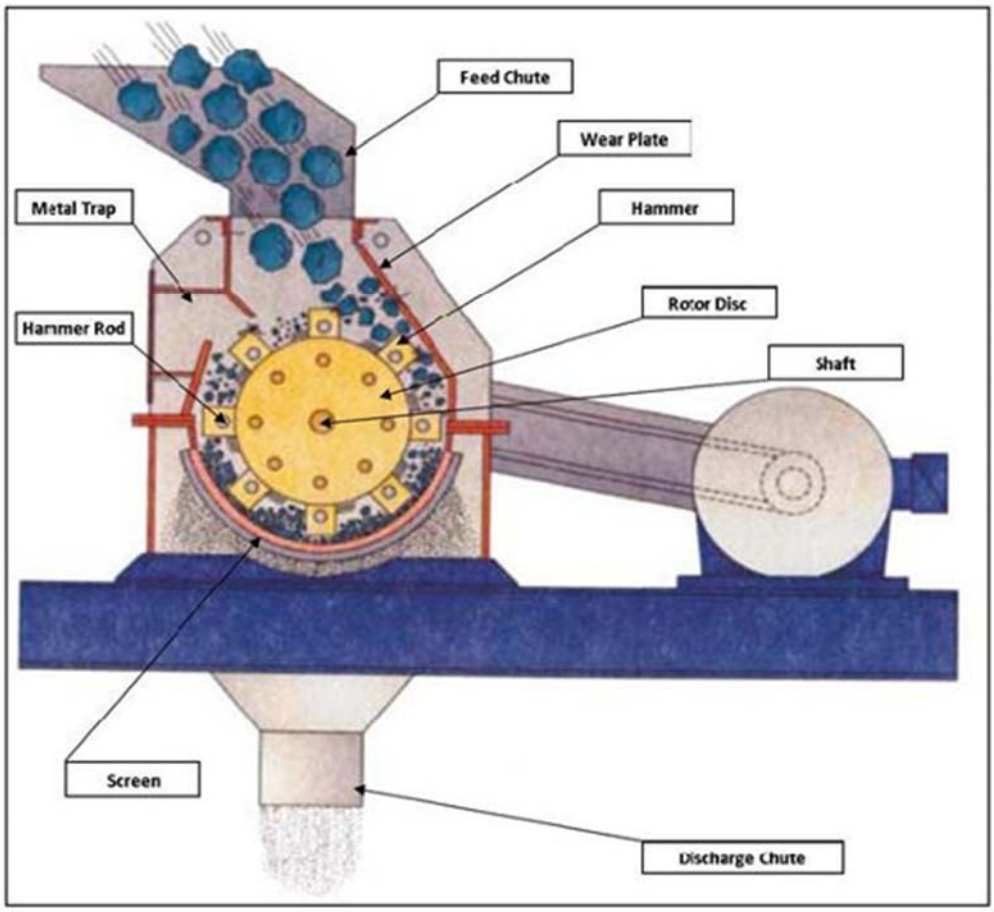

Figure 4-1: Diagrammatic representation of a hammer mill (Brown, 2014).

4.1.1.1.4 Metal Removal

To maintain the pellet mill equipment in good working order, it is essential that all potentially harmful metals of ferrous and non-ferrous nature be detected and eradicated from the waste. This process is conducted by means of magnetic separation and recovered metals can be recycled with economical value (Sahraei-nezhad and Akhlaghi-boozani, 2010).

4.1.1.1.5 Pellet Production

The production of the actual pellets is regarded as the most energy-intensive as it is where the compaction and densification of the crushed or fluffed waste material occurs in order to form the pellets (Sahraei-nezhad and Akhlaghi-boozani, 2010). A method of reducing the energy demand of pellet production is increasing the feed temperature, however keeping in consideration that temperatures in excess of the 100 °C mark would cause the emission of volatile compounds (Arshadi et al., 2008). The quality of the pellet is mainly determined by hardness and stability and to achieve this quality, the use of binders may be applied (Cherney,

2006). Pellet mills are designed in two distinct types namely the ring die pellet mill and the flat die pellet mill (PelHeat.com, 2014).

The ring die mill has its die positioned vertically, such that the material entering the mill does so through the centre of the die and is compressed through by a series of compression rollers (PelHeat.com, 2014). Stationary knives are usually attached to the outside of the ring die in order to cut the pellets to the desired length upon exiting the mill (Cherney, 2006, PelHeat.com, 2014). The ring die pellet mill is commonly designed in a manner whereby the die is powered and rotating while the compression rollers are set in motion by the friction and movement of the die (PelHeat.com, 2014).

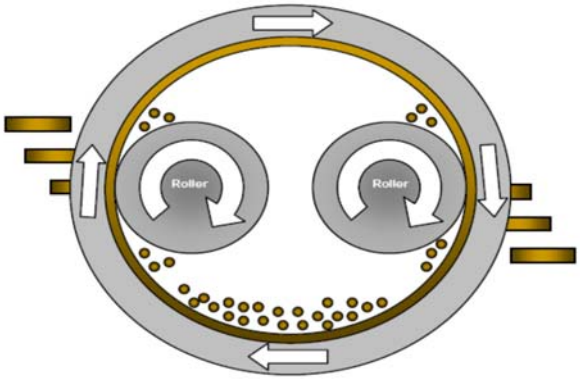

Figure 4-2: Basic design and operation of a ring die pellet mill (PelHeat.com, 2014).

The flat die pellet mill is made up of two main components namely the rollers and perforated die (Sahraei-nezhad and Akhlaghi-boozani, 2010). Feed material to the mill enters from above and moves between the rollers and is then compressed through the die. The finished pellet then emerges from the base of the die upon exiting the pellet mill (PelHeat.com, 2014)

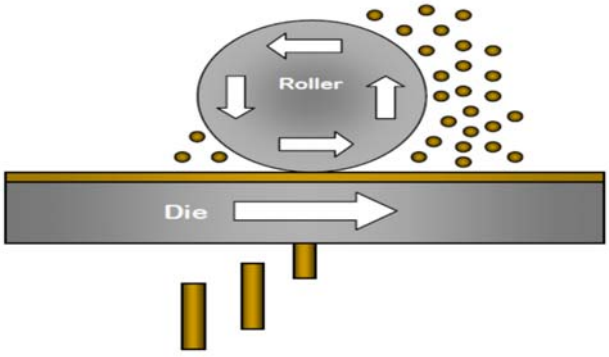

Figure 4-3: Basic design and operation of a flat die pellet mill (PelHeat.com, 2014).

4.1.2 Methodology

4.1.2.1 Source of Sample

All MSW samples used were collected from the mixed waste sections of the drop-off facilities and transfer stations around the City of Cape Town municipal area. The mixed waste section is chosen as this is the waste that is to be disposed of in the landfills. At least four sample bags of mixed waste samples were collected from each site to get a good representative of the specific sample site.

4.1.2.2 RDF Pellet Production

MSW poses a processing challenge due to its heterogeneous nature. The production of RDF pellets is put in place as a remedial strategy to this. However, due to different locations and sometimes seasonal waste, the pellets themselves may still have differing characteristics in terms of composition. To limit the variations of the RDF properties in terms of the composition and thermal properties the following steps were implemented in production:

1. The MSW samples were reduced in size proportions with regards to the large components of the collected samples by means of a hand-held scissor. All the large components of a specific sample must be cut into smaller pieces to allow for ease of handling.
2. Samples were then dried in a temperature-controlled oven at approximately 60 ℃ over a 5-hour period.
3. The dry samples were then further reduced in size using a hammer mill to form a fluff like powdered material.
4. A sample splitter was then used to obtain composites of the now powdered form MSW sample.
5. Waste material was then combined with different materials that are to act as a binder in varying ratios as per the most efficient in terms of effectiveness and amount used:

- 5 % Guar gum starch
- 5 % Modified corn starch

The starch binders were mixed in water before added to the waste to form a paste-like a mixture with adequate moisture content to allow for pelletisation to take place. Other binders used and the percentage thereof is as follows:

- 50 % Waste palm oil
- 50 % Waste engine oil

The oil binders were not mixed in water before adding to the waste because they are already in liquid form and can be readily mixed into the waste sample. The reason for the higher

percentage is because at low percentages, the mixture was not well mixed to allow pelletisation to take place, hence the ideal percentage was found at 50%.

The percentage of binder used was determined on a trial and error basis, based on the quality of the formation of the pellets after the palletisation takes place. The aim was to acquire a ratio whereby minimal binder is used to keep operating costs low in the cases where binder needs to be purchased.

6. The waste now mixed with binding material was pressed in a hydraulic press with a pressure of 10 tons which equates to 98066.5 Pa to form pellets of 13.2 mm diameter
7. The product pellets were then dried as in step 2.

Figure 4-4: Specac manual hydraulic press with ICL evacuable pellet die set.

By applying this method, the samples were expected to exhibit the same kind of properties or a very small to a negligible range of variation.

4.1.2.3 Calorific Value Determination

It is important to know the amount of energy the MSW mixed waste samples contain as a means of understanding the potential of the waste feedstock as a source of fuel. This was done by means of an E2K Bomb Calorimeter. The instrument is used to determine a sample's energy content in terms of the calorific value. This measurement is achieved by combusting the sample in a pressurized vessel which is pressurized with oxygen up to 3000 kPa. Since the vessel is filled with oxygen, the apparatus is able to achieve complete combustion of the sample in question. After the process is complete, the device gives a result as a CV value in MJ/kg. The sample mass used in the apparatus is 0.5 grams. Through the bomb calorimeter, the energy that will be liberated from the MSW during a combustion process will be determined, thus giving an idea of how and where the energy can be used. Figure 4.5 below shows the apparatus used to determine the calorific value.

Figure 4-5: e2K Bomb Calorimeter set up (Parr Instrument Company, 2007).

4.1.2.4 Thermogravimetric Analysis

The significance of understanding the thermal stability of the MSW sample is that it gives a clear picture of how the feedstock will degrade under thermal processing. This will help in the fact that it gives a guide as to how the process parameters can be manipulated during an optimization procedure. The method used in the analysis is as follows:

1. The analysis begins where the waste sample is heated in an inert environment of N_2 from (20 -900) °C at a heating rate of 20 °C/min
2. At 900 °C, the temperature is then maintained for 15 min in an N_2 environment.
3. With the temperature still maintained at 920 °C, O_2 is then introduced to the system and maintained for 15 min.

The TG curve is obtained by plotting the mass loss% against the temperature. From these curves, the data for proximate analysis can be obtained by finding the major mass loss regions and correlate them to the relevant property in terms of volatile matter, fixed carbon, ash content and moisture content

4.1.3 Results and Discussion

4.1.3.1 Calorific Value

In a preliminary study conducted, in total, 30 samples were tested amounting to 10 sample sites completed. Each sample site was analysed 3 times to ensure the integrity of the results.

The averaged results for each sample site are presented in Figure 4-6. The results presented in Figure 4.6 represent the raw milled and unpelletised samples of MSW on a dry basis. The averaged calorific value measurements, of the samples in the total range from approximately 15 to 25 MJ/kg averaging out to approximately 19 MJ/kg. In an analysis of the samples, there were samples that showed higher energy levels with one sample from Ladiesmiles maxing out at 28.9 MJ/kg. This sample and others that had calorific values above 20 MJ/kg were all found to have one thing in common and that is there was a significant amount of non-recycled plastics, like plastic bags and some plastic bottles. Columbia University Earth Engineering Centre found these plastics to have a calorific value of approximately 32 MJ/kg (Themelis and Mussche, 2014) as reported in Table 2-2 of chapter 2.

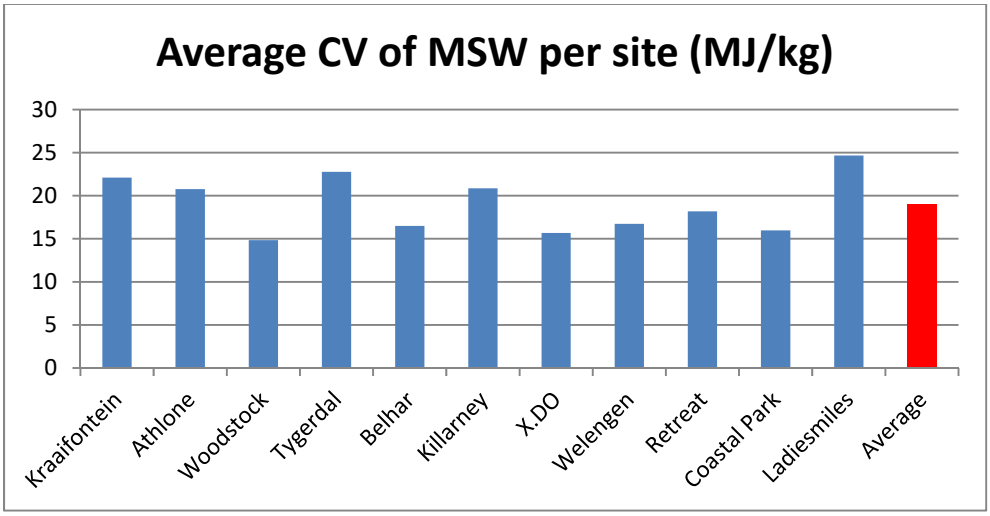

Figure 4-6: Calorific values of each site on average with the overall average (Hlaba et al., 2016).

Studies conducted in Changzhou and Guangzhou in China show raw MSW of low calorific value reporting at 3 to 4 MJ/kg while in Kuala Lumpur, Malaysia and Parona, Italy report values ranging 10 - 16.8 MJ/kg and 10.5 – 16.17 MJ/kg respectively (Zhang et al., 2010). This difference in the calorific value of the waste can be attributed to the presence or lack thereof of NRP's in the waste in question. All the locations mentioned above are developed areas in the world, which means the difference in calorific value might depend on the level of sorting and recycling practices in each area's waste management facilities, hence determining the amount of NRP's present in the waste. An example of such practices would be that practised in many communities where the NRP's are converted into oil by means of a pyrolysis process (Themelis and Mussche, 2014). This then means that the NRP's would not be present in the MSW that is to be landfilled. In the case of the Cape Town samples, however, not such processing is in place in the current waste management structure of the city municipality, however, there are still areas that show quite low calorific value. As mentioned earlier, the averaged range is between

15 and 25 MJ/kg. The areas with a calorific value of approximately 15 MJ/kg had MSW of similar composition as displayed in Figure 2.2 (Chapter 2); however, the organics fraction in these areas was found to be much higher. The Woodstock site, for instance, possesses the lowest calorific values. This is because the sample from Woodstock is mainly comprised of biomass which is essentially only wood chippings. Wood has a calorific value of about 14.4 MJ/kg according to IGNIS Energy and the average for Woodstock was 14.8 MJ/kg which is consistent. This site along with Coastal Park and Belhar exhibit similar characteristics in terms of the waste composition and calorific value. The common factor among these sites is that they are all situated near residential areas thus the waste is mainly from domestic sources which are mostly kitchen waste and garden waste, of which both fall under the organic fraction of the waste. The higher CV sample sites are situated in densely populated areas where industry and commerce are dominant meaning that the waste contains mostly plastic (packaging, bottles, carrier bags etc.), paper (office paper, cardboard packaging etc.) and still with some domestic waste from residential complexes. However, this domestic waste understandably does not have garden waste as residences are in a city centre like setting. The 15 to 25 MJ/kg result obtained is quite a vast range and just averaging from that does not give a very accurate picture in terms of the calorific value of MSW in Cape Town. Thus, it was decided that a composite sample must be prepared and analysed to get a more reputable idea of what the calorific value of the city's MSW would be on an overall basis (see Figure 4-7). In comparison to the results in Figure 4-6 and 4-7, it is deduced that the latter representing the composite sample ranges between 13 and 23 MJ/kg. However, with the composite, only one sample out of 10 runs was at the extreme low of 13 MJ/kg, as the other reading ranged from approximately 17 to 23 MJ/kg which is not as vast. This shows that the sample is close to being homogeneous which means it is a good representative sample for the overall energy content of the city's MSW.

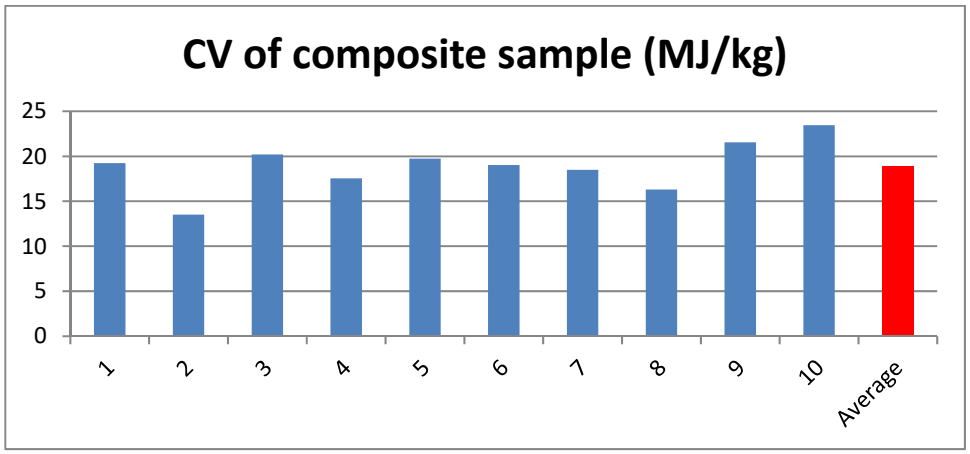

Figure 4-7: Calorific value of the composite sample and overall average (Hlaba et al., 2016)

In comparing the average CV for the composite sample and the average from the site samples, it is established that the average is reasonably close as the composite averaged out at 18.9 MJ/kg while the site sample overall average was found to be 19 MJ/kg. This indicates that it can be assumed with good reason that the average CV of the MSW is approximately 19 MJ/kg.

Studies conducted in India, Germany and Japan, show calorific values of 12-13 MJ/kg, 15-18 MJ/kg and 18 to 20 MJ/kg respectively (Jones, 2010). These calorific values were obtained from RDF pellets manufactured from MSW. On average, RDF is expected to have a calorific value ranging from 12 to 15 MJ/ kg (Jones, 2010). Interestingly so, the RDF from India with its low calorific value compared to others is used as fuel for electricity generation, thus the MSW from Cape Town is more than appropriate for the same type of application in terms of CV. It is reported that the energy–return-on-energy-invested (EROEI), for the RDF from India is in the range of 10 to 15. This is referred to as the ratio between the energy provided by a certain fuel and the energy required in the acquiring and delivery of this energy (Hall et al., 2014). The 10 to 15 range can be compared to the EROEI of a crude oil well of approximately 2000 m in depth which is quite significant (Jones, 2010).

In the preliminary study, the RDF pellets produced were of the same diameter of approximately 18 mm with varying ratio of the starch binder only used. The ratios used in terms of the ratio of starch content to MSW in the production of the pellets, ratios of 0:1, 0.5:1, 1:1 and 2:1 were used with pellet density of 326, 461, 516, and 641 kg/m^3. These results show that the pellet density is directly proportional to the amount of binder added during pelletisation (Hlaba et al., 2016). These pellets were produced using a hand-held pellet press and thus pressure could not be measured, and this method is highly subjected to human error since conditions cannot be maintained or documented. This means the density obtained from this method could not be excepted as reputable data as it is highly unreproducible. In this study, the RDF pellets produced were of the same diameter of approximately 13.2 mm with the varying binding material used. The binder materials used were guar gum powder, modified cornstarch, waste palm oil and waste engine oil in percentage mixtures with the MSW of 5 % for the guar gum and corn starch and 50 % for the waste palm and engine oil. The pellet densities are presented in Table 4-1 below:

The densities obtained using the hydraulic press at approximately 10 000 Pa show a significant difference from the ones obtained using a hand-held pellet press as these densities where much higher with the far less binding material used especially in comparison with the starch binder which was only 5 % of the total sample mass when using the hydraulic press. This then means less operating costs in terms of binder materials.

Table 4-1: Pellet densities

Binder	Density (kg/m^3)
Guar Gum	749
Corn Starch	765
Palm Oil	718
Engine Oil	743
No Binder	847

RDF pellet density is a measure of its hardness usually ranging from 250 to 700 kg/m^3 which relates to a measure of soft to very hard (Gr, 2013). The results obtained range from 718 to 847 kg/m^3 which is higher than the usual range meaning the pellets can certainly be certified as adequately rigid and stable. The pellets with no binder were found to be denser than the rest. This can be attributed to the fact that when these pellets were pressed, the samples were completely dry thus could be compressed to a higher extent as no moisture content had to be expelled during compression, meaning the waste particles can come closer together as there were no moisture molecules in between. This, however, is only applicable to the type of press used in this study as it only produces one pellet at a time which allows for more pressure to be applied during compression. Regular pelletizer machines that produce pellets in bulk would not be able to produce pellets of such high density and would normally require binder material to produce quality pellets that would not break.

The calorific value of the RDF pellets from the preliminary study was found to have the same average as the unpelletized MSW at 19 MJ/kg. This shows that the starch has no effect on the CV of the waste, however, the range of the CV from the pelletized samples was somewhat more narrow ranging from 16.8 to approximately 20 MJ/kg. This shows that the pelletized MSW or RDF is more homogenous than the unprocessed waste (Hlaba et al., 2016).

The calorific values from the new or updated study where the pellets were produced with a hydraulic press ranged from 21.1 to 27.12 MJ/kg with an average of 23.9 MJ/kg clearly showing that the density of the pellets has a direct proportionality to the calorific value of the pellets. Taking into consideration that the calorific value for the pellets with waste palm and engine oil was significantly higher at 27.1 and 26.9 MJ/kg, it could be argued that the average was elevated and better than that of the preliminary studies due to the presence of these oils. However even disregarding these pellets, the average is found to be 21.9 MJ/kg which is still higher than the 19 MJ/kg from the previous study. This then proves that pelletisation increases the caloric value of MSW.

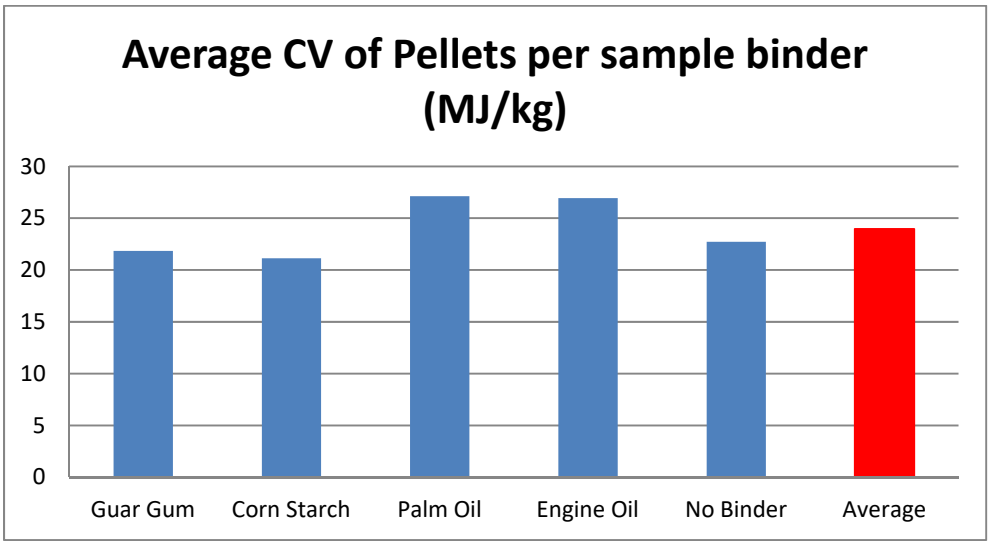

Figure 4-8: Calorific value of pellets on average including the overall average.

4.1.3.2 Thermogravimetric Analysis (TGA)

Thermal degradation of the MSW was studied using TGA. A total of 5 different samples were studied and the comparison was aimed at studying the effect of the binder material on the degradation behaviour of the RDF pellets produced. The results obtained are presented in Figure 4-9 below:

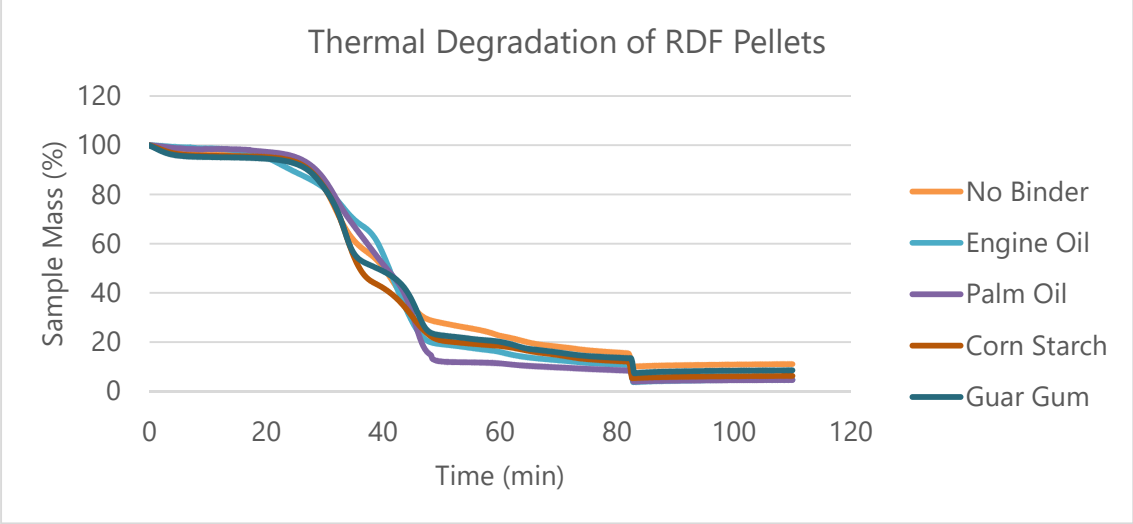

Figure 4-9: TGA curves describing the thermal degradation of produced RDF pellets

In an analysis of the results obtained, it can be deduced that all the RDF pellet samples exhibit a very synonymous trend in terms of the thermal degradation behaviour. It can be distinguished that all the samples exhibit 3 distinct major mass loss regions. Out of the 3 distinguishable regions, the second region of major mass loss is observed to have the most

significant mass loss. This is also evident in the Derivative Thermogravimetry (DTG) which describes the rate of mass loss with temperature for the samples. The third region of major mass loss is not easily disguisable from the TGA curves, however, the DTG curve shows peaks at areas where the distinguishable mass loss occurs. On the DTG curves, the second peak is observed to be the highest in all samples confirming that the second mass loss region is where the significant mass loss occurs as identified on the TGA curve.

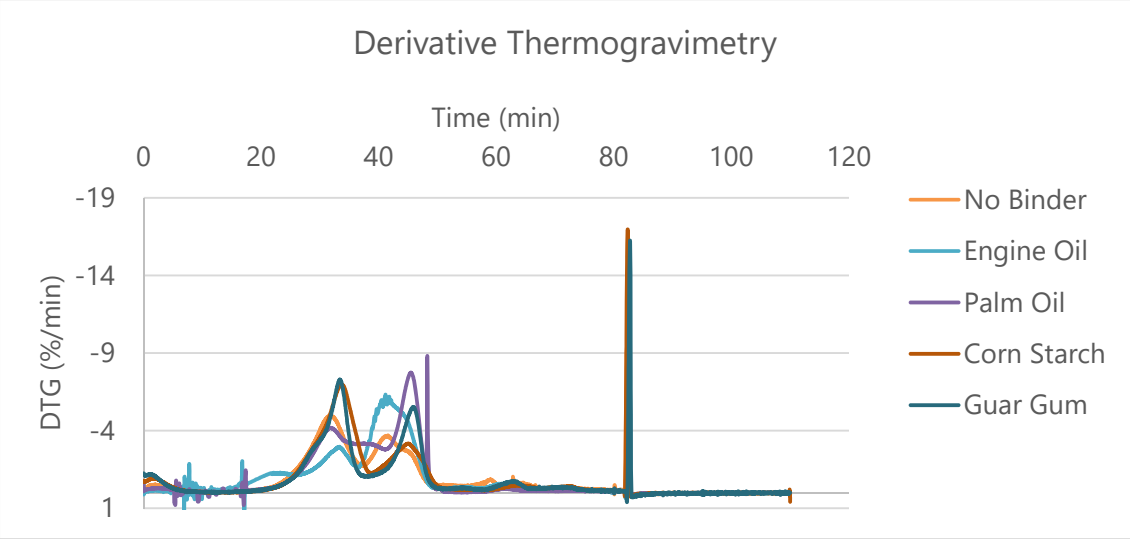

Figure 4-10: DTG curves describing the rate of mass loss of the pellets with time

Taking into consideration that the analysis took place in a nitrogen environment (inert), it can be stated that the samples were thermally degraded in pyrolytic conditions. Therefore, each degradation step can be attributed to the attributes of the samples which would be obtained in the proximate analysis. The first region of mass loss can be attributed to the removal of all moisture content present in each sample. Thus, the 2nd and 3rd regions describe the removal of all volatile matter from the samples and the point at the end of the analysis where the curve depicts a constant mass% represents the ash content of the samples. It can be argued that an assignation of the different components of MSW to the 2 peaks found describing volatile matter should be done. However, due to the constraints of this study, this could not be done. This is because the amount of each component (biomass, plastics) was not quantified as the pelletisation process was proposed as a means to eliminate the heterogeneous nature of MSW by creating a composite mix before pelletising. The composite nature of the samples before pelletisation is described in Figure 4.7. Therefore, it cannot be accurately assigned as to which of the components of MSW attributed to which peak regarding the volatile matter. This is how the proximate analysis data is then retrieved from the TGA curve (see figure 4.11). Below are the proximate analysis values as reading off the TGA curves for the pellet samples.

Table 4-2: Proximate analysis values read from the TGA curve

Pellet	Moisture %	Volatile Matter %	Fixed Carbon	Ash%
No Binder	3.50	80.9	5.60	10.0
Engine Oil	3.00	86.2	6.70	4.55
Palm Oil	2.90	88.6	4.43	4.07
Corn Starch	5.00	82.8	6.64	5.56
Guar Gum	5.60	80.9	6.12	7.38

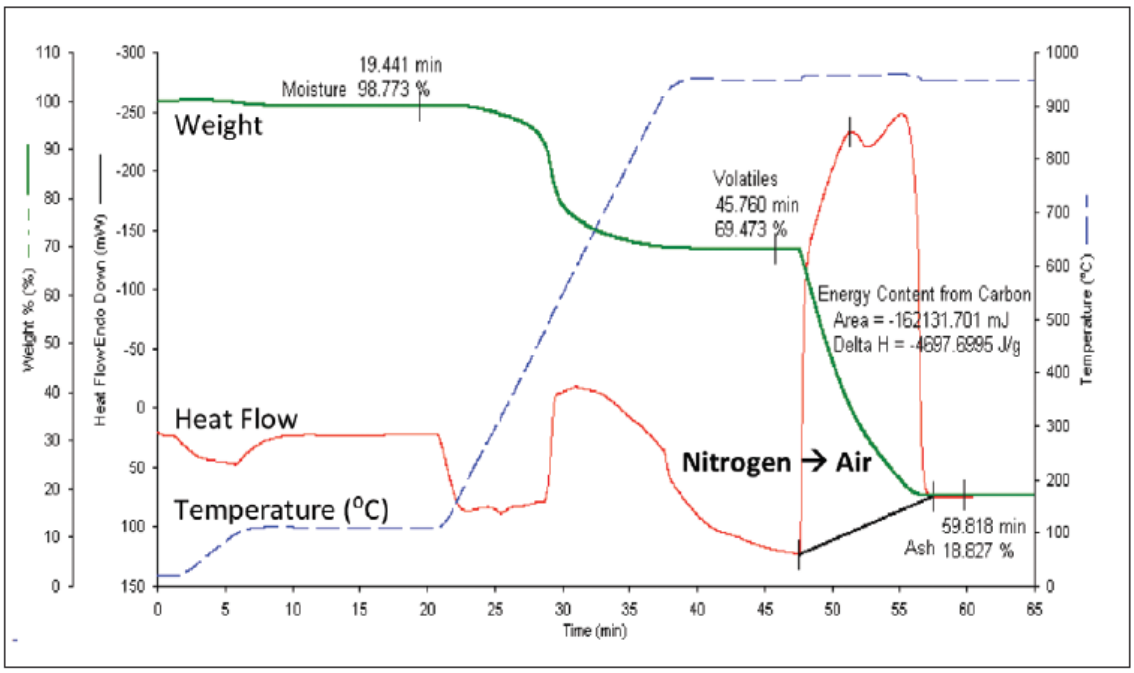

Figure 4-11: TGA proximate analysis of coal using the STA 8000 (Cassel, 2016).

In analysing the proximate analysis data read from the TGA curves, it can be deduced that the data retrieved is comparable to tests done in Malaysia and Greece, confirming the credibility of the results (Badeie, 2013, Gidarakos et al., 2006, Ismaila et al., 2013a, Jones, 2010, Kalanatarifard, 2012). The moisture content of the pellets in this study ranges from 2.90 to 5.60 %, where the pellets with corn starch and guar gum as binder had the highest moisture. This is explained by the fact that during pelletisation, the binders were mixed with water then added to the MSW fluff to form some sort of a paste-like mixture before pelletisation. The removal of moisture content begins at temperatures around 55 ℃ as the TGA and DTG curves show a slight decrease and peak respectively around this temperature and this decrease of TGA curve continues to approximately 265 ℃. The boiling point of water is 100 ℃ which explains the evaporation of moisture in this region of mass loss. A study of combustion characteristics of RDF in an oxygen environment shows similar kind of behaviour at temperatures between 50 and 150 ℃ (Li et al., 2014)

The volatile matter was highest on the pellets with palm oil and engine oil reading at 88.6 and 86.2 % respectively. The volatile nature of the binders themselves can be attributed to the volatile matter being higher than other pellets with a range of 80.9 to 88.6 %. The removal of volatile matter distinguished by a massive decrease in the TGA curve and a very high peak in the DTG curve occurs at temperatures approximately between 270 and 410 ℃. During this phase of decomposition of volatiles, taking into consideration the mixed nature of the MSW used in this study, cellulose is the major component in paper materials, hemicellulose, lignin as well as any inorganic components in the waste are completely de-volatized and the crystallinity and degree of polymerization of these polymers will impact the degradation behaviour (Bradfield, 2013, Li et al., 2014). The fixed carbon content was found to be in the range of 4.43 to 6.70 which is quite similar to the values found by (Badeie, 2013, Gidarakos et al., 2006, Ismaila et al., 2013b, Jones, 2010, Kalanatarifard, 2012). The decomposition of fixed carbon is analysed when the temperature of the TGA reaches the maximum of 900 ℃ where the TGA environment is changed from N_2 to O_2 allowing for its complete combustion. This was not the case in the preliminary study hence fixed carbon matter was not reported in that study (Hlaba et al., 2016). In terms of coal, the fixed carbon content gives a rough estimate of the heating value because this is the solid fuel left after all the volatile matter is distilled off and consists mainly of carbon (Larry, 2002). However, South African coal has a calorific value of 25.1 MJ/kg which is not significantly higher than the RDF pellets in question, although South African coal is reported to have a fixed carbon content of 51.2 %. This then brings us to the question of ash content whereby the range found for the RDF pellets was 4.07 to 10 % contrary to the 17 % reported by Larry for South African coal. Among the drawbacks brought about by ash content, the reduction of burning capacity can be attributed to the low calorific value of the coal and the low ash content of the RDF. This then explains why the calorific value is very close to that of the coal (Larry, 2002). It also needs to be considered that the RDF has high volatile matter which also contributes to the calorific value.

The degradation behaviour of these samples along with the estimated proximate analysis values approximated from the TGA data correlate with several studies conducted with RDF and raw MSW with respect to thermal processing and pretreatment (Badeie, 2013, Jones, 2010), comparison of fuel value and combustion characteristics (Li et al., 2014, Sever et al., 2016), and the pyrolysis of RDF (Kluska et al., 2014).

In terms of the effect of binder material on the thermal degradation behaviour of the samples, the overall degradation was not much affected by the binders in terms of general behaviour. However, at the end of the analysis, the amount of sample remaining was found to be different. The samples with the waste palm and engine oil binders were found to have less ash content

remaining after the calorific value determination is completed. This can be directly linked to the density of the RDF pellets produced. The density of the pellets was found to be directly proportional to the ash content, this is evidenced in the ash content of the pellets with no binder which had 10 % ash and was the densest at 847 kg/m^3.

4.1.4 Conclusion

The study conducted using MSW from the City of Cape Town Municipality in South Africa shows that the MSW has a calorific value of approximately 19 MJ/kg which is significantly high meaning that the waste can be directly used as fuel in many applications but more importantly that of electricity generation. The MSW can be converted into RDF pellets for direct use as a boiler or furnace fuel to produce high-pressure steam in power generation as the calorific value for the pelletised waste was found to be higher at 21.9 MJ/kg. In finding that South African coal has a calorific value of 25.1 MJ/kg with higher carbon content, it can be concluded that pelletised MSW would prove a suitable substitute for the fossil fuel of coal. This because MSW has far less fixed carbon content while maintaining a high calorific value. This is positive with regards to environmental considerations because the carbon footprint would be exceptionally lower than that of coal.

This is not the only possibility; more advanced thermochemical conversion techniques can also be applied to the waste to obtain high-value products like fuel gases and liquid fuel products. This then warrants the understanding of the thermal degradation behaviour of the MSW.

Using TGA, 3 distinguishable major mass loss regions were found between temperatures 55 – 265 ℃, 270 – 410 ℃ and 410 – 502 ℃. The total sample reduction was found to be more than 90 % on average which is quite a significant reduction in the waste. Studies have shown that oxygen availability in the process shows higher size reduction. This is because the process moves more towards combustion which produces CO_2 (Badeie, 2013). This is significant if a gasification process is to be applied as it also uses oxygen but less than stoichiometric requirements to create reducing conditions to produce what is called syngas which can be converted to various valuable fuel products.

4.2 Gasification

It has become a global issue to explore and exploit alternative renewable and sustainable sources of energy with the increasing demand of energy for daily living (Begum et al., 2014b). Seeing that biomass is comprised of a variety of MSW's, green waste and agricultural residues, which are found in large quantities, it is a major renewable energy contributor (Antizar-Ladislao

and Turrion-Gomez, 2008). Biomass can be processed to produce a variety of useful forms of energy such as biogas, liquid transportation fuels and syngas (Converti et al., 2009), thus making a valuable energy alternative to the conventional fossil fuels. The application of MSW gasification presents endless possibilities in energy security, mitigation of climate change and sustainable development (Begum et al., 2014b). Various thermochemical conversion techniques can transform the carbonaceous materials in biomass to a syngas product which is combustible, whereby gasification plays a lead role (Cheremisinoff and Rezaiyan, 2005). Gasification occurs when the carbonaceous material in biomass reacts with a limited gasifying agent, just enough to prevent combustion, such as oxygen, at high temperatures in a gasifier to produce combustible gas (Begum et al., 2014b, Shaohua et al., 2012).

Research on the simulation of gasification processes is somewhat limited, even though there has been a significant amount of experimental research involving MSW and other types of waste (Begum et al., 2014b). The heterogeneous nature of MSW leads to its very complex gasification process, whereby mutual influence exists and internal reactions take place (Meng et al., 2015, Zhang et al., 2013). This makes the gasification of MSW a hard process to be simulated, requiring complex mathematical modelling and iterative computations (Deng et al., 2017). Since Gibbs free energy minimisation does not require extensive knowledge of specific chemical reactions in a given process, it makes it a highly suitable thermodynamic equilibrium model to base the simulation calculation of an elaborate equilibrium system on (Shabbar and Janajreh, 2013). In recent times, researchers are making use of the Aspen Plus process simulation software to model reaction processes and solve computational problems (Deng et al., 2017). The areas of interest of these researchers have been in the combustion and gasification of coal and biomass (Mostafavi et al., 2016, Yuehong et al., 2006, Zheng et al., 2013). Aspen Plus is a large-scale software based on steady chemical process simulation, optimisation and sensitivity analysis as well as economic evaluation (Shaohua et al., 2012). The software enables researchers to simulate process operations from a single unit operation to an entire process as it provides a complete set of unit operation models (Shaohua et al., 2012).

A handful of researchers have paid attention to MSW gasification with Zheng et al. (2013) having developed an Aspen Plus model to simulate MSW gasification and melting so as to predict the composition of the gasification products. Zheng et al. (2013) along with Ramzan et al. (2011) also studied the effect of air equivalence ratio, feedstock moisture content and gasification temperature on the gasification performance. Ramzan et al. (2011) performed their study on MSW, food waste and poultry waste, and validated their model with data obtained from a hybrid biomass gasifier experiment. The effect of flue gas from the combustion section of a gasification process on syngas lower heating value (LHV) was studied by Chen (2011) using

two different types of fixed bed reactors for MSW simulation. They also studied the heat conversion efficiency and carbon conversion at different gasification temperatures and equivalence ratios. An Aspen simulation conducted by Mavukwana et al. (2013) of sugarcane bagasse gasification showed a good comparison between experimental results cited in the literature and the model results. A numerical simulation module, also developed on Aspen, of a fixed bed gasifier with varied process parameters such as equivalence ratio, gasification temperature and feedstock moisture was presented by Begum et al. (2014b). A study by Deng et al. (2017) used Aspen simulations to analyse syngas composition, LHV, and carbon conversion rate in varying process conditions such as the gasification temperature, equivalence ratio and gasifying agents.

4.2.1 Gasification Model Development

The gasification model was developed using a solid based simulation on Aspen Plus to accommodate the processing of the municipal solid waste feedstock in the form of refuse-derived fuel (RDF) pellets. This is because the simulation of heat and mass balances of a process involving solids requires a physical property model suited for solid components as physical property models used in the characterisation of a liquid substance may be deemed irrelevant for solid components (Aspentech, 2004). An advantage of having specialised property models for solids processing stems from the ability to accurately represent the solids particle size distribution which may be a crucial requirement for some processes. In this model, the operation of a fixed bed gasifier was developed for the gasification of RDF pellets on Aspen. The simulations for the process were developed on a basis of mass-energy balance and chemical equilibrium similar to the simulation studies conducted by (Begum et al., 2014b, Deng et al., 2017, Shaohua et al., 2012). The core operation of the modelled developed for this study was derived from the Aspen Plus 2004 manual titled "Getting started with solids", which gives a detailed description of the simulation model developed for the description of a coal combustion process (Aspentech, 2004). Using blocks that are consequent to reactors and other unit operations, Aspen Plus can simulate most industrial processes due to the program's vast databases comprised of thermodynamics, chemical and physical data for a wide variety of chemical compounds as well as selection of thermodynamic models that are necessary for the accurate simulation of any given chemical system (Zheng and Furimsky, 2003). As adapted from the combustion of coal simulation modelled on the Aspen manual, the developed model involves:

- The construction of a process flow using user-defined blocks to describe the gasification process.

- The specification of a global stream class, the addition of components required for gasification (conventional and nonconventional).
- Definition of non-conventional solid components (in this case RDF pellets and ash).
- Specification of physical properties for the non-conventional solid components.
- Specification of streams with the nonconvention components.
- Modification of component attributes in unit operation blocks. specification of unit operation models.
- Most importantly, the definition of Fortan blocks using fortan statements to control the drying and pyrolysis (decomposition) steps/reactions of the RDF during gasification (Aspentech, 2004).

4.2.2 Gasification Model Assumptions

Various assumptions were made in developing the model for the simulation of MSW gasification from RDF pellets. The assumptions considered are similar to those considered by (Aspentech, 2004, Begum et al., 2014b, Chen, 2011, Deng et al., 2017, Mavukwana et al., 2013, Shaohua et al., 2012, Zheng et al., 2013) and are as follows:

- The simulation model is isothermal, isobaric, kinetic free and is at steady state.
- Chemical reactions in the gasifier occur at a state of equilibrium.
- Apart from sulphur content, all elements in the model take part in the chemical reactions.
- All gases present in the model simulation are regarded as ideal, this includes hydrogen (H_2), carbon monoxide (CO), carbon dioxide (CO_2), oxygen (O_2), nitrogen (N_2), and methane (CH_4).
- The char residue is only comprised of carbon and ash in the solid phase.

4.2.3 Simulation Model Process Flow Diagram

Although a real-life gasification process occurs in a single reaction vessel, the process does undergo a certain number of steps within the vessel which can be separated into different process steps. Aspen Plus does not have a single unit operator block that acts as a gasifier, thus, an Aspen process flow was developed to describe each of the gasification steps using applicable unit operator blocks to describe and model each step of the gasification process in the simulation. The gasification process consists of drying, pyrolysis/decomposition, and the gasification step. The feed, RDF pellets, to the gasification process is specified in the model as a nonconventional component and is defined in the simulation using the proximate and ultimate analysis results obtained during the characterisation stage (Begum et al., 2014b). The

basis of the model is the minimisation of Gibb's free energy at equilibrium, with the assumption of residence time being long enough to permit the reactions to acquire a state of equilibrium.

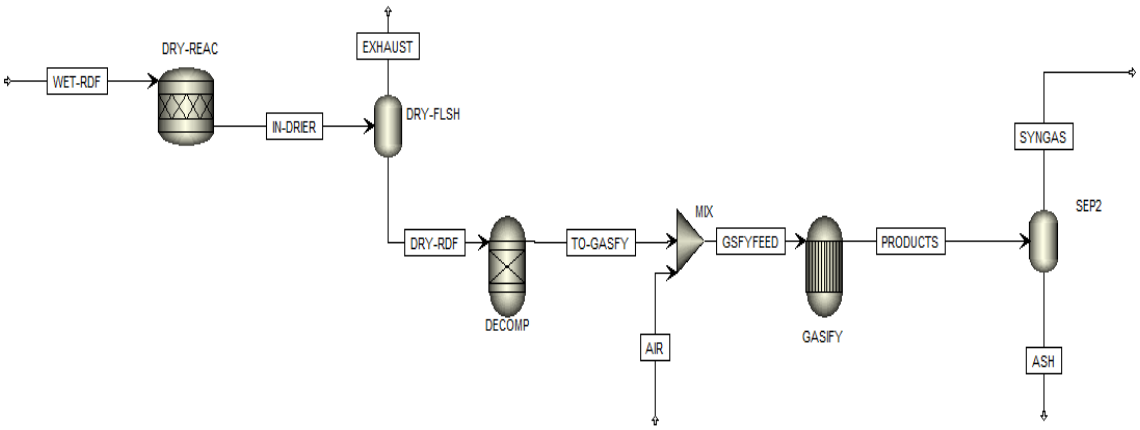

Figure 4-12: Aspen Plus model simulation process flow diagram for RDF gasification.

4.2.4 Description of the Simulation Process

The gasification simulation model was developed by using 3 main reactor types on the Aspen Plus software namely the Stoichiometric Reactor (RStoich), Yield Reactor (Ryield) and RGibbs reactors.

4.2.4.1 Drying

This section of the process is designed to simulate the drying stage of the gasification process using the RStoich reactor (DRY-REAC) on Aspen. In this step, the moisture content of the feedstock is being reduced by evaporation. Even though the RDF pellets being fed to the reactor were dried during production, there is still an amount of moisture left (WET-RDF) and that moisture content is that determined by proximate analysis. In the RStoich block, a portion of the WET-RDF feed reacts to form water, and since the reactor only has one outlet stream (IN-DRIER), a Flash 2 model separator (DRY- FLSH) was used to separate the dried RDF from the water using split fractionation and the water exits the process through the EXHAUST stream while the DRY-RDF moves to the next stage of the process. Although the drying of materials is not usually considered as a chemical reaction, a reactor model was used to simulate the process with the extent of the reaction described as WET-RDF → 0.0555084 H_2O. Aspen regards all nonconventional components as having a molecular weight of 1. Thus, the extent of reaction indicates that 1 mole of RDF reacts to form 0.0555084 mole of water. The drying process was controlled by declaring a calculator block and using FORTAN statements to describe the drying of the RDF feed.

4.2.4.2 Pyrolysis/Decomposition

After the drying step, the gasification process moves the pyrolysis/decomposition step whereby the RDF is decomposed into its constituent elements. The decomposition process model was simulated using the RYield block (DECOMP) which converts nonconvention feed components, RDF, into conventional components. Fortan statements used in a calculator block to calculate the yield distribution from the component attributes of RDF in the feed stream to the RYield model (DRY-RDF) which come in the form of an elemental composition described by the ultimate analysis of the feed stream. The converted elements include carbon, hydrogen, oxygen, nitrogen and sulphur.

4.2.4.3 Gasification

After decomposition has occurred, the converted elements are then ready for gasification. These elements in stream TO-GASFY are mixed with an AIR stream using an ASPEN Mixer block (MIX) to ensure perfect air mixing during the gasification process. The actual gasification stage of the gasification process is simulated using the RGibbs reactor model. RGibbs is a rigorous reactor model that calculates chemical and phase equilibrium by minimising Gibbs free energy of the system. Therefore, it eliminates the necessity to specify reaction stoichiometry. By minimising the Gibbs free energy and assuming complete chemical equilibrium, the reactor is then able to quantify the composition of the SYNGAS product stream. Using the heat stream Q-DECOMP, the heat of reaction associated the decomposition was passed to the RGibbs reactor. The elemental feed-air mixture enters the gasification stage (GASIFY) through stream GSFYFEED where partial oxidation occurs to constitute the gasification reactions. Part of the carbon present constitute the gas phase and undergoes devolatilization and the remaining carbon constitutes the solid phase. Using a separator model (SEP2), the syngas product was separated from the ash using split fractionation

4.2.5 Operating Parameters for Gasification

In terms of operating parameters of the gasifier system, the following will be considered:

Table 4-3: Gasification operating parameters

Parameter	Unit	Value
Feed Flow Rate	Kg/h	10
Feed Pressure	bar	1
Feed Temperature	℃	25
Air Equivalence Ratio		0 - 1
Air Pressure	bar	1
Air Temperature	℃	25
Gasifier Temperature	℃	500 - 1100
Gasifier Pressure	bar	1

As discussed in the drying and decomposition sections of the simulation process, it is important to have the proximate and ultimate analysis data of the feed materials to be able to compute the two processes respectively. Table 4-4 below shows the feed characteristics in terms of proximate and ultimate analysis for all the different RDF Pellets differentiated by the binder material used in production:

Table 4-4: RDF Pellet Characteristics

		No Binder	Waste Engine Oil	Waste Palm Oil	Corn Starch	Guar Gum Powder
Proximate Analysis (mass %) (Dry Basis)	Moisture	3.50	3.00	2.90	5.00	5.60
	Volatile Matter	80.90	86.20	88.60	82.80	80.90
	Fixed Carbon	5.60	6.70	4.43	6.64	6.12
	Ash	10.00	4.55	4.07	5.56	7.38
Ultimate Analysis (mass %)	Carbon	46.55	51.73	50.20	40.01	48.33
	Hydrogen	6.07	7.17	6.76	5.73	7.06
	Oxygen	46.81	40.03	42.11	52.84	43.48
	Nitrogen	0.31	0.64	0.64	0.79	0.83
	Sulphur	0.26	0.43	0.38	0.63	0.30
Calorific Value (MJ/kg)		22.70	26.94	27.13	21.13	21.84

4.2.6 Results and Discussion

The reference point of the gasification simulation results will be displayed for a case from which experimental outcomes were not available. Due to the absence of experimental data for RDF gasification of the Cape Peninsula University of Technology, Waste-to-Energy research

group, it has been important to utilize published data for RDF gasification models found by Ramzan et al. (2011), Chen et al. (2013a) and Násner et al. (2017), as they all utilized fixed bed gasifier systems with air as a gasifying agent. The created RDF gasification simulation was utilized to look at theoretical and the experimental data from different models with the theoretical results of chemical equilibrium model; based on Gibbs free energy minimization in this investigation.

Table 4-5 summarises desirable syngas qualities for various applications. Generally, syngas qualities and conditioning are more critical for applications in fuels and chemical synthesis rather than for hydrogen and fuel gas applications. Highly immaculate syngas (i.e. low amounts of inerts, for example, N2) is to a great degree helpful for fuels and chemicals synthesis since it considerably decreases the size and cost of downstream operations. Be that as it may, the qualities given in Table 4-5 ought not to be translated as stringent necessities. Supporting unit operations (e.g., scrubbers, blowers, coolers, and so on.) can be utilized to alter the state of the product syngas to coordinate that ideal for the coveted end-use, though, at added complexity and cost (Ciferno, 2002). In this study, no downstream operations were considered during the simulation process, the product syngas obtained is in its raw form immediately after the gasification process

Table 4-5: Desirable syngas qualities for various applications (Ciferno, 2002).

Product	**Synthetic Fuels**	**Methanol**	**Hydrogen**	**Fuel Gas**	
	FT Gasoline and Diesel			Boiler	Turbine
H_2/CO	0.6	~2.0	High	Unimportant	Unimportant
CO_2	Low	Low	Unimportant	Not Critical	Not Critical
Hydrocarbons	Low	Low	Low	High	High
N_2	Low	Low	Low	Note	Note
H_2O	Low	Low	High	Low	Note
Contaminants	<1 ppm Sulphur Low Particulates	<1 ppm Sulphur Low Particulates	<1 ppm Sulphur Low Particulates	Note	Low Part. Low Metals
Heating Value	Unimportant	Unimportant	Unimportant	High	High
Pressure, bar	~20-30	~50 (liquid phase) ~140 (vapor phase)	~28	Low	~400
Temperature, ℃	200-300 300-400	100-200	100-200	250	500-600

Figure 4-13 presents the composition of the gas obtained at baseline conditions of a temperature of 700 ℃ and air to fuel ratio of 1:1 for all the different pellet types according to a binder which was considered for this study. The results presented compares mainly the H_2 and CO composition in the gas as these are the 2 major constituents of Syngas.

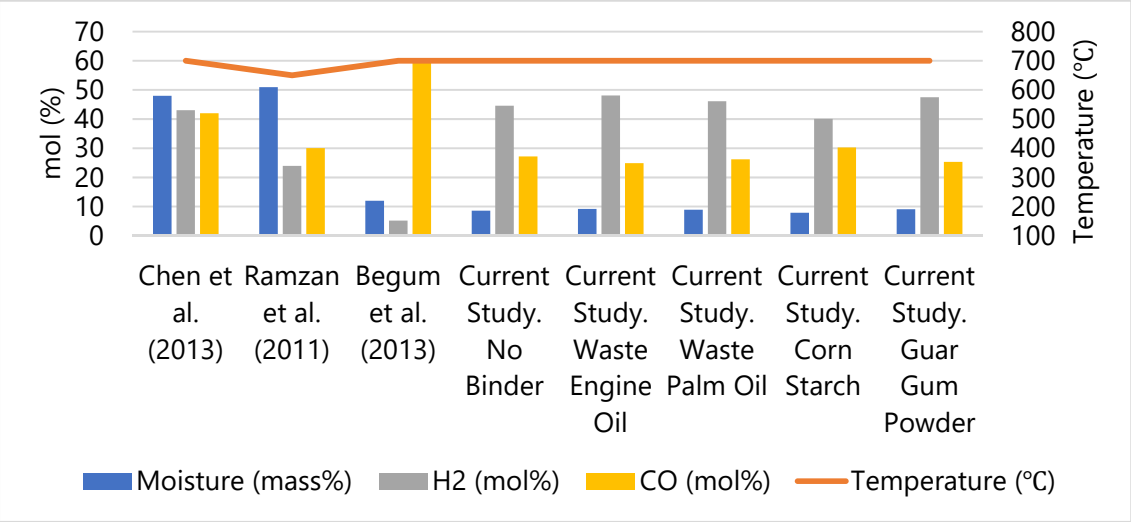

Figure 4-13: Syngas composition comparisons in terms of Moisture, Hydrogen and Carbon monoxide at constant operating conditions

The results obtained, as summarized in Figure 4-13, show that the current study has a much higher mole fraction of H_2 than CO in the product syngas with very similar operating conditions to the results being compared to. The main differences are presented in the feedstock characteristics, namely the moisture content. The other studies have a moisture content ranging between 12-48% while, in this study, the moisture was found on average at 4 % considering that the pellets were dried. The disadvantage of high moisture is that as it draws more heat towards sensible heating and moisture removal, the reactor temperature decreases which affects the gasifier performance and quality of syngas product (Wang, 2014), making the moisture content of the pellets in this study ideal in reducing the effect of temperature reduction in the reactor, thus constituting good gasifier performance and syngas product. The H_2/CO ratio of the syngas at the reference point conditions was found to fall within the range of suitability to produce Methanol at an average of 1.7 ranging between 1.3 and 1.9 which is close to the ~2.0 presented in table 4-5 (Ciferno, 2002). This was also found by Deng et al. (2017). The overall molar composition of the syngas as per different pellets is presented in Figure 4-14 as well as the average composition at the baseline conditions. From these results, the bulk molar composition of the syngas is made up of H_2 and CO, of which are the main constituents to consider in syngas when the goal of gasification is to produce transportation fuels and chemicals (i.e. methanol) as seen in Table 4-5. The other constituents that make up

the syngas product consist of CH_4, CO_2, N_2 and H_2O. These constituents with the H_2 and CO made up over 99 % of the syngas composition. Traces of NO_2, NO, SO_2 and SO_3 made up the remainder of the composition at less than 1 % in total for all the pellet types meaning they are too small to be considered to have an effect in the product gas.

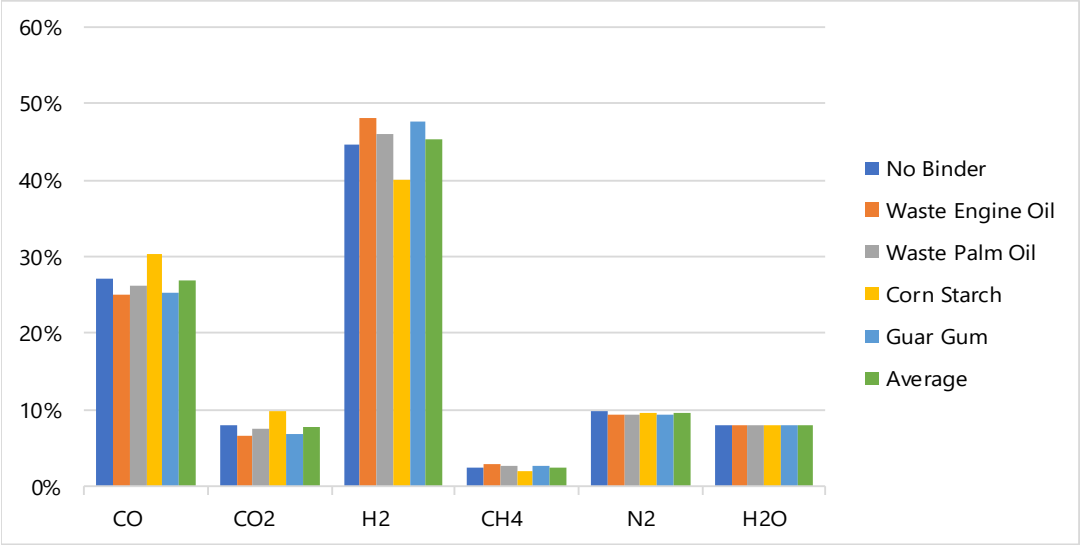

Figure 4-14: Molar composition of Syngas products for all pellet types

The CO in the syngas ranged between 25 % and 30 % with an average of 27 % across all the pellets where the corn starch pellets had the highest CO in the syngas product at 30 %. In terms of CO_2, the amount of it in the product syngas ranged from 7 % to 10 % at an average of 8 % for all the pellets where the corn starch pellets had the max at 10 % in the syngas product. As per Ciferno (2002) in Table 4-5, CO_2 content needs to be low for the syngas to be considered of either transportation fuels or methanol production, thus an average of 8 % can be deemed adequate for application in these avenues. The H_2 content in the syngas product at baseline conditions was found to range between 40 % and 48 % with an average of 45 % being the highest constituents in the syngas product for all pellets. Therefore, it was deemed that the syngas product is suitable for methanol production as the H_2/CO ratio was ~2.0 for all pellet types. CH_4 content in the syngas product represents the hydrocarbons present in the syngas product ranging from 2 % to 3 % with an average of 3 % for all pellets. According to Ciferno (2002) in Table 4-5, hydrocarbon content is required to be low for suitability of applications in transportation fuels or methanol production. N_2 and H_2O constituents in the syngas product are also required to be low for these applications and both constituents were found to average at 10 and 8 % respectively for all pellet types which can be considered as reasonable low at baseline conditions.

In the interpretation of the results obtained for the effect of various parameters on the syngas composition presented in Figures 4.15, 4.16, 4.17, 4.18, 4.19, it is important to note that they are unable to be plotted on the same scale. This is because some of the composition values have very low decimal values and some very high. The Simulation program does not allow the extraction of these so they can be plotted outside of the simulation interface. In analyzing the effect of temperature on the syngas composition for the simulation using the RDF pellets with no binder, it was found that both the composition of H_2 and CO increase in direct proportion to the temperature as seen in Figure 4-15.

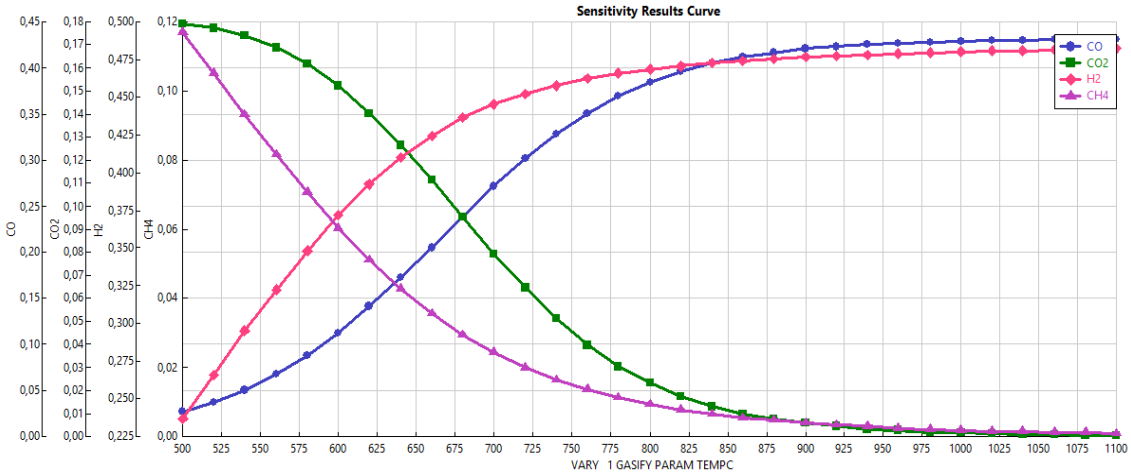

Figure 4-15: Effect of Temperature on Syngas composition for RDF pellets with no binder

The CO_2 and CH_4 decrease with an increase in temperature. It can also be deduced that as the temperature draws close to the 900 ℃ mark, the H_2/CO ratio decreases and moves towards 1 at approximately 850 ℃ where the H_2 and CO intersect. However, it needs to be noticed that each constituent is presented on their individual scale on the graph, meaning an intersection does not necessarily mean the values are equal at that point. After the 850 ℃, the H_2/CO ratio decreases but is never <1 making the syngas produced at those temperatures suitable for methanol production (Ciferno, 2002). The same effect was established on the simulation involving the pellets with waste engine oil as a binder, however, the intersection between the H_2 and CO occurred at 900 ℃ where the ratio was close to 1. However, moving passed the 900 ℃ mark the ratio remained constant at ~1 with increasing temperature. Figure 4-16 is a graphical representation of this behaviour in the syngas composition for the pellets with waste engine oil as a binder.

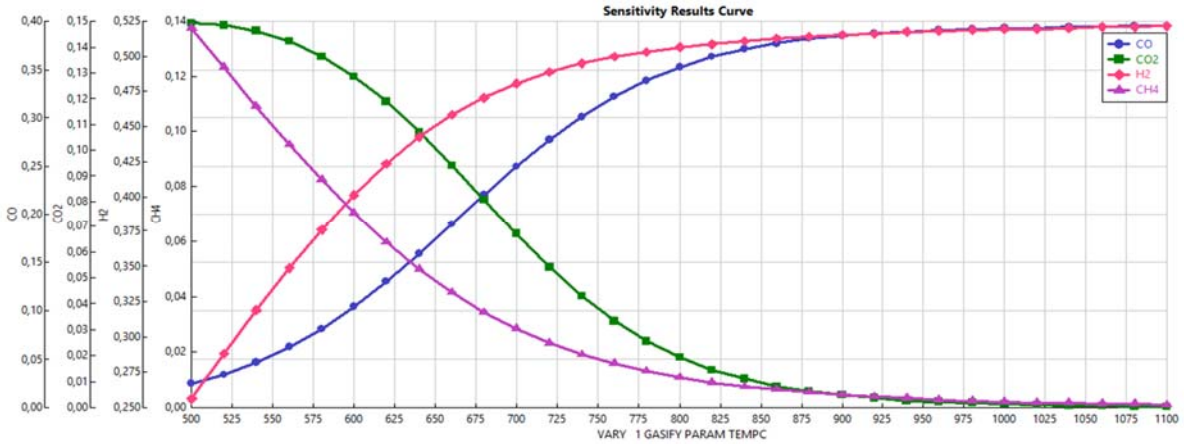

Figure 4-16: Effect of Temperature on Syngas composition for RDF pellets with engine oil as a binder

With regards to simulations considering the pellets produced using waste palm oil as binding material, a similar effect was noticed on the gas composition with increasing temperature. TheH_2 and CO composition increased, while the CH_4 and CO_2 composition decreased with increasing temperature., It was also noticed that even though the H_2/CO ratio also decreased, the ratio never goes below 1, meaning that pellets produced with waste palm oil as binder produce syngas suitable for methanol production only (Ciferno, 2002). Figure 4-17 is a graphical representation of the sensitivity analysis describing the effect of temperature on the syngas composition of pellets with waste palm oil as a binder.

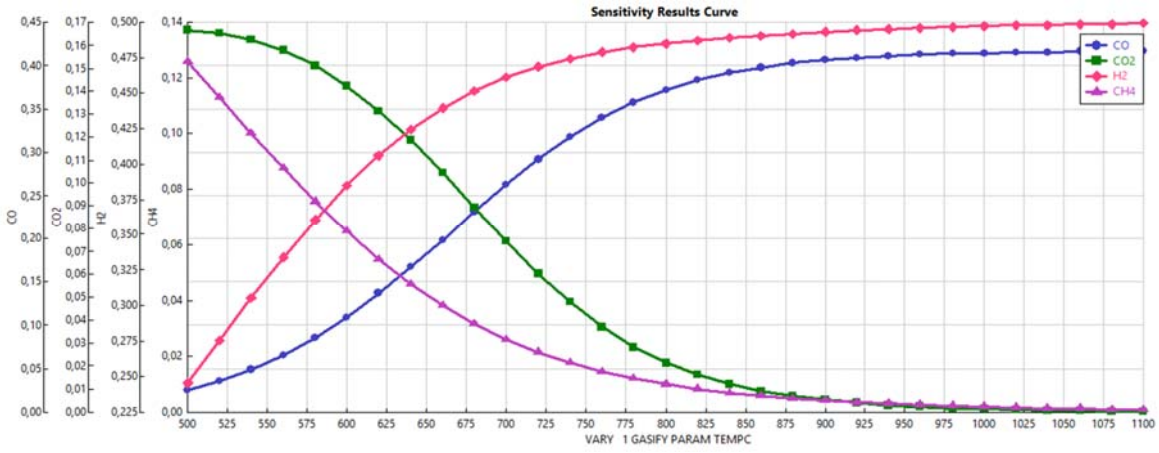

Figure 4-17: Effect of Temperature on Syngas composition for RDF pellets with waste palm oil as a binder

The syngas composition of RDF pellets produced using corn starch in the gasification simulations also show a relationship of direct proportionality to temperature with regards to H_2 and CO composition, and an inverse proportionality regarding CO_2 and CH_4 composition. As presented in Figure 4-18 below, the behaviour of the H_2/CO displayed similar behaviour

with that of the waste palm oil pellets in Figure 4-17, however at temperatures drawing closer to 1100 ℃, the ratio becomes closer to one, suggesting that at higher temperatures it can be pushed to below 1 to allow for FT Synthesis fuel production.

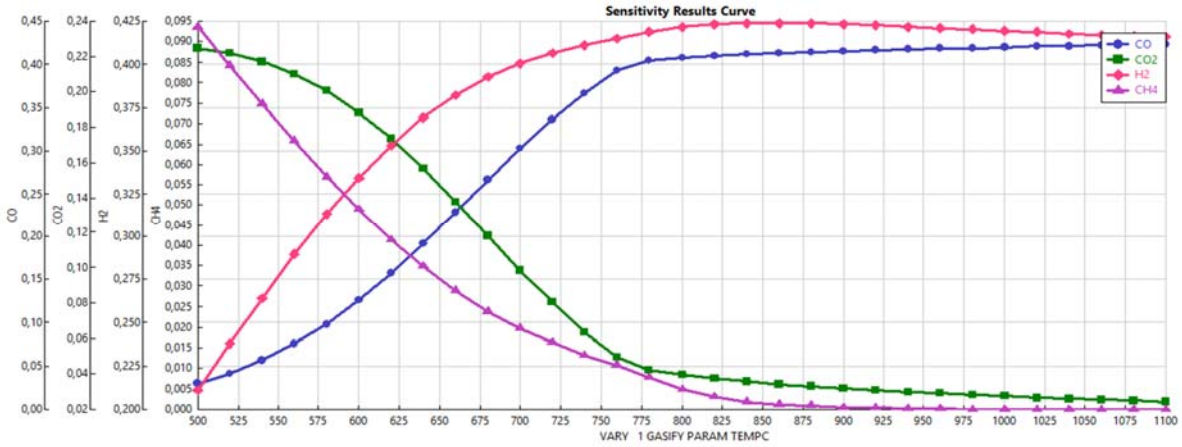

Figure 4-18: Effect of Temperature on Syngas composition for RDF pellets with corn starch as a binder

The sensitivity analysis curves for the gasification simulation of RDF pellets produced with guar gum powder as binding material showed similar behaviour, in terms of the effect of temperature on the syngas composition, to the behaviour exhibited by the simulation using waste engine oil as binding material as presented in Figure 4-19. As in Figure 4-17, it was noticed that even though the H_2/CO ratio also decreased, the H_2/CO ratio never becomes lower than 1, thus making RDF pellet with guar gum powder gasification results in syngas product suitable for methanol production.

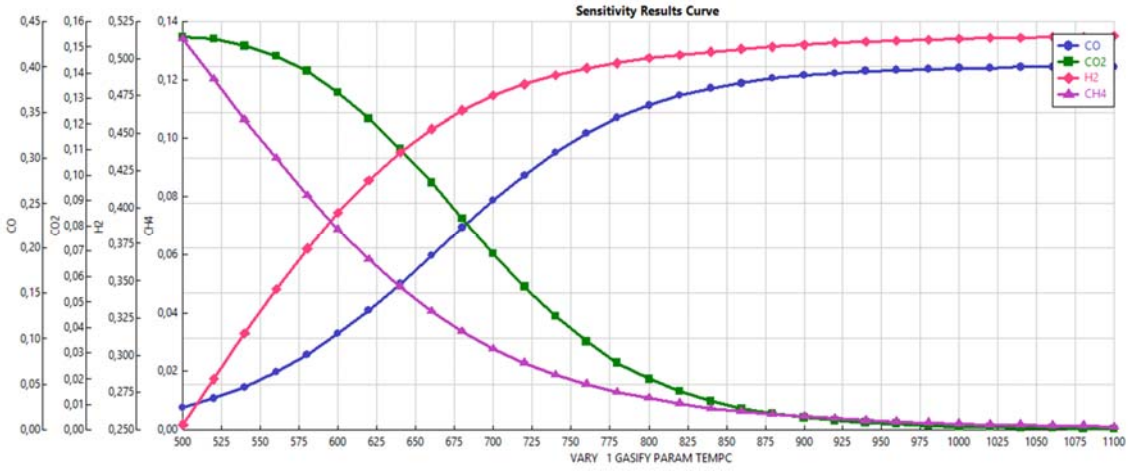

Figure 4-19: Effect of Temperature on Syngas composition for RDF pellets with guar gum powder as a binder

The effect of temperature on the carbon conversion was also studied using sensitivity analysis for all the RDF pellet types considered in the study as graphically presented in Figure 4-20 below.

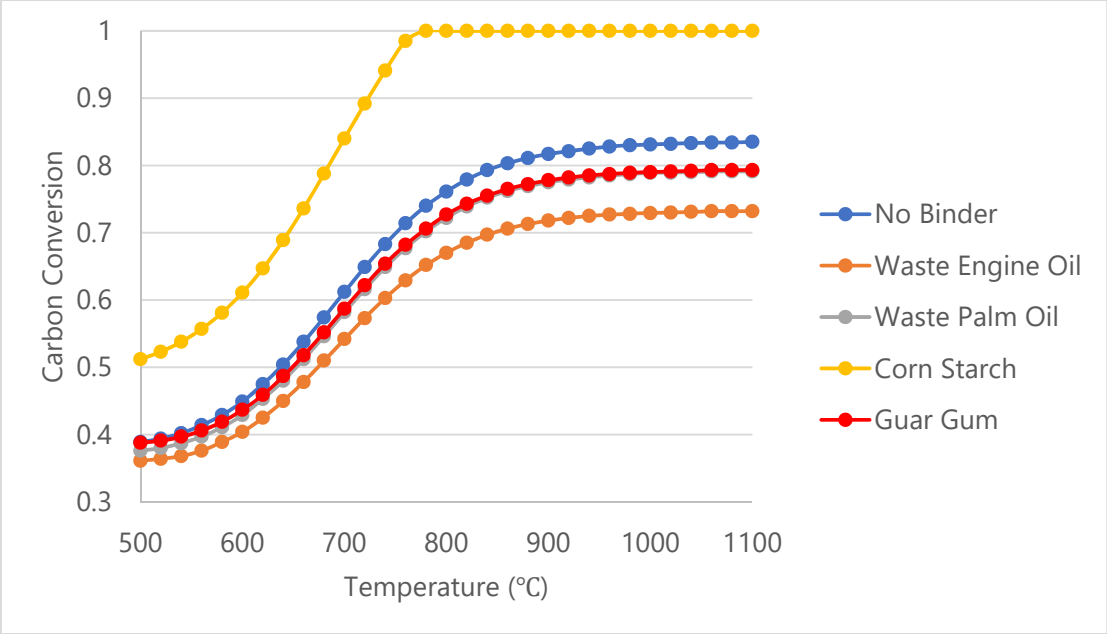

Figure 4-20: The effect of temperature on the carbon conversion of the RDF pellets.

The carbon conversion for all the RDF pellet types considered in this study was found to be directly proportional to the change in temperature, however, the extent of the conversion differed with pellet binder used. The highest conversion of carbon during the gasification simulations was found with the RDF pellets produced with corn starch as a binder and the conversion was found to be 100% at a lower temperature of 780 ℃ compared to the other pellets which had not to reach 100% carbon conversion at this point. This difference can be attributed to the ultimate analysis of the different pellets, whereby the other pellets all exhibit oxygen content between 40 and 46% presented on Table 4.4, while the oxygen content with the starch binder was 52.8%. With the higher oxygen content than the other, an increase in temperature will affect the carbon conversion much quicker than in those with lower oxygen content. All the other pellet types reached different but lower maximum carbon conversions at a higher temperature of approximately 940 ℃. The maximum carbon conversion for pellets with no binder, waste engine oil, waste palm oil and guar gum powder was found to be 83%, 73%, 79% and 79% respectively, with waste engine oil achieving the lowest carbon conversion of 73%.

With respect to the relationship between gasifying agent flowrate and syngas composition in the simulation process, the following general relationship transpired with the pellets produced

with no binder, waste engine oil, waste palm oil and guar gum powder as presented in Figure 4-21 below.

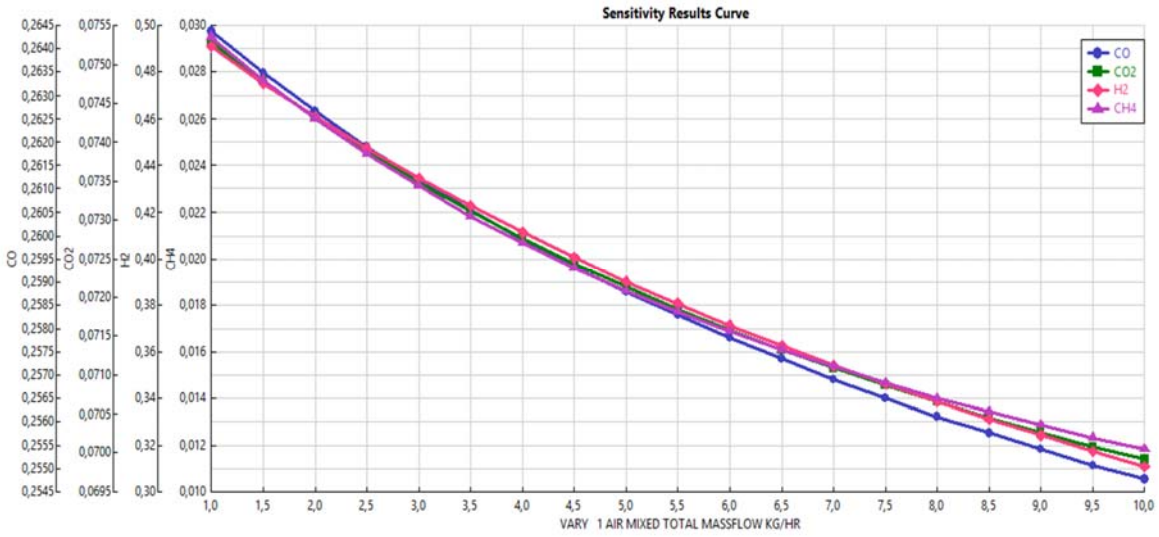

Figure 4-21: The averaged effect of airflow rate on the syngas composition of the RDF pellets produced with no binder, waste engine oil, waste palm oil and guar gum powder.

In considering the results presented in Figure 4-21, it can be deduced that the general trend with regards to the effect of airflow rate to the syngas composition is that the 4 major constituents of H_2, CO, CH_4, CO_2 that were considered for this study follow a relationship of inverse proportionality with the air flowrate. This is deduced from Figure 4.21 as the composition of each constituent decreased with increasing airflow rate. This was observed with all the four pellet types described in Figure 4-20. The pellets produced using corn starch as a binder, however, showed a slightly different effect to air flowrate in terms of the syngas composition. The sensitivity analysis describing this behaviour is presented in Figure 4-22 below.

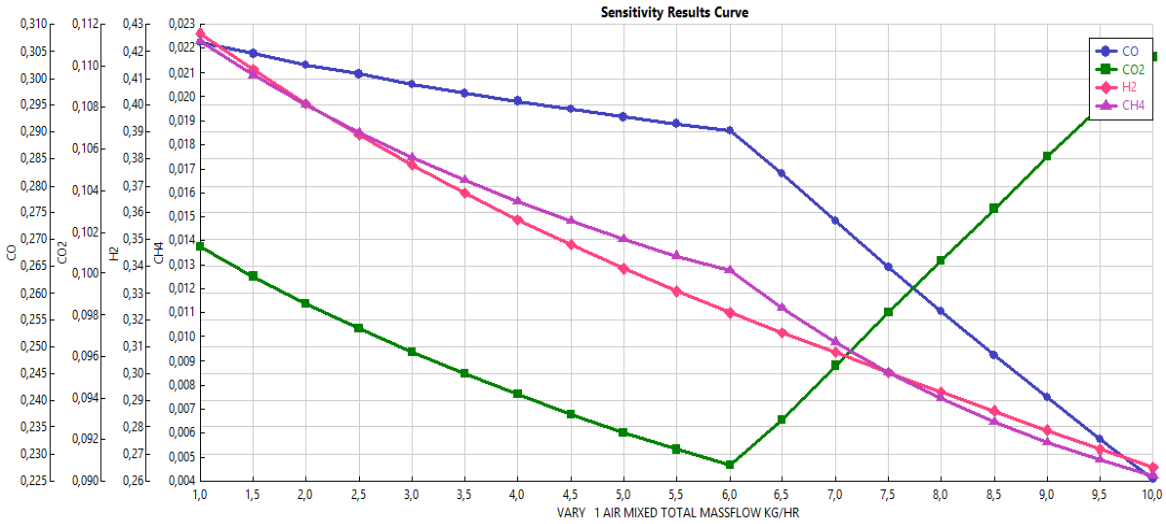

Figure 4-22: The effect of airflow rate on the syngas composition of the RDF pellets produced with corn starch.

The constituents H_2, CO, CO_2 and CH_4 in the composition of the syngas follow the same inverse proportionality to the air flowrate as with the pellets in Figure 4-20 however, when the air flowrate reached 6,0 kg/hr, the CO_2 in the syngas product increased rapidly contrary to the behaviour witnessed in the other pellet types where all constituents in the syngas composition continued to deplete with increasing airflow rate. This means that at that flow rate, the process moves into a process of combustion, hence the increase in CO_2. This is substantiated by the fact that in Figure 4-19 describing carbon conversion with temperature, the pellets with starch binder are the only batch that achieved 100 % carbon conversion with increasing temperature, meaning that at that point, the process reaches a stage of complete combustion resulting in the increase in CO_2 while the other pellets never reach the 100 % conversion within the studied air flow rate. Confirmation that the reason for this difference is due to the extent of carbon conversion between the pellet types is cemented by the behaviour of the starch pellets in the sensitivity analysis relating air flow rate to the carbon conversion for each pellet type described in Figure 4-23 below.

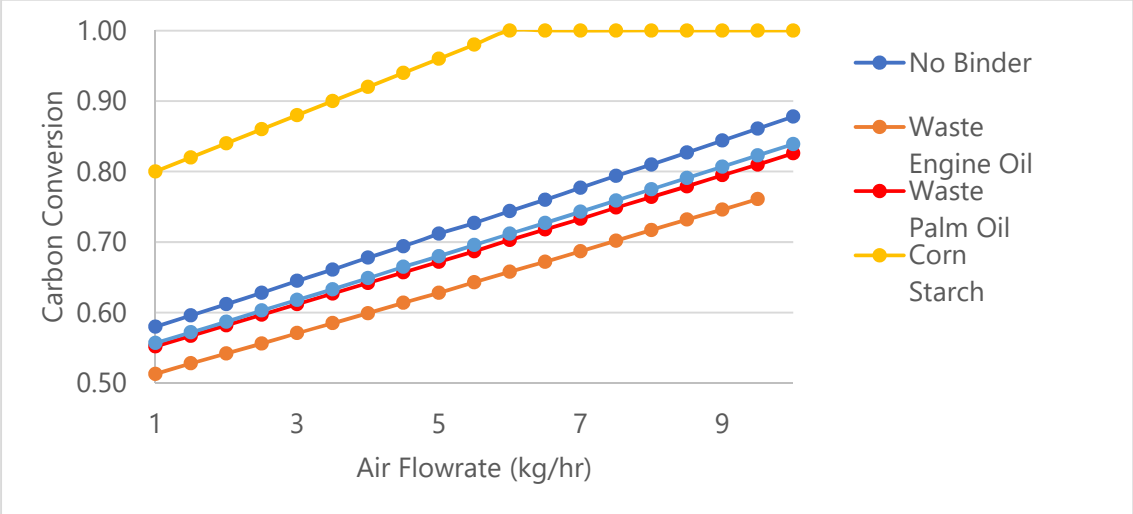

Figure 4-23: The effect of airflow rate on the carbon conversion of the RDF pellets.

At exactly an airflow rate of 6 kg/hr, the carbon conversion reaches 100% hence it correlates with the syngas composition of the starch binder pellets were at the same flow rate, the CO_2 in the syngas product increases, signifying that complete combustion is now occurring at that flow rate and above. Similarly, to the reasoning behind the effect of temperature, the higher oxygen content of the starch binder pellets can be attributed to this difference. Logically the carbon conversion should reach 100% quicker than the other pellets with an increase in airflow rate as the air also contains oxygen. In terms of the other pellet types, the carbon conversion increases linearly suggesting that at some arbitrary flow rate of air into the gasification system, they will also reach 100 % carbon conversion and reach a stage of complete combustion. This correlates with the fact that in the study parameters of a maximum airflow rate of 10 kg/hr, all the other pellets apart from the ones with starch binder do not reach 100% carbon conversion.

4.2.7 Conclusion

This study modelled a fixed bed gasifier for RDF gasification by employing Aspen Plus simulation software. The model was compared with the modelled and experimental data measured by Ramzan et al. (2011), Chen et al. (2013b) and Násner et al. (2017), Begum et al. (2014a) and Deng et al. (2017). The model can test the process in a wide variety of process parameter of which only the temperature and air to fuel ratio were modelled in this study. Further modelling was done assessing the gasification performance by optimizing operating condition using different binding materials for the feed preparation of the RDF pellets. It can be deduced that the optimal conditions were found on the simulations done with the pellets produced with corn starch binder whereby the optimal temperature was found to be 780 ℃ at an air flowrate of 6 kg/hr. These conditions are deemed optimal because the conversion of carbon at those points is at 100 %, while the syngas composition is at its highest in terms of

the important constituents of H_2 and CO and the H_2/CO ratio achieved is ideal for methanol production. The other pellets reach their maximum carbon conversion at a temperature of 940 ℃ whereby the highest conversion achieved was 83% and the air flow rate to carbon conversion graphs showed that 100% conversion could only be reached at much higher air flow rates. Higher temperatures require more energy and higher air flowrates require more capital investment and hence increase the cost of production.

CHAPTER 5. GENERAL CONCLUSION

In realisation of the energy security issue that South Africa is currently facing with insufficient petroleum reserves and the environmental threat posed by the disposal of Municipal Solid Waste (MSW) in landfill operations, Biomass to Liquid (BTL) technology was deemed to be the most suitable method of tackling these issues at the same time. Considering that MSW is highly heterogeneous in its raw form, it poses processing challenges which are normally not a factor with virgin biomass which is normally used in BTL technologies. This then prompted the use of a feed preparation step in the form of pelletisation to produce Refuse Derived Fuel (RDF) pellets from the MSW. The study investigated the production of syngas from MSW collected from the City of Cape Town waste transfer stations, drop-off sites and active landfill sites. The production of syngas was studied by means of simulating a fixed-bed, updraft gasifier system through Aspen Plus Simulation software which used air as a gasifying agent. The RDF pellets were produced using four different materials as binder, namely corn starch, waste palm oil, waste engine oil and guar gum powder. To solidify the need for an alternative method of MSW treatment, an environmental analysis of the landfill sites consisting of a radionuclide assessment and heavy metal analysis was conducted to assess the human health risk involved. Important factors that the study needed to address in order to fulfil the research objectives as per the research questions were the composition of the product syngas, the achieved H_2/CO ratio in the product syngas regarding suitability as feedstock for Fischer-Tropsch fuels and/or chemical production in light of addressing energy insecurity, the optimal conditions to maximise syngas yield in terms of temperature and equivalence ratio/gasifier feed to air ratio, and the environmental impact of the current landfilling processes in terms of Heavy Metals and Radionuclide activity.

The molar composition of the product syngas at baseline conditions of temperature 700 ℃, feed flow rate 10 kg/h and air flowrate 2 kg/hr, meaning feed to air ratio of 1:5, was 27% CO, 8% CO_2, 45% H_2, 3% CH_4, 10% N_2 and 8% H_2O on average for all the pellet types in terms of binder material used making up over 99% of the product syngas at these conditions. NO_2, NO, SO_2 and SO_3 content in the syngas product was found to be less than 1% in total on average for all pellet types at baseline conditions. The H_2/CO ratio achieved at the baseline conditions was found to average at 1.7 for all pellet types which is ~2.0 making the produced syngas suitable for methanol production. In consideration of the process optimisation, temperature, airflow rate and binder type were varied to obtain the optimum process conditions to yield the most amount of syngas with the highest content of H_2 and CO being the most important constituents of syngas. The carbon conversion was also considered to determine the optimum conditions. With regards to the effect of temperature on the syngas, varied from 500 ℃ to

1100 ℃, the H_2 and CO content were found to be directly proportional with the temperature with CH_4 and CO_2 exhibiting a relationship of inverse proportionality to temperature. This trend was found for all the pellet types regarding the effect of temperature on the composition of the syngas. Regarding the effect of temperature on the carbon conversion, only the pellets produced using corn starch were found to reach 100% carbon conversion at a temperature of 780 ℃. All the other pellets do not reach the 100% carbon conversion within the temperatures considered in the study. The other pellet types of carbon conversion ranged from 73% to 83% at a temperature of 940 ℃. Similar behaviour was observed regarding the effect of air flowrate on carbon conversion whereby only the pellets with corn starch binder reached 100% carbon conversion at 6 kg/hr while the other pellets do not reach 100% in the given test range. The effect of air flow rate on the syngas composition was found to have an inversely proportional behaviour for all the constituents for all pellet types, except that of the pellets with corn starch where the CO_2 in the syngas started to increase after the 6 kg/hr flow rate corresponding to the results of the carbon conversion thus indicating complete combustion past this point. Therefore, it can be deduced that the most suitable binder for the gasification of RDF produced from MSW is corn starch with the optimal syngas production process parameters being that of temperature at 780 ℃ and an airflow rate of 6 kg/hr translating to fuel to air feed ratio of approximately 1:2. The H_2/CO ratio was found to be always ~2.0 for all scenarios meaning the syngas at the optimum conditions would be suitable for methanol production. Methanol is an alternative, inexhaustible, ecologically and monetarily alluring fuel; it is thought to be a standout amongst the most ideal fuels for traditional fossil-based fuels. Methanol has been as of late utilized as an alternative to regular fuels for internal combustion engines to fulfil some environmental and monetary concerns (Zhen and Wang, 2015). Especially vital is the next generation, low carbon biofuels obtained from farming, forestry, municipal and industrial waste by biochemical or thermochemical processes including gasification. Ethanol, methanol or blends of these fuels can be utilized as a part of turbocharged direct injection spark ignition engines which areas or more proficient than diesel engines and furthermore, give focal points of lower-cost, bring down emanations and higher power (Bromberg and Cohn, 2010).

With regards to the environmental impact posed by landfill operations, effects stemming from radionuclide activity and heavy metal content were considered. The radioactivity concentrations of ^{238}U (^{226}Ra), ^{232}Th and ^{40}K were acquired from averaging out the radioactivity concentrations of their separate daughter radionuclides in soil tests from the Bellville, Coastal Park, and Vissershok landfill locales. With the supposition of secular equilibrium being accomplished, the dose rate in air 1m over the ground and the effective yearly dosage rates were resolved. The outcomes obtained demonstrate that the landfill sites meet worldwide norms set out by UNSCEAR and South Africa's NIASA as far as the most extreme permissible

outflows as far as the dosage rate in air and effective annual dose rates separately. In this investigation, the outcomes for heavy metal examination for landfill soil tests in the City of Cape Town Municipality demonstrate that, as far as metal chemical speciation, all the recognized metals were found be most present in the residual fraction of the Bellville site samples. Bellville site showed that each one of the metals has potential mobility of under 50%, suggesting that the metals are more disinclined to be discharged into the earth on the grounds that the plenitude of the metals is in the residual fraction. In Coastal Park site, all metals excluding Pb and Ni had potential mobility of over 50% implying that these metals are effectively released into nature with the capability of being exceptionally dangerous. Similar potential portability was seen in Vissershok site with an expansion of Cu to the metals less likely to be released into nature. Results for geo-accumulatio index showed that Bellville site was heavily contaminated with Cu and Cr while moderately contaminated with Zn and Ni. Coastal Park site showed moderate contamination for Zn and was uncontaminated to moderately contaminated with Cr, Cu, and Pb. Vissershok site was uncontaminated to moderately contaminated with Zn and Cr. Concerning the health risk assessment, it was reasoned that every one of the sites had no danger of any health hazard being related with exposure to the landfills for any of the considered metals for both adults and children of non-cancer-causing nature. Regarding the cancer risk, it was discovered that there is no danger to adults from the landfill destinations through the exposure to the metals in the investigation for adults, however, it was discovered that children are in danger of contracting cancerous health effects from exposure to Cd and As from the landfill locales.

Considering the indicated health risks of MSW landfills and the benefits of methanol fuels as a future alternative source of transportation fuels, it becomes evident that the advancement of this research into lab-scale and eventually industrial-scale applications are much warranted in the current economic climate of South Africa which is currently experiencing exceptionally high fuel prices. Advancements in this research will not only alleviate the financial strain but also bridge the ever-important energy security gap in South Africa.

References

ACKERMANN, F. 1980. A procedure for correcting the grain size effect in heavy metal analyses of estuarine and coastal sediments. *Environmental Technology,* 1**,** 518-527.

ADEFESO, I., IKHU-OMOREGBE, D. & RABIU, A. 2012. Sustainable Co-generation Plant : Refuse-Derived Fuel Gasification Integrated with High Temperature PEM Fuel Cell System. 33**,** 125--129.

ADEMOLA, A. K., OLAOYE, M. A. & ABODUNRIN, P. O. 2015. Radiological safety assessment and determination of heavy metals in soil samples from some waste dumpsites in Lagos and Ogun state, south-western, Nigeria. *Journal of Radiation Research and Applied Sciences,* 8**,** 148--153.

ADESUYI, A. A., NJOKU, K. L. & AKINOLA, M. O. 2015. Assessment of heavy metals pollution in soils and vegetation around selected industries in Lagos state, Nigeria. *Journal of Geoscience and Environment Protection,* 3**,** 11.

AGENCY STAFF, B. D. 2018. *Glencore's 2018 copper output to rise nearly 1.5-million tonnes* [Online]. Available: https://www.businesslive.co.za/bd/companies/mining/2018-02-01-glencores-2018-copper-output-to-rise-nearly-15-million-tonnes/ [Accessed 8 June 2018].

AGRICON 2017. Agricon-Pelleting Solutions.

AHMAD, N., JAAFAR, M. S., BAKHASH, M. & RAHIM, M. 2015. An overview on measurements of natural radioactivity in Malaysia. *Journal of Radiation Research and Applied Sciences,* 8**,** 136--141.

AJAYI, O. S. 2009. Measurement of activity concentrations of 40K, 226Ra and 232Th for assessment of radiation hazards from soils of the southwestern region of Nigeria. *Radiation and Environmental Biophysics,* 48**,** 323--332.

ALZAHRANI, J. H., ALHARBI, W. R., ABBADY, A. G. E. & ARABIA, S. 2011. Radiological Impacts of Natural Radioactivity and Heat Generation by Radioactive Decay of Phosphorite Deposits from Northwestern Saudi Arabia. 5**,** 683--690.

ANEKWE, U. L. & AVWIRI, G. O. 2016. Determination of Radiological Health Hazard Indices in Selected Crude Spilled Environment in River State, Nigeria. *American Journal of Scientific and Industrial Research***,** 50--59.

ANTIZAR-LADISLAO, B. & TURRION-GOMEZ, J. L. 2008. Second-generation biofuels and local bioenergy systems. *Biofuels, Bioproducts and Biorefining,* 2**,** 455--469.

ARSHADI, M., GREF, R., GELADI, P., DAHLQVIST, S. A. & LESTANDER, T. 2008. The influence of raw material characteristics on the industrial pelletizing process and pellet quality. *Fuel Processing Technology,* 89**,** 1442--1447.

ASHRAF, M. A., MAAH, M. J. & YUSOFF, I. 2012. Chemical Speciation and Potential Mobility of Heavy Metals in the Soil of Former Tin Mining Catchment. *The Scientific World Journal,* 2012**,** 125608.

ASPENTECH 2004. Aspen Plus 2004.1 Getting Started Modeling Processes with Solids.

AUCOTT, M. 2006. The fate of heavy metals in landfills : A Review by " Industrial Ecology , Pollution Prevention and the NY-NJ Harbor ".

BADEIE, A. 2013. Thermal pretreatment of municipal solid waste.

BAIRNES, M. 2013. *Combustion*, E Instrumentals International LLC.

BAKER, C. G. J. 1997. *Industrial Drying of Foods*, Springer US.

BEGUM, S., RASUL, M. & AKBAR, D. 2014a. A numerical investigation of municipal solid waste gasification using Aspen Plus. *Procedia Engineering,* 90**,** 710-717.

BEGUM, S., RASUL, M. G. & AKBAR, D. 2014b. A Numerical Investigation of Municipal Solid Waste Gasification Using Aspen Plus. *Procedia Engineering,* 90**,** 710--717.

BELGIORNO, V., DE FEO, G., DELLA ROCCA, C. & NAPOLI, R. M. A. 2003. Energy from gasification of solid wastes. *Waste Management,* 23**,** 1-15.

BENHADDYA, M. & HADJEL, H. 2013. *Spatial distribution and contamination assessment of heavy metals in surface soils of Hassi Messaoud, Algeria*.

BORGESE, L., FEDERICI, S., ZACCO, A., GIANONCELLI, A., RIZZO, L., SMITH, D. R., DONNA, F., LUCCHINI, R., DEPERO, L. E. & BONTEMPI, E. 2013. METAL FRACTIONATION IN SOILS AND ASSESSMENT OF ENVIROMENTAL CONTAMINATION IN THE VALLECAMONICA, ITALY. *Environmental science and pollution research international,* 20**,** 5067-5075.

BOZKURT, S., MORENO, L. & NERETNIEKS, I. 2000. Long term processes in waste deposit. *Science of the Total Environment,* 250**,** 101--121.

BRADFIELD, F. L. 2013. Examination of the Thermal Properties of Municipal Solid Waste and the Scalability Effect on its Degradation and Pyrolysis Products by.

BREAULT, R. W. 2010. Gasification Processes Old and New: A Basic Review of the Major Technologies.

BROMBERG, L. & COHN, D. 2010. Alcohol fueled heavy duty vehicles using clean, high efficiency engines.

BROWN, C. 2014. How Does a Hammer Mill Work?

CANADIAN NUCLEAR SAFETY COMMISSION, C. 2004. Review of Catalysts for Tar Elimination in Biomass Gasification Processes. *Industrial \& Engineering Chemistry Research,* 43**,** 6911--6919.

CASSEL, B. 2016. Proximate Analysis of Coal and Coke using the STA 8000 Simultaneous Thermal Analyzer.

CHANG, J., LIU, M., LI, X., LIN, X., WANG, L. & GAO, L. 2009. Primary research on health risk assessment of heavy metals in road dust of Shanghai. *China Environmental Science,* 29**,** 548-554.

CHEN, C. 2011. Experimental study and process simulation on MSW pyrolysis and gasification in fixed bed.

CHEN, C., JIN, Y.-Q., YAN, J.-H. & CHI, Y. 2013a. Simulation of municipal solid waste gasification in two different types of fixed bed reactors. *Fuel,* 103**,** 58--63.

CHEN, C., JIN, Y.-Q., YAN, J.-H. & CHI, Y. 2013b. Simulation of municipal solid waste gasification in two different types of fixed bed reactors. *Fuel,* 103**,** 58-63.

CHEREMISINOFF, N. P. & REZAIYAN, J. 2005. Biogasification. *Chemical Industries***,** 119--144.

CHERNEY, J. H. 2006. Grass Pelleting – The Process. *Soil Sciences***,** 2.

CIFERNO, J. A. M., J. 2002. *Benchmarking Biomass Gasification Technologies for Fuels, Chemicals and Hydrogen Production.* [Online]. National Energy Technology Laboratory. Available: https://www.netl.doe.gov/research/coal/energy-systems/gasification/gasifipedia/syngas-optimization [Accessed 27 November 2017].

CITY OF CAPE TOWN, C. 2009a. *Integrated Waste Management (IWM) Policy* [Online]. Cape Town: City of Cape Town. Available: http://sawic.environment.gov.za/documents/399.pdf [Accessed 27 June 2017].

CITY OF CAPE TOWN, C. 2009b. An Introduction to The City of Cape Town Integrated Waste Management By-law. 1--11.

CONVERTI, A., OLIVEIRA, R. P. S., TORRES, B. R., LODI, A. & ZILLI, M. 2009. Biogas production and valorization by means of a two-step biological process. *Bioresource Technology,* 100**,** 5771--5776.

COUNCIL DIRECTIVE, H. 1976. Council Directive 76/464/EEC of 4 May 1976 on pollution caused by certain dangerous substances discharged into the aquatic environment of the Community. *Official journal L,* 129**,** 0023-0029.

COUTO, N., SILVA, V. & ROUBOA, A. 2016. Municipal solid waste gasi fi cation in semi-industrial conditions using air-CO 2 mixtures. 104**,** 42--52.

CUMMER, K. R. & BROWN, R. C. 2002. Ancillary equipment for biomass gasification. *Biomass and Bioenergy,* 23**,** 113--128.

DARWISH, D. A. E., ABUL-NASR, K. T. M. & EL-KHAYATT, A. M. 2015. The assessment of natural radioactivity and its associated radiological hazards and dose parameters in granite samples from South Sinai, Egypt. *Journal of Radiation Research and Applied Sciences,* 8**,** 17--25.

DE BOECK, M., KIRSCH-VOLDERS, M. & LISON, D. 2003. Cobalt and antimony: genotoxicity and carcinogenicity. *Mutation Research/Fundamental and Molecular Mechanisms of Mutagenesis,* 533**,** 135-152.

DENG, N., LI, D., ZHANG, Q., ZHANG, A., CAI, R. & ZHANG, B. 2017. Simulation analysis of municipal solid waste pyrolysis and gasification based on Aspen plus. *Frontiers in Energy***,** 1-7.

DEPARTMENT FOR ENVIRONMENT FOOD & RURAL AFFAIRS, D. 2013. Incineration of Municipal Solid Waste.

DEPARTMENT OF ENERGY, D. 2015. Pocket Guide to South Africa 2015/2016 - Energy and Water.

DEPARTMENT OF ENVIRONMENTAL AFFAIRS AND TOURISM, D. 2006. State of Environmental Systems. South Africa. *In:* TOURISM, D. O. E. A. A. (ed.). Government Printers.

DEPARTMENT OF ENVIRONMENTAL AFFAIRS AND TOURISM, D. 2012. *National Waste Information Baseline* [Online]. South African Waste Information Centre. Available: http://www.sawic.org.za/documents/1736.pdf [Accessed 27 June 2017 2017].

DEPARTMENT OF MINERALS AND ENERGY, D. 2003. Department of Minerals And Energy Republic of South Africa White Paper

DEPARTMENT OF WATER AFFAIRS & FORESTRY, D. 1998. Minimum Requirements for Waste Disposal By Landfill. Second Edition ed. Pretoria: Department of Water Affairs & Forestry.

DIGITAL DATA SYSTEMS, D. 2010. Combustion Calorimeter System.

E4TECH 2009. Review of Technologies for Gasification of Biomass and Wastes. *Biomass***,** 125.

EISA, S. & MOHAMED, A. 2010. Investigation of Natural Radioactivity in Building Materials commonly used in Sudan.

EL-SAYED, N. 2014. Studying of Naturally Occurring Radionuclides for Some Environmental Samples and Its Hazardous Effects.

EL-TAHER, A. 2012. Assessment of natural radioactivity levels and radiation hazards for building materials used in Qassim area, Saudi Arabia. *Romanian Reports of Physics,* 57**,** 726--735.

EL-TAHER, A. & AL-ZAHRANI, J. H. 2014. Radioactivity measurements and radiation dose assessments in soil of Al-Qassim region, Saudi Arabia. *Indian Journal of Pure and Applied Physics,* 52**,** 147--154.

ENGLEDOW, S.-A. 2007. Integrated Analysis Solid Waste Baseline Report. *Environmental Conservation*.

EPA, U. 2001. Supplemental guidance for developing soil screening levels for superfund sites. *Peer Review Draft, OSWER,* 9355**,** 4-24.

ERGIN, M., SAYDAM, C., BAŞTÜRK, Ö., ERDEM, E. & YÖRÜK, R. 1991. Heavy metal concentrations in surface sediments from the two coastal inlets (Golden Horn Estuary and Izmit Bay) of the northeastern Sea of Marmara. *Chemical Geology,* 91**,** 269-285.

EUROPEAN BIOFUELS TECHNONOLOGY PLATFORM, E. 2016. *Wasted - Europe's Untapped Resource: An assessment of advanced biofuesl from wastes and residues* [Online]. Available: http://biofuelstp.eu/msw.html [Accessed 2016-09-19 2016].

FAHEEM, M., MUJAHID, S. A. & MATIULLAH 2008. Assessment of radiological hazards due to the natural radioactivity in soil and building material samples collected from six districts of the Punjab province-Pakistan. *Radiation Measurements,* 43**,** 1443--1447.

FAO FORESTRY DEPARTMENT, F. 1986. Wood Gas as Engine Fuel.

FERREIRA-BAPTISTA, L. & DE MIGUEL, E. 2005. Geochemistry and risk assessment of street dust in Luanda, Angola: A tropical urban environment. *Atmospheric Environment,* 39**,** 4501-4512.

FOGLER, H. S. 2006. *Elements of Chemical Reaction Engineering*, Prentice Hall.

FRIENDS OF THE EARTH, F. 2009. Briefing: Pyrolysis, Gasification and Plasma.

GALLAGHER, T. & PERLMAN, S. 2013. Public health: broad reception for coronavirus. *Nature,* 495**,** 176.

GDP, U. K. 2003. Waste and landfill. 37--51.

GIDARAKOS, E., HAVAS, G. & NTZAMILIS, P. 2006. Municipal solid waste composition determination supporting the integrated solid waste management system in the island of Crete. *Waste Management,* 26**,** 668--679.

GIRGIS, N., KHAYYAL, M., MCCONNELL, E. & NORTON, J. 1970. Penicillamine as an adjuvant to antimonial therapy, effect on electrocardiographic changes in dogs. *East African medical journal,* 47**,** 576-581.

GR, L. E. N. V. 2013. Review of alternative pre-treatment equipment. 1--10.

GREER, E. 1986. Selenium deficiency and toxicity in pigs. *Australian veterinary journal,* 63**,** 203-203.

GROSSEL, S. S. 1998. *Review of: "Handbook of Industrial Drying"*, Taylor \& Francis.

HALL, C. A. S., LAMBERT, J. G. & BALOGH, S. B. 2014. EROI of different fuels and the implications for society. *Energy Policy,* 64**,** 141--152.

HAMID, G. A. 2015. Microwave Digestion.

HARB, S., EL-KAMEL, A., ABD EL-MAGEED, A., ABBADY, A. & NEGM, H. Natural radioactivity measurements in soil and phosphate samples from El-Sabaea, Aswan, Egypt. IX Radiation Physics and Protection Conference. Nasr City-Cairo, 2008.

HASANBEIGI, A., LU, H., WILLIAMS, C. & PRICE, L. 2012. International Best Practices for Pre-Processing and Co-Processing Municipal Solid Waste and Sewage Sludge in the Cement Industry. 123.

HE, M., HU, Z., XIAO, B., LI, J., GUO, X., LUO, S., YANG, F., FENG, Y., YANG, G. & LIU, S. 2009. Hydrogen-rich gas from catalytic steam gasification of municipal solid waste (MSW): Influence of catalyst and temperature on yield and product composition. *International Journal of Hydrogen Energy,* 34**,** 195--203.

HE, M., XIAO, B., LIU, S., HU, Z., GUO, X., LUO, S. & YANG, F. 2010. Syngas production from pyrolysis of municipal solid waste (MSW) with dolomite as downstream catalysts. *Journal of Analytical and Applied Pyrolysis,* 87**,** 181--187.

HIMMELBLAU, D. M. & RIGGS, J. B. 2012. *Basic Principles and Calculations in Chemical Engineering*, Pearson Education Inc.

HLABA, A., RABIU, A. & OSIBOTE, O. A. 2016. Thermochemical Conversion of Municipal Solid Waste — An Energy Potential and Thermal Degradation Behavior Study. *International Journal of Environmental Science and Development,* 7**,** 661--667.

HOWARI, F. & BANAT, K. 2001. Assessment of Fe, Zn, Cd, Hg, and Pb in the Jordan and Yarmouk river sediments in relation to their physicochemical properties and sequential extraction characterization. *Water, Air, and Soil Pollution,* 132**,** 43-59.

HUANG, J. 2004. Chinese National health standards for occupational exposure to cadmium and diagnostic criteria of occupational chronic cadmium poisoning. *Biometals,* 17**,** 511-511.

HUANG, J., HUANG, R., JIAO, J. J. & CHEN, K. 2007. Speciation and mobility of heavy metals in mud in coastal reclamation areas in Shenzhen, China. *Environmental Geology,* 53**,** 221-228.

IDERIAH, T., IKPE, F. & NWANJOKU, F. 2013. Distribution and speciation of heavy metals in crude oil contaminated soils from Niger Delta, Nigeria. *World Environment,* 3**,** 18-28.

ISMAILA, A., ZAKARI, I., NASIRU, R., TIJJANI, B., ABDULLAHI, I. & GARBA, N. 2013a. Investigation on biomass briquettes as energy source in relation to their calorific values and measurement of their total carbon and elemental contents for efficient biofuel utilization. *Advances in Applied Science Research,* 4**,** 303-309.

ISMAILA, A., ZAKARI, I. Y., NASIRU, R., TIJJANI, B. I., ABDULLAHI, I. & GARBA, N. N. 2013b. Investigation on biomass briquettes as energy source in relation to their calorific values and measurement of their total carbon and elemental contents for efficient biofuel utilization. 4**,** 303--309.

JABBAR, A. 2010. PhD Thesis COMSATS Institute of Information Technology Islamabad , Pakistan.

JABBAR, A., ARSHED, W., BHATTI, A. S., AHMAD, S. S., SAEED UR, R. & DILBAND, M. 2010. Measurement of soil radioactivity levels and radiation hazard assessment in mid Rechna interfluvial region, Pakistan. *Journal of Radioanalytical and Nuclear Chemistry,* 283**,** 371--378.

JACK, C. 2005. *Ewing's Analytical Instrumentation Handbook*, Marcel Dekker Inc.

JENKINS, B. M. 1980. Down-draught gasification characteristics of major California residue-derived fuels.

JOHRI, N., JACQUILLET, G. & UNWIN, R. 2010. Heavy metal poisoning: the effects of cadmium on the kidney. *Biometals,* 23**,** 783-792.

JONES, J. C. 2010. *Thermal Processing of Waste*.

KAHL, A. 2003. KAHL Pelleting Presses. *KAHL Pelleting Presses***,** 8.

KALANATARIFARD, A. A. 2012. Identification of the Municipal Solid Waste Characteristics and Potential of Plastic Recovery at Bakri Landfill, Muar, Malaysia. *Journal of Sustainable Development,* 5**,** 11--17.

KARIM, R., KURAOKA, M., HIGUCHI, T., SEKINE, M. & IMAI, T. 2014. Assessment of Heavy Metal Contamination from Municipal Solid Waste Open Dumping Sites in Bangladesh. 2**,** 41--49.

KAUPP, A. & GOSS, J. R. 1987. State of the Art for small Scale (to 50 kW) Gas Producer- Engine Systems. U.S.D.A. Forest Service.

KHANDAKER, M. U. 2011. High purity germanium detector in gamma-ray spectrometry. *International journal of Fundamental physical sciences,* 1**,** 42--46.

KILIAN, A. 2017. Copper production growth to accelerate to 2021. Available: http://www.miningweekly.com/article/copper-production-growth-to-accelerate-to-2021-2017-06-19 [Accessed 8 June 2018].

KINGSTON, H. M. & HASWELL, S. J. 1997. *Microwave-Enhanced Chemistry, Fundamentals, Sample Preparation and Applications, American Chemical Society*.

KLUSKA, J., KLEIN, M., KAZIMIERSKI, P. & KARDAŚ, D. 2014. Pyrolysis of biomass and refuse-derived fuel performance in laboratory scale batch reactor. *Archives of Thermodynamics,* 35**,** 141-152.

KNOX, A. 2005. An Overview of Incineration and EFW Technology as Applied to the Management of Municipal Solid Waste (MSW). *Politics*.

KURODA, K., ENDO, G., OKAMOTO, A. & YOO, Y. S. 1991. Genotoxicity of beryllium, gallium and antimony in short-term assays. *Mutation Research Letters,* 264**,** 163-170.

KWON, E., WESTBY, K. J. & CASTALDI, M. J. 2010. Transforming Municipal Solid Waste (MSW) Into Fuel via the Gasification/Pyrolysis Process. *18th Annual North American Waste-to-Energy Conference,* 7**,** 53--60.

LAHTI ENERGIA, L. 2016. *Kymijärvi II power plant* [Online]. Available: http://www.lahtigasification.com/power-plant [Accessed 2018-02-28 2018].

LARRY, T. 2002. Coal Geology. 79--122.

LEE, S. 1996. *Alternative Fuels*, Taylor and Francis.

LENNTECH. 2018a. *Arsenic (As) - Chemical properties, Health and Environmental effects* [Online]. Available: https://www.lenntech.com/periodic/elements/as.htm [Accessed 10 June 2018].

LENNTECH. 2018b. *Copper (Cu) - Chemical properties, Health and Environmental effects* [Online]. Available: https://www.lenntech.com/periodic/elements/cu.htm [Accessed 8 June 2018].

LENNTECH. 2018c. *Nickel (Ni) - Chemical properties, Health and Environmental effects* [Online]. Available: https://www.lenntech.com/periodic/elements/ni.htm [Accessed 10 June 2018].

LESTANDER, T. A., JOHNSSON, B. & GROTHAGE, M. 2009. NIR techniques create added values for the pellet and biofuel industry. *Bioresource Technology,* 100**,** 1589--1594.

LI, T., ZHOU, Q., ZHANG, N. & LUO, Y. 2008. Toxic effects of chlorpromazine on Carassius auratus and its oxidative stress. *Journal of Environmental Science and Health Part B,* 43**,** 638-643.

LI, Y., JIANG, L., ZHAO, N., LI, Y., LI, R. & CHI, Y. Combustion characteristic of refuse derived fuel under oxygen-enriched atmosphere. Materials for Renewable Energy and Environment (ICMREE), 2013 International Conference on, 2014. IEEE, 462-466.

LINDELL, B. 1987. Radiation and health. *Bulletin of the World Health Organization,* 65**,** 139--148.

LIU, Z.-S., LIN, C.-L., CHANG, T.-J. & WENG, W.-C. 2016. Waste-gasification efficiency of a two-stage fluidized-bed gasification system. 48**,** 250--256.

MA, J. & SINGHIRUNNUSORN, W. 2012. Distribution and health risk assessment of heavy metals in surface dusts of Maha Sarakham municipality. *Procedia-Social and Behavioral Sciences,* 50**,** 280-293.

MARTIN, M. H. & COUGHTREY, P. J. 1982. *Biological Monitoring of Heavy Metal Pollution*, Applied Science Publishers LTD.

MAVUKWANA, A., JALAMA, K., FREEMAN, N. & HARDING, K. 2013. *Simulation of sugarcane bagasse gasification using Aspen Plus*.

MEHRA, R. & SINGH, M. 2011. Measurement of radioactivity of 238U, 226Ra, 232Th and 40K in soil of different geological origins in Northern India. *Journal of Environmental Protection,* 2**,** 960.

MENG, A., CHEN, S., ZHOU, H., LONG, Y., ZHANG, Y. & LI, Q. 2015. Pyrolysis and simulation of typical components in wastes with macro-TGA. *Fuel,* 157**,** 1--8.

MOSTAFAVI, E., PAULS, J. H., LIM, C. J. & MAHINPEY, N. 2016. Simulation of high-temperature steam-only gasification of woody biomass with dry-sorption CO2 capture. *The Canadian Journal of Chemical Engineering,* 94**,** 1648--1656.

MULLER, G. 1969. Index of Geoaccumulation in Sediments of the Rhine River. *GeoJournal,* 2**,** 108-118.

NÁSNER, A. M. L., LORA, E. E. S., PALACIO, J. C. E., ROCHA, M. H., RESTREPO, J. C., VENTURINI, O. J. & RATNER, A. 2017. Refuse Derived Fuel (RDF) production and gasification in a pilot plant integrated with an Otto cycle ICE through Aspen plus™ modelling: Thermodynamic and economic viability. *Waste Management,* 69**,** 187-201.

NATIONAL INSTITUTE OF ENVIRONMENTAL HEALTH SCIENCES, N. 2017. *Arsenic* [Online]. Available: https://www.niehs.nih.gov/health/topics/agents/arsenic/index.cfm [Accessed 10 June 2018].

NATIONAL PLANNING COMMISION, N. 2012. National Development Plan 2030: Our future - make it work.

NAVAS, A., SOTO, J. & MACHN, J. 2002. 238U 226Ra 210Pb, 232Th and 40K activities in soil profiles of the Flysch sector (Central Spanish Pyrenees). *Applied radiation and isotopes : including data, instrumentation and methods for use in agriculture, industry and medicine,* 57**,** 579--89.

NEWMAN, R. T., LINDSAY, R., MAPHOTO, K. P., MLWILO, N. A., MOHANTY, A. K., ROUX, D. G., DE MEIJER, R. J. & HLATSHWAYO, I. N. 2008. Determination of soil, sand and ore primordial radionuclide concentrations by full-spectrum analyses of high-purity germanium detector spectra. *Applied Radiation and Isotopes*.

NIU, M., HAUNG, Y., JIN, B. & WANG, X. 2014. Oxygen Gasification of Municipal Solid Waste in a Fixed-bed Gasifier. *Chinese Journal of Chemical Engineering***,** 1021--1026.

NOWROUZI, M. & POURKHABBAZ, A. 2014. Application of geoaccumulation index and enrichment factor for assessing metal contamination in the sediments of Hara Biosphere Reserve, Iran. *Chemical Speciation & Bioavailability,* 26**,** 99-105.

ODUKOYA, A. & ABIMBOLA, A. 2011. Potential soil contamination with toxic metals in the vicinity of active and abandoned dumpsites. *Agriculture and Biology Journal of North America,* 2**,** 785--790.

OGUNDIRAN, M. & OSIBANJO, O. 2009. Mobility and speciation of heavy metals in soils impacted by hazardous waste. *Chemical Speciation & Bioavailability,* 21**,** 59-69.

OLADAPO, O. O., ONI, E. A., OLAWOYIN, A. A., AKERELE, O. O. & TIJANI, S. A. 2012. Assessment of Natural Radionuclides Level in Wasteland Soils. 2**,** 38--43.

PAPP, Z., DEZSŐ, Z. & DARCZY, S. 1997. Measurement of the radioactivity of 238U, 232Th, 226Ra, 137Cs and 44K in soil using direct Ge(Li) γ-ray spectrometry. *Journal of Raa \~ oanalytical and Nuclear Chemistry,* 222**,** 171--176.

PARR INSTRUMENT COMPANY, P. 2007. Introduction to Bomb Calorimetry.

PATEL, M. L. & CHAUHAN, J. S. 2014. Municipal solid waste: alternative source of energy to the cement kilns in the state of Madhya Pradesh, India. *International Journal of Environment and Sustainable Development,* 13**,** 142.

PELHEAT.COM 2014. The Beginners Guide To Pellet Production. 12.

PRECHTHAI, T., PARKPIAN, P. & VISVANATHAN, C. 2008. Assessment of heavy metal contamination and its mobilization from municipal solid waste open dumping site. *Journal of Hazardous Materials,* 156**,** 86--94.

PROHASKA, J. R. 2000. Long-term functional consequences of malnutrition during brain development: copper. *Nutrition,* 16**,** 502-504.

RAJVANSHI, A. K. 2014. Biomass gasification. *Alternative Energy in Agriculture,* II**,** 1--21.

RAMZAN, N., ASHRAF, A., NAVEED, S. & MALIK, A. 2011. Simulation of hybrid biomass gasification using Aspen plus: A comparative performance analysis for food, municipal solid and poultry waste. *Biomass and Bioenergy,* 35**,** 3962-3969.

RAND, T., HAUKOHL, J. & MARXEN, U. 1999. Municipal solid waste incineration. *Municipal waste combustion***,** 111.

RAO, C., SAHUQUILLO, A. & SANCHEZ, J. L. 2008. A review of the different methods applied in environmental geochemistry for single and sequential extraction of trace elements in soils and related materials. *Water, Air, and Soil Pollution,* 189**,** 291-333.

RECARI, J., BERRUECO, C. & ABELL 2016. Gasi fi cation of two solid recovered fuels (SRFs) in a lab-scale fl uidized bed reactor : In fl uence of experimental conditions on process performance and release of HCl , H 2 S , HCN and NH 3. 142**,** 107--114.

REGISTRY, A. 2018. *Substance Priority List | ATSDR* [Online]. Available: https://www.atsdr.cdc.gov/spl/index.html [Accessed 23 May 2018].

ROGELJ, J., DEN ELZEN, M., HHNE, N., FRANSEN, T., FEKETE, H., WINKLER, H., SCHAEFFER, R., SHA, F., RIAHI, K. & MEINSHAUSEN, M. 2016. Paris Agreement climate proposals need a boost to keep warming well below 2 °C. *Nature,* 534**,** 631--639.

ROSSI, L., ARCIELLO, M., CAPO, C. & ROTILIO, G. 2006. Copper imbalance and oxidative stress in neurodegeneration. *The Italian journal of biochemistry,* 55**,** 212-221.

RUBIO, B., NOMBELA, M. & VILAS, F. 2000. Geochemistry of major and trace elements in sediments of the Ria de Vigo (NW Spain): an assessment of metal pollution. *Marine pollution bulletin,* 40**,** 968-980.

SADAKA, S. 2015. Gasification.

SAHRAEI-NEZHAD, F. & AKHLAGHI-BOOZANI, S. 2010. Production and Gasification of Waste Pellets.

SCHNORR, T. M., STEENLAND, K., THUN, M. J. & RINSKY, R. A. 1995. Mortality in a cohort of antimony smelter workers. *American journal of industrial medicine,* 27**,** 759-770.

SEVER, A. A., ATıMTAY, A. & SANIN, F. 2016. Comparison of fuel value and combustion characteristics of two different RDF samples. *Waste management (New York, NY),* 47**,** 217.

SHABBAR, S. & JANAJREH, I. 2013. Thermodynamic equilibrium analysis of coal gasification using Gibbs energy minimization method. *Energy Conversion and Management,* 65**,** 755--763.

SHAOHUA, L., DEYONG, C., WENGUANG, Y. & HAIGANG, W. 2012. The effect of ER on biomass gasification in a fixed bed using ASPEN PLUS simulation.

SHEHZAD, A., BASHIR, M. J. K. & SETHUPATHI, S. 2016. System analysis for synthesis gas (syngas) production in Pakistan from municipal solid waste gasification using a circulating fluidized bed gasifier. *Renewable and Sustainable Energy Reviews,* 60**,** 1302--1311.

SIMEX, S. & HELZ, G. 1981. Regional geochemistry of trace elements in Chesapeake Bay. *Environmental Geology,* 3**,** 315-323.

SROOR, A., EL-BAHI, S. M., AHMED, F. & ABDEL-HALEEM, A. S. 2001. Natural radioactivity and radon exhalation rate of soil in southern Egypt. *Applied Radiation and Isotopes,* 55**,** 873--879.

STAFF WRITER, S. 2016. Life expectancy in South Africa vs the world. Available: https://businesstech.co.za/news/lifestyle/124343/life-expectancy-in-south-africa-vs-the-world/ [Accessed 27 June 2017].

SUNDARESHAN, S. 2013. ENVIRONMENTAL RADIOACTIVITY : A CASE STUDY IN BANGALORE METROPOLITAN , INDIA Submitted by.

TESSIER, A., CAMPBELL, P. G. & BISSON, M. 1979. Sequential extraction procedure for the speciation of particulate trace metals. *Analytical chemistry,* 51**,** 844-851.

THE ENVIRONMENTAL ILLNESS RESOURCE, T. 2016. *Heavy Metal Toxicity* [Online]. Available: http://www.ei-resource.org/illness-information/related-conditions/heavy-metal-toxicity/?tmpl=component [Accessed 26 February 2017].

THEMELIS, N. J. & MUSSCHE, C. 2014. 2014 Energy and Economic Value of Municipal Solid Waste (MSW), Including Non-Recycled plastics (NRP), Currently Landfilled in the Fifty States.

TZORTZIS, M., TSERTOS, H., CHRISTOFIDES, S. & CHRISTODOULIDES, G. 2003. Gamma-ray measurements of naturally occurring radioactive samples from Cyprus characteristic geological rocks. *Radiation Measurements,* 37**,** 221--229.

U.S. DEPARMENT OF ENEGRY, U. 2000. RAIS: Risk Assessment Information System. *In:* ENERGY, U. S. D. O. (ed.). US Department of Energy: Office of Environmental Management.

UNITED NATIONS SCIENTIFIC COMMITTEE ON THE EFFECTS OF ATOMIC RADIATION, U. 2010. Exposures of the public and workers from various sources of radiation. *In:* ASSEMBLY, G. (ed.). New York: United Nations Publishers.

UNITED STATES ENVIRONMENTAL PROTECTION, A. 1989. Risk Assessment Guidance for Superfund. Vol I Human Health Evaluation Manual (Part A). Office of Emergency and Remedial Response Washington.

UNITED STATES ENVIRONMENTAL PROTECTION AGENCY, U. 1979. Water Related Fate of the 129 Priority Pollutants. US Environmental Protection Agency, Office of Water Planning and Standards Washington (DC.

USEPA, M. 1996. Soil screening guidance technical background document. *Office of Solid Waste and Emergency Response, Washington, DC EPA/540,* 95.

USLU, A., FAAIJ, A. P. C. & BERGMAN, P. C. A. 2008. Pre-treatment technologies, and their effect on international bioenergy supply chain logistics. Techno-economic evaluation of torrefaction, fast pyrolysis and pelletisation. *Energy,* 33**,** 1206--1223.

VAN DEN BERG, R. 1995. Human exposure to soil contamination: a qualitative and quantitative analysis towards proposals for human toxicology intervention values. RIVM Report no. 725201011 National Institute of Public Health and Environmental Protection (RIVM) Bilthoven. The Netherlands.

VAN DER MERWE, M. 2016. *South Africa gets its first Refuse-Derived Fuel Plant* [Online]. Daily Maverick. Available: https://www.dailymaverick.co.za/article/2016-02-18-south-africa-gets-its-first-refuse-derived-fuel-plant/ \# [Accessed 27 June 2017].

VIERHOUT, R. 2016. Enerkem biorefineries : setting a new global standard in biofuels , chemicals and waste management Enerkem at a glance.

VON BURG, R. Nickel and some nickel compounds. Journal of Applied Toxicology: An International Forum Devoted to Research and Methods Emphasizing Direct Clinical, Industrial and Environmental Applications, 1997. Wiley Online Library, 425-431.

WALI, A., COLINET, G. & KSIBI, M. 2014. Speciation of heavy metals by modified BCR sequential extraction in soils contaminated by phosphogypsum in Sfax, Tunisia. *Environmental Research, Engineering & Management,* 4**,** 14-26.

WANG, L. 2014. *Sustainable Energy Production*, CRC Press Taylor and Francis Group.

WAOO, A. A., KHARE, S. & GANGULI, S. 2014. Extraction and Analysis of Heavy Metals from Soil and Plants in the Industrial Area Govindpura , Bhopal. 1.

WILLIAMS, P. 1998. *Waste Treatment and Disposal*, John Wiley and Sons.

WORLD HEALTH ORGANIZATION, W. 1996. *Trace elements in human nutrition and health*, World Health Organization.

WORLD HEALTH ORGANIZATION, W. 2011. Guidelines for drinking-water quality. *WHO chronicle,* 38**,** 104-8.

WU, F., FU, Z., LIU, B., MO, C., CHEN, B., CORNS, W. & LIAO, H. 2011. Health risk associated with dietary co-exposure to high levels of antimony and arsenic in the world's largest antimony mine area. *Science of the Total Environment,* 409**,** 3344-3351.

XIANDENG, H. & BRADLEY, J. 2000. Inductively Coupled Plasma–Optical Emission Spectrometry. *Spectroscopy Letters,* 42**,** 58--61.

YANG, Y. X., WU, X. M., JIANG, Z. Y., WANG, W. X., LU, J. G., LIN, J., WANG, L. M. & HSIA, Y. F. 2005. Radioactivity concentrations in soils of the Xiazhuang granite area, China. *Applied Radiation and Isotopes,* 63**,** 255--259.

YUEHONG, Z., HAO, W. & ZHIHONG, X. 2006. Conceptual design and simulation study of a co-gasification technology. *Energy Conversion and Management,* 47**,** 1416--1428.

ZAFAR, S. 2009. Waste Pelletization. *Waste to Energy***,** 14--19.

ZAFAR, S. 2015. Fuel Pellets from Solid Wastes.

ZALEWSKI, M., TOMCZAK, M. & KAPAA, J. 2001. Radioactivity of Building Materials Available in Northeastern Poland. *Polish Journal of Environmental Studies,* 10**,** 183--188.

ZAMANI-AHMADMAHMOODI, R., ESMAILI-SARI, A., MOHAMMADI, J., BAKHTIARI, A. R. & SAVABIEASFAHANI, M. 2013. Spatial distribution of cadmium and lead in the sediments of the western Anzali wetlands on the coast of the Caspian Sea (Iran). *Marine pollution bulletin,* 74**,** 464-470.

ZHANG, D. Q., TAN, S. K. & GERSBERG, R. M. 2010. Municipal solid waste management in China: Status, problems and challenges.

ZHANG, J. & LIU, C. 2002. Riverine composition and estuarine geochemistry of particulate metals in China—weathering features, anthropogenic impact and chemical fluxes. *Estuarine, coastal and shelf science,* 54**,** 1051-1070.

ZHANG, Q., WU, Y., DOR, L., YANG, W. & BLASIAK, W. 2013. A thermodynamic analysis of solid waste gasification in the Plasma Gasification Melting process. *Applied Energy,* 112**,** 405--413.

ZHANG, Y., CHEN, Y., MENG, A., LI, Q. & CHENG, H. 2008. Experimental and thermodynamic investigation on transfer of cadmium influenced by sulfur and chlorine during municipal solid waste (MSW) incineration. *Journal of Hazardous Materials,* 153**,** 309--319.

ZHEN, X. & WANG, Y. 2015. An overview of methanol as an internal combustion engine fuel. *Renewable and Sustainable Energy Reviews,* 52**,** 477-493.

ZHENG, H., KALIYAN, N. & MOREY, R. V. 2013. Aspen Plus simulation of biomass integrated gasification combined cycle systems at corn ethanol plants. *Biomass and Bioenergy,* 56**,** 197--210.

ZHENG, L. & FURIMSKY, E. 2003. ASPEN simulation of cogeneration plants. *Energy Conversion and Management,* 44**,** 1845--1851.

ZHENG, N., LIU, J., WANG, Q. & LIANG, Z. 2010. Health risk assessment of heavy metal exposure to street dust in the zinc smelting district, Northeast of China. *Science of the Total Environment,* 408**,** 726-733.

ZHONG, W.-S., REN, T. & ZHAO, L.-J. 2016. Determination of Pb (Lead), Cd (Cadmium), Cr (Chromium), Cu (Copper), and Ni (Nickel) in Chinese tea with high-resolution continuum source graphite furnace atomic absorption spectrometry. *journal of food and drug analysis,* 24**,** 46-55.

Appendices

Appendix A: Sample Data and Calculations

Radionuclide Analysis

The absolute efficiency at a specific photopeak energy was determined using:

$$\text{Eff}' = \text{Eff}.\, e^{-\mu(E)\rho t}$$

Eff′ = Absolute efficiency at a specific photopeak energy after attenuation correction

Eff = Efficiency prior to specific photopeak energy attenuation correction

μ(E) = Mass attenuation at a specific gamma energy E

ρt = Average sample mass per unit area.

$$\therefore \text{Eff}' = 7.58e^{-0.882\times185.9700}$$

$$\therefore \text{Eff}' = 0.07550$$

The activity concentrations of the various radionuclides were determined using equation stipulated below:

$$A = \frac{C}{LT\times b\times m\times Eff'}$$

A = Net peak area

LT = Live time

b = Branching ratio (gamma-ray emission probability corresponding to the photopeak energy)

m = Sample mass

Eff′ = Absolute efficiency at a specific photopeak energy

$$\therefore A = \frac{613.35}{86400\times0.06167\times0.17\times0.07550}$$

$$\therefore A = 9.0816118$$

Table F1: Radionuclide analysis readings and activity concentrations.

									Eff	7.58	-0.882		
	BV7												
		background	240941	sample									
	E (keV)	Cbg	Cbg (cor)	Cspec	C	LT	b	m(kg)	Eff	A(Bq/kg)	A(Bq/kg)av		
Ra	185.9700	4433.00	1589.65	2203	613.35	86400	0.06167	0.17	0.07550	9.086118	9.08612	2.12	
Pb	239.2000	45.00	16.14	5669	5652.86	86400	0.07498	0.17	0.06047	85.99572			
	295.2200	329.00	117.98	1026	908.02	86400	0.18496	0.17	0.05022	6.742109			
	351.9100	417.00	149.53	1800	1650.47	86400	0.35792	0.17	0.04302	7.393985	33.3773	45.5701	
Bi	609.1100	339.00	121.56	1383	1261.44	86400	0.44791	0.17	0.02651	7.326412			
	767.8000	4.00	1.43	177	175.57	86400	0.04799	0.17	0.02162	11.67318			
	964.3400	23.00	8.25	196	187.75	86400	0.03029	0.17	0.01768	24.17887			
	1119.8600	115.00	41.24	309	267.76	86400	0.14797	0.17	0.01550	8.054738			
	1238.4200	15.00	5.38	141	135.62	86400	0.05859	0.17	0.01418	11.26008			
	1377.4700	28.00	10.04	57	46.96	86400	0.03919	0.17	0.01291	6.4019			
	1729.4800	20.00	7.17	49	41.83	86400	0.02879	0.17	0.01056	9.486797			
	1763.9700	218.00	78.17	286	207.83	86400	0.15357	0.17	0.01038	8.993261			
	2203.9500	80.00	28.69	91	62.31	86400	0.04859	0.17	0.00853	10.37158	9.34452	2.58682	

The results of the radionuclide analysis show the activity concentrations of the progenies relating to the parent radionuclides of ^{238}U, ^{232}Th, and ^{40}K respectively. The parent concentrations were determined by averaging the progenies or daughter radionuclides which were identified as Radium (^{226}Ra), Lead (^{214}Pb), Bismuth (^{214}Bi) for ^{238}U, Actinium (^{228}Ac) and Thallium (^{208}Tl) for ^{232}Th, as well as the individual naturally occurring radionuclide Potassium (^{40}K).

Table A2: Activity concentrations for daughter radionuclides and their related parent radionuclides.

	Ra		Pb		Bi		Ac		Tl		K						
	A(Bq/Kg)	σ	A(Bq/Kg)	σ	A(Bq/Kg)	σ	A(Bq/Kg)	σ	A(Bq/Kg)	σ	A(Bq/Kg)	σ				U	Th	K
bvcput	7.650	1.604	8.373	1.490	10.228	3.687	9.989	0.385	12.220	2.729	91.169	9.614			bvcput	8.8	11.1	91.2
bv7	9.086	2.117	33.377	45.570	9.345	2.587	11.198	0.983	11.982	3.813	81.257	8.636			bv7	17.3	11.6	81.3
bv8	9.572	2.009	35.556	44.563	16.256	4.485	10.146	1.858	17.659	4.283	99.553	10.565			bv8	20.5	13.9	99.6
bv10	8.570	2.016	25.775	32.459	10.017	1.841	9.039	0.145	8.510	3.394	69.550	7.563			bv10	14.8	8.8	69.6
bv11	2.582	1.635	21.163	27.194	7.603	3.926	6.943	0.610	8.588	3.181	47.669	5.700			bv11	10.4	7.8	47.7
bv11,2	4.463	1.571	20.411	27.463	8.256	1.941	8.054	2.462	7.962	3.227	45.031	5.181			bv11,2	11.0	8.0	45.0
bv16	9.482	2.230	34.549	45.829	12.320	2.592	12.707	0.013	12.384	3.451	109.991	11.563			bv16	18.8	12.5	110.0
bv285	12.492	2.527	37.348	49.021	10.965	4.778	12.974	0.782	19.080	6.612	100.772	10.544			bv285	20.3	16.0	100.8
bv486	14.359	2.586	39.461	50.293	18.747	2.971	15.849	0.028	20.814	5.965	122.014	12.799			bv486	24.2	18.3	122.0
bv1813	9.052	2.513	21.220	27.520	9.454	7.462	7.135	1.485	8.354	3.447	50.254	5.814			bv1813	13.2	7.7	50.3
bv3817	11.553	2.788	32.922	40.805	13.229	6.181	10.760	1.523	12.304	4.216	82.524	8.970			bv3817	19.2	11.5	82.5
bv9815	9.907	2.637	22.718	30.255	11.110	1.732	8.298	1.709	14.107	4.274	56.999	6.567			bv9815	14.6	11.2	57.0
bv12814	9.581	2.019	21.685	27.317	7.611	3.016	8.854	0.434	12.607	5.028	51.258	6.154			bv12814	13.0	10.7	51.3
cp7	7.720	2.114	27.503	33.973	8.632	1.540	10.533	0.936	15.606	4.486	79.779	8.762			cp7	14.6	13.1	79.8
cp688	9.439	2.680	31.936	40.968	9.265	2.808	12.514	1.272	16.558	4.203	63.910	7.027			cp688	16.9	14.5	63.9
vk3	19.384	3.912	58.314	68.756	20.398	5.007	19.702	1.524	26.342	8.222	248.150	25.232			vk3	32.7	23.0	248.1
vk10	14.400	2.540	42.417	50.976	14.934	1.923	14.621	0.381	16.945	4.448	155.766	16.074			vk10	23.9	15.8	155.8
vk384	25.063	4.105	73.725	88.408	25.032	2.908	24.790	2.217	27.518	6.665	352.432	35.706			vk384	41.3	26.2	352.4

The radium equivalent is calculated by the equation:

$$Ra_{eq} = C_{Ra} + 1.43C_{Th} + 0.077C_K$$

Where C_{Ra}, C_{Th} and C_K are the activity concentrations of ^{226}Ra, ^{232}Th and ^{40}K respectively.

$$Ra_{eq} = 15.847 + 1.43(11.481) + 0.077(77.542)$$

$$Ra_{eq} = 38.237$$

The external hazard index is calculated as follows:

$$H_{ex} = \frac{C_{Ra}}{370\ Bq/kg} + \frac{C_{Th}}{259\ Bq/kg} + \frac{C_K}{4810\ Bq/kg}$$

Where C_{Ra}, C_{Th} and C_K are the activity concentrations in Bq/kg for ^{226}Ra, ^{232}Th and ^{40}K respectively.

$$H_{ex} = \frac{15.847}{370} + \frac{11.481}{259} + \frac{77.542}{4810}$$

$$H_{ex} = 0.103$$

The internal hazard index is determined by the following equation:

$$H_{in} = \frac{C_{Ra}}{158\ Bq/kg} + \frac{C_{Th}}{259\ Bq/kg} + \frac{C_K}{4810\ Bq/kg}$$

$$H_{in} = \frac{15.847}{158} + \frac{11.481}{259} + \frac{77.542}{4810}$$

$$H_{in} = 0.146$$

The representative level index is calculated as follows:

$$I_{\gamma r} = \frac{C_{Ra}}{150\ Bq/kg} + \frac{C_{Th}}{100\ Bq/kg} + \frac{C_K}{1500\ Bq/kg}$$

$$I_{\gamma r} = \frac{15.847}{150} + \frac{11.481}{100} + \frac{77.542}{1500}$$

$$I_{\gamma r} = 0.2722$$

Table A3: Averaged activity concentrations for parent radionuclides for each site and hazard indices.

	U	Th	K	Radium Equivalent (Bq/Kg)
Bellville	15.847	11.481	77.5416	38.237
Coastal Park	15.749	13.803	71.8444	41.019
Vissershok	32.630	21.653	252.1159	83.007
Site	H_{ex}	H_{in}	$I_{\gamma r}$	
Bellville	0.103	0.146	0.2722	
Coastal Park	0.111	0.153	0.2909	
Vissershok	0.224	0.312	0.6021	

The absorbed dose rate is determined as follows:

$$D = 0.462C_{Ra} + 0.604C_{Th} + 0.0417C_K$$

$$D = 0.462(15.847) + 0.604(11.481) + 0.0417(77.5416)$$

$$D = 17.490\ (\mathrm{nGy/h})$$

Annual effective dose rate outdoors is determined as follows:

$$E = D(\mathrm{nGy/h}) \times 8760(\mathrm{h/y}) \times 0.2 \times 0.7(\mathrm{Sv/Gy}) \times 10^{-6}$$

$$E = 17.490 \times 8760 \times 0.2 \times 0.7 \times 10^{-6}$$

$$E = 0.0214\ (\mathrm{mSv/y})$$

Annual effective dose rate indoors is determined as follows:

$$E = D(\mathrm{nGy/h}) \times 8760(\mathrm{h/y}) \times 0.8 \times 0.7(\mathrm{Sv/Gy}) \times 10^{-6}$$

$$E = 17.490 \times 8760 \times 0.8 \times 0.7 \times 10^{-6}$$

$$E = 0.0858\ (\mathrm{mSv/y})$$

The effective lifetime cancer risk (ELCR) is determined as follows:

$$ECLR = E \times DL \times RF$$

Where E is the annual effective dose rate (mSv/y), DL is the duration of life or life expectancy of which is 62.9 years in South Africa and RF is the risk factor (Sv^{-1}) which indicates fatal cancer per Sievert.

$$ECLR = 0.0214 \times 62.9 \times 0.05$$

$$ECLR = 0.0675$$

Heavy Metal Analysis

Table A4: Heavy metal analysis readings for Bellville site from Inductively Coupled Plasma Optical Emission Spectroscopy (ICP-OES) showing fractions 1 to 4 of digestion process

Sample No.	Sample ID	Heavy Metal concentration (µg/g)								
		Zn	**Cr**	**Cd**	**Se**	**Sb**	**Cu**	**Pb**	**Ni**	**As**
		µg/g	µg/g	µg/g	µg/g	µg/g	µg/g	µg/g	µg/g	µg/g
1	F1	11.480	0.880	0.120	3.480	1.800	3.800	0.440	0.360	1.360
	F2	9.320	1.080	0.080	1.080	1.440	2.320	1.640	0.480	0.760
	F3	3.850	0.550	0.350	10.850	1.300	0.450	1.600	0.950	4.050
	R	65.040	21.640	1.040	70.920	12.520	24.040	21.000	20.280	13.600
2	F1	30.000	1.000	0.080	5.040	1.440	0.280	0.720	0.000	2.160
	F2	9.200	1.240	0.120	1.440	0.960	0.320	0.600	0.320	0.640
	F3	4.900	0.900	0.300	10.550	1.150	0.900	1.150	0.350	3.800
	R	11.440	5.720	0.000	11.280	2.800	3.440	5.000	3.480	2.400
3	F1	5.800	0.480	0.040	14.200	3.200	0.080	1.920	0.400	3.800
	F2	4.720	1.200	0.120	3.240	1.160	0.040	0.440	0.200	0.720
	F3	6.100	0.600	0.250	14.300	1.200	0.550	1.100	0.350	3.950
	R	12.760	11.800	0.760	60.240	11.560	5.320	11.280	5.120	9.480
4	F1	37.360	0.520	0.120	16.040	3.480	1.960	8.400	1.600	4.360
	F2	12.800	1.160	0.120	2.200	1.360	0.560	10.840	0.320	0.800
	F3	12.000	2.100	0.300	12.100	1.400	6.250	4.750	2.350	4.100
	R	69.560	23.600	1.160	74.960	12.320	27.360	62.480	20.600	15.440
5	F1	27.400	0.400	0.160	19.640	3.960	6.680	4.920	1.120	5.280
	F2	11.000	1.120	0.120	4.400	1.400	0.320	2.400	0.200	0.960
	F3	7.950	0.800	0.300	12.600	1.250	14.700	1.300	0.650	4.250
	R	50.040	13.840	0.680	50.760	8.680	24.960	27.680	15.720	9.080
6	F1	20.360	0.800	0.040	7.520	2.160	11.920	1.560	1.000	2.440
	F2	4.200	0.760	0.000	2.200	0.760	2.840	0.600	0.360	1.120
	F3	4.250	0.500	0.300	9.750	0.850	4.750	1.200	1.050	3.750
	R	65.640	15.720	0.760	51.480	8.720	28.760	22.680	18.960	11.240
7	F1	10.240	0.720	0.040	6.920	1.920	3.960	1.560	1.840	2.360
	F2	2.880	1.160	0.160	2.160	1.040	0.720	1.240	0.800	0.440
	F3	6.200	0.150	0.300	9.600	1.050	0.250	0.900	1.350	3.700
	R	50.680	14.040	0.600	46.800	7.880	16.040	14.200	17.080	8.280
8	F1	11.560	0.560	0.080	14.680	3.040	2.280	4.240	1.240	4.080
	F2	4.600	1.240	0.160	1.240	0.880	0.000	3.320	0.120	0.560
	F3	3.000	0.200	0.300	13.000	0.900	0.100	0.650	0.050	3.550
	R	31.000	11.160	0.400	33.960	6.280	12.560	13.480	9.880	6.400
9	F1	6.320	1.040	0.120	5.520	22.800	3.440	1.200	3.320	10.640
	F2	2.120	1.240	0.160	2.280	2.520	0.720	1.120	0.040	0.720
	F3	4.850	0.900	0.300	12.450	1.150	0.050	0.950	0.200	3.950
	R	59.120	12.040	0.600	47.040	8.280	20.440	18.440	17.360	8.200
10	F1	378.600	0.600	0.280	21.840	5.760	487.520	6.640	2.920	6.680
	F2	89.520	12.080	0.000	8.840	2.000	373.680	14.280	5.240	1.400
	F3	75.100	15.150	0.250	11.850	1.500	424.100	1.900	7.800	3.750
	R	101.000	904.840	1.360	88.320	15.360	258.120	33.800	76.000	14.720

The mean for each element in each site for each fraction was calculated as follows (NB calculations shown for only Bellville site for Zn metal):

$$\text{Mean F1} = \frac{11.480+30.000+5.800+37.360+27.400+20.360+10.240+11.560+6.320+378.600}{10}$$

$$\text{Mean F1} = 53.91\ \mu g/g$$

$$\text{Mean F2} = \frac{9.320+9.200+4.720+12.800+11.000+4.200+2.880+4.600+2.120+89.520}{10}$$

$$\text{Mean F2} = 15.04\ \mu g/g$$

$$\text{Mean F3} = \frac{3.850+4.900+6.100+12.000+7.950+4.250+6.200+3.000+4.850+75.100}{10}$$

$$\text{Mean F3} = 12.82\ \mu g/g$$

$$\text{Mean R} = \frac{65.040+11.440+12.760+69.560+50.040+65.640+50.680+31.000+59.120+101.000}{10}$$

$$\text{Mean R} = 51.63\ \mu g/g$$

The mobile phases are calculated by adding fractions 1 to 3 for each element on each sample for each site. The mean of each mobile phases is given below or can be calculated by adding the mean of F1 to that of F2 and 3.

$$\text{Mobile Phases (MP)} = \text{F1} + \text{F2} + \text{F3}$$

$$\text{Mobile Phases (MP)} = 53.91 + 15.04 + 12.82$$

$$\text{Mobile Phases (MP)} = 81.77\ \mu g/g$$

The 95% confidence level is obtained as follows:

$$95\%\ \text{Confidence level} = \bar{X} \pm (Z \times \sigma \times n)$$

Where $\bar{X}$ is the sample mean, Z is (1 – confidence level), σ is the sample standard deviation and n is the samples size.

$$95\%\ \text{Confidence level} = 81.77 \pm ((1 - 0.95) \times 162.9 \times 10)$$

$$95\%\ \text{Confidence level} = 81.77 \pm 81.45$$

$$95\%\ \text{Confidence level} = 163.22 \text{ or } 0.32$$

The upper limit is used for further calculations:

$$\therefore 95\%\ \text{Confidence level} = 163.22\ \mu g/g$$

Table A5: Mean activity levels for each site with standard deviation and 95% confidence level.

		Zn		Cr		Cd		Se		Sb		Cu		Pb		Ni		As	
Site	Fraction	MEAN	SD	MEAN	SD	MEAN	SD	MEAN	SD	MEAN	SD	MEAN	SD	MEAN	SD	MEAN	SD	MEAN	SD
Bellville	F1	53.91	114.59	0.70	0.22	0.11	0.07	11.49	6.58	4.96	6.40	52.19	153.00	3.16	2.74	1.38	1.08	4.32	2.74
	F2	15.04	26.42	2.23	3.46	0.10	0.06	2.91	2.30	1.35	0.54	38.15	117.90	3.65	4.85	0.81	1.57	0.81	0.28
	F3	12.82	22.03	2.19	4.59	0.30	0.03	11.71	1.50	1.18	0.20	45.21	133.21	1.55	1.18	1.51	2.31	3.89	0.21
	R	51.63	27.38	103.44	281.63	0.74	0.39	53.58	21.82	9.44	3.59	42.10	76.41	23.00	16.16	20.45	20.46	9.88	4.00
	MP	81.77	162.90	5.11	8.00	0.51	0.08	26.10	9.24	7.48	6.89	135.55	404.04	8.36	8.21	3.70	4.48	9.01	2.87
	Total	133.40	190.42	108.55	289.91	1.24	0.55	79.68	32.20	16.92	10.74	177.66	480.51	31.36	24.93	24.15	25.42	18.90	7.24
	95% from MEAN	81.45		4.00		0.04		4.62		3.44		202.02		4.11		2.24		1.43	
	95% Confidence Level	**163.22**		**9.12**		**0.55**		**30.72**		**10.93**		**337.58**		**12.46**		**5.94**		**10.45**	
Coastal Park	F1	160.88	385.76	0.65	0.27	0.42	0.37	24.78	15.89	5.02	2.68	2.62	5.11	6.57	4.51	2.15	2.05	6.78	4.47
	F2	45.32	97.99	0.78	0.30	0.12	0.08	9.94	7.41	2.54	1.22	0.33	0.21	2.85	1.78	0.30	0.35	2.58	1.96
	F3	22.49	23.14	1.63	1.38	0.17	0.08	14.04	2.49	1.66	0.53	8.12	9.54	1.67	3.02	0.56	0.47	4.27	0.74
	R	33.00	40.79	11.00	10.21	0.22	0.18	24.06	8.60	4.68	1.46	7.55	7.53	24.82	30.52	5.78	5.55	5.28	2.37
	MP	228.69	505.91	3.06	1.60	0.71	0.39	48.76	22.00	9.21	3.67	11.07	13.03	11.08	8.64	3.00	2.51	13.63	5.96
	Total	261.69	547.69	14.05	12.15	0.93	0.71	72.81	34.40	13.89	5.89	18.62	22.39	35.90	39.83	8.78	8.42	18.91	9.54
	95% from MEAN	252.96		0.80		0.19		11.00		1.83		6.51		4.32		1.25		2.98	
	95% Confidence Level	**481.65**		**3.86**		**0.90**		**59.76**		**11.05**		**17.59**		**15.40**		**4.25**		**16.61**	
Vissershok	F1	14.54	7.51	0.50	0.27	0.20	0.15	20.62	9.48	4.31	1.55	1.45	2.73	4.72	1.85	2.26	4.63	5.61	2.53
	F2	12.81	8.94	0.86	0.31	0.09	0.09	8.64	7.44	2.17	1.26	0.40	0.39	2.85	1.08	0.50	0.40	2.01	2.46
	F3	4.51	2.89	0.95	0.74	0.25	0.02	13.22	1.78	1.43	0.20	3.17	3.28	1.19	2.13	0.51	0.19	3.76	0.25
	R	21.40	11.15	11.50	3.65	0.48	0.28	41.14	16.60	7.47	2.84	6.84	2.83	22.63	15.87	4.98	1.69	7.42	2.50
	MP	33.43	538.13	2.21	1.41	0.54	0.39	42.72	20.02	7.99	3.43	4.90	12.40	8.62	8.71	3.11	2.62	11.51	5.60
	Total	53.26	30.49	13.80	4.97	1.01	0.55	83.62	35.30	15.38	5.84	11.86	9.23	31.38	20.93	8.25	6.91	18.80	7.74
	95% from MEAN	269.06		0.71		0.20		10.01		1.71		6.20		4.36		1.31		2.80	
	95% Confidence Level	**302.49**		**2.91**		**0.74**		**52.73**		**9.71**		**11.10**		**12.98**		**4.42**		**14.31**	
Control	F1	2.41	3.45	0.16	0.21	0.41	0.02	37.28	0.45	7.09	0.10	0.43	0.16	6.69	0.18	1.07	0.29	10.47	0.17
	F2	6.72	1.14	0.24	0.07	0.32	0.14	27.35	7.64	5.56	1.15	0.57	0.12	5.20	1.43	0.67	0.43	7.64	1.96
	F3	4.00	1.59	0.13	0.06	0.17	0.08	17.20	2.44	2.23	0.68	3.87	4.10	1.03	1.05	0.58	0.03	5.17	0.90
	R	12.77	1.38	6.19	1.85	0.07	0.05	15.32	4.41	3.04	0.77	3.27	1.06	9.47	4.35	3.92	0.92	3.19	0.89
	MP	13.13	3.36	0.53	0.14	0.90	0.23	81.83	5.83	14.89	0.66	4.87	4.33	12.93	1.79	2.32	0.73	23.27	1.45
	Total	25.91	7.57	6.72	2.19	0.97	0.29	97.15	14.95	17.93	2.71	8.13	5.44	22.39	7.02	6.24	1.67	26.46	3.91
	95% from MEAN	0.50		0.02		0.04		0.87		0.10		0.65		0.27		0.11		0.22	
	95% Confidence Level	**13.64**		**0.56**		**0.94**		**82.70**		**14.99**		**5.52**		**13.19**		**2.43**		**23.49**	

The 95% confidence level concentration is then used to determine the health risk. Below is the sample calculation and data for the health risk determination or adults at the Bellville site.

Table A6: Parameter meaning and value of daily dose model of heavy metals in urban surface dusts (Ma and Singhirunnusorn, 2012)(Ma and Singhirunnusorn, 2012)

Parameter	**Meaning and Unit**	**Values**	
		Child	Adult
C	Exposure-point concentration, mg/µg	95%UCL	
IngR	Ingestion rate, mg/d	200	100
InhR	Inhalation rate m^3/d	7.6	20
PEF	Particle emission factor, m^3/kg	1.36×10^9	
SA	Exposure skin area, cm^2	2800	5700
SL	Skin adherence factor $mg/(cm^2h)$	0.2	0.7
ABS	Dermal absorption factor, unitless	0.001	
ED	Exposure duration, y	6	24
EF	Exposure frequency, d/y	180	

BW	Average body weight, kg	15 70
AT	Average time, d	ED X 365 (non-carcinogens) 70 X 365 (carcinogens)
RfDo	Reference Dose	0.003
GAIBS	Gastrointestinal Absorption Factor	Metal Dependant
RfCi	Inhalation Reference Concentration	Metal Dependant
IUF	Inhalation Unit Risk	Metal Dependant
CF	Conversion Factor	100

D_{ing} is the everyday measurement by means of hand-to-mouth ingestion of substrate particles

$$\mathrm{D_{ing}} = \mathrm{C} \times \frac{\mathrm{IngR} \times \mathrm{EF} \times \mathrm{ED}}{\mathrm{BW} \times \mathrm{AT}} \times 10^{-6}$$

$$\mathrm{D_{ing}} = 163.22 \times \frac{100 \times 350 \times 24}{70 \times 8760} \times 10^{-6}$$

$$\mathrm{D_{ing}} = 2.24 \times 10^{-4}$$

D_{inh} is the day by day dosage by means of inhalation of re-suspended particles through mouth and nose.

$$\mathrm{D_{inh}} = \mathrm{C} \times \frac{\mathrm{InhR} \times \mathrm{EF} \times \mathrm{ED}}{\mathrm{PEF} \times \mathrm{BW} \times \mathrm{AT}}$$

$$\mathrm{D_{inh}} = 163.22 \times \frac{20 \times 350 \times 24}{1.36 \times 10^{9} \times 70 \times 8760}$$

$$\mathrm{D_{inh}} = 3.29 \times 10^{-8}$$

D_{dermal} is the day by day dosage by means of dermal retention of trace components in particles clung to uncovered skin.

$$\mathrm{D_{dermal}} = \mathrm{C} \times \frac{\mathrm{SL} \times \mathrm{SA} \times \mathrm{ABS} \times \mathrm{EF} \times \mathrm{ED}}{\mathrm{BW} \times \mathrm{AT}} \times 10^{-6}$$

$$\mathrm{D_{dermal}} = 163.22 \times \frac{0.07 \times 5700 \times 0.001 \times 350 \times 24}{70 \times 8760} \times 10^{-6}$$

$$\mathrm{D_{dermal}} = 8.92 \times 10^{-7}$$

For non-carcinogens the dosages computed for every component and exposure pathway are in this way divided by the corresponding reference dose (RfDo) to give a hazard quotient (HQ).

$$\mathrm{HQ} = \left(\frac{\mathrm{D_{ing}}}{\mathrm{RfDo}}\right) + \left(\frac{\mathrm{D_{dermal}}}{\mathrm{GAIBS} \times \mathrm{RfDo}}\right) + \left(\frac{\mathrm{D_{inh}}}{\mathrm{RfCi} \times \mathrm{CF}}\right)$$

$$\mathrm{HQ} = \left(\frac{2.24 \times 10^{-4}}{0.003}\right) + \left(\frac{8.92 \times 10^{-7}}{1 \times 0.003}\right) + \left(\frac{3.29 \times 10^{-8}}{0.005 \times 100}\right)$$

$$\mathrm{HQ} = 7.48 \times 10^{-2}$$

For carcinogens, the dose is multiplied by the corresponding slope factor (SFO) to create a gauge of cancer risk (CR).

$$CR = \left(\frac{SFO \times D_{dermal}}{GAIBS}\right) + (IUR \times D_{inh}) + (SFO \times D_{ing})$$

$$CR = \left(\frac{0 \times 8.9 \times 10^{-7}}{1}\right) + (0.9 \times 3.29 \times 10^{-8}) + (0 \times 2.24 \times 10^{-4})$$

$$CR = 2.96 \times 10^{-8}$$

Table A7: Data and results for Dose, Hazard Quotient and Cancer Risk for Adults in the Bellville site.

Parameters	Values Test	Zn	Cr	Cd	Se	Sb	Cu	Pb	Ni	As
conc at 95% confidence level ( )	1	163.215966	9.115038	0.545228	30.72146	10.92594	337.5764	12.46324	5.940449	10.44597
Body Weight (BW)	70	70	70	70	70	70	70	70	70	70
Averaging Time (AT)	1	8760	25550	25550	25550	25550	8760	25550	25550	25550
Exposure Frequency (EF)	1	350	350	350	350	350	350	350	350	350
Exposure Duration (ED)	1	24	24	24	24	24	24	24	24	24
Ingestion Rate (soil) (IngR)	1	100	100	100	100	100	100	100	100	100
GI absorption factor (GI)	1	1	1	1	1	1	1	1	1	1
Surface Area Exposed Skin (SA)	1	5700	5700	5700	5700	5700	5700	5700	5700	5700
Soil to Skin Adherence Factor (AF)	1	0.07	0.07	0.07	0.07	0.07	0.07	0.07	0.07	0.07
Dermal Absorption Factor (ABSi)	1	0.001	0.001	0.001	0.001	0.001	0.001	0.001	0.001	0.03
Inhalation Rate (air) (InhR)	1	20	20	20	20	20	20	20	20	20
Particulate Emission Factor(PEF)	1	1360000000	1.36E+09	1.36E+09	1.36E+09	1.36E+09	1.36E+09	1.36E+09	1.36E+09	1.36E+09
Soil to Air VolatilisationFactor(VF)	1									2
Skin adherence factor (SL)	1	0.07	0.07	0.07	0.07	0.07	0.07	0.07	0.07	0.07
refrence dose (RfDo)	1	0.003	0.003	0.001	0.005	0.0004	0.04	0.02	0.02	0.0003
inhalation reference concentration $RfCi$	1	0.005	0.0001	0.0001	0.005	0.2	0.075	0.0002	0.00009	0.000015
gastrointestinalabsorption factor (GAIBS)	1	1	0.025	0.025	1	0.15	0.3	0.025	0.04	1
inhalation unit risk (IUR)	1	0.9	0.084	0.0018			2.4	0.15	0.00026	0.0043
conversion factor	100	100	100	100	1	100	100	100	100	100
SFO	1		0.5	6.1				0.5	0.84	1.5
D_{ing}	1.43E-08	2.24E-04	4.28E-06	2.56E-07	1.44E-05	5.13E-06	4.62E-04	5.85E-06	2.79E-06	4.91E-06
D_{inh}	1.43E-02	3.29E-08	6.30E-10	3.77E-11	2.12E-09	7.55E-10	6.80E-08	8.61E-10	4.10E-10	7.21E-10
D_{dermal}	1.43E-08	8.92E-07	1.71E-08	1.02E-09	5.76E-08	2.05E-08	1.85E-06	2.34E-08	1.11E-08	5.87E-07
H_{ing}	1.43E-08	7.45E-02	1.43E-03	2.56E-04	2.89E-03	1.28E-02	1.16E-02	2.93E-04	1.40E-04	1.64E-02
H_{inh}	1.43E-04	6.58E-08	6.30E-08	3.77E-09	4.24E-07	3.77E-11	9.07E-09	4.30E-08	4.56E-08	4.81E-07
H_{dermal}	1.43E-08	2.97E-04	2.28E-04	4.09E-05	1.15E-05	3.41E-04	1.54E-04	4.67E-05	1.39E-05	1.96E-03
HQ	1.43E-04	7.48E-02	1.65E-03	2.97E-04	2.90E-03	1.32E-02	1.17E-02	3.39E-04	1.53E-04	1.83E-02
C_{ing}	1.43E-08	0.00E+00	2.14E-06	1.56E-06	0.00E+00	0.00E+00	0.00E+00	2.93E-06	2.34E-06	7.36E-06
C_{inh}	1.43E-02	2.96E-08	5.29E-11	6.78E-14	0.00E+00	0.00E+00	1.63E-07	1.29E-10	1.07E-13	3.10E-12
C_{dermal}	1.43E-08	0.00E+00	3.42E-07	2.49E-07	0.00E+00	0.00E+00	0.00E+00	4.67E-07	2.34E-07	8.81E-07
CR	1.43E-02	2.96E-08	2.48E-06	1.81E-06	0.00E+00	0.00E+00	1.63E-07	3.39E-06	2.58E-06	8.24E-06

Gasification Model

Table A8: Gasification model stream data for simulation of RDF pellets bound with guar-gum powder.

Material											
Stream Name	Units	AIR	DRY-RDF	EXHAUST	GASES	GSFYFEED	IN-DRIER	PRODUCTS	SOLIDS	TO-GASFY	WET-RDF
Description											
From			DRY-FLSH	DRY-FLSH	02-Sep	MIX	DRY-REAC	GASIFY	02-Sep	DECOMP	
To		MIX	DECOMP			GASIFY	DRY-FLSH	02-Sep		MIX	DRY-REAC
Stream Class		MCINCPSD	MCINCPSD		MCINCPSD	MCINCPSD	MCINCPSD	MCINCPSD	MCINCPSD	MCINCPSD	MCINCPSD
Maximum Relative Error											
Cost Flow	$/hr										
Total Stream											
Temperature	C	25	250 648		700	234 334	25	700	700	25	25
Pressure	bar	101 353	101 353		101 353	101 353	101 353	101 353	101 353	101 353	101 353
Mass Vapor Fraction		1	0		1	0,517599	0	0,79501	0	0,419763	0
Mass Liquid Fraction		0	0		0	0,064573	0	0	0	0,078849	0
Mass Solid Fraction		0	1		0	0,417825	1	0,20499	1	0,50139	1
Mass Enthalpy	kcal/kg	-6.48E-10	-1252,45		-835 605	-310 364	-1252,48	-627 066	181 708	-372 436	-1128,43
Mass Density	kg/cum	117 958	1232,64		0,196543	0,980865	1232,64	0,247216	2488,35	0,944758	1232,64
Enthalpy Flow	Gcal/hr	-1.30E-15	-0,0125245		-0,00797 177	-0,00372 436	-0,0125 248	-0,00752 479	0,00044 698	-0,00372 436	-0,0112 843
Mass Flows	kg/hr	2	10		954 012	12	10	12	245 988	10	10
H2O	kg/hr	0	0		0,869122	1	0	0,869122	0	1	0
N2	kg/hr	153 417	0		160 887	160 887	0	160 887	0	0,0747	0
O2	kg/hr	0,465834	0		0	371 483	0	7.98E-17	0	3 249	0
RDF	kg/hr	0	10		0	0	10	0	0	0	10
NO2	kg/hr	0	0		0	0	0	3.13E-22	0	0	0
NO	kg/hr	0	0		0	0	0	2.25E-10	0	0	0
S	kg/hr	0	0		0,000532549	0,027	0	0,000532549	0	0,027	0
SO2	kg/hr	0	0		0,052879 4	0	0	0,052879 4	0	0	0

SO3	kg/hr	0	0		0	0	0	1.05E-07	0	0	0
H2	kg/hr	0	0		0,582334	0,6354	0	0,582334	0	0,6354	0
CL2	kg/hr	0	0		0	0	0	0	0	0	0
HCL	kg/hr	0	0		0	0	0	0	0	0	0
C	kg/hr	0	0		0	43 497	0	179 568	179 568	43 497	0
CO	kg/hr	0	0		431 056	0	0	431 056	0	0	0
CO2	kg/hr	0	0		184 639	0	0	184 639	0	0	0
ASH	kg/hr	0	0		0	0,6642	0	0,6642	0,6642	0,6642	0
CH4	kg/hr	0	0		0,269429	0	0	0,269429	0	0	0
Mass Fractions											
H2O		0	0		0,0911018	0,0833333	0	0,0724269	0	0,1	0
N2		0,767083	0		0,168642	0,134072	0	0,134072	0	0,00747	0
O2		0,232917	0		0	0,30957	0	6.65E-18	0	0,3249	0
RDF		0	1		0	0	1	0	0	0	1
NO2		0	0		0	0	0	2.61E-23	0	0	0
NO		0	0		0	0	0	1.87E-11	0	0	0
S		0	0		5.58E+00	0,00225	0	4.44E+00	0	0,0027	0
SO2		0	0		0,00554285	0	0	0,00440662	0	0	0
SO3		0	0		0	0	0	8.71E-09	0	0	0
H2		0	0		0,0610405	0,05295	0	0,0485278	0	0,06354	0
CL2		0	0		0	0	0	0	0	0	0
HCL		0	0		0	0	0	0	0	0	0
C		0	0		0	0,362475	0	0,14964	0,729987	0,43497	0
CO		0	0		0,451835	0	0	0,359214	0	0	0
CO2		0	0		0,19354	0	0	0,153866	0	0	0
ASH		0	0		0	0,05535	0	0,05535	0,270013	0,06642	0
CH4		0	0		0,0282417	0	0	0,0224524	0	0	0
Volume Flow	cum/hr	169 552	0,00811266		485 396	122 341	0,00811266	485 406	0,000988558	105 847	0,00811266

MIXED Substream											
Phase		Vapor	Missing		Vapor	Mixed	Missing	Vapor	Missing	Mixed	Missing
Temperature	C	25			700	234 334		700		25	
Pressure	bar	101 353			101 353	101 353		101 353		101 353	
Molar Vapor Fraction		1			1	0,92231		1		0,909403	
Molar Liquid Fraction		0			0	0,0776898		0		0,0905974	
Molar Solid Fraction		0			0	0		0		0	
Mass Vapor Fraction		1			1	0,889078		1		0,841867	
Mass Liquid Fraction		0			0	0,110922		0		0,158133	
Mass Solid Fraction		0			0	0		0		0	
Molar Enthalpy	kcal/mol	-1.87E-11			-131 108	-659 643		-131 108		-756 044	
Mass Enthalpy	kcal/kg	-6.48E-10			-835 605	-514,67		-835 605		-721,38	
Molar Entropy	cal/mol-K	102 009			15 923	-139 031		15 923		-236 499	
Mass Entropy	cal/gm-K	0,0353579			101 484	-0,108476		101 484		-0,225656	
Molar Density	kmol/cum	0,040886			0,0125265	0,0445613		0,0125265		0,0449558	
Mass Density	kg/cum	117 958			0,196543	0,571134		0,196543		0,47116	
Enthalpy Flow	Gcal/hr	-1.30E-15			-0,00797177	-0,00359553		-0,00797177		-0,00359687	
Average MW		288 504			156 902	128 168		156 902		104 805	
Mole Flows	kmol/hr	0,0693231			0,608031	0,545073		0,608031		0,475749	
H2O	kmol/hr	0			0,0482436	0,0555084		0,0482436		0,0555084	
N2	kmol/hr	0,0547653			0,0574319	0,0574319		0,0574319		0,00266657	
O2	kmol/hr	0,0145579			0	0,116093		2.49E-18		0,101535	
NO2	kmol/hr	0			0	0		6.80E-24		0	
NO	kmol/hr	0			0	0		7.49E-12		0	
S	kmol/hr	0			1.66E+00	0,000842013		1.66E+00		0,000842013	
SO2	kmol/hr	0			0,000825405	0		0,000825405		0	
SO3	kmol/hr	0			0	0		1.31E-09		0	

H2	kmol/hr	0			0,288873	0,315197		0,288873		0,315197	
CL2	kmol/hr	0			0	0		0		0	
HCL	kmol/hr	0			0	0		0		0	
C	kmol/hr	0			0	0		0		0	
CO	kmol/hr	0			0,153892	0		0,153892		0	
CO2	kmol/hr	0			0,041954 2	0		0,041954 2		0	
CH4	kmol/hr	0			0,016794 4	0		0,016794 4		0	
Mole Fractions											
H2O		0			0,079344	0,101837		0,079344		0,116676	
N2		0,79			0,094455	0,105366		0,094455		0,005605	
O2		0,21			0	0,212986		4.10E-18		0,213421	
NO2		0			0	0		1.12E-23		0	
NO		0			0	0		1.23E-11		0	
S		0			2.73E+00	0,001544 77		2.73E+00		0,001769 87	
SO2		0			0,001357 51	0		0,001357 51		0	
SO3		0			0	0		2.15E-09		0	
H2		0			0,475096	0,578267		0,475096		0,662528	
CL2		0			0	0		0		0	
HCL		0			0	0		0		0	
C		0			0	0		0		0	
CO		0			0,253098	0		0,253098		0	
CO2		0			0,069001	0		0,069001		0	
CH4		0			0,027621	0		0,027621		0	
Mass Flows	kg/hr	2			954 012	69 861		954 012		49 861	
H2O	kg/hr	0			0,869122	1		0,869122		1	
N2	kg/hr	153 417			160 887	160 887		160 887		0,0747	
O2	kg/hr	0,465834			0	371 483		7.98E-17		3 249	
NO2	kg/hr	0			0	0		3.13E-22		0	

NO	kg/hr	0			0	0		2.25E-10		0	
S	kg/hr	0			0,000532549	0,027		0,000532549		0,027	
SO2	kg/hr	0			0,0528794	0		0,0528794		0	
SO3	kg/hr	0			0	0		1.05E-07		0	
H2	kg/hr	0			0,582334	0,6354		0,582334		0,6354	
CL2	kg/hr	0			0	0		0		0	
HCL	kg/hr	0			0	0		0		0	
C	kg/hr	0			0	0		0		0	
CO	kg/hr	0			431 056	0		431 056		0	
CO2	kg/hr	0			184 639	0		184 639		0	
CH4	kg/hr	0			0,269429	0		0,269429		0	
Mass Fractions											
H2O		0			0,0911018	0,143141		0,0911018		0,200558	
N2		0,767083			0,168642	0,230295		0,168642		0,0149816	
O2		0,232917			0	0,531746		8.36E-18		0,651611	
NO2		0			0	0		3.28E-23		0	
NO		0			0	0		2.36E-11		0	
S		0			5.58E+00	0,00386482		5.58E+00		0,00541505	
SO2		0			0,00554285	0		0,00554285		0	
SO3		0			0	0		1.10E-08		0	
H2		0			0,0610405	0,090952		0,0610405		0,127434	
CL2		0			0	0		0		0	
HCL		0			0	0		0		0	
C		0			0	0		0		0	
CO		0			0,451835	0		0,451835		0	
CO2		0			0,19354	0		0,19354		0	
CH4		0			0,0282417	0		0,0282417		0	
Volume Flow	cum/hr	169 552			485 396	12 232		485 396		105 826	

Vapor Phase											
Molar Enthalpy	kcal/mol	-1.87E-11			-131 108	-162 202		-131 108		-177 074	
Mass Enthalpy	kcal/kg	-6.48E-10			-835 605	-131 284		-835 605		-182 509	
Molar Entropy	cal/mol-K	102 009			15 923	161 065		15 923		108 232	
Mass Entropy	cal/gm-K	0,0353579			101 484	0,130364		101 484		0,111554	
Molar Density	kmol/cum	0,040886			0,0125265	0,0411019		0,0125265		0,040886	
Mass Density	kg/cum	117 958			0,196543	0,507815		0,196543		0,396683	
Enthalpy Flow	Gcal/hr	-1.30E-15			-0,00797177	-0,000815431		-0,00797177		-0,000766107	
Average MW		288 504			156 902	12 355		156 902		970 219	
Mole Flows	kmol/hr	0,0693231			0,608031	0,502726		0,608031		0,432648	
H2O	kmol/hr	0			0,0482436	0,0140236		0,0482436		0,0132643	
N2	kmol/hr	0,0547653			0,0574319	0,0574268		0,0574319		0,0026663	
O2	kmol/hr	0,0145579			0	0,11608		2.49E-18		0,101522	
NO2	kmol/hr	0			0	0		6.80E-24		0	
NO	kmol/hr	0			0	0		7.49E-12		0	
S	kmol/hr	0			1.66E+00	1.11E-04		1.66E+00		1.08E-04	
SO2	kmol/hr	0			0,000825405	0		0,000825405		0	
SO3	kmol/hr	0			0	0		1.31E-09		0	
H2	kmol/hr	0			0,288873	0,315195		0,288873		0,315195	
CL2	kmol/hr	0			0	0		0		0	
HCL	kmol/hr	0			0	0		0		0	
C	kmol/hr	0			0	0		0		0	
CO	kmol/hr	0			0,153892	0		0,153892		0	
CO2	kmol/hr	0			0,0419542	0		0,0419542		0	
CH4	kmol/hr	0			0,0167944	0		0,0167944		0	
Mole Fractions											
H2O		0			0,079344	0,027895		0,079344		0,0306583	
N2		0,79			0,0944555	0,114231		0,0944555		0,00616275	

O2		0,21			0	0,230901		4.10E-18		0,234653	
NO2		0			0	0		1.12E-23		0	
NO		0			0	0		1.23E-11		0	
S		0			2.73E+00	2.20E-04		2.73E+00		2.50E-04	
SO2		0			0,00135751	0		0,00135751		0	
SO3		0			0	0		2.15E-09		0	
H2		0			0,475096	0,626973		0,475096		0,728526	
CL2		0			0	0		0		0	
HCL		0			0	0		0		0	
C		0			0	0		0		0	
CO		0			0,253098	0		0,253098		0	
CO2		0			0,0690001	0		0,0690001		0	
CH4		0			0,027621	0		0,027621		0	
Mass Flows	kg/hr	2			954 012	621 118		954 012		419 763	
H2O	kg/hr	0			0,869122	0,252638		0,869122		0,238959	
N2	kg/hr	153 417			160 887	160 872		160 887		0,0746924	
O2	kg/hr	0,465834			0	371 443		7.98E-17		324 858	
NO2	kg/hr	0			0	0		3.13E-22		0	
NO	kg/hr	0			0	0		2.25E-10		0	
S	kg/hr	0			0,000532549	3.55E-03		0,000532549		3.47E-03	
SO2	kg/hr	0			0,0528794	0		0,0528794		0	
SO3	kg/hr	0			0	0		1.05E-07		0	
H2	kg/hr	0			0,582334	0,635396		0,582334		0,635396	
CL2	kg/hr	0			0	0		0		0	
HCL	kg/hr	0			0	0		0		0	
C	kg/hr	0			0	0		0		0	
CO	kg/hr	0			431 056	0		431 056		0	
CO2	kg/hr	0			184 639	0		184 639		0	

CH4	kg/hr	0			0,269429	0		0,269429		0	
Mass Fractions											
H2O		0			0,0911018	0,0406747		0,0911018		0,0569272	
N2		0,767083			0,168642	0,259005		0,168642		0,0177939	
O2		0,232917			0	0,598022		8.36E-18		0,773909	
NO2		0			0	0		3.28E-23		0	
NO		0			0	0		2.36E-11		0	
S		0			5.58E+00	5.71E-04		5.58E+00		8.26E-04	
SO2		0			0,00554285	0		0,00554285		0	
SO3		0			0	0		1.10E-08		0	
H2		0			0,0610405	0,102299		0,0610405		0,15137	
CL2		0			0	0		0		0	
HCL		0			0	0		0		0	
C		0			0	0		0		0	
CO		0			0,451835	0		0,451835		0	
CO2		0			0,19354	0		0,19354		0	
CH4		0			0,0282417	0		0,0282417		0	
Liquid Phase											
Molar Enthalpy	kcal/mol					-656 512				-656 765	
Mass Enthalpy	kcal/kg					-3587,62				-3590,21	
Molar Entropy	cal/mol-K					-370 169				-369 685	
Mass Entropy	cal/gm-K					-202 285				-202 089	
Molar Density	kmol/cum					550 578				549 884	
Mass Density	kg/cum					1007,52				1005,92	
Enthalpy Flow	Gcal/hr					-0,0027801				-0,00283077	
Average MW						182 994				182 932	
Mole Flows	kmol/hr					0,0423466				0,0431017	
H2O	kmol/hr					0,0414849				0,0422442	

N2	kmol/hr					5.03E-01				2.73E-02	
O2	kmol/hr					1.28E-01				1.30E+00	
NO2	kmol/hr					0				0	
NO	kmol/hr					0				0	
S	kmol/hr					0,000842012				0,000842012	
SO2	kmol/hr					0				0	
SO3	kmol/hr					0				0	
H2	kmol/hr					1.87E-01				2.21E-01	
CL2	kmol/hr					0				0	
HCL	kmol/hr					0				0	
C	kmol/hr					0				0	
CO	kmol/hr					0				0	
CO2	kmol/hr					0				0	
CH4	kmol/hr					0				0	
Mole Fractions											
H2O						0,979652				0,980105	
N2						0,000118875				6.33E-01	
O2						0,000301511				0,000301648	
NO2						0				0	
NO						0				0	
S						0,019883 8				0,019535 5	
SO2						0				0	
SO3						0				0	
H2						4.41E+00				5.12E+00	
CL2						0				0	
HCL						0				0	
C						0				0	
CO						0				0	

CO2						0				0	
CH4						0				0	
Mass Flows	kg/hr					0,774915				0,788469	
H2O	kg/hr					0,747362				0,761041	
N2	kg/hr					0,000141019				7.64E-01	
O2	kg/hr					0,00040856				0,000416034	
NO2	kg/hr					0				0	
NO	kg/hr					0				0	
S	kg/hr					0,027				0,027	
SO2	kg/hr					0				0	
SO3	kg/hr					0				0	
H2	kg/hr					3.76E-01				4.45E-01	
CL2	kg/hr					0				0	
HCL	kg/hr					0				0	
C	kg/hr					0				0	
CO	kg/hr					0				0	
CO2	kg/hr					0				0	
CH4	kg/hr					0				0	
Mass Fractions											
H2O						0,964443				0,965213	
N2						0,00018198				9.69E-01	
O2						0,000527231				0,000527648	
NO2						0				0	
NO						0				0	
S						0,0348425				0,0342435	
SO2						0				0	
SO3						0				0	
H2						4.85E-01				5.64E-01	

CL2						0				0	
HCL						0				0	
C						0				0	
CO						0				0	
CO2						0				0	
CH4						0				0	
CIPSD Substream											
Temperature	C					234 334		700	700	25	
Pressure	bar					101 353		101 353	101 353	101 353	
Molar Liquid Fraction						0		0	0	0	
Molar Solid Fraction						1		1	1	1	
Mass Liquid Fraction						0		0	0	0	
Mass Solid Fraction						1		1	1	1	
Molar Enthalpy	kcal/mol					-0,00317111		315 055	315 055	1.24E-11	
Mass Enthalpy	kcal/kg					-0,264017		262 305	262 305	1.04E-09	
Molar Entropy	cal/mol-K					-0,010664		492 021	492 021	3.12E-11	
Mass Entropy	cal/gm-K					-0,000887851		0,409642	0,409642	2.60E-12	
Molar Density	kmol/cum					187,33		187,33	187,33	187,33	
Mass Density	kg/cum					2250,02		2250,02	2250,02	2250,02	
Enthalpy Flow	Gcal/hr					-1.15E-02		0,000471017	0,000471017	4.51E-15	
Average MW						12 011		12 011	12 011	12 011	
Mole Flows	kmol/hr					0,362143		0,149503	0,149503	0,362143	
H2O	kmol/hr					0		0	0	0	
N2	kmol/hr					0		0	0	0	
O2	kmol/hr					0		0	0	0	
NO2	kmol/hr					0		0	0	0	
NO	kmol/hr					0		0	0	0	

S	kmol/hr					0		0	0	0	
SO2	kmol/hr					0		0	0	0	
SO3	kmol/hr					0		0	0	0	
H2	kmol/hr					0		0	0	0	
CL2	kmol/hr					0		0	0	0	
HCL	kmol/hr					0		0	0	0	
C	kmol/hr					0,362143		0,149503	0,149503	0,362143	
CO	kmol/hr					0		0	0	0	
CO2	kmol/hr					0		0	0	0	
CH4	kmol/hr					0		0	0	0	
Mole Fractions											
H2O						0		0	0	0	
N2						0		0	0	0	
O2						0		0	0	0	
NO2						0		0	0	0	
NO						0		0	0	0	
S						0		0	0	0	
SO2						0		0	0	0	
SO3						0		0	0	0	
H2						0		0	0	0	
CL2						0		0	0	0	
HCL						0		0	0	0	
C						1		1	1	1	
CO						0		0	0	0	
CO2						0		0	0	0	
CH4						0		0	0	0	
Mass Flows	kg/hr					43 497		179 568	179 568	43 497	
H2O	kg/hr					0		0	0	0	

N2	kg/hr					0		0	0	0	
O2	kg/hr					0		0	0	0	
NO2	kg/hr					0		0	0	0	
NO	kg/hr					0		0	0	0	
S	kg/hr					0		0	0	0	
SO2	kg/hr					0		0	0	0	
SO3	kg/hr					0		0	0	0	
H2	kg/hr					0		0	0	0	
CL2	kg/hr					0		0	0	0	
HCL	kg/hr					0		0	0	0	
C	kg/hr					43 497		179 568	179 568	43 497	
CO	kg/hr					0		0	0	0	
CO2	kg/hr					0		0	0	0	
CH4	kg/hr					0		0	0	0	
Mass Fractions											
H2O						0		0	0	0	
N2						0		0	0	0	
O2						0		0	0	0	
NO2						0		0	0	0	
NO						0		0	0	0	
S						0		0	0	0	
SO2						0		0	0	0	
SO3						0		0	0	0	
H2						0		0	0	0	
CL2						0		0	0	0	
HCL						0		0	0	0	
C						1		1	1	1	
CO						0		0	0	0	

CO2						0		0	0	0	
CH4						0		0	0	0	
Volume Flow	cum/hr					0,00193 318		0,00079 8073	0,00079 8073	0,00193 318	
PSD											
0 - 20 mu						0		0	0	0	
- 40 mu						0		0	0	0	
- 60 mu						0		0	0	0	
- 80 mu						0		0	0	0	
- 100 mu						0		0	0	0	
- 120 mu						0		0	0	0	
- 140 mu						0,1		0,1	0,1	0,1	
- 160 mu						0,2		0,2	0,2	0,2	
- 180 mu						0,3		0,3	0,3	0,3	
- 200 mu						0,4		0,4	0,4	0,4	
NCPSD Substream											
Temperature	C		250 648			234 334	25	700	700	25	25
Pressure	bar		101 353			101 353	101 353	101 353	101 353	101 353	101 353
Mass Enthalpy	kcal/kg		-1252,45			-192 232	-1252,48	-361 888	-361 888	-191 945	-1128,43
Mass Density	kg/cum		1232,64			3486,88	1232,64	3486,88	3486,88	3486,88	1232,64
Enthalpy Flow	Gcal/hr		-0,0125245			-0,00012 7681	-0,0125 248	-2.40E+00	-2.40E+00	-0,00012 749	-0,0112 843
Mass Flows	kg/hr		10			0,6642	10	0,6642	0,6642	0,6642	10
RDF	kg/hr		10			0	10	0	0	0	10
ASH	kg/hr		0			0,6642	0	0,6642	0,6642	0,6642	0
Mass Fractions											
RDF			1			0	1	0	0	0	1
ASH			0			1	0	1	1	1	0
Volume Flow	cum/hr		0,00811266			0,00019 0485	0,0081 1266	0,00019 0485	0,00019 0485	0,00019 0485	0,0081 1266

Component Attributes											
ASH											
PROXANAL											
Moisture						0		0	0	0	
FC						0		0	0	0	
VM						0		0	0	0	
Ash						100		100	100	100	
SULFANAL											
Pyritic						0		0	0	0	
Sulfate						0		0	0	0	
Organic						0		0	0	0	
ULTANAL											
Ash						100		100	100	100	
Carbon						0		0	0	0	
Hydrogen						0		0	0	0	
Nitrogen						0		0	0	0	
Chlorine						0		0	0	0	
Sulfur						0		0	0	0	
Oxygen						0		0	0	0	
RDF											
PROXANAL											
Moisture			10				10				5,6
FC			6,12				6,12				6,12
VM			80,9				80,9				80,9
Ash			7,38				7,38				7,38
SULFANAL											
Pyritic			0				0				0
Sulfate			0				0				0

Organic			0,3				0,3				0,3
ULTANAL											
Ash			7,38				7,38				7,38
Carbon			48,33				48,33				48,33
Hydrogen			7,06				7,06				7,06
Nitrogen			0,83				0,83				0,83
Chlorine			0				0				0
Sulfur			0,3				0,3				0,3
Oxygen			36,1				36,1				36,1
PSD											
0 - 20 mu			0			0	0	0	0	0	0
- 40 mu			0			0	0	0	0	0	0
- 60 mu			0			0	0	0	0	0	0
- 80 mu			0			0	0	0	0	0	0
- 100 mu			0			0	0	0	0	0	0
- 120 mu			0			0	0	0	0	0	0
- 140 mu			0,1			0,1	0,1	0,1	0,1	0,1	0,1
- 160 mu			0,2			0,2	0,2	0,2	0,2	0,2	0,2
- 180 mu			0,3			0,3	0,3	0,3	0,3	0,3	0,3
- 200 mu			0,4			0,4	0,4	0,4	0,4	0,4	0,4
Heat											
Stream Name	Q1	Q2	S1								
QCALC Gcal/hr	0,001240 50778	- 0,0075596 0088	- 0,0037591 7001								
TBEGIN C	25,	250 648 468									
TEND C	25,	25,									

Table A9: Sensitivity analysis data for the effect of temperature on the syngas composition for guar gum powder pellets

Row/Case	Status							
		VARY 1	(CIN-C)/	C	CO	CO2	H2	CH4
		GASIFY	CIN					
		PARAM						
		TEMP						
		C		KMOL/HR				
1	OK	500	0,387946	0,221651	0,0247064	0,154048	0,253159	0,134134
2	OK	520	0,390958	0,22056	0,0344986	0,153088	0,284354	0,120228
3	OK	540	0,396591	0,21852	0,0471287	0,150658	0,314991	0,106426
4	OK	560	0,405629	0,215247	0,0629945	0,146505	0,344333	0,0930578
5	OK	580	0,418774	0,210487	0,0823718	0,140413	0,371704	0,0804088
6	OK	600	0,436554	0,204048	0,105327	0,132265	0,396538	0,0687037
7	OK	620	0,4592	0,195847	0,131626	0,122095	0,41842	0,0581014
8	OK	640	0,486531	0,185949	0,160671	0,110136	0,437131	0,0486926
9	OK	660	0,517859	0,174604	0,19148	0,096848	0,452657	0,0405041
10	OK	680	0,551957	0,162256	0,222765	0,0828822	0,465193	0,0335058
11	OK	700	0,587172	0,149503	0,253098	0,0690001	0,475096	0,027621
12	OK	720	0,621662	0,137012	0,281151	0,0559404	0,482823	0,0227393
13	OK	740	0,653748	0,125393	0,305931	0,0442856	0,488844	0,0187308
14	OK	760	0,682222	0,115081	0,326919	0,0343741	0,49357	0,0154606
15	OK	780	0,706498	0,10629	0,344076	0,0262877	0,497324	0,0128008
16	OK	800	0,726546	0,0990294	0,357715	0,0199067	0,500339	0,0106382
17	OK	820	0,742673	0,0931891	0,368328	0,014994	0,502795	0,00887752
18	OK	840	0,75533	0,0886054	0,376447	0,0112746	0,504836	0,00744098
19	OK	860	0,76504	0,0850889	0,382573	0,00848768	0,506567	0,00626523
20	OK	880	0,772365	0,0824366	0,387156	0,00641124	0,508055	0,00529911
21	OK	900	0,777839	0,0804541	0,390572	0,00486708	0,509336	0,0045017
22	OK	920	0,781919	0,0789764	0,39312	0,00371756	0,510436	0,00384056
23	OK	940	0,784964	0,0778737	0,395029	0,00285905	0,511376	0,00328996
24	OK	960	0,787243	0,0770484	0,396466	0,00221481	0,512179	0,00282947
25	OK	980	0,788956	0,0764283	0,397554	0,00172857	0,512863	0,00244276
26	OK	1000	0,790248	0,0759603	0,398383	0,00135921	0,513445	0,00211671
27	OK	1020	0,791227	0,0756057	0,399019	0,00107674	0,513942	0,00184075
28	OK	1040	0,791972	0,0753358	0,39951	0,000859211	0,514365	0,00160629
29	OK	1060	0,792542	0,0751296	0,399891	0,000690524	0,514728	0,00140636
30	OK	1080	0,792978	0,0749715	0,400189	0,000558804	0,515038	0,00123528
31	OK	1100	0,793314	0,0748499	0,400424	0,000455249	0,515305	0,00108837

Table A10: Sensitivity analysis data for the effect of air flow rate on the syngas composition for guar gum powder pellets.

Row/Case	Status							
		VARY 1	(CIN-C)/	C	CO	CO2	H2	CH4
		AIR	CIN					
		MIXED						
		TOTAL MASSFLOW						
		KG/HR		KMOL/HR				
1	OK	1	0,556639	0,16056	0,254215	0,0696103	0,505649	0,0312878
2	OK	1,5	0,571868	0,155045	0,253633	0,0692919	0,489883	0,0293671
3	OK	2	0,587172	0,149503	0,253098	0,0690001	0,475096	0,027621
4	OK	2,5	0,602545	0,143936	0,252606	0,0687318	0,461199	0,0260287
5	OK	3	0,617982	0,138345	0,252151	0,0684845	0,44811	0,0245724
6	OK	3,5	0,633479	0,132733	0,25173	0,0682559	0,435761	0,0232367
7	OK	4	0,64903	0,127101	0,251339	0,0680441	0,424089	0,0220085
8	OK	4,5	0,664633	0,121451	0,250975	0,0678475	0,413039	0,0208765
9	OK	5	0,680283	0,115783	0,250637	0,0676645	0,402561	0,0198308
10	OK	5,5	0,695977	0,1101	0,25032	0,0674938	0,392611	0,0188626
11	OK	6	0,711712	0,104401	0,250025	0,0673344	0,38315	0,0179645
12	OK	6,5	0,727486	0,0986889	0,249748	0,0671852	0,374142	0,0171297
13	OK	7	0,743297	0,0929633	0,249487	0,0670453	0,365555	0,0163524
14	OK	7,5	0,759141	0,0872254	0,249243	0,0669139	0,357359	0,0156274
15	OK	8	0,775017	0,0814759	0,249013	0,0667904	0,349528	0,01495
16	OK	8,5	0,790924	0,0757155	0,248796	0,066674	0,342038	0,0143161
17	OK	9	0,806858	0,0699449	0,248591	0,0665642	0,334866	0,0137221
18	OK	9,5	0,82282	0,0641646	0,248397	0,0664605	0,327993	0,0131646
19	OK	10	0,838806	0,0583751	0,248213	0,0663624	0,3214	0,0126406

Table A11: Sensitivity analysis data for the effect of temperature on carbon conversion.

Temperature	No Binder	Waste Engine Oil	Waste Palm Oil	Corn Starch	Guar Gum
500	0.389	0.36	0.38	0.51	0.39
520	0.394	0.36	0.38	0.52	0.39
540	0.402	0.37	0.39	0.54	0.40
560	0.414	0.38	0.40	0.56	0.41
580	0.429	0.39	0.41	0.58	0.42
600	0.449	0.40	0.43	0.61	0.44
620	0.475	0.43	0.45	0.65	0.46
640	0.504	0.45	0.48	0.69	0.49
660	0.538	0.48	0.51	0.74	0.52
680	0.574	0.51	0.55	0.79	0.55
700	0.612	0.54	0.58	0.84	0.59
720	0.649	0.57	0.62	0.89	0.62

740	0.683	0.60	0.65	0.94	0.65
760	0.714	0.63	0.68	0.99	0.68
780	0.74	0.65	0.70	1.00	0.71
800	0.761	0.67	0.72	1.00	0.73
820	0.779	0.69	0.74	1.00	0.74
840	0.793	0.70	0.75	1.00	0.76
860	0.803	0.71	0.76	1.00	0.77
880	0.811	0.71	0.77	1.00	0.77
900	0.817	0.72	0.78	1.00	0.78
920	0.821	0.72	0.78	1.00	0.78
940	0.825	0.73	0.78	1.00	0.79
960	0.828	0.73	0.79	1.00	0.79
980	0.83	0.73	0.79	1.00	0.79
1000	0.831	0.73	0.79	1.00	0.79
1020	0.832	0.73	0.79	1.00	0.79
1040	0.833	0.73	0.79	1.00	0.79
1060	0.834	0.73	0.79	1.00	0.79
1080	0.834	0.73	0.79	1.00	0.79
1100	0.835	0.73	0.79	1.00	0.79

Table A11: Sensitivity analysis data for the effect of temperature on carbon conversion

Air Flow Rate (kg/hr)	No Binder	Waste Engine Oil	Waste Palm Oil	Corn Starch	Guar Gum
1	0.58	0.51	0.55	0.80	0.56
1.5	0.60	0.53	0.57	0.82	0.57
2	0.61	0.54	0.58	0.84	0.59
2.5	0.63	0.56	0.60	0.86	0.60
3	0.65	0.57	0.61	0.88	0.62
3.5	0.66	0.59	0.63	0.90	0.63
4	0.68	0.60	0.64	0.92	0.65
4.5	0.69	0.61	0.66	0.94	0.67
5	0.71	0.63	0.67	0.96	0.68
5.5	0.73	0.64	0.69	0.98	0.70
6	0.74	0.66	0.70	1.00	0.71
6.5	0.76	0.67	0.72	1.00	0.73
7	0.78	0.69	0.73	1.00	0.74
7.5	0.79	0.70	0.75	1.00	0.76
8	0.81	0.72	0.76	1.00	0.78
8.5	0.83	0.73	0.78	1.00	0.79
9	0.84	0.75	0.80	1.00	0.81
9.5	0.86	0.76	0.81	1.00	0.82
10	0.88	0.78	0.83	1.00	0.84

Appendix B: Conference Proceeding Publications

In *Proceedings of the 7th International Conference on Informatics, Environment, Energy and Applications* 2018

Environmental Emissions Assessment of Coal and Refuse Derived Fuel Incineration Processes by Simulation

Otolorin Adelaja Osibote
Department of Mathematics and Physics
Cape Peninsula University of Technology
Cape Town 8000, South Africa
27 21 460 9092
osibotea@cput.ac.za

Aviwe Hlaba
Department of Chemical Engineering
Cape Peninsula University of Technology
Cape Town 8000, South Africa
+27 730171799
Aviwe.t@gmail.com

Ademola Rabiu
Department of Chemical Engineering
Cape Peninsula University of Technology
Cape Town 8000, South Africa
27 21 460 3449
rabiua@cput.ac.za

ABSTRACT

Coal has been the predominant source of energy for electricity production in South Africa. Coal combustion process for energy recovery is regarded as a heavy pollutant emissions process. Waste derived alternative fuels are widely used for substituting the thermal energy requirement from fossil fuels and reducing the pollutant emission. This paper is a comparison between the burning of coal and RDF as far as fuel qualities and emissions. The ignition of fuel derived from MSW is a promising low-cost retrofitting procedure for coal power plants, having the additional advantage of lessening the volume of waste transfer in landfills. Moreover, co-burning of RDF and coal, as opposed to changing to RDF ignition alone straight from the onset of devoted power plants, permits plant administrators to be adaptable to varieties in the RDF supply.

CCS Concepts

• Computing methodologies- Modelling and Simulation- Simulation evaluation

Keywords

Municipal solid waste; refuse-derived fuel; emissions; greenhouse gases; global warming; waste-to-energy.

1. INTRODUCTION

The conversion of Municipal Solid Waste (MSW) in Waste-to-Energy facilities has been perceived globally as a way to save fossil fuels and enhance ecological quality by decreasing the measure of waste to be landfilled [1]. 130 million tons of MSW globally are combusted yearly in WTE facilities that create power, also steam for region warming. In the US alone, around 30 million tons of MSW are combusted in WTE plants to create around 2.8 GW of power and some steam for region warming [2], which is roughly 0.3 % of aggregate US power generation. The WTE emissions of concern are trace organic compounds, especially polychlorinated dioxins and furans, unstable trace metals, for example, mercury, lead and cadmium, total particulate matter, and acidic gases, for example, hydrogen chloride, hydrogen fluoride, sulfur dioxide and nitrogen oxides [2].

IEEA'18, March 28–31, 2018, Beijing, China.

ACM ISBN 978-1-4503-6362-4/18/03…$15.00
DOI: https://doi.org/10.1145/3208854.3208870

An expansion in ozone harming substance discharges because of burning of non-renewable energy sources for the production if fuels and electricity has brought about outflows of around 25 billion tons of carbon dioxide (CO_2) per annum [3]. Greenhouse gas emissions from anthropogenic sources have expanded from 27 gigatons CO_2 proportionality for every year ($GtCO_2$/yr.) to 49 $GtCO_2$/yr. amid the time of 1970 to 2010 with the expansion being most astounding in mankind's history amid the time of 2000-2010 [4]. Future projections show that Africa will be a standout amongst the most influenced mainland's by environmental change due to its helplessness to other financial and social difficulties, for example, destitution and illnesses [5]. According to the United States Environmental Protection Agency [6]; 46 billion tons were evaluated to have been sourced from human exercises in 2010, speaking to a 35% expansion when contrasted with 1990. CO_2 is a noteworthy anthropogenic ozone-harming substance and has contributed an aggregate of 75% to worldwide aggregate emissions in 2010 [7]. The ignition of petroleum products for power generation is the biggest contributor to worldwide CO_2 emissions. Figure 1 shows a comparison of natural greenhouse gases to man-made depicting CO_2 as the highest contributor in manmade emissions.

South Africa is the 13th biggest emitting nation considering 2008 petroleum product CO_2 outflows and the biggest radiating nation on the landmass of Africa. With a local economy controlled by coal, South Africa has encountered a seven-overlap increment in non-renewable energy source CO_2 emanations since 1950, with 80-90% of outflows from coal. For 2008, 85% of South Africa's petroleum product CO_2 outflows of 119 million metric tons of carbon was from coal, another 11.6% were from oil utilization, and the rest of from cement making and flammable gas and coke-broiler gas utilization [8].

1.1 Greenhouse Gas Effect on Climate Change

Greenhouse gasses retain and transmit long-wave (infrared) radiation, in this way catching and holding heat inside the climate. Greenhouse gasses aggregately make up under 1% of the Earth's environment. The greenhouse gasses which have the biggest warming impact inside the air are water vapor (mists) and carbon dioxide. Other greenhouse gasses incorporate methane and nitrogen oxides – these have less effect on the general warming

impact. Water vapor is the richest ozone-depleting substance in the air, yet isn't delivered as a result of human action [9].

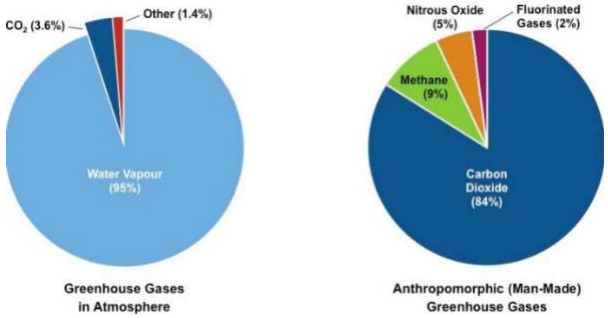

Figure 1. Proportion of greenhouse gases (natural vs anthropomorphic) [9].

There are two elements which decide the amount of the effect an ozone harming substance will have in warming the climate, these elements are also graphically represented in Figure 2:

1. Capacity to ingest long-wave radiation

Gasses that have a more prominent ability to ingest long-wave radiation will have a more prominent warming effect (per atom)

2. Fixation inside the climate

The more noteworthy the centralization of a gas, the more noteworthy its warming effect will be inside the environment.

The greenhouse impact functions to trap warmth in the atmosphere and thus counteract fast temperature fluctuations.

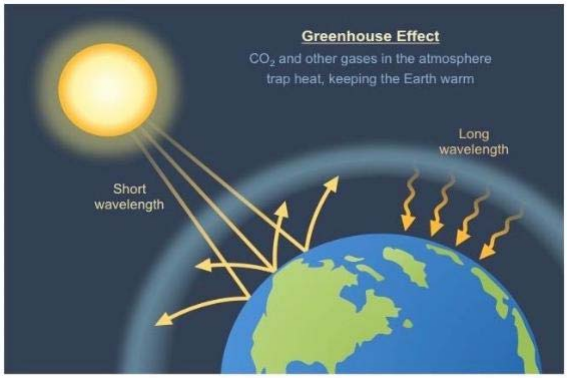

Figure 2. The greenhouse effect [9].

While greenhouse gasses happen normally, man is expanding ozone-depleting substance emissions by means of various exercises, including deforestation and expanded cultivating/agribusiness. The ozone-harming substance that is expanding most quickly in the air is carbon dioxide and the primary driver is burning. The expanded dependence on petroleum products following the mechanical upheaval has brought about ~38% expansion in CO2 levels [9].

Greenhouse gasses assume an urgent part in deciding worldwide temperatures and climate patterns because of their ability to hold warmth. As these gasses trap warmth, increments in ozone-depleting substance concentrations should connect with an expansion in worldwide temperature. Long-term climate patterns (atmosphere) may likewise be impacted by ozone-harming substance concentrations. Researchers foresee that increments in ozone-depleting substance concentrations will prompt an increased greenhouse impact, bringing about:

More incessant outrageous climate conditions (e.g. warm waves, violent winds, more powerful typhoons, and so forth.).

Some areas to become more drought affected, while different territories turn out to be more inclined to times of substantial rainfall.

Changes to circulating ocean currents – which may cause longer El Nino (warming) and La Nina (cooling) conditions [9].

This has been experienced severely in South Africa during the past year with the rainfall received during October 2017 was near normal to above normal over large parts of the country. Only a few isolated areas across the country received below-normal rainfall. During the 3-month period from August to October 2017, large parts of the western half of the country received below-normal rainfall. The eastern half of the country received mostly near normal to above-normal rainfall; however, isolated areas received below-normal rainfall. During October 2017, isolated areas across the country experienced somewhat dry conditions. During the three-month period from August to October 2017, moderately dry to severely dry conditions were mostly experienced in isolated areas of the Northern and Western Cape. Somewhat dry conditions occurred in isolated areas across the rest of South Africa [10].

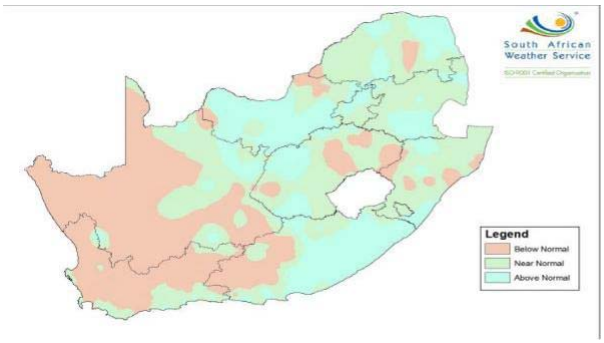

Figure 3. Assessment of rainfall for August 2017 to October 2017 [10].

The 12-month (November 2016 to October 2017) as well as 24-month (November 2015 to October 2017) SPI maps give an indication of areas where prolonged droughts exist, in other words, where below-normal rainfall occurred over a period of one year or longer. On the 12- month SPI map presented on Figure 3, severely dry to extremely dry conditions are most noticeable in the Western Cape as well as adjacent areas of the Northern Cape. On the 24-month SPI map as shown in Fig. 4, moderately dry to severely dry conditions are most noticeable in the Northern, Western, and Eastern Cape, but also in isolated areas of the Free State and Mpumalanga [10].

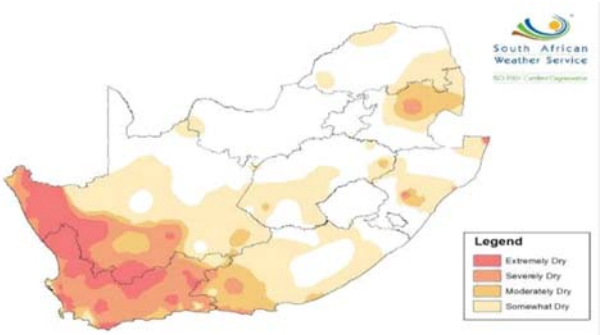

Figure 4. Standardize precipitation index for November 2016 to October 2017 [10].

The connection between worldwide temperatures and carbon dioxide concentrations as shown in Fig. 5 was built up by breaking down information over a long-time period. Ice cores taken from the Vostok station in Antarctica give proof of the natural conditions at the season of solidifying. Information gathered from the Vostok ice core exhibits that there is a strong positive correlation between carbon dioxide concentrations and temperature ($\uparrow CO_2$ levels $\propto \uparrow$ temperature).

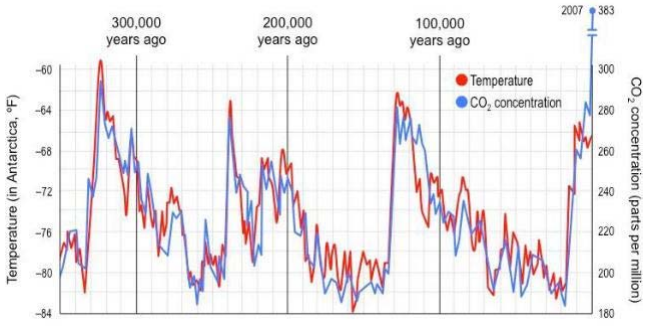

Figure 5. Vostok ice core data – temperature versus carbon dioxide concentration [9].

1.2 Electricity Generation and CO2 Emissions

CO_2 emissions from power generation and heat represented the biggest ozone harming substance outflows in 2013 as this area is high carbon intensive. Universally, total essential energy supply in 2013 represented 44% of CO_2 outflows, for the most part because of the high carbon content per unit of energy discharged. Therefore, CO_2 discharges emerging from the burning of coal for power generation expanded by 4.9% to 13.7 $GtCO_2$ in 2013 [3]. Coal at present takes care of the developing demand for power generation in South Africa where there are extensive coal holds and restricted assets of other energy sources. Coal stays to be South Africa's most abundant energy source and a large portion of the coal that ESKOM utilizes is of low quality, low calorific incentive at 15-16 MJ/kg and high ash content of around 42% [5]. ESKOM depends on this coal to generate 90 % of South Africa's power supply [6]. Be that as it may, South Africa's coal quality results in various burdens with respect to waste and discharges originating from sulphur, nitrogen oxides, natural mixes, substantial metals, radioactive components and greenhouse gases [11], [12].

Coal supplies 33% of all energy utilized worldwide and makes up 40% of power generation, and in addition assuming a critical part in ventures, for example, iron and steel. Notwithstanding authentic worries about air contamination and ozone-depleting substance outflows, coal use will keep on being significant later. Hence more noteworthy endeavors are required by government and industry to grasp not so much dirtying but rather more proficient advancements to guarantee that coal turns into a much cleaner wellspring of energy in the decades to come [13].

A lot of power generation in South Africa will keep on being sourced from coal-fired power stations within the foreseeable future [14]. South Africa is a middle-income nation, however, has one of the most elevated amounts of CO_2 outflows per capita on the planet fundamentally because of the ignition of coal with the end goal of power generation [15]. One of the difficulties that were experienced by South Africa's fundamental power supplier in 2010 was an expansion in outright CO_2 discharges from 221.7 megatons in 2009 to 224.7 megatons in 2010 which was highlighted by the producer as a reason for great concern [16]. Clearly, South Africa needs to secure a superior comprehension of ozone-harming substance emissions from power generation because of the ignition of coal and further concentration to alleviation endeavors in this segment. The fundamental opportunity for South Africa to diminish its ozone-harming substance emissions from power generation is to execute energy productivity, demand administration and move towards a less greenhouse gas discharges concentrated energy blend. Treating residual waste with different Waste-to-Energy (WtE) advancements is a feasible choice for disposal of Municipal Solid Waste and energy generation [17]. The present pattern of monetary development and way of life of individuals increments municipal waste (MSW) generation and consequences for current landfill situation, inaccessibility of land, open burning landfill causes contamination what's more, has significantly consequences for general wellbeing. There is direness for a compelling solid waste administration because of these reasons. WTE incineration helps in diminishing greenhouse gasses by abstaining from dumping to landfill foils the methane emissions from landfill and producing renewable energy in the form of electrical power which additionally helps in diminishing reliance on petroleum products. As of now the biggest wellspring of GHGs in the form of methane (CH_4) discharges on the planet are landfills with an appraisal of almost 21% of the aggregate methane generation. As a GHG Methane is 21 times more grounded than carbon dioxide generation [18].

This paper is a comparison between the burning of coal and RDF as far as fuel qualities and emissions using an ASPEN simulation model to model the combustion of both MSW derived Refuse Derived Fuel (RDF) pellets and coal. The environmental assessment will be based on the amount of the major GHG's produced from the combustion of each fuel, namely the CH4 and CO_2 produced.

2. METHODOLGY

2.1 Model Description

In real life applications, the combustion of fuel would happen in one combustion vessel. However, since ASPEN Plus does not have a single reactor block to model a combustion process, a number of blocks in combination were used to model the combustion of coal and RDF. This combustion was adopted from the ASPEN Plus guide dealing with solids processing specifically the combustion of coal [19].

The fuel is first fed into the RStoich block of ASPEN plus to simulate the drying of the fuel being combusted, representing the first step of the combustion process (DRY-REAC). The moisture

is removed from the feedstock by means of evaporation and the resultant moisture is separated from the dried feedstock by means of a Flash 2 model separator (DRY-FLSH) using the principle of split fractionation then the moisture leaves the process through the MOIST stream.

The RGibbs model is used to simulate the combustion of the dry feedstock in the BURN block. RGibbs models chemical equilibrium by minimizing Gibbs free energy. However, the Gibbs free energy of coal cannot be calculated because it is a nonconventional component in ASPEN Plus. Before feeding the dried feedstock to the RGibbs block, it is required to decompose the feedstock into its constituent elements which ASPEN will recognize as conventional components. This is done in the RYield block, DECOMP. The heat of reaction associated with the decomposition of the feedstock needs to be taken into consideration in the combustion process. Use of a heat stream to carry this heat of reaction from the RYield block to the RGibbs block is employed

Finally, the combustion gases are separated from the ash using the Aspen Plus model SSplit for this separation. The complete process flow combining all these blocks to complete the process is presented in Figure 6.

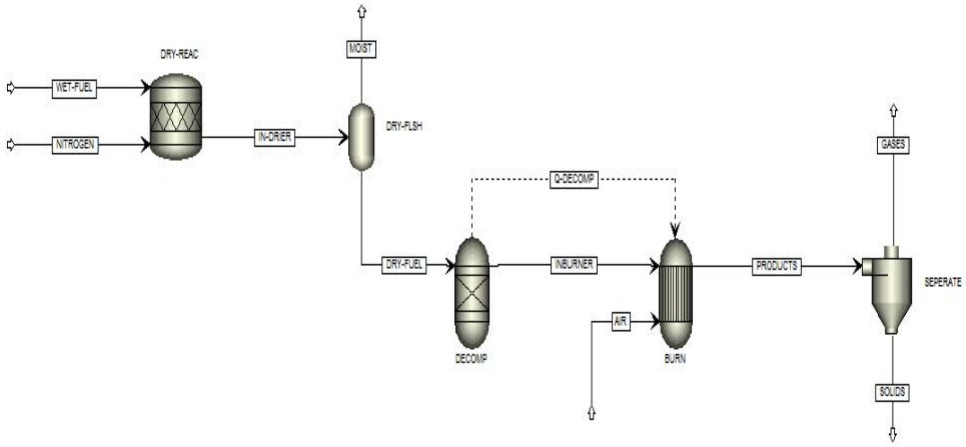

Figure 6. ASPEN Plus process flow diagram for combustion model simulation

2.2 Model Assumptions

A numerous amount of assumptions was taken into consideration during the development of the simulation model of the combustion of coal and RDF pellet feedstocks.

The process was assumed to occur at steady state in isothermal, isobaric and kinetic free conditions.

Reactions in the combustion vessel occur in an equilibrium state.

The decomposition of the feedstock tool place instantaneously and the constituents consisted of NO_2, NO, S, SO_2, SO_3, H_2, Cl_2, HCl, C, CO, CO_2, and Ash.

Gases including H_2, CO, CO_2, O_2, N_2, and CH_4 are all regarded as ideal.

The char residue is only made up of ash and carbon in solid phase.

The carbon is assumed to have completely reacted.

2.3 Initial Operating Parameters

2.3.1 Combustion vessel

Regarding the initial operating parameters for the combustion process, the following were considered:

Table 1. Combustion operating parameters

Parameter	Value	Unit
Feed Flow Rate	1000	Kg/h
Feed Pressure	1	bar
Feed Temperature	25	℃
Nitrogen Rate	5000	Kg/h
Nitrogen Temperature	132	℃
Air Pressure	1	bar
Air Temperature	25	℃
Combustor Pressure	1	bar

2.3.2 Feed characteristics

The clear majority of South Africa's coal is of a bituminous thermal grade [20]. The characteristic of South African coal adapted for the model simulation of combustion of coal were obtained from analysis conducted by Nel [21], at the North West University in South Africa. The feed characteristics in terms of proximate and ultimate analysis are presented in Figure 7.

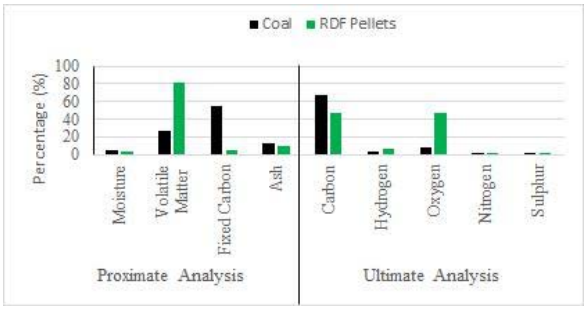

Figure 7. Proximate and Ultimate Analysis of feedstocks.

The RDF pellets were produced from Municipal Solid Waste samples collected from transfer stations and drop off sites around the City of Cape Town Municipal region. MSW in its raw form poses and handling and processing challenge due to its heterogenous nature. The pelletisation of the MSW to form RDF

was performed to limit these challenges which in turn helps in terms of process control parameters and handling. The characterization in terms of proximate and ultimate analysis were conducted at Roediger Agencies cc. and the Central Analytical Facility of Stellenbosch University respectively.

3. RESULTS AND DISCUSSION

The simulation uses a pre-heated nitrogen stream in the feed to preheat the feed temperature to start the combustion process. The temperature of the combustion chamber is not set to a certain value, only the temperate of the feed was considered. It is to be noted that the emissions data received from this are compiled with no gas cleaning procedures being applied to the gas stream as it would be done in industry applications at power and heat generation facilities. The emission reported in this study focus on mainly for CO_2, NO_X, SO_2 emissions compared between the combustion of coal and RDF. The results obtained are summarized in Figure 8.

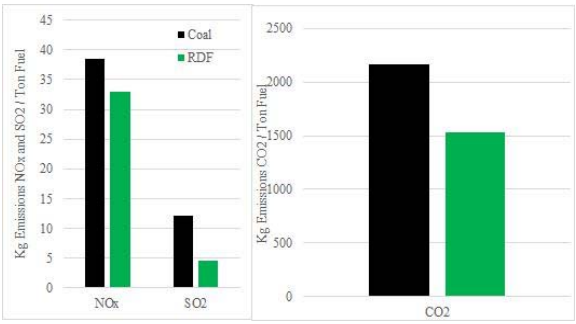

Figure 8. Emissions comparisons between coal and RDF.

The results obtained in Figure 9 show that the CO_2 emissions are inherently higher in coal combustion than with RDF combustion with no gas cleaning in both processes. The percentage saving on CO_2 emissions amounts to approximately 32.1% when using RDF in this combustion process. Kaplan, DeCarolis and Barlaz [22] reported similar finding in waste-to-energy applications while O'Brien and Swana [23] reported savings of over 60% on CO_2 emissions. The United States Environmental Protection Agency [24] reported savings of over 50% in terms of CO_2 emission and Christensen, Damgaard and Astrup [25] concluded that The more fossil fuels that are substituted in the energy sector by the electricity and heat production from the WtE plants, the larger the CO_2 savings offered.

In terms of the SO_2 and NO_X, it can be distinguished from the simulation results that the NO_X emissions in kg/ ton fuel is lower in the RDF than in the coal, as well as the SO_2. Research from various others also show significantly lower NO_X and SO_2 emissions in waste-to-energy facilities than in coal fired plants [22-25], which then validates the authenticity of the results obtained. The reduction in SO_2 emissions from the coal to the RDF was found to be 62% and the reduction of NO_X was found to be 14%. Albina [26] and [27] also states that the emission factors of SO_2 and NO_X are significantly lower in waste-to-energy facilities than in coal fired plants.

4. CONCLUSION

The results obtained from the study clearly show that the combustion of RDF is a viable option for an alternative to coal in terms of the emissions contributing to the greenhouse effect. South Africa is currently facing the effects of global warming through the irregular weather patterns that have seen the Western Cape Province experience severe water shortages for almost a year now. It is evident that a solution is required and fast. As for the criteria of air toxins, waste-to-energy facilities transmit fundamentally less carbon dioxide than any of the petroleum product power plants. They radiate essentially less sulfur dioxide than coal-fired power plants. They are comparable to coal-and oil-fired power plants as for nitrogen oxide emissions. In terms of South Africa, further research into the applications of RDF as a coal substitute is required before any field applications can be investigated. A comparison of waste-to-energy and coal plant emissions is required to be conducted per unit of energy as a basis, then cost implications can follow to assess the feasibly of a complete change from coal to RDF and reduced impacts due to less landfill operations. The ignition of fuel derived from MSW is a promising low-cost retrofitting procedure for coal power plants, having the additional advantage of lessening the volume of waste transfer in landfills. Moreover, co-burning of RDF and coal, as opposed to changing to RDF ignition alone straight from the onset of devoted power plants, permits plant administrators to be adaptable to varieties in the RDF supply.

The study demonstrates that substituting some portion of the coal supply by processed high-calorific value waste.

5. ACKNOWLEDGMENTS

All the authors would like to thank the Cape Peninsula University of Technology for funding towards the project and attendance at the conference.

6. REFERENCES

[1] Themelis, N. An overview of the global waste-to-energy industry. James LTD, City, 2003.

[2] Albina, D. O. and Themelis, N. J. Emissions from Waste-to-Energy: A Comparison with Coal-fired Power Plants.

[3] International Energy Agency, I. Annual Report. 2014.

[4] Change, I. P. O. C. Climate Change 2014 Impacts, Adaptation, and Vulnerability Part A: Global and Sectoral Aspects. 2014a.

[5] Meehl, G. A., Stocker, T. F., Collins, W. D., Friedlingstein, A., Gaye, A. T., Gregory, J. M., Kitoh, A., Knutti, R., Murphy, J. M. and Noda, A. Global climate projections2007).

[6] United States Environmental Protection Agency, U. Available and Emerging Technologies for Reducing Greenhouse Gas Emissions from The Pulp And Paper Manufacturing Industry U.S. Environmental Protection Agency, North Carolina, 2010.

[7] International Energy Agency, I. IEA Statistics-CO2 Emissions from Fuel Combustion Highlights. Paris: International Energy Agency, 2010.

[8] Boden, T. A., Marland, G. and Andres, R. J. Global, Regional, and National Fossil-Fuel CO2 Emissions. Oak Ridge National Laboratory, City, 2011.

[9] BioNinja, B. Greenhouse Gases. City, 2017.

[10] South Africa Weather Service, S. Drought Monitoring. City, 2017.

[11] Deng, N., Li, D., Zhang, Q., Zhang, A., Cai, R. and Zhang, B. Simulation analysis of municipal solid waste pyrolysis and gasification based on Aspen plus. Frontiers in Energy2017), 1-7.

[12] Zheng, H., Kaliyan, N. and Morey, R. V. Aspen Plus simulation of biomass integrated gasification combined cycle systems at corn ethanol plants. Biomass and Bioenergy, 562013), 197--210.

[13] International Energy Agency, I. Medium-Term Coal Market Report. City, 2016.

[14] Manzini, L. and aspects, E. p. p.-E. Greenhouse gas emissions assessment for electricity generation from coal: an Eskom power station. City, 2016.

[15] Bogner, J., Pipatti, R., Hashimoto, S., Diaz, C., Mareckova, K., Diaz, L., Kjeldsen, P., Monni, S., Faaij, A. and Gao, Q. Mitigation of global greenhouse gas emissions from waste: conclusions and strategies from the Intergovernmental Panel on Climate Change (IPCC) Fourth Assessment Report. Working Group III (Mitigation). Waste Management & Research, 26, 1 2008), 11-32.

[16] Electricity Supply Commission, E. Eskom Integrated Report 2011 | Fact sheets - Climate change. City, 2011.

[17] World Energy Council, W. World Energy Resources, Waste to Energy City, 2016.

[18] Gupta, S. and Mishra, R. Estimation of Electrical Energy Generation from Waste to Energy using Incineration Technology. International Journal, 3, 4 2015), 631-634.

[19] Aspentech Aspen Plus 2004.1 Getting Started Modeling Processes with Solids. City, 2004.

[20] Anglo American, A. Mining and Processing in South Africa Coal Mining and Processing in South Africa. City, 2017.

[21] Nel, S. Catalytic steam gasification of large coal particles. North-West University, 2011.

[22] Kaplan, P., DeCarolis, J. and Barlaz, M. Life Cycle Comparison of Waste-to-Energy to Sanitary Landfill, 2012.

[23] O'Brien, J. K. and Swana, P. E. Comparison of Air Emissions from Waste-to-Energy Facilities to Fossil Fuel Power Plants In Proceedings of the 14th North American Waste to Energy Conference (Tampa, Florida USA 2006). NAWTEC14-3187, [insert City of Publication],[insert 2006 of Publication].

[24] United States Environmental Protection Agency, U. Air Emissions from MSW Combustion Facilities. City, 2005.

[25] Christensen, T. H., Damgaard, A. and Astrup, T. Waste to Energy: The Carbon Perspective. City, 2015.

[26] Albina, D. O. Comparitive Analysis of Emissions from WTE and Coal-fired Power Plants. Columbia University, City, 2003.

[27] Vekemans, O. and Chaouki, J. Municipal Solid Waste Cofiring in Coal Power Plants: Combustion Performance. InTech, City, 2016.

Proceedings of the 7th International Conference on Informatics, Environment, Energy and Applications (pp. 59-64). 2018

Process Simulation of Municipal Solid Waste Derived Pellet Gasification for Fuel Production

Aviwe Hlaba
Department of Chemical Engineering
Cape Peninsula University of Technology
Cape Town 8000, South Africa
+27 73 017 1799
aviwe.t@gmail.com

Ademola Rabiu
Department of Chemical Engineering
Cape Peninsula University of Technology
Cape Town 8000, South Africa
+27 21 460 3449
RabiuA@cput.ac.za

Otolorin Adelaja Osibote
Department of Mathematics and Physics
Cape Peninsula University of Technology
Cape Town 8000, South Africa
27 21 460 9092
osibotea@cput.ac.za

ABSTRACT

This investigation proposes a model of syngas creation from Refuse Derived Fuel (RDF) Pellet gasification with air in fixed bed reactor. The model (utilizing Aspen Plus process simulation software) is utilized to model the anticipated results of RDF gasification and to give some processes fundamentals concerning syngas generation from RDF gasification. The fixed bed reactors is an updraft fixed bed reactor which can be divided into 3 sections n (devolatilization, partial oxidation, and steam reforming). The model is based on a combination of modules that the Aspen Plus simulator provides, representing the three stages of gasification. Thermodynamics package used in the simulation comprised the Non- Random Two-Liquid (NRTL) model. The model works on the principle of Gibbs free energy minimization and was validated with experimental data of MSW gasification found in literature. The RYield module was combined with the RGibbs module to describe pyrolysis section, while the RGibbs module was used for the gasification section individually. Proximate and ultimate analysis of RDF pellets and operating conditions used in the model are discussed. The sensitivity analysis module of Aspen Plus was used to research the effect of air equivalence ratio ER and temperature value on the syngas composition, and carbon conversion The results indicate that higher temperature improves gasification as the composition of H_2 and CO increase, as well as carbon conversion, until a temperature of 900℃, and higher air equivalence ratio increases the carbon conversion while decreasing syngas quality as there is an increase in CO_2 and H. Results obtained are in good agreement of experimentally measured data in literature.

CCS Concepts

3. **Computing methodologies – Modelling and Simulation – Simulation evaluation**

IEEA'18, March 28–31, 2018, Beijing, China.

ACM ISBN 978-1-4503-6362-4/18/03…$15.00
DOI: https://doi.org/10.1145/3208854.3208869

Keywords

Refuse derived fuel; gasification; equivalence ratio; conversion; syngas.

1. INTRODUCTION

It has become a global issue to explore and exploit alternative renewable and sustainable sources of energy with the increasing demand of energy for daily living. Seeing that biomass is comprised of a variety of MSW's, green waste and agricultural residues, which are found in large quantities, it is a major renewable energy contributor [1], [2]. Biomass can be processed to produce a variety of useful forms of energy such as biogas, liquid transportation fuels and syngas [3], thus making a valuable energy alternative to the conventional fossil fuels. The application of MSW gasification presents endless possibilities in the energy security, mitigation of climate change and sustainable development [2]. Various thermochemical conversion techniques can transform the carbonaceous materials in biomass to a syngas product which is combustible, whereby gasification plays a lead role [4]. Gasification occurs when the carbonaceous material in biomass reacts with limited gasifying agent, just enough to prevent combustion, such as oxygen, at high temperatures in a gasifier to produce combustible gas [2], [5].

Research on the simulation of gasification processes is somewhat limited, even though there has been a significant amount of experimental research involving MSW and other types of waste [25] The heterogenous nature of MSW leads to its very complex gasification process, whereby mutual influence exists and internal reactions take place [6], [7]. This makes the gasification of MSW a hard process to be simulated, requiring complex mathematical modelling and iterative computations [8]. Since Gibbs free energy minimization does not require extensive knowledge of specific chemical reactions in a given process, it makes it a highly suitable thermodynamic equilibrium model to base the simulation calculation of an elaborate equilibrium system on [9]. In recent times, researchers are making use of the Aspen Plus process simulation software to model reaction processes and solve computational problems [8]. The areas of interest of these researchers have been in the combustion and gasification of coal and biomass [7], [10], [11]. Aspen Plus is a large-scale software based on steady chemical process simulation, optimization and sensitivity analysis as well as economic evaluation [5]. The software enables researchers to simulate process operations from a

single unit operation to an entire process as it provides a complete set of unit operation models [5].

A handful of researchers have paid attention to MSW gasification with Zheng, Kaliyan and Morey [7] having developed an Aspen Plus model to simulate MSW gasification and melting so as to predict the composition of the gasification products. Zheng, Kaliyan and Morey [7] along with Ramzan, Ashraf, Naveed and Malik [12] also studied the effect of air equivalence ratio, feedstock moisture content and gasification temperature on the gasification performance. Ramzan, Ashraf, Naveed and Malik [12]performed their study on MSW, food waste and poultry waste, and validated their model with data obtained from a hybrid biomass gasifier experiment. The effect of flue gas from the combustion section of a gasification process on syngas lower heating value (LHV) was studied by Chen, Jin, Yan and Chi [13] using two different types of fixed bed reactors for MSW simulation. They also studied the heat conversion efficiency and carbon conversion at different gasification temperatures and equivalence ratios. An Aspen simulation conducted by Mavukwana, Jalama, Freeman and Harding [14] of sugarcane bagasse gasification showed a good comparison between experimental results cited in literature and the model results. A numerical simulation mode, also developed on Aspen, of a fixed bed gasifier with varied process parameters such as equivalence ratio, gasification temperature and feedstock moisture was presented by Begum, Rasul and Akbar [2]. A study by Deng, Li, Zhang, Zhang, Cai and Zhang [8] used Aspen simulations to analyse syngas composition, LHV, and carbon conversion rate in varying process conditions such as the gasification temperature, equivalence ratio and gasifying agents.

2. METHODOLGY

2.1 Gasification Model Development

The gasification model was developed using a solid based simulation on Aspen Plus to accommodate the processing of the municipal solid waste feedstock in the form of refuse derived fuel (RDF) pellets. This is because the simulation of heat and mass balances of a process involving solids requires a physical property model suited for solid components as physical property models used in the characterization of a liquid substance may be deemed irrelevant for solid components [15]. An advantage of having specialized property models for solids processing stems from the ability to accurately represent the solids particle size distribution which may be a crucial requirement for some processes. In this model, the operation of a fixed bed gasifier was developed for the gasification of RDF pellets on Aspen. The simulations for the process were developed on a basis of mass-energy balance and chemical equilibrium similar to the simulation studies conducted by Begum, Rasul and Akbar [2], Shaohua, Deyong, Wenguang and Haigang [5] and Deng, Li, Zhang, Zhang, Cai and Zhang [8]. The core operation of the modelled developed for this study was derived from the Aspen Plus 2004 manual titled “Getting started with solids”, which gives a detailed description of simulation model developed for the description of a coal combustion process [12] Using blocks that are consequent to reactors and other unit operations, Aspen Plus can simulate most industrial processes due to the program’s vast databases comprised of thermodynamic, chemical and physical data for a wide variety of chemical compounds as well as selection of thermodynamic models that a necessary for the accurate simulation of any given chemical system [16]. As adapted from the combustion of coal simulation modelled on the Aspen manual, the developed model involves:

The construction of a process flow using user defined blocks to describe the gasification process.

The specification of a global stream class, addition of components required for gasification (conventional and nonconventional).

Definition of nonconventional solid components (in this case RDF pellets and ash).

Specification of physical properties for the nonconventional solid components.

Specification of streams with the non- conventional components.

Modification of component attributes in unit operation blocks. specification of unit operation models.

Most importantly, definition of Fortan blocks using fortan statements to control the drying and pyrolysis (decomposition) steps/reactions of the RDF during gasification [15].

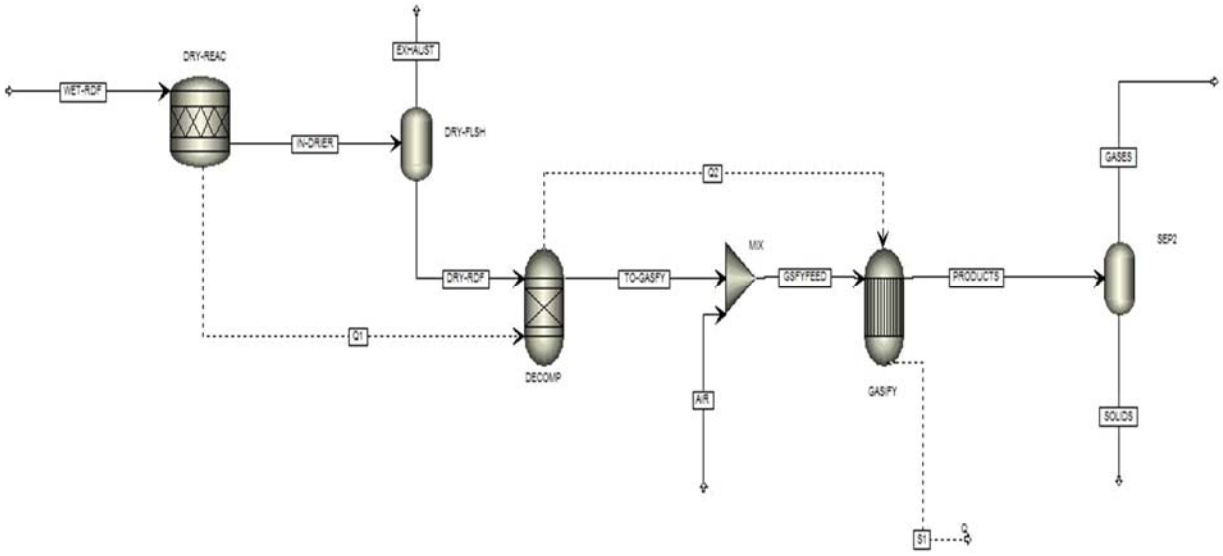

Figure 1. Aspen plus model simulation process flow diagram for RDF gasification.

2.2 Model Assumptions

Various assumptions were made in developing the model for the simulation of MSW gasification from RDF pellets. The assumptions considered are similar to those considered by several authors and are as follows [2], [5], [8], [15]:

The simulation model is isothermal, isobaric, kinetic free and is at steady state.

Chemical reactions in the gasifier occur at a state of equilibrium.

Apart from sulphur content, all elements in the model take part in the chemical reactions.

All gases present in the model simulation are regarded as ideal, this includes hydrogen (H_2), carbon monoxide (CO), carbon dioxide (CO_2), oxygen (O_2), nitrogen (N_2), and methane (CH_4).

The char residue is only comprised of carbon and ash in solid phase.

2.3 Model Process Flow Diagram

Although a real-life gasification process occurs in a single reaction vessel, the process does undergo a certain number of steps within the vessel which can be separated into different process steps. Aspen Plus does not have a single unit operator block that acts as a gasifier, thus, an Aspen process flow was developed to describe each of the gasification steps using applicable unit operator blocks to describe and model each step of the gasification process in the simulation as depicted in Figure 1.

The gasification process consists of a drying, pyrolysis/decomposition, and the gasification step. The feed, RDF pellets, to the gasification process is specified in the model as a nonconventional component and is defined in the simulation using the proximate and ultimate analysis results obtained during the characterization stage. The basis of the model is the minimization of Gibb's free energy at equilibrium, with the assumption of residence time being long enough to permit the reactions to acquire a state of equilibrium.

2.4 Simulation Process Description

The gasification simulation model was developed by using 3 main reactor types on the Aspen Plus software namely the Stoichiometric Reactor (RStoich), Yield Reactor (Ryield) and RGibbs reactors. The combination of all the process steps to follow is graphically presented by the process flow diagram in Figure 1.

2.4.1 Drying

This section of the process is designed to simulate the drying stage of the gasification process using the RStoich reactor (DRY-REAC) on Aspen. In this step, the moisture content of the feedstock is being reduced by evaporation. Even though the RDF pellets being fed to the reactor were dried during production, there is still an amount of moisture left (WET-RDF) and that moisture content is that determined by proximate analysis. In the RStoich block, a portion of the WET-RDF feed reacts to form water, and since the reactor only has one outlet stream (IN-DRIER), a Flash 2 model separator (DRY- FLSH) was used to separate the dried RDF from the water using split fractionation and the water exits the process through the EXHAUST stream while the DRY-RDF moves to the next stage of the process. Although the drying of materials is not usually considered as a chemical reaction, a reactor model was used to simulate the process with the extent of the reaction described as WET-RDF → 0.0555084 H_2O. Aspen regards all nonconventional components as having a molecular weight of 1. Thus, the extent of reaction indicates that 1 mole of RDF reacts to form 0.0555084 mole of water. The drying process was controlled by declaring a calculator block and using FORTAN statements to describe the drying of the RDF feed.

2.4.2 Pyrolysis/Decomposition

After the drying step, the gasification process moves the pyrolysis/decomposition step whereby the RDF is decomposed into its constituent elements. The decomposition process model was simulated using the RYield block (DECOMP) which converts non convention feed components, RDF, into conventional components. Fortan statements used in a calculator block to calculate the yield distribution from the component attributes of RDF in the feed stream to the RYield model (DRY-RDF) which

come in the form of an elemental composition described the ultimate analysis of the feed stream. The converted elements include carbon, hydrogen, oxygen, nitrogen and sulphur.

2.4.3 Gasification

After decomposition, has occurred, the converted elements are then ready for gasification. These elements in stream TO-GASFY are mixed with an AIR stream using an ASPEN Mixer block (MIX) to ensure perfect air mixing during the gasification process. The actual gasification stage of the gasification process is simulated using the RGibbs reactor model. RGibbs is a rigorous reactor model that calculates chemical and phase equilibrium by minimizing Gibbs free energy of the system. Therefore, it eliminates the necessity to specify reaction stoichiometry. By minimizing the Gibbs free energy and assuming complete chemical equilibrium, the reactor is then able to quantify the composition of the SYNGAS product stream. Using the heat stream Q-DECOMP, the heat of reaction associated the decomposition was passed to the RGibbs reactor. The elemental feed-air mixture enters the gasification stage (GASIFY) through stream GSFYFEED where partial oxidation occurs to constitute the gasification reactions. Part of the carbon present constitute the gas phase and undergoes devolatisation and the remaining carbon constitutes the solid phase. Using a separator model (SEP2), the syngas product was separated from the ash using split fractionation

2.5 Operating Parameters

2.5.1 Gasifier

Table 1 shows the operating parameters of the gasifier system and Table 2 is a description of the feed characteristics to be considered in the simulation process, the following will be considered:

Table 1. Gasification operating parameters

Parameter	Value	Unit
Feed Flow Rate	100	Kg/h
Feed Pressure	1	bar
Feed Temperature	25	℃
Equivalence Ratio	0-1	
Air Pressure	1	bar
Air Temperature	25	℃
Gasifier Temperature	500-900	℃
Gasifier Pressure	1	bar

2.5.2 Feed Characteristics

Table 2. RDF Pellet Characteristics

Proximate Analysis (mass %) (Dry Basis)	Moisture	3.50
	Volatile Matter	80.9
	Fixed Carbon	5.60
	Ash	10.0
Ultimate Analysis (mass %)	Carbon	44.6
	Hydrogen	8.94
	Oxygen	27.6
	Nitrogen	4.74
	Sulphur	4.18
Calorific Value (MJ/kg)		22.7

3. RESULTS AND DISCUSSION

The baseline of the gasification simulation results will be presented for a case from which experimental results were unavailable. Due to the lack of experimental data referred to RDF gasification of the Cape Peninsula University of Technology, Waste-to-Energy research group, it has been necessary to use reported data for RDF gasification models, obtained by Ramzan, Ashraf, Naveed and Malik [12], Chen, Jin, Yan and Chi [17] and Násner, Lora, Palacio, Rocha, Restrepo, Venturini and Ratner [18], as they all used fixed bed gasifier systems with air as a gasifying agent. The developed RDF gasification model was used to compare theoretical and the experimental data from other models with the theoretical results of chemical equilibrium model based on Gibbs free energy minimization in this study. The results presented in Figure 2 below compares mainly the H_2 and CO composition in the gas as these are the 2 major constituents of Syngas.

The results obtained, as summarized in Figure 2, show that the current study has a much higher mole fraction of H_2 than CO in the product syngas with very similar operating conditions to the results being compared to. The main differences are presented in the feedstock characteristics, namely the moisture content. The other studies have moisture content ranging between 12-48% while in this study the moisture was 3.5% as the feedstock was dried.

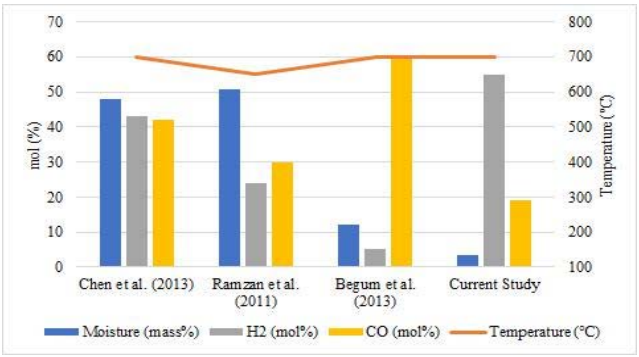

Figure 2. Aspen Plus model simulation process flow diagram for RDF gasification.

The disadvantage of high moisture is that as it draws more heat towards sensible heating and moisture removal, the reactor temperature decreases which affects the gasifier performance and quality of syngas product [19]. The H_2:CO ratio of the syngas found at the baseline conditions is deemed suitable for H_2 production at 3:1 [20]. This was also found by Deng, Li, Zhang, Zhang, Cai and Zhang [8]

In analyzing the effect of temperature on the syngas composition, it was found that both the composition of H_2 and CO increase in direct proportion to the temperature as seen in Figure 3.

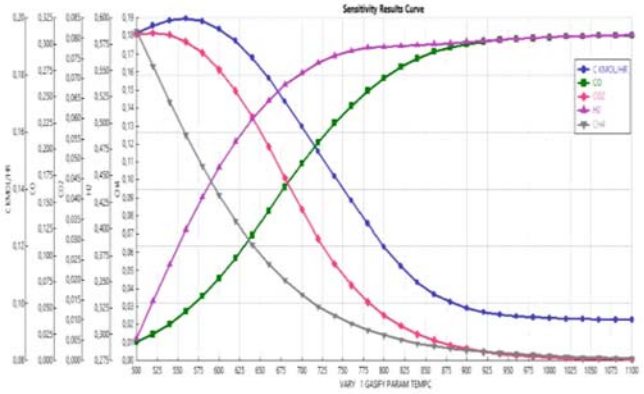

Figure 3. Effect of Temperature on Syngas composition.

Also in Figure 3, it can be deduced that the C, CO_2 and CH_4 all decrease with an increase in temperature. It can also be deduced that as the temperature draws close to the 900℃ mark, the H_2: CO ratio decreases and remains as 2:1 making the gas ideal for methanol production. [20].

In terms of the effect of temperature on the conversion of carbon, it was found to increase with an increase in temperature up to 72% conversion at 900℃ and remained constant thereafter as presented in Figure 4.

Taking into consideration, the effect of the gasifying agent to fuel ratio, the relationship presented on Figure 5 transpired. The CO_2 and CO composition in the product syngas were found to be directly proportional to the amount of air supplied into the system. This is because with increasing the air supply, the process moves more to a combustion type of process, hence the increase in CO_2 which is opposite to the effect of temperature while keeping the air supply constant.

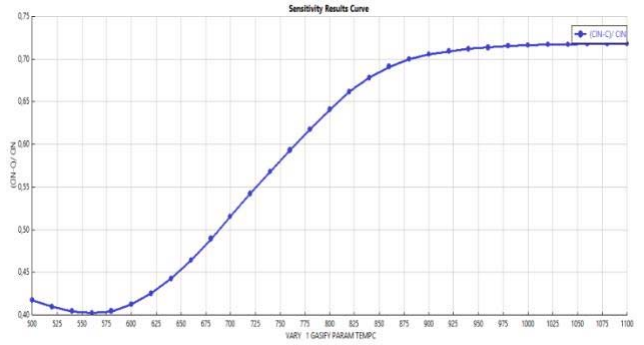

Figure 4. Effect of Temperature on Carbon conversion.

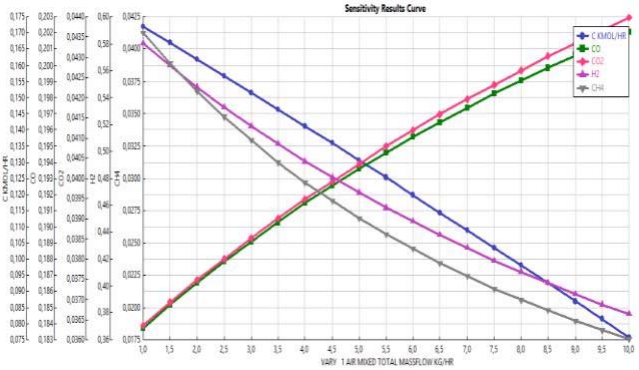

Figure 5. Effect of air: Fuel ratio on gas composition.

The relation of air supply to carbon conversion also resembled direct proportionality due to the same effect of the process moving into more of a combustion type process due to the excess amount of oxidizing agent. At the air: fuel ratio of 1:1 (air flow 10 kg/h), the carbon conversion was found to be 77.5% and was found to be increasing linearly, contrary to the effect of temperature where the conversion came to a constant value.

These results confirm what was found by Ramzan, Ashraf, Naveed and Malik [12], Chen, Jin, Yan and Chi [17], Begum, Rasul and Akbar [2] and Deng, Li, Zhang, Zhang, Cai and Zhang [8].

4. CONCLUSION

This study modelled a fixed bed gasifier for RDF gasification by employing Aspen Plus simulation software. The model was compared with the modelled and experimental data measured by Ramzan, Ashraf, Naveed and Malik [12], Chen, Jin, Yan and Chi [20] and Násner, Lora, Palacio, Rocha, Restrepo, Venturini and Ratner [18], Begum, Rasul and Akbar [2] and Deng, Li, Zhang, Zhang, Cai and Zhang [8]. The findings produced from this study were in good agreement with those cited, making the model suitable for simulation of RDF gasification and several other biomass feedstocks. The model has the ability of testing the process in a wide variety of process parameter of which only the temperature and air to fuel ratio were modelled in this study. Further modelling will be done assessing the gasification performance by optimizing operating condition using different binding materials for the feed preparation of the RDF pellets.

5. ACKNOWLEDGMENTS

All the authors would like to thank the Cape Peninsula University of Technology for funding towards the project and attendance at the conference.

6. REFERENCES

[28] Antizar-Ladislao, B. and Turrion-Gomez, J. L. Second-generation biofuels and local bioenergy systems. Biofuels, Bioproducts and Biorefining, 2, 5 2008), 455--469.

[29] Begum, S., Rasul, M. and Akbar, D. A numerical investigation of municipal solid waste gasification using Aspen Plus. Procedia Engineering, 902014), 710-717.

[30] Converti, A., Oliveira, R. P. S., Torres, B. R., Lodi, A. and Zilli, M. Biogas production and valorization by means of a two-step biological process. Bioresource Technology, 100, 23 2009), 5771--5776.

[4] Cheremisinoff, N. P. and Rezaiyan, J. Biogasification. Chemical Industries2005), 119--144.

[5] Shaohua, L., Deyong, C., Wenguang, Y. and Haigang, W. The effect of ER on biomass gasification in a fixed bed using ASPEN PLUS simulation. City, 2012.

[6] Meng, A., Chen, S., Zhou, H., Long, Y., Zhang, Y. and Li, Q. Pyrolysis and simulation of typical components in wastes with macro-TGA. Fuel, 1572015), 1--8.

[7] Zheng, H., Kaliyan, N. and Morey, R. V. Aspen Plus simulation of biomass integrated gasification combined cycle systems at corn ethanol plants. Biomass and Bioenergy, 562013), 197--210.

[8] Deng, N., Li, D., Zhang, Q., Zhang, A., Cai, R. and Zhang, B. Simulation analysis of municipal solid waste pyrolysis and gasification based on Aspen plus. Frontiers in Energy2017), 1-7.

[9] Shabbar, S. and Janajreh, I. Thermodynamic equilibrium analysis of coal gasification using Gibbs energy minimization method. Energy Conversion and Management, 652013), 755--763.

[10] Mostafavi, E., Pauls, J. H., Lim, C. J. and Mahinpey, N. Simulation of high-temperature steam-only gasification of woody biomass with dry-sorption CO2 capture. The Canadian Journal of Chemical Engineering, 94, 9 2016), 1648--1656.

[11] Yuehong, Z., Hao, W. and Zhihong, X. Conceptual design and simulation study of a co-gasification technology. Energy Conversion and Management, 47, 11-12 2006), 1416--1428.

[12] Ramzan, N., Ashraf, A., Naveed, S. and Malik, A. Simulation of hybrid biomass gasification using Aspen plus: A comparative performance analysis for food, municipal solid and poultry waste. Biomass and Bioenergy, 35, 9 2011), 3962-3969.

[13] Chen, C., Jin, Y.-Q., Yan, J.-H. and Chi, Y. Simulation of municipal solid waste gasification in two different types of fixed bed reactors. Fuel, 1032013), 58-63.

[14] Mavukwana, A., Jalama, K., Freeman, N. and Harding, K. Simulation of sugarcane bagasse gasification using Aspen Plus, 2013.

[15] Aspentech Aspen Plus 2004.1 Getting Started Modeling Processes with Solids. City, 2004.

[16] Zheng, L. and Furimsky, E. ASPEN simulation of cogeneration plants. Energy Conversion and Management, 44, 11 2003), 1845--1851.

[17] Chen, C., Jin, Y.-Q., Yan, J.-H. and Chi, Y. Simulation of municipal solid waste gasification in two different types of fixed bed reactors. Fuel, 1032013), 58-63.

[18] Násner, A. M. L., Lora, E. E. S., Palacio, J. C. E., Rocha, M. H., Restrepo, J. C., Venturini, O. J. and Ratner, A. Refuse Derived Fuel (RDF) production and gasification in a pilot plant integrated with an Otto cycle ICE through Aspen plus™ modelling: Thermodynamic and economic viability. Waste Management, 692017), 187-201.

[19] Wang, L. Sustainable Energy Production. CRC Press Taylor and Francis Group, 2014.

[20] Ciferno, J. A. M., J. Benchmarking Biomass Gasification Technologies for Fuels, Chemicals and Hydrogen Production. National Energy Technology Laboratory, City, 2002.

International Proceedings of Chemical, Biological and Environmental Engineering, V0l. 102 (2017)
DOI: 10.7763/IPCBEE. 2017. V102. 12

Landfill Operations Effects on Natural Radionuclide Activities

Aviwe Hlaba [1], Peane Maleka [2] Ademola Rabiu [1], Otolorin Adelaja Osibote [3+]

Department of Mathematics & Physics, Faculty of Applied Science, Cape Peninsula University of Technology, Cape Town 8000, South Africa

Department of Chemical Engineering, Faculty of Engineering, Cape Peninsula University of Technology, Cape Town 8000, South Africa

iThemba LABS, Faure, Cape Town, 7131, South Africa

Abstract. Naturally occurring radionuclide activity was investigated at landfill sites from the City of Cape Town using a Hyper-Pure Geranium detector with appropriate shielding coupled to a Palmtop Multichannel Analyzer. Activity concentrations of the radionuclides ^{238}U, ^{232}Th and ^{40}K were obtained from the activity concentrations of their respective daughter radionuclides. To obtain the overall combined effect in terms of activity concentration from the 3 parent radionuclides, the radium equivalent was calculated and 38.273, 41.019 and 83.007 Bq/Kg were obtained from Bellville, Coastal Park, and Vissershok respectively. Other radiological hazards in terms of Internal and External hazard indices and Representative hazard index were determined and found to be within safe limits. Dose rate in air at 1m above the ground was determined to obtain a characteristic of the external gamma-ray and was found to be 17.490, 18.609 and 38.667 nGy/y for Bellville, Coastal Park, and Vissershok respectively. The health effects of the radiation in terms of annual effective dose and excess lifetime cancer risk were determined to be 0.031 mSv/y and 0.0961×10^{-3} which are lower than limits set by the United Nations Scientific Committee on the Effects of Atomic Radiation (UNSCEAR) and the Nuclear Industry Association of South Africa (NIASA).

Keywords: Solid Waste, Radionuclide, Activity Concertation, Dose Rate, gamma-ray, Radiological Hazard.

1. Introduction

Naturally Occurring Radionuclide Materials (NORM) are any material that contains radioactive elements and is found in the environment. [1]. These elements originate from the earth's crust and approximately 90 % of the radiation exposure to humans can be attributed to natural origins such as exposure to radon gas, cosmic radiation and surface dwelling radionuclides [2]. Contact is mainly through direct external exposure or incorporation of the radionuclide into the body by inhalation or ingestion respectively [3]. Soil is among the most considerable sources of radiation exposure and the migration of radionuclides to humans and the immediate environment [4]. Exposure is a direct result of gamma ray emissions that are produced by terrestrial radionuclides which are the members of the Uranium (^{238}U) and Thorium (^{232}Th) series, as well as the Potassium (^{40}K) series, of which concentrations vary according to the type of soil and the geology of the area [3], [5], [6].

Solid waste management is an ever-growing challenge in South Africa due to rapid urbanisation and population growth. This growth in urban communities comes with increased volumes of waste generation posing a challenge to municipalities with regards to its management. Materials containing radionuclides are disposed of in MSW landfills [7]. Poor siting, design and operation of waste disposal facilities is among the historical problems experienced with MSW which have detrimental effects on the quality of life and

+ Corresponding author. Tel.: + 27 21 460 9092 fax: +.27 21 460 3854
E-mail address: osibotea@cput.ac.za.

immediate environment [8]. Approximately 1.9 mega tons of waste are generated annually in Cape Town alone, with only a small percentage of the waste being processed in recycling efforts. Waste contributors in South Africa are generally industrial, commercial, and household with a composition of approximately 38 % non-recyclable waste, 22 % mainline recyclables, 22 % builders' rubble and 16 % organic waste of which only the recyclable waste is not going to the landfill site [9], [10].

The aim of the study is to conduct radionuclide analysis of environmental soil samples collected from 3 active landfill sites in Cape Town, South Africa, namely Vissershok, Bellville, and Coastal Park landfill sites of which are operated by the City of Cape Town (CoCT) municipality. The objective of this analysis is to quantify the activities of NORM namely ^{238}U, ^{232}Th and ^{40}K in landfill soil, and thereof, assess the gamma radiation which will give an indication of the dose that humans are potentially exposed to.

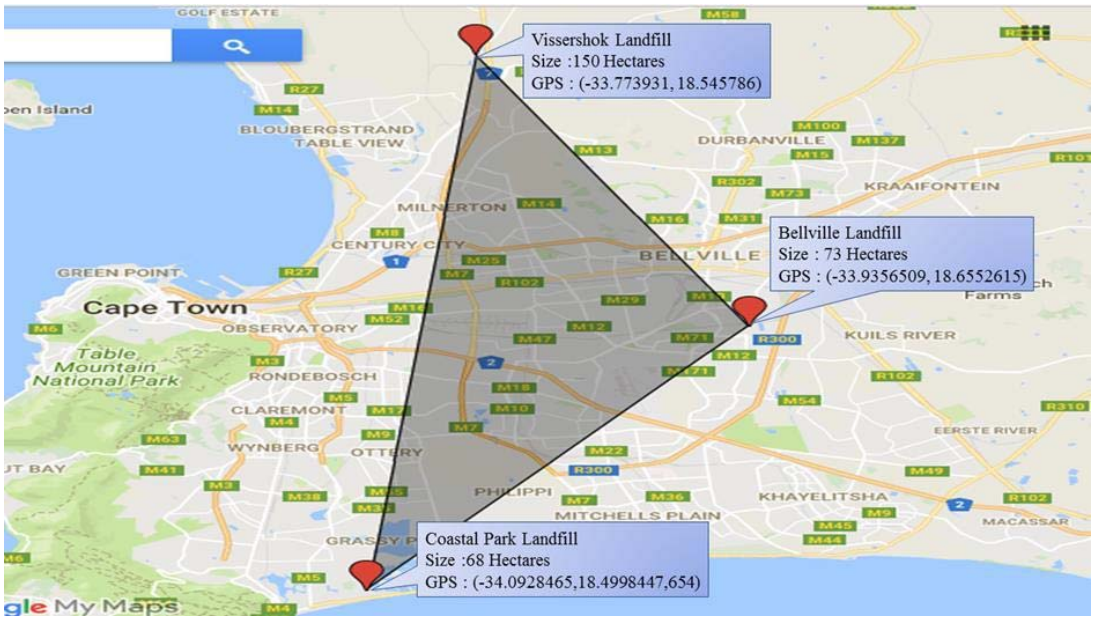

Fig. 1: Size and GPS coordinates of the 3 landfill sites studied.

2. Materials and Methods

2.1. Source of Sample

A total number of 42 (14 per site) soil samples were collected at approximately 1 kg each. Soil samples were collected at a depth of approximately 5 – 10 cm depth at the base of the landfill sites approximately 40 – 50 m to ensure a good representative.

2.2. Sample Preparation

Samples were air-dried at room temperature for a period of 5 to 7 days. in a controlled environment to prevent resident dust contamination. The samples were then homogenized by means of a crushing and grinding process to attain a pre-set particle size per specifications dictated by the analytical requirements. The ground samples were then passed through a sieve of 35 mm mesh. The samples were then stored in air-tight Marinelli beakers with geometry which is identical to that of the reference material. The beakers containing the samples were hermetically sealed and stored for a period of approximately 4 weeks before gamma-ray spectrometry commenced. This is to ensure that secular radioactive equilibrium was reached after their progeny [2], [3], [5], [11].

2.3. Gamma-ray Measurements

Radionuclide analysis of the soil samples was carried out by means of the gamma-ray spectroscopy method. The analysis setup comprised of a Hyper-Pure Germanium (HPGe) detector coupled via a computerized interface to a Palmtop Multichannel Analyzer (MCA). The detector was a coaxial n-type detector with an energy resolution of 2.0 keV (full width at half maximum, FWHM) at 1332 keV, shielded with lead blocks in order to prevent scattered radiation from the shield [12]. The efficiency of the detector,

which is typical of HPGe detectors was 30 % [12]. Each sample was analyzed for naturally occurring radionuclide activity for a period of 86400 seconds and the accumulated spectra data was analyzed by the palmtop MCA software (MCA8k-01). The gamma ray transition energy lines of 186 keV for ^{226}Ra, 2614.6 keV for ^{208}Tl and 1460 keV for ^{40}k were used to obtain the activity concentrations ^{238}U, ^{232}Th and ^{40}K respectively. The activity concentrations were computed using the photopeaks of the gamma ray spectra of the decay series. Since the parent radionuclides do not inherently emit intense gamma rays but have progenies with more intense gamma rays and equal in activity to their parents at secular equilibrium, the radionuclide analysis was dependent on the detection of the emissions from these progenies.

The activity concentration, A, was determined using the following relationship: A = C/(LT×b×m× Eff'), where C is the net peak area, LT is the live time, b is the branching ratio, m is the sample mass and Eff' is the absolute efficiency at a specific photopeak energy [3], [11], [13]-[15].

3. Results and Discussion

In order to obtain the activity concentrations of the parent radionuclide ^{238}U and ^{235}U, gamma ray energies of 186 keV from ^{226}Ra were used, under the assumption that ^{235}U/^{238}U isotopic ratio is constant for varying sample type and composition at 7.2×10^{-3} [5]. Regarding the fact that secular equilibrium can be assumed as reached between ^{238}U and ^{232}Th and their respective decay products as per methodology waiting period, ^{238}U and ^{232}Th activity concentrations were determined by computing the mean activity concentrations of their decay products, namely ^{226}Ra, ^{214}Pb and ^{214}Bi for ^{238}U and ^{228}Ac and ^{208}Tl for ^{232}Th [16]. The results obtained are summarized in Fig. 2.

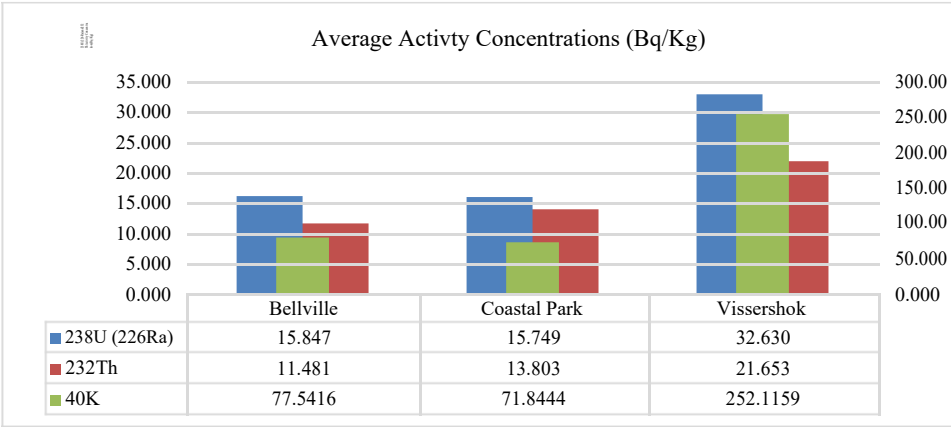

Fig. 2: Summary of results showing the activity concentrations of ^{238}U, ^{232}Th and singly occurring ^{40}K in (Bq/Kg) as an average of each radionuclide from all samples in each site

In consideration of the results obtained, it can be distinguished that the ^{238}U activity concentration in the Bellville site ranges between 8.750 and 24.189 Bq/Kg with a mean concentration of 15.847 Bq/Kg. Activity for ^{232}Th at the same site ranges between 7.774 – 18.331 Bq/Kg with an average of 11.791 Bq/Kg and ^{40}K averaging at 77.542 Bq/Kg range 45.031 – 122.041 Bq/Kg.

The Coastal Park landfill site shows a ^{238}U activity range of 14.618 – 16.880 Bq/Kg with an average activity of 15.749 Bq/Kg while ^{232}Th and ^{40}K averaged at 13.803 and 71.844 Bq/Kg with ranges 13.069 – 14.536 Bq/Kg and 63.910 – 79.779 Bq/Kg respectively while at the Vissershok site, ^{238}U activity concentration was found in the range 23.917 – 41.273 Bq/Kg with an average of 32.630 Bq/Kg, 15.783 – 26.154 Bq/Kg with a mean activity of 21.653 Bq/Kg for ^{232}Th and 155.766 – 352.432 Bq/Kg at an average activity of 252.116 Bq/Kg for ^{40}K.

Several radiological parameters were determined from the activity concentrations obtained from the soil samples. The parameters include the radium equivalent, external and internal hazard indices, representative gamma index, absorbed dose rate, annual effective dose rate (indoor and outdoor), lifetime dose rate, and the excess lifetime cancer risk.

The distribution of the naturally occurring radionuclides ^{238}U, ^{232}Th and ^{40}K is not by any means uniform in the soil. Therefore, in order to compare the combined radiological effect of the soil containing these radionuclides by a single quantity, a collective index called the Radium Equivalent was used to describe the gamma radiation from the varying mixtures of the radionuclides in the soil [5], [11], [17]. The radium equivalent, Ra_{eq}, is calculated by using the $Ra_{eq} = C_{Ra} + 1.43C_{Th} + 0.077C_K$ [18], where C_{Ra}, C_{Th} and C_K are the activity concentrations of ^{226}Ra, ^{232}Th and ^{40}K respectively. The index represents a weighted total of the above-mentioned radionuclides' activity concentrations on the basis of an assumption that states that 1 Bq/Kg of ^{226}Ra, 0.7 Bq/Kg of ^{232}Th and 13 Bq/Kg of ^{40}K produce an equal amount of gamma radiation dose rates [16], [19], [20].

The results obtained show that the Vissershok landfill has the highest amount of radiation at 79.608 Bq/Kg. This site also showed the highest amounts of the activity concentrations of the 3 radionuclides ^{238}U (^{226}Ra), ^{232}Th and ^{40}K. This can be attributed to that fact that Vissershok is the largest of the 3 landfill sites and most amounts of all types of waste, ranging from motor oil, household, medical and industrial waste are disposed of at this site.

This then explains the overall high radiation activity at this landfill site. Coastal Park landfill displayed the second highest amount of radiation with regards to the radium equivalent. Breaking down this reading of 38.042 Bq/Kg, it was noticed that potassium was particularly high as compared to the other radionuclides. This can be attributed to the fact that the Coastal Park landfill was mostly used for the disposal of builders' rubble. According to research conducted around the world, it was observed that building materials show a particularly high radioactivity concentration of potassium [21]-[23]. Similarly, with the Coastal Park site, the Bellville site exhibited a synonymous distribution of the 3 radionuclides and having a radium equivalent of 31.610 Bq/Kg. The Bellville reading is a bit lower compared to Coastal Park, since the Bellville site had a more even distribution of household, builders' rubble and garden waste compared to coastal park and had a lower thorium concentration compared to coastal park.

External Hazard Index is a commonly used hazard index to denote the external exposure and is obtained using the equation $H_{ex} = C_{Ra} / (370\ Bq/kg) + C_{Th} / (259\ Bq/kg) + C_K / (4810\ Bq/kg)$ [24]-[27], where C_{Ra}, C_{Th} and C_K are the activity concentrations in Bq/kg for ^{226}Ra, ^{232}Th and ^{40}K respectively, as with the other indices to be discussed. This is a model proposed by several authors which creates a scenario for a room in the house where the inhabitants live with infinitely thick walls without windows and doors [28]. The value of the external hazard index must be less then unity, which essentially means that the objective of the index is to maintain the radiation dose to the accepted dose limit of 1 mSv/y which corresponds to the upper limit of Ra_{eq} 370 Bq/kg [24], [26], [29].

The calculated values for external hazard index illustrated on Fig. 3 range from 0.103 – 0.224 with a mean value of 0.146 and a standard deviation of 0.068. All the values obtained are below the critical value of unity being 1 which corresponds to the accepted dose limit of 1 mSv/y [24], [26], [29].

In addition to the external irradiation, radon along with its short-lived products are regarded hazardous to respiratory organs through inhalation of alpha particles emitted from these products. The internal exposure to radon and its daughter products are quantified by the internal hazard index which, which needs to be less than 1, is given by the equation $H_{in} = C_{Ra} / (158\ Bq/kg) + C_{Th} / (259\ Bq/kg) + C_K / (4810\ Bq/kg)$. The calculated values of the external hazard index presented in Fig. 3 were found to range from 0.146 to 0.312 with a mean value of 0.204 and standard deviation of 0.094. All the values obtained do not exceed the recommended limit of 1 with Bellville landfill site showing the lowest at 0.146 and Visserhok the highest at 0.312.

Representative level index is used for the approximation of gamma radiation associated with natural radionuclide activity in the soil and is defined by the equation $I_{\gamma r} = C_{Ra} / (150\ Bq/kg) + C_{Th} / (100\ Bq/kg) + C_K / (1500\ Bq/kg)$ [24]-[29]. The values obtained for the representative level index as presented also in Fig. 3 were found to range from 0.272 to 0.602 with a mean value of 0.388 and a standard deviation of 0.185. The limit for the representative level index is set to be ≤ 1 (Ajayi 2009), of which all the values obtained fall below the limit. Therefore, it can be concluded that based on these results, with respect to the radium equivalent, internal and external hazard indices, as well as the representative level index, there is no evidence

of any threat of a health hazard from the landfill soil of Bellville, Coastal Park and Vissershok respectively in regards to gamma radiation.

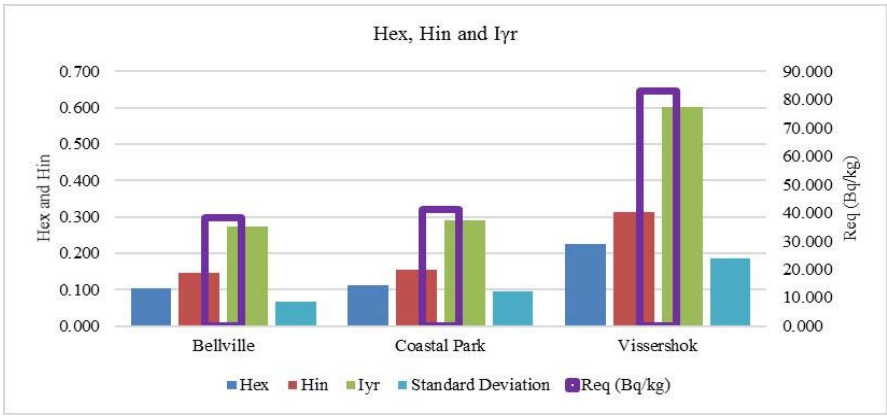

Fig. 3: Radium equivalent, average activity internal and external hazard indices with representative level index in landfill soil

To provide a characteristic of the external gamma ray, it is necessary to calculate the absorbed rate at 1m above the ground. The absorbed dose rate D (nGy/h) was calculated using equation: $D = 0.462C_{Ra} + 0.604C_{Th} + 0.0417C_K$ [28]. The values obtained for absorbed dose rate in air at 1m above ground averaged at 17.490, 18.609 and 38.667 nGy/h for the Bellville, Coastal Park, and Visserhok landfills respectively. The United Nations Scientific Committee on the Effects of Atomic Radiation (UNSCEAR) reports a global average of approximately 55 to 60 nGy/h absorbed rate 1m above the ground of which all 3 sites are lower [5], [11], [28]. Results in summary in Fig. 4.

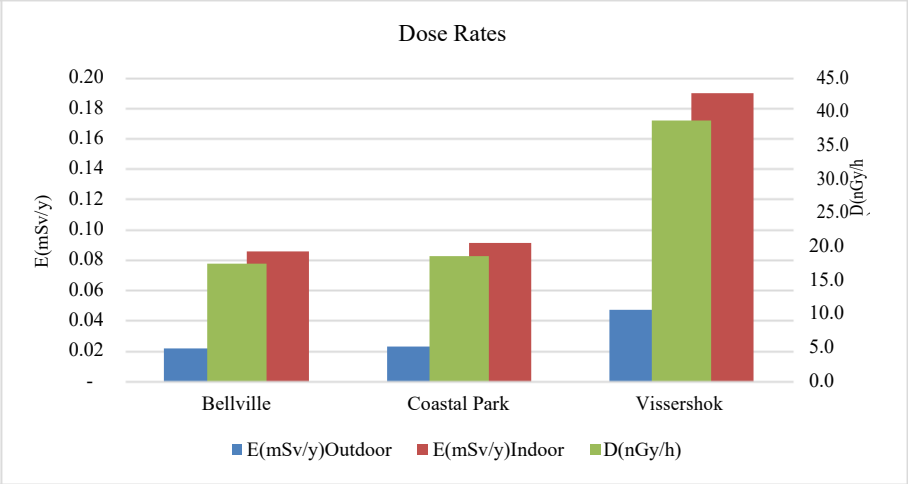

Fig. 4: Summary of results for absorbed dose rates and annual effective dose rate (indoor and outdoor) per year for each site.

It is also necessary to assess the overall effects of this radiation on health due to the absorbed dose rate. This is done by determining the annual effective dose rate E (mSv/y) using the equation $E = D(nGy/h) \times 8760(h/y) \times 0.2 \times 0.7(Sv/Gy) \times 10^{-6}$ [28]. The equation, as used by the UNSCEAR, takes into account a conversion coefficient of 0.7 Sv/Gy from the absorbed dose in air 1m above the ground and outdoor occupancy factor of 0.2 [5], [11]. The annual effective dose rate for indoors was also determined which then considers an indoor occupancy factor of 0.8, being the fraction of time spent indoors, instead of 0.2 which the corresponds to the fraction of time spent outdoors in the equation above [26], [28]. To approximate the annual effective dose, the conversion coefficient from absorbed dose in air to effective dose needs to be taken into consideration, as well as the outdoor occupancy factor [26]. The annual effective dose rates determined using the outdoor occupancy factor for outdoor terrestrial gamma radiation in landfill soil were 0.0214, 0.0228 and 0.0474 mSv/y for Bellville, Coastal Park, and Vissershok respectively, which are all

lower than the reported global average of 0.07 mSv/y [28]. The corresponding values for annual effective dose rate for indoor exposure were found to be 0.086, 0.091 and 0.190 mSv/y for Bellville, Coastal Park and Vissershok landfill sites respectively. The results obtained for all 3 sites fall under the world-wide average of 0.34 mSv/y. It can be deduced from the result of absorbed dose rate and annual effective dose rate that the soil in the 3 City of Cape Town landfill sites still fall under the category of normal levels of radiation, meaning the soil radioactivity of the sites remains less hazardous to the environment and human health. Summary of these result given in Fig. 4.

These results are also lower in comparison to the combined limit of indoor and outdoor annual effective dose rate specified by UNSCEAR of 0.460 mSv/y for terrestrial radionuclides of an area regarded to have normal background radiation [11]. These results also meet the standards set out by the Nuclear Industry Association of South Africa (NIASA) that state that no member of the general public may receive more than 1 mSv/y in addition to natural background exposure of approximately 2.4 mSv/y [30].

Excess lifetime cancer risk (ELCR) describes the probability of developing cancer in a population of individuals over a lifetime at a specific level of exposure. This was calculated using the equation ELCR = E ×DL ×RF where E is the annual effective dose rate (mSv/y), DL is the duration of life or life expectancy of which is 62.9 years in South Africa [31], and RF is the risk factor (Sv^{-1}) which indicates fatal cancer per Seviert. The International Commission on Radiological Protection (ICRP 106), for stochastic effects, used a value of 0.5 for RF for the public [25], [26], [29]. The results obtained for ELCR as well as lifetime dose to rate which is calculated by multiplying the life expectancy with the annual effective dose rate are presented on Fig. 5.

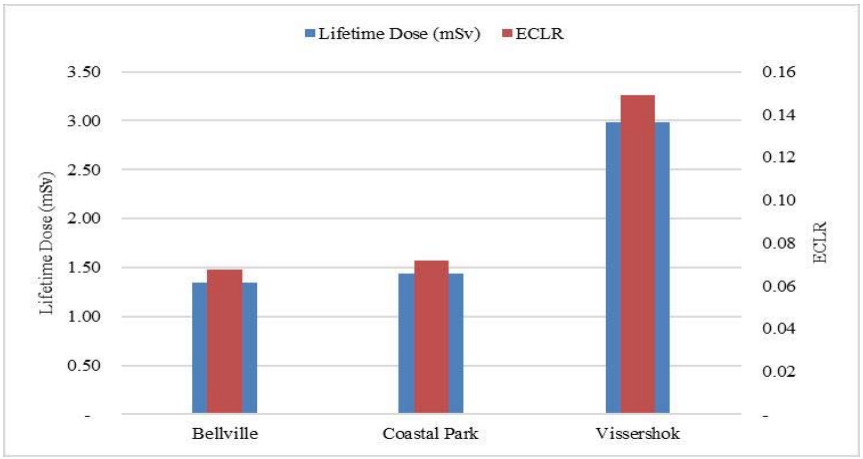

Fig. 5: Summary of results for life time dose and excess lifetime cancer risk

The results obtained for ELCR are 0.0675, 0.0718 and 0.1491 ($\times 10^{-3}$) lifetime cancer risk. The presented values are lower than the global average 0.29 ($\times 10^{-3}$) lifetime cancer risk presented by the UNSCEAR [28].

4. Conclusion

Radionuclide analysis of soil samples from 3 active landfill sites around the City of Cape Town Municipal area was conducted. The analysis was carried out by means of gamma-ray spectroscopy with a Hyper-Pure Germanium detector with appropriate shielding connected to a Palmtop Multichannel Analyzer.

The radioactivity concentrations of ^{238}U, ^{232}Th and ^{40}K were obtained from averaging out the radioactivity concentrations of their respective daughter radionuclides in soil samples from the Bellville, Coastal Park, and Vissershok landfill sites.

With the assumption of secular equilibrium being attained, the dose rate in air 1m above ground and the effective annual dose rates were determined. The results obtained show that the landfill sites meet global standards set out by UNSCEAR and South Africa's NIASA in terms of the maximum allowable emissions in terms of the dose rate in air and effective annual dose rates respectively.

5. Acknowledgements

All the authors would like to thank the Cape Peninsula University of Technology for funding towards the project and Ithemba Labs for the Radionuclide Analysis required for the study.

6. References

[21] International Atomic Energy Agency, *Naturally Occurring Radioactive Material*. in *Naturally Occurring Radioactive Material Symposium*. 2010. Marrakesh, Morocco: International Atomic Energy Agency.

[22] Ademola, A.K., M.A. Olaoye, and P.O. Abodunrin, *Radiological safety assessment and determination of heavy metals in soil samples from some waste dumpsites in Lagos and Ogun state, south-western, Nigeria.* Journal of Radiation Research and Applied Sciences, 2015. **8**(1): p. 148--153.

[23] Jabbar, A., et al., *Measurement of soil radioactivity levels and radiation hazard assessment in mid Rechna interfluvial region, Pakistan.* Journal of Radioanalytical and Nuclear Chemistry, 2010. **283**: p. 371--378.

[24] Ahmad, N., et al., *An overview on measurements of natural radioactivity in Malaysia.* Journal of Radiation Research and Applied Sciences, 2015. **8**(1): p. 136--141.

[25] Mehra, R., *Measurement of Radioactivity of ^{238}U, ^{226}Ra, ^{232}Th and ^{40}K in Soil of Different Geological Origins in Northern India.* Journal of Environmental Protection, 2011. **02**(07): p. 960--966.

[26] Navas, A., J. Soto, and J. Machn, *^{238}U, ^{226}Ra, ^{210}Pb, ^{232}Th and ^{40}K activities in soil profiles of the Flysch sector (Central Spanish Pyrenees).* Applied radiation and isotopes : including data, instrumentation and methods for use in agriculture, industry and medicine, 2002. **57**(4): p. 579--89.

[27] Aucott, M., *The fate of heavy metals in landfills : A Review by " Industrial Ecology, Pollution Prevention and the NY-NJ Harbor "*. 2006, New York Academy of Sciences: New York.

[28] Department of Environmental Affairs and Tourism, *State of Environmental Systems. South Africa*, D.o.E.A.. Tourism, Editor. 2006, Government Printers.

[29] City of Cape Town, *Integrated Waste Management (IWM) Policy* 2009 [cited 2017 27 June]; 1--11]. Available from: http://sawic.environment.gov.za/documents/399.pdf.

[30] Department of Environmental Affairs and Tourism, *National Waste Information Baseline*. 2012 [cited 2017 27 June 2017]; 1--28]. Available from: http://www.sawic.org.za/documents/1736.pdf.

[31] Oladapo, O.O., et al., *Assessment of Natural Radionuclides Level in Wasteland Soils.* 2012. **2**(3): p. 38--43.

[32] Khandaker, M.U., *High purity germanium detector in gamma-ray spectrometry.* International journal of Fundamental physical sciences, 2011. **1**(2): p. 42--46.

[33] El, N.A., *Studying of Naturally Occurring Radionuclides for Some Environmental Samples and Its Hazardous Effects*. 2014, Fayoum University.

[34] Jabbar, A., *PhD Thesis COMSATS Institute of Information Technology Islamabad , Pakistan.* 2010.

[35] Tzortzis, M., et al., *Gamma-ray measurements of naturally occurring radioactive samples from Cyprus characteristic geological rocks.* Radiation Measurements, 2003. **37**: p. 221--229.

[36] Harb, S., et al. *Natural radioactivity measurements in soil and phosphate samples from El-Sabaea, Aswan, Egypt*. in *IX Radiation Physics and Protection Conference. Nasr City-Cairo*. 2008.

[37] El-Sayed, N., *Studying of Naturally Occurring Radionuclides for Some Environmental Samples and Its Hazardous Effects*. 2014.

[38] Yang, Y.X., et al., *Radioactivity concentrations in soils of the Xiazhuang granite area, China.* Applied Radiation and Isotopes, 2005. **63**(2): p. 255--259.

[39] Alzahrani, J.H., et al., *Radiological Impacts of Natural Radioactivity and Heat Generation by Radioactive Decay of Phosphorite Deposits from Northwestern Saudi Arabia.* 2011. **5**(6): p. 683--690.

[40] Papp, Z., Z. Dezső, and S. Darczy, *Measurement of the radioactivity of ^{238}U, ^{232}Th, ^{226}Ra, ^{137}Cs and ^{40}K in soil using direct Ge(Li) gamma-ray spectrometry.* Journal of Radioanalytical and Nuclear Chemistry, 1997. **222**: p. 171--176.

[41] Eisa, S. and A. Mohamed, *Investigation of Natural Radioactivity in Building Materials commonly used in Sudan.*

2010 (December).

[31] El-Taher, A., *Assessment of natural radioactivity levels and radiation hazards for building materials used in Qassim area, Saudi Arabia.* Romanian Reports of Physics, 2012. **57**(3-4): p. 726--735.

[32] Zalewski, M., M. Tomczak, and J. Kapaa, *Radioactivity of Building Materials Available in Northeastern Poland.* Polish Journal of Environmental Studies, 2001. **10**(3): p. 183--188.

[33] Ajayi, O.S., *Measurement of activity concentrations of ^{40}K, ^{226}Ra and ^{232}Th for assessment of radiation hazards from soils of the southwestern region of Nigeria.* Radiation and Environmental Biophysics, 2009. **48**(3): p. 323-- 332.

[34] Anekwe, U.L. and G.O. Avwiri, *Determination of Radiological Health Hazard Indices in Selected Crude Spilled Environment in River State, Nigeria.* American Journal of Scientific and Industrial Research, 2016: p. 50--59.

[35] El-Taher, A. and J.H. Al-Zahrani, *Radioactivity measurements and radiation dose assessments in soil of Al-Qassim region, Saudi Arabia.* Indian Journal of Pure and Applied Physics, 2014. **52**(3): p. 147--154.

[36] Sroor, A., et al., *Natural radioactivity and radon exhalation rate of soil in southern Egypt.* Applied Radiation and Isotopes, 2001. **55**(6): p. 873--879.

[37] United Nations Scientific Committee on the Effects of Atomic Radiation, *Exposures of the public and workers from various sources of radiation.*, Assembly, Editor. 2010, United Nations Publishers: New York. p. 223--463.

[38] Darwish, D.A.E., K.T.M. Abul-Nasr, and A.M. El-Khayatt, *The assessment of natural radioactivity and its associated radiological hazards and dose parameters in granite samples from South Sinai, Egypt.* Journal of Radiation Research and Applied Sciences, 2015. **8**(1): p. 17--25.

[39] Lindell, B., *Radiation and health.* Bulletin of the World Health Organization, 1987. **65**(2): p. 139--148.

[40] Staff Writer, S. *Life expectancy in South Africa vs the world*. 2016.

International Proceedings of Chemical, Biological and Environmental Engineering, V0l. 102
(2017) DOI: 10.7763/IPCBEE. 2017. V102. 11

Refuse Derived Fuel Pellets as a Renewable Energy Source

Aviwe Hlaba [1], Ademola Rabiu [1] and Adelaja Otolorin Osibote [2+]

Department of Mathematics and Physics, Cape Peninsula University of Technology, Cape Town 8000, South Africa

Department of Chemical Engineering, Cape Peninsula University of Technology, Cape Town 8000, South Africa

Abstract. The South African Government, through the National Development Plan of South Africa, aims to provide access to the grid and off-grid electrical power to a minimum of 95 % of the population by 2030, of which 20 GW of the required 29 GW required for this needs to come from alternative and renewable energy sources. The study conducted using MSW from the City of Cape Town Municipality in South Africa shows that the MSW has a calorific value of approximately 19 MJ/kg which is significantly high, meaning that the waste can be directly used as fuel in many applications but more importantly that of electricity generation. The calorific value for the pelletised waste was found to be higher at an average of 23.9 MJ/kg which can be compared with South African coal being 25.1 MJ/kg. Using TGA, 3 distinguishable major mass loss regions were found between temperatures 55 - 265℃, 270 - 410℃ and 410 - 502℃. The total sample reduction was found to be more than 90% on average which is a reduction of the waste.

Keywords: Refuse Derived Fuel, Pelletisation, Calorific Value, Thermal Degradation, Renewable, Sustainable

1. Introduction

By the year 2030, the National Development Plan of South Africa foresees that the country's energy sector will promote development and economic growth through substantial energy infrastructure investments [41] The document also states that South Africa will possess adequate electricity and liquid fuels supply, ensuring economic activity and welfare remain undisrupted. The plan also states that a minimum of 95 % of the population will attain access to the grid and off-grid electrical power [1].

Renewable energy sources are proposed in the plan for viable alternatives to coal and will supply 20 000 MW of the additional 29 000 MW electrical power requirements of 2013 [2]. Considering that South Africa has already faced a problem with regards to balancing electricity demand with supply, forcing the Electricity Supply Commission (ESKOM) to resort to a relief strategy where planned power cuts were implemented at scheduled times in a process colloquially known to South Africans as "Load Shedding". This is why energy security remains at the helm of current and future industrial and technological advancements [2].

Amongst other Department of Energy (DoE) goals, one is to ensure secure energy supply and well managed demand while ensuring an efficient and diverse energy mix allowing universal access within a transformed sector [3]. The DoE looks to implement policies that adapt to minimize the effects of climate, especially considering the recent Paris Agreement on Climate change which aims to significantly reduce carbon emissions from industries such as the energy industry [3], [4]. The DoE also emphasizes the expansion of electricity supplies such as biomass and other renewable energy sources namely, solar, wind and hydro in order to satisfy the country's future electricity demands and reduce emissions [2].

+ Corresponding author. Tel.: + 27 21 460 9092 fax: +27 21 460 3854
E-mail address: osibotea@cput.ac.za

2. South Africa's Electricity Generation and Energy Resources

Coal remains to be South Africa's most abundant energy source and most of the coal that ESKOM uses is of low quality, low calorific value at 15-16 MJ/kg and high ash content of approximately 42 % [5]. ESKOM relies on this coal to produce 90 % of South Africa's electricity supply [6]. However, South Africa's coal quality results in a number of disadvantages regarding waste and emissions stemming from sulphur, nitrogen oxides, organic compounds, heavy metals, radioactive elements, greenhouse gases and once again high ash content [7], [8].

Approximately 60 % of South Africa's crude oil requirements are supplemented by imports from the Middle East and Africa due to the country's limited reserves [2]. South Africa's fuel production is comprised of 5 % of gas produced by PetroSA [9], 35 % from coal including Sasol being the largest coal-to-chemicals producer in the world with its proprietary Fisher Tropsch Synthesis process [9] and approximately 50 % from local crude oil refineries [2]. About 10 % of the fuel is imported from refineries across the globe [2].

3. The Opportunity for Refuse Derived Fuel (RDF) Applications in South Africa

Considering the world's drive towards green energy solutions and the recent Paris Agreement on Climate Change, which aims to maintain the global warming to substantially lower the 2℃ and hopefully to some extent attempt to set the limit at 1.5℃ [4], it is evident that the world is moving away from fossil fuels and more towards renewable energy solutions.

The South African government as per the Integrated Resource Plan of 2010 has been looking into giving substantial assistance to sustainable green energy initiatives by means of sundry clean energy options range on a countrywide scale [9], [10]. In the envisaged 20-year term of the plan, approximately 42 % of electricity generated must come from renewable resources.

Municipal Solid Waste (MSW) is an inferior quality fuel in its raw form. Thus, the production of RDF pellets improves the fuel's consistency, storage and handling characteristics, combustion behaviour and calorific value remediating the issue of its heterogeneity [11], [12]. There are 2 generic types of RDF systems with substantial commercial applications in the US and parts of Europe like the UK in the form of coarse RDF pellets and fluff RDF [11]. This study focuses on the production of coarse RDF pellets. Interwaste announced the launch of South Africa's first RDF plant in 2016 [13]. The plant capacity of waste converted to fuel currently stands at 12 000 tons for use in South Africa's manufacturing sector [13]. The South African white paper on renewable energy 2003 set a target of 10 000 GWh of energy from alternative and renewable sources by 2013 [14]. Despite South Africa's abundance of sunlight and the wind for electricity generation, the potential for RDF should not be underestimated. Resource Availability and Current Waste Management Practices

MSW also termed as rubbish, trash, refuse or garbage is general waste which contains everyday items which are disposed of by the public. City of Cape Town municipality website reports that approximately 1.9 mega tons of waste are generated annually in the city [15]-[17]. Modelled waste data shows that South Africa as a whole generated 59 million tons of general waste in 2011 [16]. Recycling efforts only account for an estimated 5.8 million tons while the balance of 53 million tons.

The composition of general waste in South Africa as contributed by industrial, commercial and household waste streams can be represented in terms of 6 % plastic, 7 % paper, 4 % glass, 1 % tyres, 13 % organic waste, 21 % construction and demolition waste, and 34 % non-recyclable municipal waste.

In most developing countries, landfilling is the most commonly placed waste disposal method due to its cheapness and convenience despite threats to the environment [16], [18]-[21]. In excess of 95 % of waste generated in South Africa is landfilled with the global average currently sitting at 85 % [16], [22]. The City of Cape Town Municipality (CoCT) waste management division currently operates 25 drop-off facilities for temporary storage of collected waste and 3 landfill sites. When ill-managed, landfills can have negative effects in the short and long term. The short-term effects may include issues such as noise, flies, odour, air pollution, unsightliness and the wind scattered litter. The long-term effects are comprised of problems like

water source pollution through leached heavy metals and landfill gas generation. The long-term effects are normally factors of incorrect site selection, design, preparation and/or operation of the landfill site.

Therefore, producing RDF for energy or fuel generation purposes does not only contribute towards the goals of attaining renewable sources of energy, but also alleviating the environmental burden that MSW places on the planet in terms of pollution.

4. Materials and Methodology

4.1. Source of Sample

All MSW samples used were collected from the mixed waste sections of the drop-off facilities and transfer stations around the City of Cape Town municipal area. The mixed waste section is chosen as this is the waste that is to be disposed of in the landfills. At least four sample bags of mixed waste samples were collected from each site to get a good representative of the specific sample site.

4.2. RDF Pellet Production

To limit the variations of the RDF properties in terms of the composition and thermal properties due to its heterogenous nature, the following steps were implemented in production to reduce processing challenges:

The MSW samples were reduced in size proportions with regards to the large components of the collected samples by means of a hand-held scissor. All the large components of a specific sample must be cut into smaller pieces to allow for ease of handling. Samples were then dried in a temperature controlled oven at approximately 60 ℃ over a 5-hour period. The dry samples were then further reduced in size using a hammer mill to form a fluff like powdered material. A sample splitter was then used to obtain composites of the now powdered form MSW sample. Waste material was then combined with different materials that are to act as a binder in varying ratios as per the most efficient in terms of effectiveness and amount used:

- 5 % Guar gum starch
- 5 % Modified corn starch
- The starch binders were mixed in water before added to the waste to form a paste-like a mixture with adequate moisture content to allow for pelletisation to take place. Other binders used and the percentage thereof are as follows:
- 50 % Waste palm oil
- 50 % Waste engine oil
- The oil binders were not mixed in water before addition to the waste because they are already in liquid form and can be readily mixed into the waste sample. The reason for the higher percentage is because at low percentages, the mixture was not well mixed to allow pelletisation to take place, hence the ideal percentage was found at 50 %.

The waste now mixed with binding material was pressed in a hydraulic press with a pressure of 10 tons which equates to 98066.5 Pa to form pellets of 13.2 mm diameter. The product pellets were then dried as previously described the same way as the raw waste.

4.3. Calorific Value Determination

It is important to know the amount of energy the MSW mixed waste samples contain as means of understanding the potential of the waste feedstock as a source of fuel. This was done by means of an E2K Bomb Calorimeter. The instrument was used to determine a sample's energy content in terms of the calorific value. This measurement is achieved by combusting the sample in a pressurized vessel which is pressurized with oxygen up to 3000 kPa. Since the vessel is filled with oxygen, the apparatus can achieve complete combustion of the sample in question. After the process is complete, the device gives a result as a CV value in MJ/kg. The sample mass used in the apparatus is 0.5 grams. Through the bomb calorimeter, the energy that will be liberated from the MSW during a combustion process will be determined, thus giving an idea of how and where the energy can be used.

4.4. Thermogravimetric Analysis

The significance in understanding the thermal stability of the MSW sample is that it gives a clear picture of how the feedstock will degrade under thermal processing. This will help in the fact that it gives a guide as to how the process parameters can be manipulated during an optimization procedure. The method used in the analysis is as follows:

- The analysis begins where the waste sample is heated in an inert environment of N2 from 20 °C-900 °C at a heating rate of 20 °C/min
- At 900 °C the temperature is then maintained for 15 min in the N2 environment.
- With the temperature still maintained at 900 °C, O2 is then introduced to the system and maintained for 15 min.

The TG curve is obtained from plotting the mass loss % against the temperature. From these curves, the data for proximate analysis can be obtained by finding the major mass loss regions and correlate them to the relevant property in terms of volatile matter, fixed carbon, ash content and moisture content.

5. Results and Discussion

5.1. Calorific Value

The calorific value of RDF pellets in this study was found to range between 21.1 and 27.12 MJ/kg with an average of 23.9 MJ/kg, and a density range of 718 to 847 kg/m^3. Both measurements were found to be higher than those from the previous study [23] which shows a relationship of direct proportionality between density and calorific value. The relationship between density and calorific value is presented in Fig. 1.

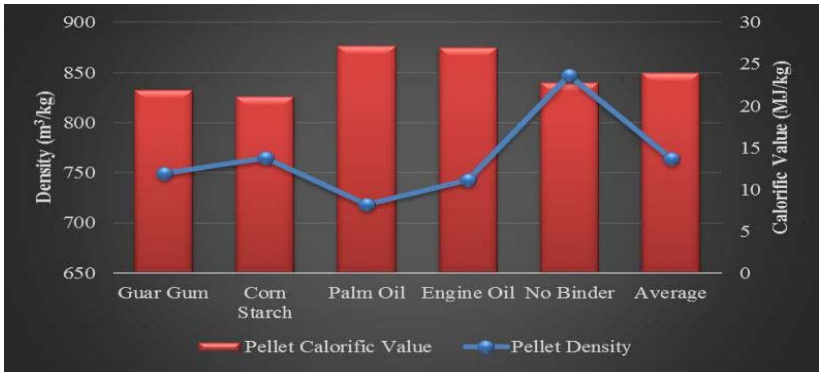

Fig. 1: The density and calorific value of pellets on average including overall average

The pellets with no binder were found to be denser than the rest. This can be attributed to the fact that when these pellets were pressed, the samples were completely dry thus could be compressed to a higher extent as no moisture content had to be expelled during compression, meaning the waste particles can come closer together as there were no moisture molecules in between. Taking into consideration that the calorific value for the pellets with waste palm and engine oil was significantly higher at 27.1 and 26.9 MJ/kg, it could be argued that the average was elevated and better than that of the preliminary studies due to the presence of these oils, however, the pellets with no binder showed calorific value of 22.7 MJ/kg at a density of 847 kg/m^3 which is higher than the previous study calorific value [23].

A proposal presented by Clean Globe to construct a Waste to Energy plant reported that based on Cape Town waste generation statistics, using a mean calorific value of 8.5 MJ/kg, the electricity that can be produced would amount to approximately 116 MW/day [24]. Studies conducted in Japan, India and Germany using RDF pellets produced calorific value results ranging between 12-20 MJ/kg, and most of these countries are already producing electricity and heat commercially [25]. The energy –return-on-energy-invested (EROEI) of the MSW from India is reported to be between 10 and 15 which is comparable to the EROEI of a crude oil well of approximately 2000 m in depth which is relatively large [25] The results obtained from this study for calorific value are significantly high making the RDF highly suited for the application of electricity generation.

5.2. Thermogravimetric Analysis (TGA) and Derivative Thermogravimetry (DTG)

Thermal degradation of the MSW was studied using TGA. A total of 5 different samples were studied and the comparison was aimed at studying the effect of the binder material on the degradation behaviour of the RDF pellets produced. In an analysis of the results obtained, it can be deduced that all the RDF pellet samples exhibit a very synonymous trend in terms of the thermal degradation behavior. It can be distinguished that all the samples exhibit 3 distinct major mass loss regions. Out of the 3 distinguishable regions, the second region of major mass loss is observed to have the most significant mass loss. This is also evident in the Derivative Thermogravimetry (DTG) which describes the rate of mass loss with temperature for the samples. The third region of major mass loss is not easily disguisable from the TGA curves, however, the DTG curve shows peaks at areas where the distinguishable mass loss occurs. On the DTG curves, the second peak is observed to be the highest in all samples confirming that the second mass loss region is where the significant mass loss occurs as identified on the TGA curve. The results obtained are presented in Fig. 2 below.

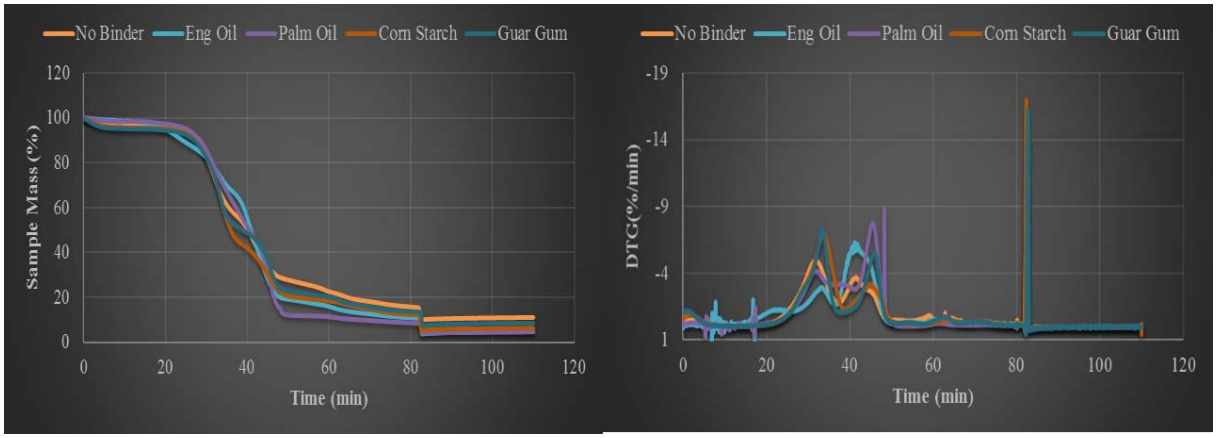

Fig. 2: TGA curves describing the thermal degradation of produced RDF pellets (left), and. DTG curves describing the rate of mass loss of the pellets with time (right).

The first region of mass loss can be attributed to the removal of all moisture content present in each sample. Thus, the 2nd and 3rd regions describe the removal of all volatile matter from the samples and the point at the end of the analysis where the curve depicts a constant mass % represents the ash content of the samples. This is how the proximate analysis data is then retrieved from the TGA curve. Fig. 3 is a representation of the proximate analysis values as read off the TGA curves for the pellet samples comprised of the different binder materials.

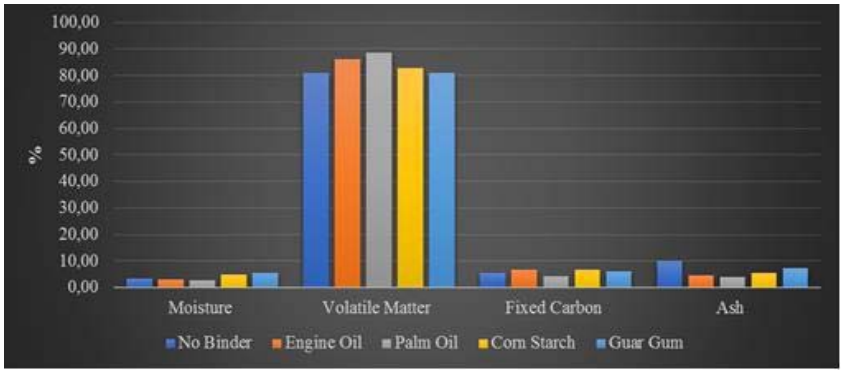

Fig. 3: Proximate Analysis Data Retrieved for TGA Curves

In analysing the proximate analysis data read from the TGA curves, it can be deduced that the data retrieved is comparable to tests done in Malaysia and Greece, confirming the credibility of the results [25-29]. The moisture content of the pellets in this study ranges from 2.90 to 5.60 %, where the pellets with corn

starch and guar gum as binder had the highest moisture. This collates well with the favourably high calorific value obtained in comparison to raw MSW which is higher in moisture and hence lower calorific value [24]. This is explained by the fact that during pelletisation, the binders were mixed with water then added to the MSW fluff to form some sort of a paste-like a mixture before pelletisation. With biomass in general, a moisture content of up to 15 % is regarded suitable to facilitate a gasification process which is efficient [30]. Although biomass with higher moisture content results in H2 rich syngas, it does, however, have the disadvantage that as it draws more heat towards sensible heating and moisture removal, the reactor temperature decreases which affects the gasifier performance and quality of syngas product [30]. The removal of moisture content begins at temperatures around 55 ℃ as the TGA and DTG curves show a slight decrease and peak respectively around this temperature and this decrease of TGA curve continues to approximately 265 ℃. The boiling point of water is 100℃ which explains the evaporation of moisture in this region of mass loss. A study of combustion characteristics of RDF in oxygen environment shows similar kind of behaviour at temperatures between 50 and 150 ℃ [31].

Volatile matter generally makes up most the biomass ranging between 70 % and 85 % by mass [30]. The volatile matter was highest on the pellets with palm oil and engine oil reading at 88.6 and 86.2 % respectively. The volatile nature of the binders themselves can be attributed the volatile matter being higher than s other pellets with a range of 80.9 to 88.6 %. The volatile matter is directly proportional to the biomass reactivity and conversion efficiency [30]. The removal of volatile matter distinguished by a massive decrease in the TGA curve and a very high peak in the DTG curve occurs at temperatures approximately between 270 and 410 ℃. During this phase of decomposition of volatiles, taking into consideration the mixed nature of the MSW used in this study, cellulose being the major component in paper materials, hemicellulose, lignin as well as any inorganic components in the waste are completely de-volatilized and the crystallinity and degree of polymerization of these polymers will impact the degradation behaviour [31], [32].

Fixed carbon content is the solid residue excluding the ash that remains after devolatilization of the biomass an inert environment. Biomass with high fixed carbon content results in high energy throughput in the gasifier and syngas with more char but less tar [30]. The fixed carbon content was found to be in the range of 4.43 to 6.70 % which is quite like the values found by [25]-[29]. The decomposition of fixed carbon is analysed when the temperature of the TGA reaches the maximum of 900 ℃ where the TGA environment is changed from N2 to O2 allowing for its complete combustion. This was not the case in the preliminary study hence fixed carbon matter was not reported in that study [23]. In terms of coal, the fixed carbon content gives a rough estimate of the heating value because this is the solid fuel left after all the volatile matter is distilled off and consists mainly of carbon [33]. However, South African coal has a calorific value of 25.1 MJ/kg which is not significantly higher than the RDF pellets in question, although South African coal is reported to have a fixed carbon content of 51.2 %.

This then brings us to the question of ash content whereby the range found for the RDF pellets was 4.07 to 10 % contrary to the 17 % reported by Larry for South African coal [33]. Among the drawbacks brought about by ash content, the reduction of burning capacity can be attributed to the low calorific value of the coal and the low ash content of the RDF explains why the calorific value is very close to that of the coal [33]. It also needs to be considered that the RDF has high volatile matter which also contributes to the calorific value. At high temperatures, ash melts and fuses together to form clinker which then brings the gasification process to a grinding halt. A lower ash content is regarded adequate for biomass feedstock considering that ash does not possess any energy [30].

The degradation behaviour of these samples along with the estimated proximate analysis values approximated from the TGA data correlate with several studies conducted with RDF and raw MSW with respect to thermal processing and pre-treatment [25], [26], comparison of fuel value and combustion characteristics [31], [34], and the pyrolysis of RDF [35].

6. Conclusion

The MSW can be converted into RDF pellets for direct use as a boiler or furnace fuel to produce high-pressure steam in power generation as the calorific value for the pelletised waste was found to be high. In finding that South African coal has a calorific value comparable to the RDF with higher carbon content, it

can be concluded that pelletised MSW would prove a suitable substitute for the fossil as it has far less fixed carbon content while maintaining a high calorific value which is a positive with regards to environmental considerations because the carbon footprint would be exceptionally lower than that of coal.

7. Acknowledgements

All the authors would like to thank the Cape Peninsula University of Technology for funding towards the project and attendance at the conference.

8. References

[1] National Planning Commission, *National Development Plan 2030: Our future - make it work*, Presidency, Editor. 2012, Government Printers: Pretoria.

[2] Department of Energy, *Pocket Guide to South Africa 2015/2016 - Energy and Water*, Energy, Editor. 2015, Government Printers: Pretoria.

[3] Department of Energy, *DoE Strategic Plan 2015-2020*, Energy, Editor. 2015, Submerge Publishers: Pretoria.

[4] Rogelj, J., et al., *Paris Agreement climate proposals need a boost to keep warming well below 2 degrees* . Nature, 2016. **534**(7609): p. 631-9.

[5] Electricity Supply Commison, . *Fact Sheet - The Formation of Coal*. 2016 [cited 2017 26 June]; Available from: http://www.eskom.co.za/AboutElectricity/FactsFigures/Documents/CO0009FormationCoalRev9.pdf.

[6] Electricity Supply Commison, *Understanding Electricity*. 2017 [cited 2017 26 June]; Available from: http://www.eskom.co.za/AboutElectricity/ElectricityTechnologies/Pages/Understanding_Electricity.aspx.

[7] Electricity Supply Commison, E. *Coal Power*. 2017 [cited 2017 26 June 2017]; Available from: http://www.eskom.co.za/AboutElectricity/ElectricityTechnologies/Pages/Coal_Power.aspx.

[8] Pretorius, I., et al., *A perspective on South African coal fired power station emissions.* Journal of Energy in Southern Africa, 2015. **26**: p. 27-40.

[9] South African Information Reporter, S. *South Africa's energy supply*. 2012 [cited 2017 27 June]; Available from: https://www.brandsouthafrica.com/investments-immigration/business/economy/infrastructure/energy.

[10] Department of Energy, *Integrated Resource Plan For Electricity*, Energy, Editor. 2010, Government Printers: Pretoria.

[11] Williams, P., *Waste Treatment and Disposal*. 1998: John Wiley and Sons.

[12] Zafar, S., *Fuel Pellets from Solid Wastes*. 2015.

[13] Van Der Merwe, M. *South Africa gets its first Refuse-Derived Fuel Plant*. 2016 [cited 2017 27 June]; Available from: https://www.dailymaverick.co.za/article/2016-02-18-south-africa-gets-its-first-refuse-derived-fuel-plant/ \#.

[14] Department of Minerals and Energy, *Department of Minerals And Energy Republic of South Africa White Paper* 2003.

[15] City of Cape Town, *Integrated Waste Management (IWM) Policy* 2009 [cited 2017 27 June]; 1--11]. Available from: http://sawic.environment.gov.za/documents/399.pdf.

[16] Department of Environmental Affairs and Tourism, *National Waste Information Baseline*. 2012 [cited 2017 27 June 2017]; 1--28]. Available from: http://www.sawic.org.za/documents/1736.pdf.

[17] Engledow, S., *Integrated Analysis Solid Waste Baseline Report.* Environmental Conservation, 2007.

[18] Adefeso, I.B., A.M. Rabiu, and D.I. Ikhu-Omoregbe, *Refuse-derived fuel gasification for hydrogen production in high temperature proton exchange membrane fuel cell base CHP system.* Waste and Biomass Valorization, 2015. **6**(6): p. 967-974.

[19] Adesuyi, A.A., K.L. Njoku, and M.O. Akinola, *Assessment of heavy metals pollution in soils and vegetation around selected industries in Lagos state, Nigeria.* Journal of Geoscience and Environment Protection, 2015. **3**(07): p. 11.

[20] Aucott, M., *The fate of heavy metals in landfills: A Review by " Industrial Ecology, Pollution Prevention and the NY-NJ Harbor "*. 2006, New York Academy of Sciences: New York.

[21] Odukoya, A. and Abimbola A., *Potential soil contamination with toxic metals in the vicinity of active and abandoned dumpsites.* Agriculture and Biology Journal of North America, 2011. **2**(5): p. 785--790.

[22] Department of Water Affairs & Forestry, D., *Minimum Requirements for Waste Disposal By Landfill*. 1998, Department of Water Affairs & Forestry: Pretoria.

[23] Hlaba, A., A. Rabiu, and O.A. Osibote, *Thermochemical Conversion of Municipal Solid Waste — An Energy Potential and Thermal Degradation Behavior Study.* International Journal of Environmental Science and Development, 2016. **7**(9): p. 661--667.

[24] Clean Globe, *MSW as an Energy Source*. 2011, National Energy Regulator of South Africa: COFit Presentation.

[25] Jones, J.C., *Thermal Processing of Waste*. 2010. 1--99.

[26] Badeie, A., *Thermal pretreatment of municipal solid waste.* 2013(7).

[27] Gidarakos, E., G. Havas, and P. Ntzamilis, *Municipal solid waste composition determination supporting the integrated solid waste management system in the island of Crete.* Waste Management, 2006. **26**(6): p. 668--679.

[28] Ismaila, A., et al., *Investigation on biomass briquettes as energy source in relation to their calorific values and measurement of their total carbon and elemental contents for efficient biofuel utilization.* Advances in Applied Science Research, 2013. **4**(4): p. 303-309.

[29] Kalanatarifard, A.A., *Identification of the Municipal Solid Waste Characteristics and Potential of Plastic Recovery at Bakri Landfill, Muar, Malaysia.* Journal of Sustainable Development, 2012. **5**(7): p. 11--17.

[30] Wang, L., *Sustainable Energy Production*. 2014: CRC Press Taylor and Francis Group.

[31] Li, Y., et al. *Combustion characteristic of refuse derived fuel under oxygen-enriched atmosphere*. in *Materials for* Renewable *Energy and Environment (ICMREE), 2013 International Conference on*. 2014. IEEE.

[32] Bradfield, F.L., *Examination of the thermal properties of municipal solid waste and the scalability of its pyrolysis*. 2014, Stellenbosch: Stellenbosch University.

[33] Thomas, L., *Coal Geology*. 2012: Wiley.

[34] Sever, A.A., A. Atımtay, and F. Sanin, *Comparison of fuel value and combustion characteristics of two different RDF samples.* Waste management (New York, NY), 2016. **47**(Pt B): p. 217.

[35] Kluska, J., et al., *Pyrolysis of biomass and refuse-derived fuel performance in laboratory scale batch reactor.* Archives of Thermodynamics, 2014. **35**(1): p. 141-152.

Thermochemical Conversion of Municipal Solid Waste — An Energy Potential and Thermal Degradation Behavior Study

A. Hlaba, A. Rabiu, and O. A. Osibote

***Abstract*—Solid waste management has become an ever growing problem world-wide due to rapid urbanization and population growth. South Africa was found to have generated 59 million tons of general waste in 2011 with the Western Cape generating 675kg/capita/annum. The convention of management has been that of landfilling, however this method is fast becoming insignificant due to the lack of space and detrimental nature to environment. In light of the energy security issue South Africa is facing, and the global drive of finding alternate sources of fuel with the depletion of fossil fuel, attention has turned to MSW as a sustainable source of energy while remediating its effect on the environment. Thermochemical conversions of Municipal Solid Waste (MSW), thus presents an attractive means of harnessing the potential value in this waste stream thus thermochemical conversion pose an attractive means of converting this waste stream into valuable fuel products. Study was conducted making use of RDF pellets produced from the MSW. Pellet density was varied by varying the starch binder to MSW ratio, thus the effect of this on energy content and thermal degradation behavior was studied. The energy content of MSW in Cape Town was investigated using a bomb calorimeter and the thermal degradation behavior was studied using Thermogravimetric Analysis (TGA). The MSW calorific value was found to average at 19MJ/kg and 3 distinguishable major mass loss regions were found between temperatures 55 – 265^{o}C, 270 - 410^{o}C and 410 - 502^{o}C. The total mass reduction was found to be 76%.**

***Index Terms*—Calorific value (CV), proximate analysis, refuse derived fuel (RDF), thermo-gravimetric analysis (TGA), derivative thermogravimetry (DTG).**

[13] INTRODUCTION

Solid waste management is an ever growing challenge for any major city, not only in South Africa, but on a global scale. Due to urbanization, populations of major cities grow immensely on an annual basis. It stands to reason that with an increasing amount of people flocking into an area, the amount of solid waste generated would also show a substantial increase, exhibiting a relationship of direct proportionality. This then poses a challenge to the municipalities with regards to the management of the ever increasing volumes of waste generated.

Comprehensive Municipal Solid Waste (MSW) characterization data is not available in more recent documentation, however, a study conducted by the DEAT in conjunction with the Council for Scientific and Industrial Research(CSIR) South Africa in 2011 reports that generation data according to per capita per annum was found to be still relevant in 2011 [1].

Table I illustrates clearly the link between urbanization and waste generation. Gauteng followed by the Western Cape Province show the highest amount of waste generation being 761 and 675 kg/capita/annum respectively. These respective provinces are also considered as the two most urbanized provinces in South Africa

According to the Population Education report published by the City of Cape Town in 2011, the population of the city increases by 2.6% every year. In this document, Statistics South Africa reported that in 2011, the population of Cape Town was 3.74 million. With a population growth rate of 2.6% annually, it means that Cape Town currently has a population of 4.03 million showing an increase of approximately 290 000 people over the past 3 years. Treasury reports that approximately an average of 0.8 to 3 kg per capita per day is generated suburban areas in South Africa. This amounts to quite a substantial amount when considering all the contributors of MSW in a specific town, city, or metropolitan area. City of Cape Town municipality website reports that approximately 1.9 mega tons of waste is generated annually in the city [2]-[4].

Modeled waste data shows that South Africa as a whole generated 59 million tons of general waste in 2011 (see Table [21] [3]. Recycling efforts only account for an estimated 5.8 million tons while the balance of 53 million tons.

The composition of general waste in South Africa as contributed by industrial, commercial and household waste streams can be represented in terms of plastic, paper, glass, tyres, organic waste, construction and demolition waste, and non-recyclable municipal waste. Paper, plastics, glass and tyres are regarded as the mainline recyclables.

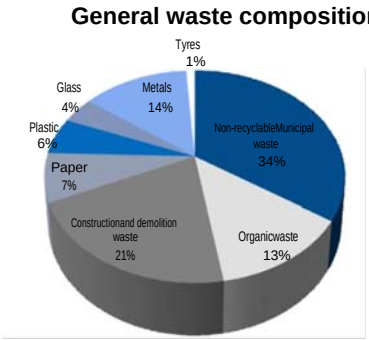

Fig. 1. The waste composition for general waste, 2011 (percentage by mass) [3].

Manuscript received September 8, 2015; revised November 13, 2015. The authors are with the Cape Peninsula University of Technology, South Africa (e-mail: aviwe.t@gmail.com).

doi: 10.18178/ijesd.2016.7.9.858

Taking a closer look at the composition of the MSW namely in the City of Cape Town and the Gauteng province of South Africa, only a few studies of characterization have been carried out to date . With regards to the organic fraction of the waste, it can be split into putrescibles, greens and garden waste. Adding these streams together however and reporting them as organic waste shows that the City of Cape Town alone is very closely comparable to the whole province of Gauteng.

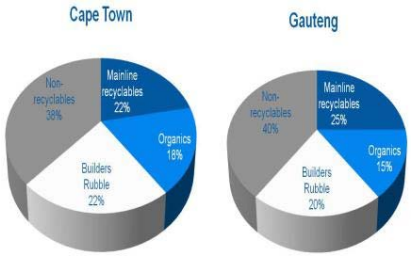

Fig. 2. Municipal waste composition (Percentage by Mass) [3].

In most developing countries, burning and landfilling are the common placed methods for MSW management, with glass and plastics being recycled. These methods are however largely inadequate and also pose a threat to the environment, public health, quality of air, landscape and ground water [5].

Thermo-chemical conversion thus provides an attractive means to managing waste whilst obtaining an alternative sustainable energy source.

Landfilling in particular is increasingly being globally recognized as an unsustainable method for waste management due to the adverse effects it has on the environment in terms of polluting contaminants [6]-[9]. Waste-To-Energy (WTE) conversion technologies are largely gaining positive acclaim with numerous municipalities worldwide [10]. These technologies can be separated into biological/chemical, physical or thermal technologies.

Biological/chemical technologies are low temperature operations running below 200^{o}C and hence with low reaction rate as reaction rate is directly proportional to reaction temperature [11]. Some technologies are comprised of the manufacturing of products by means of physical chemistry and chemical processes applied in multiple steps. A vast range of by-products are obtained ranging between compost, chemicals and electricity.

Physical technologies deal with the changing of the characteristics of the organic fraction from the MSW feedstock. These organic materials may be separated, shredded and dried resulting in a material formally known as refuse-derived fuel (RDF). This fuel can come in the form of densified or pelletized homogenous fuel pellets which are used in thermal technologies.

Thermal technologies, unlike the biological/chemical technologies, operate at much higher temperatures ranging from 400^{o}C to 5000^{o}C. Electricity is commonly the primary by-product from most thermal technologies currently in application. Thermal technologies include advanced thermal conversion processes in the form of incineration, pyrolysis, and gasification.

This paper focuses on understanding the energy potential of Refuse Derived Fuel (RDF) pellets from MSW in the City of Cape Town and their respective thermal degradation behavior. This can be regarded as a preliminary study in order to understand the thermal characteristics of this alternate source of energy as a basis for application in thermo-chemical conversion technologies in future applications for the production of energy, be it in the form of electricity or even transportation fuels. This is in light of the current energy security issue that South Africa faces in terms of insignificant fossil fuel reserves in terms of coal and natural gas.

South Africa's most abundant energy source is coal and most of the coal is of low quality, low heating value and high ash content. According to the Electricity Supply Commission, also known as "ESKOM" in South Africa, the organization relies on this coal to generate 90% of South Africa's electrical energy supply. Even with the coal, South Africa is still facing a crisis in terms of balancing power supply with demand which has resulted in ESKOM resorting to a relief procedure known to South African citizens as "Load shedding".

Sasol uses the gasification of coal to produce syng as for petroleum production. However, coal is somewhat, "dirty" source of fuel due to its polluting nature. Petro SA converts natural gas into liquid fuels, however reserves are low.

MSW on the other hand offers a sustainable, non-exhaustible and non-season dependent source of raw material for the production of any form of energy.

Materials and Methodology

Source of Sample

All MSW samples used were collected from the mixed waste sections of the drop-off facilities and transfer stations around the City of Cape Town municipal area. The mixed waste section is chosen as this is the waste that is to be disposed off in the landfills. At least four sample bags of mixed waste samples were collected from each site in order to get a good representative of the specific sample site.

B. RDF Production

MSW poses a processing challenge due to its heterogeneous nature. The production of RDF pellets is put in place as a remedial strategy to this. However, due to different locations and sometimes seasonal waste, the pellets themselves may still have differing characteristics in terms of composition. In order to limit the variations of the RDF properties in terms of the composition and thermal properties the following steps were implemented in production:

[21] The MSW samples were reduced in size proportions with regards to the large components of the collected samples by means of a hand held scissor. All the large components of a specific sample must be cut into smaller pieces to allow for ease of handling.

[22] Samples are then dried in a temperature controlled oven at approximately 60^{o}C over a 5 hour period.

[23] The dry samples are then further reduced in size using a hammer mill.

[36] A sample splitter is then used to obtain composites of the now powdered form MSW sample.
[37] Modified corn starch mixed with water is then used as a binder where the starch to MSW ratio is varied and the pellets are formed using a hand held pellet press.
[38] Pellets are then dried as in step 2.

By applying this method, the sample should exhibit the same kind of properties or a very small to negligible range of variation.

C. Calorific Value Determination

It is important to know the amount of energy the MSW mixed waste samples contain as means of understanding the potential of the waste feed stock as a source of fuel. This was done by means of an E2K Bomb Calorimeter. The instrument is used to determine a sample's energy content in terms of the calorific value. This measurement is achieved by combusting the sample in a pressurized vessel which is pressurized with oxygen up to 3000 kPa. Since the vessel is filled with oxygen, the apparatus is able to achieve complete combustion of the sample in question. After the process is complete, the device gives a result as a CV value in MJ/kg. The sample mass used in the apparatus is 0.5 grams. Through the bomb calorimeter, the energy that will be liberated from the MSW during a combustion process will be determined, thus giving an idea of how and where the energy can be used.

D. Thermo-Gravimetric Analysis

The significance in understanding the thermal stability of the MSW sample is that it gives a clear picture of how the feedstock will degrade under thermal processing. This will help in the fact that it gives a guide as to how the process parameters can be manipulated during an optimization procedure.

The method used in the analysis is as follows:

1) The analysis begins where the waste sample is heated in an inert environment of N2 from 20°C-920°C at a heating rate of 20°C/min
2) At 920°C the temperature is then maintained for 15 min in N2environment.
3) With the temperature still maintained at 920°C, $O_2$is then introduced to the system and maintained for 15 min.

The TG curve is obtained from plotting the mass loss% against the temperature. From these curves, the data for proximate analysis can be obtained by finding the major mass loss regions and correlate them to the relevant property in terms of volatile matter, fixed carbon, ash content and moisture content

III. Results and Discussion

A. Calorific Value

In total, 30 samples were tested amounting to 10 sample sites completed. Each sample site was analyzed 3 times to ensure the integrity of the results. The averaged results for each sample site are presented on Fig. 3.

The results presented in Fig. 3 represent the raw ground up samples of MSW on a dry basis. The averaged calorific value measurements, of the samples in total range from approximately 15 to 25 MJ/kg averaging out to approximately 19 MJ/kg. In analysis of the samples, there were samples that showed higher energy levels with one sample from Ladiesmiles maxing out at 28.9 MJ/kg. This sample and others that had calorific values above 20 MJ/kg were all found to have one thing in common and that is there was a significant amount of non-recycled plastics, like plastic bags and some plastic bottles. Columbia University Earth Engineering Center, these plastics have a calorific value of approximately 32 MJ/kg [12].

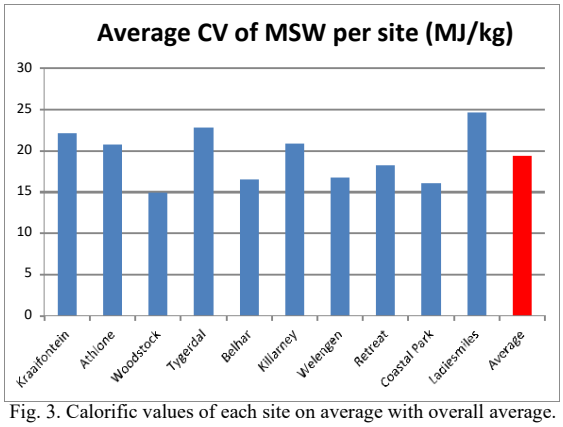

Fig. 3. Calorific values of each site on average with overall average.

TABLE I: Calorific Value of Non-Recyclable Plastics (NRP) Broken down into the Different Constituents That Makes up the Material [12]

Materials	% in NRP	MJ/kg	MJ/kg NRP
Polyethylene terephthalate (PET)	12.4	24	2.93
High density polyethylene (HDPE)	17.8	44	7.76
Polyvinyl chloride (PVC)	5.5	19	1.05
Low density polyethylene/ Linear low density polyethylene (LDPE/LLDPE)	19.6	28	5.39
Polypropylene (PP)	13.9	44	6.08
Polystyrene (PS)	8.70	41	3.56
Other	22.0		5.55
Total NRP	100		31.96

Studies conducted in Changzhou and Guangzhou in China show raw MSW of low calorific value reporting at 3 to 4 MJ/kg while in Kuala Lumpur,Malaysia and Parona, Italy report values ranging 10 - 16.8 MJ/kg and 10.5 – 16.17 MJ/kg respectively [13]. This difference in calorific value of the waste can be attributed to the presence or lack thereof of NRP's in the waste in question. All the locations mention above are fairly developed areas in the world, which means the difference in calorific value might depend on the level of sorting and recycling practices in each area's waste management facilities, hence determining the amount of NRP's present in the waste. An example of such practices would be that practiced in many communities where the NRP's are converted into oil by means of a pyrolysis process [12]. This then means that the NRP's would not be present in the MSW that is to be landfilled. In the case of the Cape Town samples however, no such process is in place in the current waste management structure of the city municipality, however, there are still areas that show quite low calorific

value. As mentioned earlier, the averaged range is between 15 and 25 MJ/kg. The areas with calorific value of approximately 15 MJ/kg had MSW of similar composition as displayed in Fig. 2; however the organics fraction in these areas was found to be much higher. The Woodstock site for instance possesses the lowest calorific values. This is due to the fact that the sample from Woodstock is mainly comprised of biomass which is essentially only wood chippings. Wood has a calorific value of about 14.4 MJ/kg according IGNIS Energy and the average for Woodstock was 14.8 MJ/kg which is fairly consistent. This site along with Coastal Park and Belharexhibit similar characteristics in terms the waste composition and calorific value. The common factor among these sites is that they are all situated near residential areas thus the waste is mainly from domestic sources which is mostly kitchen waste and garden waste, of which both fall under the organic fraction of the waste. The higher CV sample sites are situated in densely populated areas where industry and commerce are dominant meaning that the waste contains mostly plastic (packaging, bottles, carrier bags etc.), paper (office paper, cardboard packaging etc.) and still with some domestic waste from residential complexes. However this domestic waste understandable doesn't have garden waste as residences are in a city center like setting.

TABLE II: PERCENTAGE MUNICIPAL WASTE CONTRIBUTION BY PROVINCE IN SOUTH AFRICA, 2011 [3]

Province	kg/capita/annum	Waste generated as % of Total waste
Western Cape	675	20
Eastern Cape	113	4
Northern Cape	547	3
Free State	199	3
KwaZulu Natal	158	9
North West	68	1
Gauteng	761	45
Mpumalanga	518	10
Limpopo	103	3

TABLE III: MODELED WASTE DATA [3]

General Waste 2011	Generated	Recycled	Disposed	Recycled
	Tonnes			%
Municipal waste	7, 88	-	7, 88	0
Organic waste	2, 95	1, 03	1, 92	35
Construction and demolition waste	4, 73	0, 756	3, 97	16
Paper	1, 69	0, 966	0,728	57
Plastic	1, 28	0, 230	1, 05	18
Glass	0, 938	0, 300	0, 637	32
Metals	3, 12	2, 49	0, 624	80
Tyres	0, 247	0.00987	0, 237	4
Other	36,2	-	36,2	0
Total general waste [T]	59, 0	5, 79	53, 2	10

The 15 to 25 MJ/kg result obtained is quite a vast range and just averaging from that does not give a very accurate picture in terms of the calorific value of MSW in Cape Town. Thus it was decide that a composite sample must be prepared and analysed to get a more reputable idea of what the calorific value of the city's MSW would be on an overall basis (see Fig. 4). In comparison of the results in Fig. 3 and Fig. 4, it is deduced that the latter representing the composite sample ranges between 13 and 23 MJ/kg. However, with the composite, only one sample out of 10 runs was at the extreme low of 13 MJ/kg, as the other reading ranged from approximately 17 to 23 MJ/kg which is not as vast. This shows that the sample is fairly close to being homogeneous which means it is a good representative sample for the overall energy content of the city's MSW.

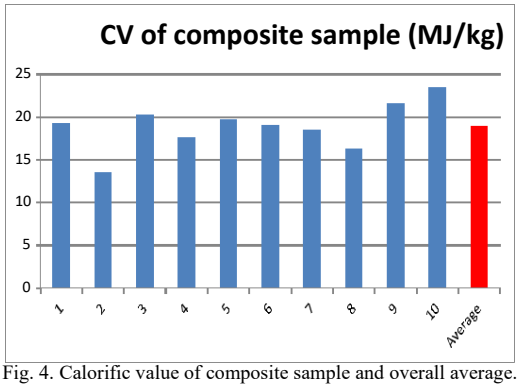

Fig. 4. Calorific value of composite sample and overall average.

In comparing the average CV for the composite sample and the average from the site samples, it is established that the average is reasonable close as the composite averaged out at 18.9 MJ/kg while the site sample overall average was found to be 19 MJ/kg. This indicates that it can be assumed with good reason that the average Calorific Value of the MSW is approximately 19 MJ/kg.

Studies conducted in India, Germany and Japan, show calorific values of 12-13 MJ/kg, 15-18 MJ/kg and 18 to 20MJ/kg respectively [14]. These calorific values were obtained from RDF pellets manufactured from MSW. On average, RDF is expected to have calorific value ranging from 12 to 15 MJ/ kg [14]. Interestingly so, the RDF from India with its low calorific value compared to others is used as fuel for electricity generation, thus the MSW from Cape Town is more than appropriate for the same type of application in terms of CV. It is reported that the energy –return-on-energy-invested (EROEI), for the RDF from India is in the range of 10 to 15. This is referred to as the ratio between the energy provided by a certain fuel and the energy required in the acquiring and delivery of this energy [15]. The 10 to 15 range can be compared to the EROEI of a crude oil well of approximately 2000m in depth which is quite significant [14].

In this study, the RDF pellets produced were of the same diameter of approximately 18mm with varying ratio of the starch binder used. The ratio's used in terms of starch content to MSW in the production of the pellets were 0:1, 0.5:1, 1:1 and 2:1 with pellet density of 326, 461, 516, and 641 kg/m^3. RDF pellet density is a measure of its hardness ranging from 250 to 700 kg/m^3 which relates to a measure of soft to very hard [16]. These results show that the pellet density is directly proportional to the amount of binder added during pelletization.

The calorific value of the RDF pellets was found to have the same average as the unpelletized MSW at 19 MJ/kg. This shows that the starch has no effect on the CV of the waste,

however the range of the CV from the pelletized samples was somewhat more narrow ranging from 16.8 to approximately 20 MJ/kg. This shows that the pelletized MSW or RDF is more homogenous than the unprocessed waste.

B. Thermal Degradation Behavior of MSW

Thermal degradationof the MSW was studied using TGA. A total of 6 different samples were studied and the comparison was aimed at studying the effect of the starch content on the degradation behavior of the RDF pellets produced. Also the thermal degradation of the unpelletized MSW was analyzed including that of virgin biomass which is normally the conventional feedstock for alternative fuel production applications due to its homogenous nature in terms of composition which allows ease of operation in production plants. The results obtained are presented in Fig. 5 below.

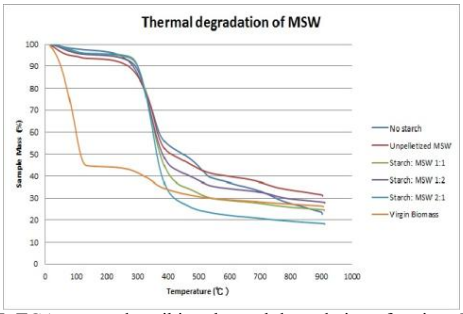

Fig. 5. TGA curves describing thermal degradation of various RDF.

In analysis of the results obtained, it can be deduced that from all the RDF pellet samples including the unpelletized MSW sample exhibit a similar trend in terms of the thermal degradation behavior. It can be distinguished that all the samples, except the virgin biomass, show 3 distinct regions of major mass loss. Out of the 3 distinguishable regions, the second region of major mass loss is observed to have the most significant mass loss.

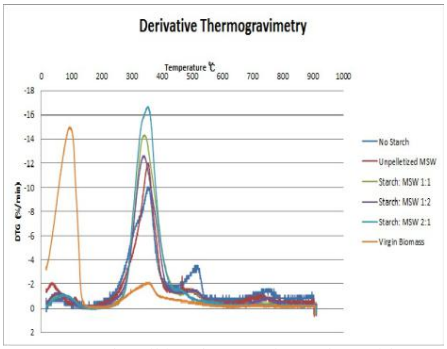

Fig. 6. DTG curves describing the rate of mass loss with temperature.

This is also evident in the Derivative Thermogravimetry (DTG) which describes the rate of mass loss with temperature for the samples. A third region of major mass loss is not easily disguisable from the TGA curves, however the DTG shows slight peaks after the second major peak which indicates a third region of mass loss. Taking into consideration that the analysis takes place in a nitrogen environment (inert), it can be stated that the samples were thermally degraded in pyrolytic conditions. Therefore, each degradation step can be attributed to the attributes of the samples which would be obtained in proximate analysis. The first region of mass loss can be attributed to the removal of all moisture content present in each sample. Thus the 2nd and 3rd regions describe the removal of all volatile matter from the samples. The average percentage of mass remaining at the end of the analysis for the pellet samples and the unpelletized MSW was found to be approximately 24% which is attributed to the ash content. This means that the samples are degraded by approximately 76% which is quite significant if looking at it in the perspective of size reduction of the waste.

The removal of moisture content begins at temperatures around 55°C as the TGA and DTG curves show a slight decrease and peak respectively around this temperature and this decrease of TGA curve continues to approximately 265°C. On average, for all pelletized MSW samples (RDF) and the unpelletized MSW, this amount to approximately 7% of the sample degraded thus can be correlated to a moisture content of about 7% for these samples. The boiling point of water is 100°C which explains the evaporation of moisture in this region of mass loss. A study of combustion characteristics of RDF in oxygen environment shows similar kind of behavior at temperatures between 50 and 150°C [17].

The removal of volatile matter distinguished by a massive decrease in the TGA curve and a very high peak in the DTG curve occurs at temperatures approximately between 270 and 410°C accounting to an average mass loss for the unpelletized MSW and RDF pellets of 51% from the previous degradation region. During this phase of decomposition of volatiles, taking into consideration the mixed nature of the MSW used in this study, cellulose being the major component in paper materials, hemicellulose, lignin as well as any inorganic components in the waste are completely de-volatized and the crystallinity and degree of polymerization of these polymers will impact the degradation behavior [17], [18]. Decomposition of fixed carbon is not expected as analysis is carried out in an inert atmosphere.

The third major loss region is not so evident in the TGA curve; however slight peaks are noticeable in the DTG curves, more especially with the 'No Starch' pellet sample as this shows a region of increase in rate of decomposition. This mass loss phase is attributed to the removal of more volatile matter from temperatures of approximately 410°C from the preceding peak to approximately 502°C. In total, the amount of volatile matter removed on average for all samples was found to be approximately 69% of the MSW samples (RDF Pellets and unpelletized).

The degradation behavior of these samples along with the estimated proximate analysisvalues approximated from the TGA data correlate with several studies conducted with RDF and raw MSW with respect to thermal processing and pretreatment [14] and [19], comparison of fuel value and combustion characteristics [17], [20] and the pyrolysis of RDF [21].

In terms of the effect of starch content on the thermal degradation behavior of the samples, the overall degradation was not much affected by the starch content in terms of the general behavior. However at the end of the analysis, the amount of sampleremaining was found to be different. With increasing starch content, the ash content remaining was

found to be decreasing. This can be directly linked to the density of the RDF pellets produced. The starch to MSW ratio was found to be directly proportional to the density of the final pellet product. This then shows that the more dense the sample is, the more stable the thermal degradation behavior observed. Taking into consideration, the pellet sample of starch to MSW ratio 2:1 being the sample with the most amount of starch was found to have less than 20% ash content and all others were found to be above 20% with each ratio varying in terms of the fact that starch content was inversely proportional to the ash content at the end of analysis. This sample was also found to show the most stability in terms of thermal degradation behavior.

IV. Conclusion

The study conducted using MSW from the City of Cape Town Municipality in South Africa shows that the MSW has a calorific value of approximately 19 MJ/kg which is significantly high meaning that the waste can be directly used as fuel in many applications but more importantly that of electricity generation. The MSW can be convertedinto RDF pellets for direct use as boiler or furnace fuel for the production of high pressure steam in power generation.

This is not the only possibility, more advanced thermochemical conversion techniques can also be applied to the waste in order to obtain high value products like fuel gases and liquid fuel products. This then warrants the understanding of the thermal degradation behavior of the MSW.

Using TGA in inert atmosphere, which can be related to that of pyrolysis, 3 distinguishable major mass loss regions were found between temperatures 55 - 265°C, 270 - 410°C and 410 - 502°C. The total sample reduction was found to be 76% which is quite significant reduction of the waste. Studies have shown that oxygen availability in the process shows higher size reduction. This is because the process moves more towards combustion which produces CO_2 [19].

This is significant if a gasification process is to be applied as it also uses oxygen but less than stoichiometric requirements to create reducing conditions for the production of what is called syngas which can be converted to various valuable fuel products.

Acknowledgment

All the authors would like to thank Cape Peninsula University of Technology for funding towards the project and attendance at the conference.

References

[1] D. Kilian, H. Fiehn, J. Ball, and S. Lewis, "National state of the environment project background research paper produced for the South Africa," December, pp. 1–37, 2005.
[2] S.-A. Engledow, "Integrated analysis solid waste baseline report," *Environ. Conserv.*, 2007.
[3] DEA and D. of E. Affairs, "National waste information baseline report," 2012.
[4] C. Town, "An introduction to the city of cape town integrated waste management by-law," 2009.
[5] I. Adefeso, D. Ikhu-Omoregbe, and A. Rabiu, "Sustainable co-generation plant: Refuse-derived fuel gasification integrated with high temperature PEM fuel cell system," vol. 33, pp. 125–129, 2012.
[6] M. Aucott, "The fate of heavy metals in landfills: A review by 'industrial ecology, pollution prevention and the NY-NJ Harbor,'" February, 2006.
[7] DEAT, "State of environmental systems," 2006.
[8] A. A. Adesuyi, K. L. Njoku, and M. O. Akinola, "Assessment of heavy metals pollution in soils and vegetation around selected industries in Lagos State , Nigeria," September, pp. 11–19, 2015.
[9] A. Odukoya and A. Abimbola, "Potential soil contamination with toxic metals in the vicinity of active and abandoned dumpsites," *Agric. Biol. J. North Am.*, vol. 2, no. 5, pp. 785–790, 2011.
[10] D. P. Zine, J. Hahn, B. Parks, and G. Smith, "Evaluation of alternative solid waste processing technologies," p. 500, September 2005.
[11] H. S. Fogler, *Elements of Chemical Reaction Engineering*, vol. 42. Prentice Hall, 2006.
[12] N. J. Themelis and C. Mussche, "2014 energy and economic value of municipal solid waste (MSW), including non-recycled plastics (NRP), currently landfilled in the fifty states," 2014.
[13] Y. Zhang, Y. Chen, A. Meng, Q. Li, and H. Cheng, "Experimental and thermodynamic investigation on transfer of cadmium influenced by sulfur and chlorine during municipal solid waste (MSW) incineration," *J. Hazard. Mater.*, vol. 153, no. 1–2, pp. 309–319, 2008.
[14] J. C. Jones, *Thermal Processing of Waste*. 2010.
[15] C. A. S. Hall, J. G. Lambert, and S. B. Balogh, "EROI of different fuels and the implications for society," *Energy Policy*, vol. 64, pp. 141–152, 2014.
[16] L. E. N. V Gr, "Review of alternative pre-treatment equipment," pp. 1–10, 2013.
[17] Y. Li, L. Jiang, N. Zhao, Y. Li, R. Li, and Y. Chi, "Combustion characteristic of refuse derived fuel under oxygen-enriched atmosphere," pp. 1–5, 2003.
[18] F. L. Bradfield, "Examination of the thermal properties of municipal solid waste and the scalability effect on its degradation and pyrolysis products by," December 2013.
[19] A. Badeie, "Thermal pretreatment of municipal solid waste," no. 7, 2013.
[20] A. Sever Akdağ, A. Atımtay, and F. D. Sanin, "Comparison of fuel value and combustion characteristics of two different RDF samples," *Waste Manag.*, 2015.
[21] J. Kluska and M. Klein, "Pyrolysis of biomass and refuse-derived fuel performance in laboratory scale batch reactor," vol. 35, no. 1, pp. 141–152, 2014.

A.Hlaba was born in the town Umtata and raised in Butterworth, Eastern Cape Province in South Africa on April 11, 1991. Hlaba obtained his national diploma in chemical engineering in 2013 and the B-Tech degree in chemical engineering in 2015 both at the Cape Peninsula University of Technology, South Africa. He is currently completing his master's program at the same institution.

A.Rabiu holds a BSc (Hons) and an MSc in chemical engineering from Obafemi Awolowo University, Nigeria, the B-Tech in project management and the MPhil in commercial law. Ademola is presently a senior lecturer with Cape Peninsula University of Technology, CPUT where he is teaching process design and petroleum production technology. His research interests are sustainable energy technology which include thermo-chemical conversion of wastes to fuels; processing of conventional and non-conventional petroleum resources and sustainable resources.

Adelaja Otolorin Osibote completed her undergraduate studies at Ogun State University, Nigeria (now Olabisi Onabanjo University) in physics in 1992 and received her M.Sc. in engineering physics (medical and health physics option) from Obafemi Awolowo University, also in Nigeria in 1999. She obtained her Ph.D (medical physics) from Escola Nacional de Saude Publica (National School of Public Health)-FIOCRUZ, Brazil in 2006. She was a postdoctoral research fellow in the Department of Nuclear Energy, Universidade Federal de Pernambuco (Federal University of Pernambuco), Brazil in 2007 and in the Department of Human Biology (Biomedical Engineering) of University of Cape Town, South Africa in 2008. She was a junior research associate, of the Abdus Salam International Center for Theoretical Physics from 2002 to 2006.

Dr. Osibote assumed a faculty position in the Department of Physics, Olabisi Onabanjo University in 1995 and presently in the Department of Mathematics and Physics, Cape Peninsula University of Technology, South Africa. She has carried out research on several areas including irradiation of foodstuffs, measurement of radioactivity in food and environmental fields, quality assurance in diagnostic radiology and in the developments of algorithms for automated focusing of a microscope for the detection of tuberculosis. She teaches several courses in physics at the University and supervises a number of students.